

Xenorhabdus bovienii bacteria – *Steinernema* spp. nematode interactions as a model of
evolution and mechanisms within broad-host range symbioses

By

Kristen E. Murfin

A dissertation submitted in partial fulfillment of
the degree requirements for the degree of

Doctor of Philosophy

(Microbiology)

at the

UNIVERSITY OF WISCONSIN-MADISON

2015

Date of final oral examination: 5/5/2015

This dissertation is approved by the following members of the Final Oral Committee:

Heidi Goodrich-Blair, Bacteriology

Cameron Currie, Bacteriology

Edward Ruby, Medical Microbiology and Immunology

Caitilyn Allen, Plant Pathology

Kenneth Raffa, Entomology

Xenorhabdus bovienii bacteria – *Steinernema* nematode spp. interactions as a model of evolution and mechanisms within broad-host range symbioses

By

Kristen E. Murfin

Under the supervision of Professor Heidi Goodrich-Blair

At the University of Wisconsin-Madison

ABSTRACT

Mutually beneficial symbioses (mutualism) between bacterial symbionts and plant or animal hosts are ubiquitous, and quite frequently these associations are broad host-range in nature, in that the bacterial symbiont can associate with several different hosts. Although broad host-range mutualisms are widespread and fundamentally important to our understanding of biological systems, our basic knowledge of how these systems are maintained and evolve is limited. The work detailed in this thesis describes the development of the *Xenorhabdus bovienii* bacterial strain – *Steinernema* spp. nematode association as a model for exploring such questions. In the work described here I characterize a suite of nine *X. bovienii* bacterial strains that associate with six different nematode host species. Through genomic and phenotypic analysis, I demonstrate that these bacterial strains are functionally diverse, providing the potential for variability in symbiotic interactions. Experimental testing demonstrates that indeed variability in symbiotic interactions occurs and that these differences are likely due to coevolution between nematode host species and bacterial strain symbionts. Further comparative genomic analyses provide insight into which bacterial functions are diverse and

may contribute to variability in symbiotic interactions. Finally, I provide an in-depth analysis of the incompatible relationship between *S. feltiae* nematodes and the symbionts of *S. intermedium* and *S. affine* nematodes, which demonstrates that bacterial symbionts can influence the outcome of host competition. In total, these experiments define features of the *X. bovienii* bacterial strain – *Steinernema* spp. association to begin to answer basic biological questions about broad host-range symbiosis, such as the impact of interactions on the ecology of organisms and the maintenance of associations through evolutionary time. Additionally, the described characterizations will enable the use of the system as a model for future experimentation to understand broad host-range symbioses.

ACKNOWLEDGMENTS

I would first and foremost like to thank my thesis advisor Dr. Heidi Goodrich-Blair for providing a rich scientific environment that has enabled me to grow as a scientist. I am deeply grateful for the opportunities that she has given me and her continued outstanding mentorship. Heidi has given me the best guidance and “cheerleading” that I could ask for, and I would like to thank her for it. Working with her has truly been a pleasure, and I know that I am a better scientist because of it.

I also would like to thank all of the lab mates, undergraduates, and collaborators that I’ve worked with throughout the years for their scientific support. It has been great to bounce ideas around with them, and they have given me some wonderful advice. I would like to specifically thank Jonathan Klassen for his help with bioinformatics. I also wish to particularly thank my current office-mates Mengyi Cao, Ángel Cassanova-Torres, and Terra Mauer for their encouragement during the thesis writing process.

Additionally, I would like to thank all of my friends and family for their continued encouragement and support throughout my graduate school career. Having them to lean on has made this a better experience for me. In particular I would like to thank my husband Joe for his understanding, love, and support. I am so glad that we went through this together.

Thank you all for everything that you have done to support me in this endeavor.

Sincerely,

Kristen

TABLE OF CONTENTS

Abstract	i
Acknowledgements	iii
Table of Contents	iv
List of Figures	ix
List of Tables	xiii
Chapter 1 Introduction and literature review	1
Abstract	2
Symbiosis and mutualism	3
Broad host-range mutualistic associations	4
Entomopathogenic nematode – bacterial associations	6
“Omics” as a tool for studying EPN – bacterial mutualisms	7
<i>X. bovienii</i> strains – <i>Steinernema</i> spp. nematodes as a model of broad host-range associations	12
Conclusions	15
Thesis Plan	17
References	19
Chapter 2 <i>Xenorhabdus bovienii</i> interactions with <i>Steinernema</i> spp. nematodes ...	26
Abstract	27
Introduction	28
Results	32
Conclusions	43

Acknowledgements	46
Materials and Methods	47
References	50
Chapter 3 <i>Xenorhabdus bovienii</i> bacterial strain diversity impacts coevolution and symbiotic maintenance with <i>Steinernema spp.</i> nematode hosts	54
Abstract	55
Importance	56
Introduction	57
Results	59
Conclusions	71
Acknowledgements	76
Materials and Methods	77
References	82
Supplemental Materials	87
Chapter 4 Comparison of <i>Xenorhabdus bovienii</i> bacterial strain genomes reveals diversity in secondary metabolites and symbiotic functions.	99
Abstract	100
Introduction	102
Results and Discussion	104
Conclusions	127
Author Contributions	129
Acknowledgements	129

Materials and Methods	130
References	133
Supplemental Materials	142

Chapter 5 *Xenorhabdus bovienii* symbionts provide an advantage to their

Steinernema affine nematode hosts by killing competitor *Steinernema feltiae*

nematodes	155
Abstract	156
Introduction	157
Results	161
Conclusions	172
Acknowledgements	175
Materials and Methods	176
References	182
Supplemental Materials	185

Chapter 6 Conclusion and future directions: *Xenorhabdus bovienii* bacteria –

<i>Steinernema</i> species associations as a model of broad host range symbioses	189
Introduction	190
Development of the <i>X. bovienii</i> – <i>Steinernema</i> spp. system model	191
Principles of broad-host range symbiosis determined using the <i>X. bovienii</i> –	
<i>Steinernema</i> spp. model system	197
Future directions	201
Conclusions	204

References	205
Appendix 1 Identification of bacterial colonization in nematodes using florescent	
microscopy	211
Abstract	212
Protocol Text	214
Representative Results	223
Figures	224
Conclusions	229
Acknowledgements	232
References	233
Appendix 2 Phenotypic variation and host interactions of <i>Xenorhabdus bovienii</i> SS-	
2004, the entomopathogenic symbiont of <i>Steinernema jolietii</i> nematodes	235
Abstract	236
Introduction	237
Results and Discussion	241
Conclusions	257
Acknowledgements	259
Materials and Methods	260
References	266
Appendix 3 Previously unrecognized stages of species-specific colonization in the	
<i>Xenorhabdus-Steinernema</i> mutualism	273

Abstract274
Introduction275
Results279
Conclusions297
Acknowledgements302
Materials and Methods303
References309

Appendix 4 The CRISPR/cas system of *Xenorhabdus nematophila* contributes to

colonization of symbiotic host nematodes	313
Abstract314
Introduction315
Results319
Conclusions339
Acknowledgements342
Materials and Methods344
References354
Supplemental Materials361

LIST OF FIGURES

Chapter 1

- Figure 1.1 EPN-bacteria lifecycle in insect host8
- Figure 1.2 *Steinernema* sp. Nematode hosts of *X. bovienii*14

Chapter 2

- Figure 2.1 *Steinernema* nematode and *Xenorhabdus* bacteria life cycle29
- Figure 2.2 Morphological differences in primary and secondary form *X. bovienii* . . 34
- Figure 2.3 Phenotypic variation affects progeny IJ development36
- Figure 2.4 Colonization percentage of *Steinernema* nematode hosts by *X. bovienii* strains in various nutritional conditions38
- Figure 2.5 Colonization of *S. feltiae* life stages 40
- Figure 2.6 Progression of colonization in *S. feltiae* life cycle42

Chapter 3

- Figure 3.1 *X. bovienii* bacteria – *Steinernema* nematode – *Galleria mellonella* insect interactions 58
- Figure 3.2 Co-phylogeny of nematode spp. hosts and bacterial symbiont strains . .61
- Figure 3.3 Measurement of mutualist interaction parameters 64
- Figure 3.4 Nematode and bacterial combinations show measurements consistent with co-adaptation68
- Figure 3.5 Contribution of increased benefits in maintenance of symbiosis 73
- Figure 3.S1 Bayesian distance phylogenies88
- Figure 3.S2 Schematic diagram of mutualistic testing 89
- Figure 3.S3 Possible causes of progeny infective fitness defects 90

Figure 3.S4	Heatmap of overrepresented and underrepresented genes	91
Chapter 4		
Figure 4.1	<i>Xenorhabdus</i> bacteria and <i>Steinernema</i> nematode life cycle	103
Figure 4.2	Genome synteny between finished and draft <i>X. bovienii</i> genomes . . .	107
Figure 4.3	Annotated toxin genes in <i>X. bovienii</i> genomes	114
Figure 4.4	Tc toxin protein phylogenetic analyses	122
Figure 4.S1	Distribution of amino acid sequence divergence in proteins	153
Figure 4.S2	Phylogenies of partitioned nucleic acid sequence	154
Chapter 5		
Figure 5.1	<i>Steinernema</i> nematodes and <i>Xenorhabdus</i> bacteria lifecycle	158
Figure 5.2	<i>S. feltiae</i> and <i>S. affine</i> competition experiments	164
Figure 5.3	Xb-Sa kills <i>S. feltiae</i> nematodes rather than inhibiting development . .	167
Figure 5.4	Xb-Sa killing of <i>S. feltiae</i> is infection mediated	170
Figure 5.5	<i>S. feltiae</i> nematodes have narrowed intestines when exposed to Xb-Sa	173
Figure 5.S1	Natural superinfections	185
Figure 5.S2	Superinfection of cadavers by <i>S. feltiae</i> nematodes	186
Figure 5.S3	Xb-Sa also localizes to <i>S. feltiae</i> nematode eggs	187
Chapter 6		
Figure 6.1	Nematode and bacterial life cycle	193
Appendix 1		
Figure A1.1	Schematic outline of the experiment	224
Figure A1.2	Depiction of adult females containing eggs	225
Figure A1.3	Example microscope images of nematode-bacterial association	226

Appendix 2

Figure A2.1	Colony and cell morphology of <i>X. bovienii</i> primary and secondary variants	242
Figure A2.2	<i>S. carpocapsae</i> (A-B) and <i>S. jolietii</i> (C-F) intestinal receptacle	244
Figure A2.3	<i>X. bovienii</i> colonization frequency	247
Figure A2.4	Nematode-infected <i>G. mellonella</i> with primary form, but not secondary form <i>X. bovienii</i> produce infective juveniles and are flaccid and liquefied	251
Figure A2.5	<i>X. bovienii</i> virulence in <i>M. sexta</i> larvae	254

Appendix 3

Figure A3.1	Model for nematode reproduction	276
Figure A3.2	<i>X. nematophila</i> bacteria localize specifically to the anterior intestinal caecum (AIC) in adult and juvenile <i>S. carpocapsae</i> nematodes	280
Figure A3.3	Bacterial colonization and intestinal constriction of nematode pre-IJ stages	283
Figure A3.4	<i>X. nematophila</i> requires SR1 for localization to the AIC and PIV	288
Figure A3.5	<i>X. nematophila</i> SR1 confers upon <i>X. szentirmaii</i> the ability to colonize the AIC and PIV of <i>S. carpocapsae</i> nematodes	291
Figure A3.6	Spatial and temporal events in the <i>X. nematophila</i> / <i>S. carpocapsae</i> association are observed in the association between <i>X. bovienii</i> and <i>S.</i> <i>feltiae</i>	294
Figure A3.7	Spatial and temporal bacterial colonization events during <i>Steinernema</i> development	299

Appendix 4

Figure A4.1	Schematic representation of the <i>niID</i> CRISPR locus	316
-------------	--	-----

Figure A4.2	Wild type, but not mutant <i>niID</i> provided in trans complements the colonization defect of the <i>niID6::Tn5</i> mutant325
Figure A4.3	The <i>niID</i> locus of <i>X. nematophila</i> encodes a small RNA328
Figure A4.4	<i>cas6e</i> is necessary for presence of CRISPR RNA, but not for NiID RNA or colonization of <i>S. carpocapsae</i> nematodes	331
Figure A4.5	<i>cas6e</i> is necessary for colonization in the <i>niID6::Tn5 attTn7::Tn7/niID</i> background334
Figure A4.S1	Deletion analysis of the <i>niID</i> region indicates neither <i>orf1</i> nor <i>orf2</i> is required in its entirety to rescue the colonization defect of the <i>niID6::Tn5</i> mutant in plasmid complementation assays361
Figure A4.S2362
Figure A4.S3364

LIST OF TABLES

Chapter 2

Table 2.1	Bacterial strains and plasmids used in this study	33
-----------	---	----

Chapter 3

Table 3.S1	Bacterial strains and nematode host species used in this study.	93
------------	---	----

Table 3.S2	Average nucleotide identity of <i>X. bovienii</i> strains used in these experiments94
------------	---	-----

Table 3.S3	Unique genomic content differences between <i>X. bovienii</i> strains.	95
------------	--	----

Table 3.S4	Virulence of <i>S. feltiae</i> nematodes alone and <i>X. bovienii</i> co-injections. . .	96
------------	--	----

Table 3.S5	Table of statistical analysis of linear regression analyses of data shown in Table 3.S4, Figure 3.3, and Figure 3.4 relative to bacterial phylogenetic distance97
------------	---	-----

Table 3.S6	Cook's distance of native symbiont clade average point derived from linear regression analyses of parameters from Table 3.S5 and Figure 3.398
------------	---	-----

Chapter 4

Table 4.1	<i>Xenorhabdus bovienii</i> genomes used in this study	105
-----------	--	-----

Table 4.2	Phenotypes of <i>X. bovienii</i> bacterial strains	110
-----------	--	-----

Table 4.3	NRPS and PKS clusters	126
-----------	---------------------------------	-----

Table 4.S1	Secretion system genes	142
------------	----------------------------------	-----

Table 4.S2	Bacterial genes predicted to encode select symbiotic activities	136
------------	---	-----

Table 4.S3	Regulatory proteins found within <i>X. bovienii</i> strains	145
------------	---	-----

Table 4.S4	<i>X. bovienii</i> genes predicted to encode LysR family transcription factors	146
------------	--	-----

Table 4.S5	<i>X. bovienii</i> genes predicted to encode two-component regulatory systems	147
Table 4.S6	Annotated toxin genes	149
Table 4.S7	Best BlastP hits of Xb-Si putative Shiga toxin	150
Table 4.S8	Tc subunit genes from <i>X. bovienii</i> genomes	151
Chapter 5		
Table 5.1	Bacterial strains and plasmids used in this study	160
Table 5.2	Development of <i>S. feltiae</i> nematodes on <i>X. bovienii</i> bacterial strains .	162
Table S1	Testing of pre-conditioned media for adult nematode survival	186
Appendix 1		
Table A1.1	Example scoring of a nematode population for bacterial presence . . .	227
Table A1.2	Fluorescent protein containing plasmids	228
Appendix 2		
Table A2.1	Strains and plasmids used in this study	240
Table A2.2	Fluorescent protein containing plasmids	242
Table A2.3	Toxicity of <i>X. bovienii</i> concentrated protein samples against selected insect pests of plants	256
Appendix 3		
Table A3.1	Composite <i>S. carpocapsae</i> colonization data	286
Table A3.2	Composite frequency of <i>X. bovienii</i> tissue localization in <i>S. feltiae</i> . . .	296
Table A3.3	Bacterial strains and plasmids used in this study	304
Appendix 4		
Table A4.1	Strains and plasmids used in this study	323
Table A4.2	A <i>nilD::kan</i> mutation does not confer a colonization defect in the HGB081 and HGB800 backgrounds	333

Table A4.3	<i>nilD</i> is required for <i>X. nematophila</i> colonization of <i>S. anatoliense</i> and <i>S. websteri</i> nematodes	337
Table A4.S1	Regions of genome differences between XnSc 081 and XnSc 800 . . .	365
Table A4.S2	CRISPR loci of <i>X. nematophila</i> (HGB800) designated alphabetically according to their chromosomal position	367
Table A4.S3	Colonization analysis of HGB315 (<i>nilD6::Tn5</i>) carrying SR2 deletion constructs	368
Table A4.S4	Oligonucleotides used in this study	369

CHAPTER 1

Introduction and literature review

Sections of this work have been published as:

Murfin KE, Dillman AR, Foster JM, Bulgheresi S, Slatko BE, Sternberg PW, and Goodrich-Blair H. "Nematode-Bacterium Symbioses - Cooperation and Conflict Revealed in the 'Omics' Age." Biol Bull. 2012 Aug; 223(1):85-102.

ABSTRACT

Beneficial symbiotic associations between microbial symbionts and host plants or animals are diverse and occur within all trophic levels and ecosystems. As such, they are integrally important to our understanding in many scientific areas, such as ecology, evolution, and health. Beneficial symbiosis can be specific associations, where one symbiont species associates with one host species, but quite often, beneficial symbioses are generalist in nature, where at least one of the partners can associate with several different partner species. This is frequently the case in symbioses involving bacterial partners, where a bacterial symbiont species has the ability to associate with several different plant or animal host species. In this chapter, the diversity of microbial symbioses is described with emphasis on broad interactions. Specific focus is also given to the potential for utilizing the association between *Xenorhabdus bovienii* bacterial symbionts and their *Steinernema* spp. nematode hosts as a model for broad interactions.

SYMBIOSIS AND MUTUALISM

Symbioses, the intimate living together of two or more unlike organisms, is a widespread phenomenon that occurs across all trophic levels in all ecosystems, and as such, symbioses are integrally important to ecosystem dynamics (1), evolution (2), and health of the symbiotic partners (3-5). Symbioses can range from mutually beneficial associations (i.e. mutualisms) to interactions that are harmful towards one partner (i.e. parasitism). Perhaps the most prominent symbioses involve microbial symbionts due to microbial abundance. Mutualisms between microbial symbionts and host plants or animals are complex and diverse, often involving the exchange of many different goods and services.

Many microbial mutualisms are nutritionally based, where one or both partners produce nutrients in exchange for different nutrients or other goods and services. For example, within the interaction between *Rhizobium* bacteria and legume plants, the plant host provides a carbon source to the bacterial symbiont in exchange for fixed nitrogen from the bacterium (6). Common nutrients exchanged in mutualism are vitamins (7, 8), amino acids (9, 10), energy sources (e.g. carbon) (11-13), and nitrogen (6, 10, 14-17). In some of these associations, the exchange of nutrients is through direct transfer of metabolites, as in nitrogen fixation by plant mutualistic bacteria (6, 10, 15-17). However, in other systems, symbionts contribute to host nutrition through direct degradation of food substrates, thereby increasing their bioavailability for the host. For example, within the termite-intestinal microbiota mutualism, the termites consume woody plant material that is broken down by the symbiotic microorganisms that reside within the termite digestive tract, and this digestion releases nutrients for both the host and symbionts (13). It was recently discovered that nutritional mutualisms can also be a hybrid of these two approaches, as is the case in wood-consuming bivalve, *Bankia setacea*, that has gill-associated bacterial symbionts (18). The gill-associated symbionts produce enzymes that are transported to the bivalve's cecum for digestion of wood consumed by the host (12).

Another common function in symbioses is defense of the symbiont, host, or both from predators, pathogens, or competitors. It is likely that hosts almost always have a defensive role through providing a protected niche for the symbiont. Additionally, the symbiont can provide protection to the host through the production of compounds, such as toxins or antibiotics, that kill or deter competing organisms. For example, some secondary symbionts of aphids produce toxins that provide protection from parasitoid wasps that lay eggs in the aphid host (19). These toxins kill the developing wasp and allow the aphid to survive. Host protection by symbionts likely also occurs through the microbe filling a niche and competitively excluding other microbes, including potential pathogens, as is proposed for certain animal – microbiota associations (20). Symbionts also have been linked to other roles that may directly or indirectly provide defensive benefits, such as influencing development at a variety of stages (4, 21), educating and modulating the immune system (22), and altering animal behavior (4, 23).

In addition to nutrition and defense, other less common goods or services can be exchanged between hosts and symbionts. Alternate goods and services include benefits such as transport through sulfide gradients (24), water filtering (25), and heat tolerance (26). In all of these examples, the good or service provided is specific to the needs of the symbiont or host due to a particular life cycle feature.

BROAD HOST-RANGE MUTUALISTIC ASSOCIATIONS

Many different mutualistic associations have been studied as individual host-symbiont pairs to investigate details of interactions between one symbiont and one host. For example, the interactions between *Steinernema carpocapsae* nematodes and *Xenorhabdus nematophila* bacteria have been studied to understand bacterial mechanisms of host tissue colonization (27, 28) and defensive symbiosis (29, 30). Additionally, investigations of interactions between *Vibrio fischeri* bacteria and *Euprymna scolopes* squid have resulted in detailed knowledge of host

detection of and physiological changes in response to specific bacterial signals (31, 32). These findings on representative pairs are helping reveal general paradigms applicable to many other symbioses (33, 34), including those that are more complex and difficult to study (35).

Although there is much value in investigating detailed mechanisms by which individual pairs associate with each other, many mutualisms, including those developed for study, are actually generalist associations. In mutualism, associations may be specialist (one host and one symbiont) or generalist (host and/or symbiont may associate with several potential partners). This can be true in both binary associations (only one host and one symbiont associate at a time) and in a microbial consortium (the host has multiple microbial constituents that fill different niches). Perhaps the most common of the generalist associations are those where the symbiont species is able to associate with several host species or genera (e.g. broad-host range mutualisms). For instance, many of the plant-associated nitrogen-fixing bacterial species (e.g. *Bradyrhizobium* and *Rhizobium*) can associate with several different host genera and species (6, 16, 17, 36). This also occurs among animal symbioses, such as in the previously mentioned squid-*Vibrio* system (37). Additionally, broad host-range associations occur between *Symbiodinium* dinoflagellate species with coral reef invertebrates, where the *Symbiodinium* symbiont provides energy through photosynthesis to the invertebrate host (38). Similarly, the intestinal bacterium *Bifidobacterium pseudolongum* subsp. *globosum* can associate with bovine, cheetah, and canine hosts, and other *Bifidobacterium* spp. also associate with a variety of hosts (39, 40).

Studies on broad host-range interactions are beginning to elucidate how microbial diversity in symbiont species can affect mutualistic activities and their specificity with different hosts. Bacterial strains within a species, including those associated with hosts (15, 41, 42), have a large genetic diversity that likely causes differences in bacterial function and the ability to engage in symbiosis with different partners. Indeed in the mutualism between squid and their *V.*

fischeri symbionts, diversity in bacterial genes involved in host colonization impacts competitive colonization of the squid by native *V. fischeri* bacterial strains (43). Additionally genetic diversity impacts the ability of *Rhizobium* bacteria to interact with legume hosts (44, 45). Because broad host-range associations are likely common, understanding their function and stability within the context of multiple potential partners will be integral to our understanding of host-microbe mutualisms. Remaining questions about broad host-range associations include understanding how symbiont isolate diversity impacts host health, if symbiont isolates are maintained with specific hosts, how symbiotic maintenance occurs, and how coevolution and coadaptation between diverse host and symbiont isolates impacts specificity in symbiosis. For study of these questions, there are many mutualistic associations that would be feasible to utilize, such as the mutualisms that occur between entomopathogenic (i.e. insect-parasitizing) nematodes and their bacterial symbionts.

ENTOMOPATHOGENIC NEMATODE – BACTERIAL ASSOCIATIONS

At least two genera of entomopathogenic nematodes (EPNs), *Steinernema* and *Heterorhabditis*, have evolved binary mutualistic associations with gammaproteobacteria, *Xenorhabdus* and *Photorhabdus* respectively, that allow them to kill insects and utilize the cadavers as food sources (46). Within these associations, a vast majority of the partnerships are broad host-range in nature and therefore represents an excellent resource for understanding broad host-range mutualism. Within the *Photorhabdus* genus there are three species recognized: *P. temperata*, *P. luminescens*, and *P. asymbiotica*. The last was isolated originally from human wounds, but recently was discovered to colonize, like the other species, a heterorhabditid nematode host, of which there are 18 recognized species (47, 48). In contrast, there are 22 species of *Xenorhabdus* (49, 50) that colonize one or more of the >70 known species of *Steinernema* nematodes (47, 48).

In EPN – bacterial associations, the partners engage in symbiosis that allows them to complete a parasitic life cycle within an insect host (Figure 1.1). Within the environment, a specialized infective stage of EPNs carries a population of the symbiont within the intestine, and releases them upon invasion of an insect host. There, the bacteria contribute to killing the insect, help degrade the insect cadaver for nutrients, and protect the cadaver from opportunists. Once the insect resources are consumed, the EPN progeny nematodes develop into the colonized infective stage and emerge to hunt for a new insect host (51, 52). In EPN associations, the bacteria and nematodes can be cultivated independently or together, and molecular genetic techniques are available for the bacteria and, in some cases, for the nematodes (51, 53, 54). This technical tractability has enabled the use of EPNs and bacteria as models of mutualism, virulence, evolution, behavior, ecology, and drug discovery (51, 55-61). Furthermore, since these nematode-bacterium complexes are pathogenic toward a wide but varying range of insects, an additional goal in studying EPNs is improving their use in biological control of insect pests (62). In particular, investigators have focused on identifying nematode traits associated with host range and successful parasitism to help improve the field efficacy of EPNs, and on identifying products of the entomopathogenic bacteria with insecticidal properties, efforts facilitated by sequencing of both bacterial and nematode genomes (63-66).

“OMICS” AS A TOOL FOR STUDYING EPN – BACTERIAL MUTUALISMS

The advent of “omics” techniques (e.g. genomics, transcriptomics, proteomics) has greatly furthered our understanding of many mutualisms, such as microbiota communities (39, 41, 67). This is also true within EPN – bacterial associations. Genomics and transcriptomics of bacterial symbionts have furthered our understanding of differences among binary symbiotic associations and differences in bacterial species, such as coding potential and mechanisms of

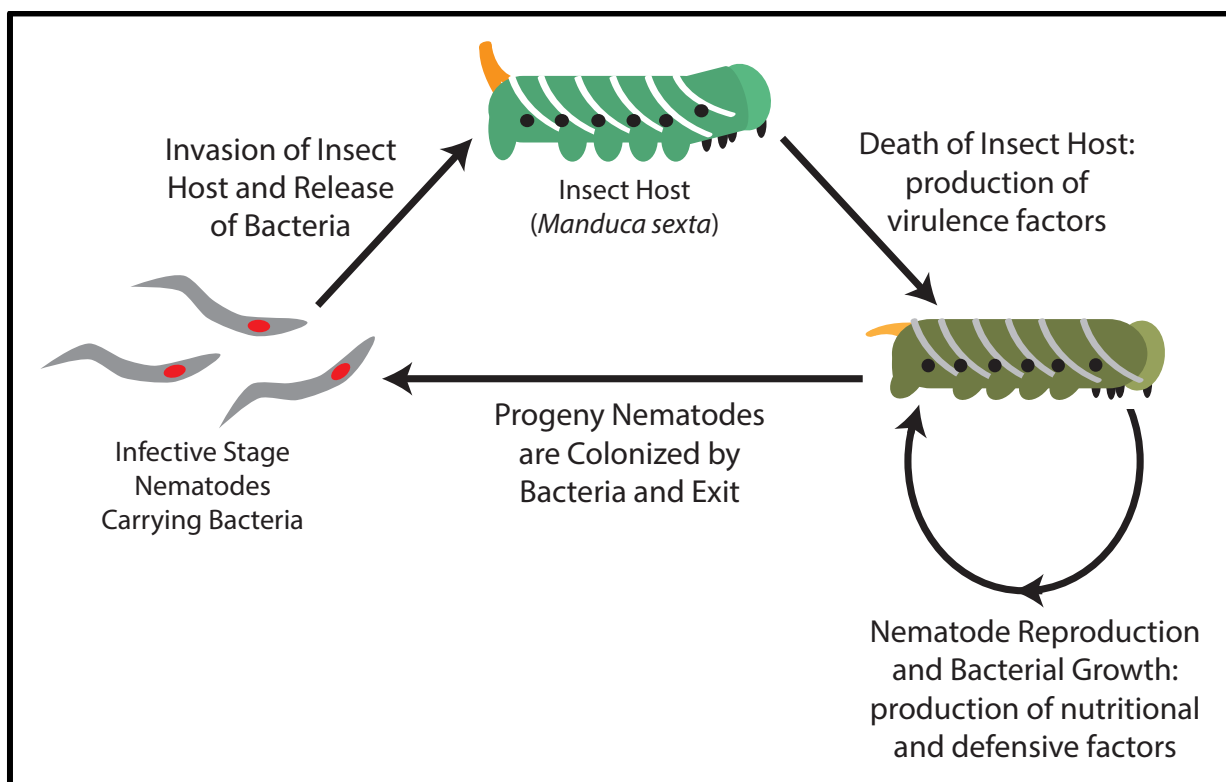


Figure 1.1 EPN-bacteria lifecycle in insect host. The schematic depicts the lifecycle of EPN nematodes (grey) with their bacterial symbionts (red) in an insect host (green). Environmental stage nematodes carry the bacterial symbiont in a specialized portion of their intestine and seek out insect hosts in the soil. The nematodes then infect the insect host and release the bacterial symbiont into the insect's blood cavity. The nematodes and bacteria then produce virulence factors and kill the insect host. The nematodes and bacteria then grow and reproduce inside the insect cadaver. During growth, the bacteria produce factors that provide nutrients, likely through degrading insect tissue, and that protect the cadaver environment from competitor microbes and scavenging insects. Once nutrients are depleted, the nematodes and bacteria re-associate into environmental stage nematodes and exit the insect cadaver.

interacting with both the nematode and insect host. Additionally this work has demonstrated several conserved phenomena that may be generally applicable to EPN associations.

Photorhabdus and *Xenorhabdus* bacteria are closely related to each other phylogenetically, and both infect a similar range of insect hosts, but each associates with an EPN from a different clade (68). Both bacteria make similar symbiotic contributions to the fitness of their nematode hosts: helping establish infection in insects, defending the insect host from predators and competitors, and promoting normal nematode development (69). However, comparative analyses of the four sequenced bacterial genomes (*P. luminescens*, *P. asymbiotica*, *X. nematophila*, and *X. bovienii*) (64, 65) revealed these similar fitness traits are the product of convergent evolution (63). For example, each symbiont limits the growth of competitor microbes, but does so through the production of different types of antimicrobial compounds (63). In contrast, the genes involved in entomopathogenicity, such as those encoding insecticidal toxins, appear to be conserved among the four bacterial species. Based on the apparent convergent evolution of genes involved in nematode-association and conservation of those involved in insect virulence, this study also predicted which bacterial genes may be involved in either of these symbiotic behaviors (63). The analysis was based on the idea that genes present in both *Xenorhabdus* and *Photorhabdus* but absent in non-insect pathogens may be enriched for those that encode activities necessary for killing and digesting insects. Similarly, genes that are unique to either *Xenorhabdus* or *Photorhabdus* should be enriched for those that are necessary for interactions with the nematode host. The study found 243 *X. nematophila* genes common to *Xenorhabdus* and *Photorhabdus* but absent in non-insect pathogens, including many with predicted roles in pathogenesis, and 290 genes specific to *Xenorhabdus*. Perhaps not surprisingly, genes of unknown function predominate in the latter "nematode host interaction" category, suggesting that bacterial genes involved in nematode

interactions remain to be functionally characterized (63). Further application of proteomic and "panning" approaches would be useful for exploring this set of potential host-interaction genes.

In addition to comparative genome approaches, genome sequencing of EPN symbionts facilitated genetic screens that lent insights into the biology involved in host-microbe interactions. As with all mutualistic symbiotic associations a key component of the EPN-bacterium symbiosis is transmission of the bacterial symbiont to the next generation. In EPNs this occurs by bacterial colonization of the intestines of progeny infective juveniles and carriage to the next insect host. Bacterial colonization of the infective juvenile stage can be highly selective, such that in some EPN-bacterium associations only one species of bacterium is capable of colonizing a particular species of nematode (51, 53). Transposon mutagenesis screens in both *X. nematophila* and *P. luminescens* have revealed novel genes involved in this specificity (28, 70, 71). In one study, nine *X. nematophila* genes essential for normal colonization of the infective stage of *S. carpocapsae* nematodes were identified. Three of these genes, *nilA*, *B*, and *C*, are encoded together on a 3.5-kb locus (28). Further study revealed that this locus is not present in other *Xenorhabdus* bacterial symbionts and is sufficient to confer colonization of *S. carpocapsae* on naturally non-colonizing bacteria, establishing for the first time a genetic element conferring host range expansion in an animal-bacterial association (72). *nilB* is similar to genes found in animal associated microbes, including mucosal pathogens (28, 73), supporting the idea that common molecules or mechanisms maintain many host-bacterial interactions regardless of whether the outcome of the interaction is mutualistic or pathogenic (74). The function of NilB, a surface exposed outer membrane protein (73) remains unclear, but analysis of the EPN symbiont genome sequences has provided some clues. Relaxed search parameters revealed that each of the four sequenced genomes of EPN symbionts, including *X. nematophila* itself, encodes a NilB-like protein in a conserved genomic context. Adjacent genes are predicted to encode TonB-like transporters and TonB-dependent receptors, involved in

metabolite transport across the membrane. This finding leads to the hypothesis that NilB and NilB-like proteins may be involved in transport of a class of molecules that varies among different nematode hosts, allowing their function to dictate host range specificity (73). Alternatively, the NilB-like orthologs may play a role in other aspects of the EPN symbiont biology, such as insect virulence.

Consistent with the latter hypothesis, screens for *P. luminescens* mutants defective in colonizing their nematode host *H. bacteriophora* did not reveal the NilB-like ortholog, nor any of the other colonization genes identified in *X. nematophila* (28, 70, 71). This finding further supports the convergent abilities of *Xenorhabdus* and *Photorhabdus* to mutualistically associate with their respective nematodes (63). Putative *P. luminescens* nematode colonization genes revealed by mutant screens include those involved in lipopolysaccharide metabolism, fimbriae biosynthesis, and regulation (70, 71). Subsequent microarray work established that the colonization gene *hdfR* encodes a transcription factor that regulates more than 100 genes, including many involved in metabolic processes. Nematodes co-cultivated with the *hdfR* mutant display a developmental lag, suggesting that *hdfR* is required for normal nematode development (75). As the roles of bacteria in EPN development are elucidated, it will be particularly interesting to compare these findings among host-symbiont pairs to determine if common themes are revealed.

Another avenue toward elucidating the molecular dynamics of nematode-bacterium mutualism is identification of genes that are expressed specifically during association. Such an approach has been applied to *P. luminescens* and *P. temperata*. Using selective capture of transcribed sequences (SCOTS), 106 *P. temperata* transcripts were identified to have altered levels when cells were grown in liquid culture versus colonizing the nematode host (76). The authors identified genes involved in cell surface structure, regulation, stress response, nucleic acid modification, transport, and metabolism, and found that half of the transcriptional changes

overlap with that of the bacterial starvation response (76). This overlap as well as the metabolic shifts that occur in sugar metabolism and amino acid biosynthesis indicate that it is likely that the nematode is a nutrient poor environment.

These studies have revealed several key interactions that are common within nematode – bacterial interactions, such as specificity of colonization events. However, they also highlight that while the themes are common, the molecular mechanisms underlying them are likely specific to the system, as in diversity of genetic factors that facilitate colonization. These features are likely to be diverse among different species pairs. However it is unclear if the genetic mechanisms would be conserved in broad host range nematode bacterial associations, as genomic and functional analyses have only been done on specific binary partner pairs.

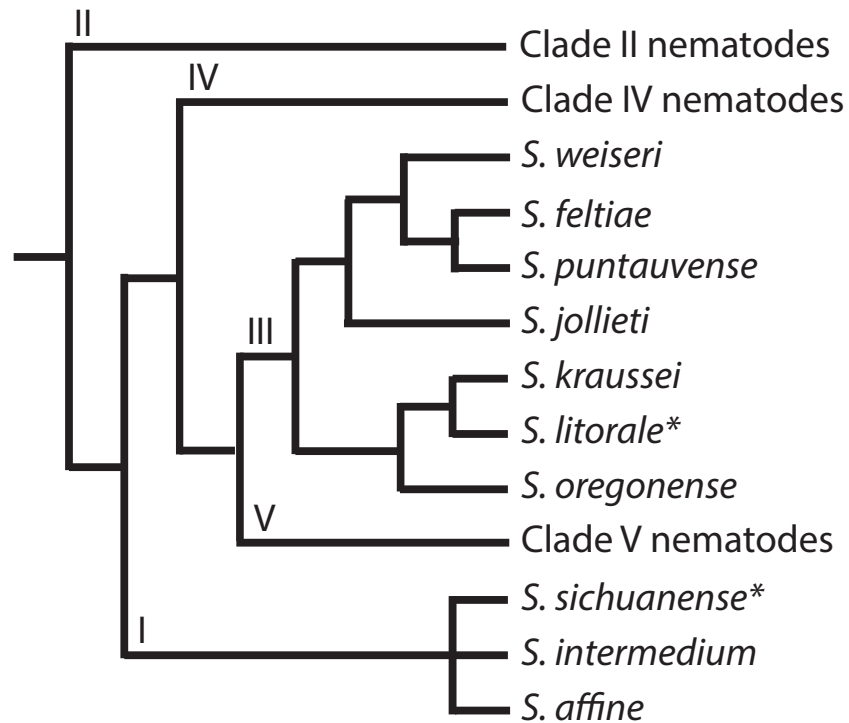
***X. BOVIENII* BACTERIAL STRAINS – *STEINERNEMA* SPP. NEMATODES AS A MODEL OF BROAD-HOST RANGE ASSOCIATIONS**

The work described above mainly focused on binary interactions between individual species of EPNs and bacterial symbionts. The extensive knowledge of mutualism specificity and partner contributions within EPN associations and their experimental tractability make them particularly attractive for development to understand broad host-range mutualism. Of the *Steinernema* nematode-bacterial pairings, *X. bovienii* is the most promiscuous, associating with at least 10 *Steinernema* nematode species from two distinct clades (Figure 1.2) and as such lends itself to investigations of the questions as outlined in the previous section.

Previous work on *X. bovienii* – *Steinernema* spp. associations has shown that it is an obligate mutualism, in that the bacterial symbiont is necessary for nematode development within the insect and the bacteria can only be transmitted by the nematode vector (77, 78). For example, *S. feltiae* nematodes and their *X. bovienii* bacterial symbiont both contribute to virulence towards the insect host (78, 79). Also, examination of individual *X. bovienii* bacterial

strain virulence revealed diversity of insecticidal activities, which may reflect a varied natural insect host range (80, 81). Additionally, a potential defensive role has been identified for the bacterial symbiont. *X. bovienii* produces several effective antimicrobials and a bacteriocin that can protect the host and symbiont from competitor or pathogenic microbes within the insect cadaver (82-84).

Figure 1.2



***Steinerinema* sp. nematode hosts of *X. bovienii*.** The phylogenetic tree shows the clades of *Steinerinema* nematodes and names the hosts known to carry *X. bovienii* bacterial strains.

Roman numerals indicate the nematode clades. The tree is based on a cophylogenetic study by Lee and Stock (68). Nematodes not carrying *X. bovienii* have been omitted and clades with no *X. bovienii* hosts have been collapsed down to one branch. * indicate nematode species not included within the original study but are known to carry *X. bovienii*. The likely placement of these strains within the tree is based on known morphology and comparison of 28s rRNA sequences.

Although many *X. bovienii* – *Steinernema* pairs had been isolated (68, 85), they had not, at the time this thesis work began, been studied at the cellular and molecular level. It was expected that interactions between *X. bovienii* and their nematode hosts would have the same general characteristics as those of other, better studied, *Xenorhabdus* – *Steinernema* associations. However, the specific mechanisms underpinning the interactions, such as the identity of bacterial proteins necessary to colonize host tissues (28), are expected to differ from other *Xenorhabdus* species. Diversity among the *X. bovienii* strains in these features that will impact their ability to engage with different nematode host species was also expected. At the start of this work, such analyses had not been conducted, nor had the impact of bacterial strain diversity on mutualistic interactions and their stability been investigated.

CONCLUSIONS

Broad mutualistic associations are common within natural environments and are represented within all trophic levels and among diverse environments. As bacteria that associate with hosts are genetically diverse, it is likely that they vary in mutualistic functions and their ability to interact with hosts. Diversity in benefits may influence how symbioses are maintained and competition between different partner pairs. Such information will likely prove to be important in many ecological and evolutionary areas, such as in preservation of coral reefs. For example, it is likely that the *Symbiodinium* variations are linked to more or less tolerance for temperature changes, which may prove to be useful for reef restoration (38). Additionally, information on broad host-range symbioses will provide insights into basic functions and stabilities of symbioses, such as the maintenance of particular partner pairs. Characterization of *X. bovienii* – *Steinernema* spp. associations in a directly comparable way will facilitate the utilization of this system as a model for understanding fundamental principles underlying the evolution, maintenance and ecology of broad mutualistic associations, such as those mentioned above. As both experimental and “omics” approaches have been shown to be highly effective in studying the interactions between EPNs and their bacterial symbionts, integration of both approaches will likely be effective in defining these associations.

THESIS PLAN

Broad mutualistic associations are wide-spread and fundamentally important to our understanding of symbiotic maintenance, evolution, and ecology. However, there exists a gap in our knowledge regarding mechanistic functions that enable and stabilize these associations. For example, it is likely that symbiont factors that facilitate colonization in binary interactions vary among symbiont isolates that associate with different hosts, but it is unclear if the same determinants are diversified or if different determinants are utilized. Towards understanding mechanisms such as these, the association between *X. bovienii* bacteria and *Steinernema* spp. hosts is a candidate model that can be utilized to address fundamental principles regarding symbiotic maintenance and evolution as well as the impact of symbiont diversity on symbiotic interactions. This thesis details the work in developing the *X. bovienii* – *Steinernema* spp. mutualism as a model:

Chapter 2 describes work undertaken to define the general characteristics of the association between *X. bovienii* and their *Steinernema* spp. hosts. Included in this chapter are the characterizations of individual bacterial strains, a description of the process by which *X. bovienii* colonizes a nematode host, and several methods for study of these organisms.

Chapter 3 defines the specificity that occurs between *S. feltiae* nematodes and *X. bovienii* bacterial strain symbionts. This work provides foundational insights into how bacterial symbiont strain diversity can impact success in mutualistic interactions and contribute to symbiotic maintenance.

Chapter 4 details work on comparative genomic analysis of *X. bovienii* bacterial strains to define diversity in potential symbiosis factors among the strains. This work extends the previous

chapter by providing insights into potential mechanisms that could contribute to specificity in symbiosis.

Chapter 5 presents an investigation of the incompatible interaction between *S. feltiae* nematodes and the symbionts of *S. intermedium* and *S. affine* nematodes. The data supports the idea that this incompatibility provides a competitive advantage to a nematode host in establishing a mono-species productive infection in insects.

Chapter 6 summarizes the work from chapters 1-5 and appendices 1-4 to provide a cohesive view of *X. bovienii* – *Steinernema* spp. associations. Additionally, this provides the framework for further use of these interactions as a model for broad mutualism. Also included are potential future directions and uses for this model.

REFERENCES

1. **Saavedra S, Stouffer DB, Uzzi B, Bascompte J.** 2011. Strong contributors to network persistence are the most vulnerable to extinction. *Nature* **478**:233-235.
2. **Weyl EG, Frederickson ME, Yu DW, Pierce NE.** 2010. Economic contract theory tests models of mutualism. *Proc Natl Acad Sci U S A* **107**:15712-15716.
3. **Berg G.** 2009. Plant-microbe interactions promoting plant growth and health: perspectives for controlled use of microorganisms in agriculture. *Appl Microbiol Biotechnol* **84**:11-18.
4. **McFall-Ngai M, Hadfield MG, Bosch TC, Carey HV, Domazet-Lozo T, Douglas AE, Dubilier N, Eberl G, Fukami T, Gilbert SF, Hentschel U, King N, Kjelleberg S, Knoll AH, Kremer N, Mazmanian SK, Metcalf JL, Nealson K, Pierce NE, Rawls JF, Reid A, Ruby EG, Rumpho M, Sanders JG, Tautz D, Wernegreen JJ.** 2013. Animals in a bacterial world, a new imperative for the life sciences. *Proc Natl Acad Sci U S A* **110**:3229-3236.
5. **Nicholson JK, Holmes E, Kinross J, Burcelin R, Gibson G, Jia W, Pettersson S.** 2012. Host-gut microbiota metabolic interactions. *Science* **336**:1262-1267.
6. **Rogel MA, Bustos P, Santamaria RI, Gonzalez V, Romero D, Cevallos MA, Lozano L, Castro-Mondragon J, Martinez-Romero J, Ormeno-Orrillo E, Martinez-Romero E.** 2014. Genomic basis of symbiovar mimosae in *Rhizobium etli*. *BMC Genomics* **15**:575.
7. **Aksoy S.** 2000. Tsetse--A haven for microorganisms. *Parasitol Today* **16**:114-118.
8. **Salem H, Bauer E, Strauss AS, Vogel H, Marz M, Kaltenpoth M.** 2014. Vitamin supplementation by gut symbionts ensures metabolic homeostasis in an insect host. *Proc Biol Sci* **281**.
9. **Douglas AE.** 2006. Phloem-sap feeding by animals: problems and solutions. *J Exp Bot* **57**:747-754.
10. **Prell J, Bourdes A, Kumar S, Ludwig E, Hosie A, Kinghorn S, White J, Poole P.** 2010. Role of symbiotic auxotrophy in the *Rhizobium*-legume symbioses. *PLoS One* **5**:e13933.
11. **Aylward FO, Burnum KE, Scott JJ, Suen G, Tringe SG, Adams SM, Barry KW, Nicora CD, Piehowski PD, Purvine SO, Starrett GJ, Goodwin LA, Smith RD, Lipton MS, Currie CR.** 2012. Metagenomic and metaproteomic insights into bacterial communities in leaf-cutter ant fungus gardens. *ISME J* **6**:1688-1701.
12. **O'Connor RM, Fung JM, Sharp KH, Benner JS, McClung C, Cushing S, Lamkin ER, Fomenkov AI, Henrissat B, Londer YY, Scholz MB, Posfai J, Malfatti S, Tringe SG, Woyke T, Malmstrom RR, Coleman-Derr D, Altamia MA, Dedrick S, Kaluziak ST, Haygood MG, Distel DL.** 2014. Gill bacteria enable a novel digestive strategy in a wood-feeding mollusk. *Proc Natl Acad Sci U S A* **111**:E5096-5104.

13. **Brune A.** 2014. Symbiotic digestion of lignocellulose in termite guts. *Nat Rev Microbiol* **12**:168-180.
14. **Ben-Yosef M, Pasternak Z, Jurkevitch E, Yuval B.** 2014. Symbiotic bacteria enable olive flies (*Bactrocera oleae*) to exploit intractable sources of nitrogen. *J Evol Biol* doi:10.1111/jeb.12527.
15. **Galardini M, Mengoni A, Brilli M, Pini F, Fioravanti A, Lucas S, Lapidus A, Cheng JF, Goodwin L, Pitluck S, Land M, Hauser L, Woyke T, Mikhailova N, Ivanova N, Daligault H, Bruce D, Detter C, Tapia R, Han C, Teshima H, Mocali S, Bazzicalupo M, Biondi EG.** 2011. Exploring the symbiotic pangenome of the nitrogen-fixing bacterium *Sinorhizobium meliloti*. *BMC Genomics* **12**:235.
16. **Moulin L, Klonowska A, Caroline B, Booth K, Vriezen JA, Melkonian R, James EK, Young JP, Bena G, Hauser L, Land M, Kyrpides N, Bruce D, Chain P, Copeland A, Pitluck S, Woyke T, Lizotte-Waniewski M, Bristow J, Riley M.** 2014. Complete genome sequence of *Burkholderia phymatum* STM815(T), a broad host range and efficient nitrogen-fixing symbiont of *Mimosa* species. *Stand Genomic Sci* **9**:763-774.
17. **Teamtisong K, Songwattana P, Noisangiam R, Piromyou P, Boonkerd N, Tittabutr P, Minamisawa K, Nantagij A, Okazaki S, Abe M, Uchiumi T, Teaumroong N.** 2014. Divergent nod-containing *Bradyrhizobium* sp. DOA9 with a megaplasmid and its host range. *Microbes Environ.*
18. **Distel DL, Beaudoin DJ, Morrill W.** 2002. Coexistence of multiple proteobacterial endosymbionts in the gills of the wood-boring Bivalve *Lyrodus pedicellatus* (Bivalvia: Teredinidae). *Appl Environ Microbiol* **68**:6292-6299.
19. **Oliver KM, Russell JA, Moran NA, Hunter MS.** 2003. Facultative bacterial symbionts in aphids confer resistance to parasitic wasps. *Proc Natl Acad Sci U S A* **100**:1803-1807.
20. **Reid G, Bruce AW, McGroarty JA, Cheng KJ, Costerton JW.** 1990. Is there a role for lactobacilli in prevention of urogenital and intestinal infections? *Clin Microbiol Rev* **3**:335-344.
21. **Shin SC, Kim SH, You H, Kim B, Kim AC, Lee KA, Yoon JH, Ryu JH, Lee WJ.** 2011. *Drosophila* microbiome modulates host developmental and metabolic homeostasis via insulin signaling. *Science* **334**:670-674.
22. **Kandasamy S, Chattha KS, Vlasova AN, Rajashekara G, Saif LJ.** 2014. Lactobacilli and Bifidobacteria enhance mucosal B cell responses and differentially modulate systemic antibody responses to an oral human rotavirus vaccine in a neonatal gnotobiotic pig disease model. *Gut Microbes* doi:10.4161/19490976.2014.969972:0.
23. **Sharon G, Segal D, Ringo JM, Hefetz A, Zilber-Rosenberg I, Rosenberg E.** 2010. Commensal bacteria play a role in mating preference of *Drosophila melanogaster*. *Proc Natl Acad Sci U S A* **107**:20051-20056.
24. **Ott JA, Novak R, Schiemer F, Hentschel U, Nebelsick M, Polz M.** 1991. Tackling the sulfide gradient: A novel strategy involving marine nematodes and chemoautotrophic ectosymbionts. *Marine Ecology* **12**:261-279.

25. **Tsubaki R, Kato M.** 2014. A novel filtering mutualism between a sponge host and its endosymbiotic bivalves. *PLoS One* **9**:e108885.
26. **Marquez LM, Redman RS, Rodriguez RJ, Roossinck MJ.** 2007. A virus in a fungus in a plant: three-way symbiosis required for thermal tolerance. *Science* **315**:513-515.
27. **Bhasin A, Chaston JM, Goodrich-Blair H.** 2012. Mutational analyses reveal overall topology and functional regions of NilB, a bacterial outer membrane protein required for host association in a model of animal-microbe mutualism. *J Bacteriol* **194**:1763-1776.
28. **Heungens K, Cowles CE, Goodrich-Blair H.** 2002. Identification of *Xenorhabdus nematophila* genes required for mutualistic colonization of *Steinernema carpocapsae* nematodes. *Mol Microbiol* **45**:1337-1353.
29. **Gulcu B, Hazir S, Kaya HK.** 2012. Scavenger deterrent factor (SDF) from symbiotic bacteria of entomopathogenic nematodes. *J Invertebr Pathol* **110**:326-333.
30. **Zhou X, Kaya HK, Heungens K, Goodrich-Blair H.** 2002. Response of ants to a deterrent factor(s) produced by the symbiotic bacteria of entomopathogenic nematodes. *Appl Environ Microbiol* **68**:6202-6209.
31. **Foster JS, Apicella MA, McFall-Ngai MJ.** 2000. *Vibrio fischeri* lipopolysaccharide induces developmental apoptosis, but not complete morphogenesis, of the *Euprymna scolopes* symbiotic light organ. *Dev Biol* **226**:242-254.
32. **Nyholm SV, Stewart JJ, Ruby EG, McFall-Ngai MJ.** 2009. Recognition between symbiotic *Vibrio fischeri* and the haemocytes of *Euprymna scolopes*. *Environ Microbiol* **11**:483-493.
33. **Ghedin E, Hailemariam T, DePasse JV, Zhang X, Oksov Y, Unnasch TR, Lustigman S.** 2009. *Brugia malayi* gene expression in response to the targeting of the *Wolbachia* endosymbiont by tetracycline treatment. *PLoS Negl Trop Dis* **3**:e525.
34. **Hamilton PT, Leong JS, Koop BF, Perlman SJ.** 2014. Transcriptional responses in a *Drosophila* defensive symbiosis. *Mol Ecol* **23**:1558-1570.
35. **Chaston J, Goodrich-Blair H.** 2010. Common trends in mutualism revealed by model associations between invertebrates and bacteria. *FEMS Microbiol Rev* **34**:41-58.
36. **Rogel MA, Ormeno-Orrillo E, Martinez Romero E.** 2011. Symbiovars in rhizobia reflect bacterial adaptation to legumes. *Syst Appl Microbiol* **34**:96-104.
37. **Nishiguchi MK, Nair VS.** 2003. Evolution of symbiosis in the Vibrionaceae: a combined approach using molecules and physiology. *Int J Syst Evol Microbiol* **53**:2019-2026.
38. **Tonk L, Sampayo EM, Weeks S, Magno-Canto M, Hoegh-Guldberg O.** 2013. Host-specific interactions with environmental factors shape the distribution of symbiodinium across the Great Barrier Reef. *PLoS One* **8**:e68533.
39. **D'Aimmo MR, Modesto M, Mattarelli P, Biavati B, Andlid T.** 2014. Biosynthesis and cellular content of folate in bifidobacteria across host species with different diets. *Anaerobe* **30**:169-177.

40. **Lugli GA, Milani C, Turrone F, Duranti S, Ferrario C, Viappiani A, Mancabelli L, Mangifesta M, Taminiu B, Delcenserie V, van Sinderen D, Ventura M.** 2014. Investigation of the evolutionary development of the genus *Bifidobacterium* by comparative genomics. *Appl Environ Microbiol* **80**:6383-6394.
41. **Hansen EE, Lozupone CA, Rey FE, Wu M, Guruge JL, Narra A, Goodfellow J, Zaneveld JR, McDonald DT, Goodrich JA, Heath AC, Knight R, Gordon JI.** 2011. Pan-genome of the dominant human gut-associated archaeon, *Methanobrevibacter smithii*, studied in twins. *Proc Natl Acad Sci U S A* **108 Suppl 1**:4599-4606.
42. **Lee SM, Donaldson GP, Mikulski Z, Boyajian S, Ley K, Mazmanian SK.** 2013. Bacterial colonization factors control specificity and stability of the gut microbiota. *Nature* **501**:426-429.
43. **Chavez-Dozal AA, Gorman C, Lostroh CP, Nishiguchi MK.** 2014. Gene-swapping mediates host specificity among symbiotic bacteria in a beneficial symbiosis. *PLoS One* **9**:e101691.
44. **Heath KD.** 2010. Intergenomic epistasis and coevolutionary constraint in plants and rhizobia. *Evolution* **64**:1446-1458.
45. **Thrall PH, Laine AL, Broadhurst LM, Bagnall DJ, Brockwell J.** 2011. Symbiotic effectiveness of rhizobial mutualists varies in interactions with native Australian legume genera. *PLoS One* **6**:e23545.
46. **Dillman AR, Chaston JM, Adams BJ, Ciche TA, Goodrich-Blair H, Stock SP, Sternberg PW.** 2012. An entomopathogenic nematode by any other name. *PLoS pathogens* **8**:e1002527.
47. **Nguyen KB.** 11/16/11 2010. Morphology and taxonomy of entomopathogenic nematodes. <http://entnem.ifas.ufl.edu/nguyen/morph/namespp.HTM>. Accessed
48. **Stock SP, Goodrich-Blair H.** 2012. Nematode parasites, pathogens and associates of insects and invertebrates of economic importance, p 375-425. *In* Lacey LA (ed), *Manual of Techniques in Invertebrate Pathology*, 2 ed. Elsevier Press.
49. **Tailliez P, Laroui C, Ginibre N, Paule A, Pages S, Boemare N.** 2010. Phylogeny of *Photorhabdus* and *Xenorhabdus* based on universally conserved protein-coding sequences and implications for the taxonomy of these two genera. Proposal of new taxa: *X. vietnamensis* sp. nov., *P. luminescens* subsp. caribbeanensis subsp. nov., *P. luminescens* subsp. hainanensis subsp. nov., *P. temperata* subsp. khanii subsp. nov., *P. temperata* subsp. tasmaniensis subsp. nov., and the reclassification of *P. luminescens* subsp. thracensis as *P. temperata* subsp. thracensis comb. nov. *Int J Syst Evol Microbiol* **60**:1921-1937.
50. **Tailliez P, Pages S, Edgington S, Tymo LM, Buddie AG.** 2011. Description of *Xenorhabdus magdalenensis* sp. nov., the symbiotic bacterium associated with *Steinernema australe*. *Int J Syst Evol Microbiol* doi:10.1099/ijs.0.034322-0.
51. **Clarke DJ.** 2008. *Photorhabdus*: a model for the analysis of pathogenicity and mutualism. *Cellular microbiology* **10**:2159-2167.

52. **Herbert EE, Goodrich-Blair H.** 2007. Friend and foe: the two faces of *Xenorhabdus nematophila*. *Nat Rev Microbiol* **5**:634-646.
53. **Goodrich-Blair H.** 2007. They've got a ticket to ride: *Xenorhabdus nematophila*-*Steinernema carpocapsae* symbiosis. *Current opinion in microbiology* **10**:225-230.
54. **Ciche TA, Sternberg PW.** 2007. Postembryonic RNAi in *Heterorhabditis bacteriophora*: a nematode insect parasite and host for insect pathogenic symbionts. *BMC Dev Biol* **7**:101.
55. **Richards GR, Goodrich-Blair H.** 2009. Masters of conquest and pillage: *Xenorhabdus nematophila* global regulators control transitions from virulence to nutrient acquisition. *Cell Microbiol* **11**:1025-1033.
56. **Eleftherianos I, French-Constant RH, Clarke DJ, Dowling AJ, Reynolds SE.** 2010. Dissecting the immune response to the entomopathogen *Photorhabdus*. *Trends in microbiology* **18**:552-560.
57. **Bashey F, Young SK, Hawlena H, Lively CM.** 2012. Spiteful interactions between sympatric natural isolates of *Xenorhabdus bovienii* benefit kin and reduce virulence. *Journal of evolutionary biology* **25**:431-437.
58. **Bode HB.** 2009. Entomopathogenic bacteria as a source of secondary metabolites. *Curr Opin Chem Biol* **13**:224-230.
59. **Adhikari BN, Lin CY, Bai X, Ciche TA, Grewal PS, Dillman AR, Chaston JM, Shapiro-Ilan DI, Bilgrami AL, Gaugler R, Sternberg PW, Adams BJ.** 2009. Transcriptional profiling of trait deterioration in the insect pathogenic nematode *Heterorhabditis bacteriophora*. *BMC Genomics* **10**:609.
60. **Ram K, Preisser EL, Gruner DS, Strong DR.** 2008. Metapopulation dynamics override local limits on long-term parasite persistence. *Ecol* **89**:3290-3297.
61. **Hallem EA, Dillman AR, Hong AV, Zhang Y, Yano JM, DeMarco SF, Sternberg PW.** 2011. A sensory code for host seeking in parasitic nematodes. *Current biology : CB* **21**:377-383.
62. **Stock SP.** 2004. Insect parasitic nematodes: from lab curiosities into model organisms. *Journal of Invertebrate Pathology* **89**:57-66.
63. **Chaston JM, Suen G, Tucker SL, Andersen AW, Bhasin A, Bode E, Bode HB, Brachmann AO, Cowles CE, Cowles KN, Darby C, de Léon L, Drace K, Du Z, Givaudan A, Herbert Tran EE, Jewell KA, Knack JJ, Krasomil-Osterfeld KC, Kukor R, Lanois A, Latreille P, Leimgruber NK, Lipke CM, Liu R, Lu X, Martens EC, Marri PR, Médigue C, Menard ML, Miller NM, Morales-Soto N, Norton S, Ogier J-C, Orchard SS, Park D, Park Y, Qurollo BA, Sugar DR, Richards GR, Rouy Z, Slominski B, Slominski K, Snyder H, Tjaden BC, van der Hoeven R, Welch RD, Wheeler C, Xiang B, Barbazuk B, et al.** 2011. The entomopathogenic bacterial endosymbionts *Xenorhabdus* and *Photorhabdus*: Convergent lifestyles from divergent genomes. *PLoS One* **6**:e27909.

64. **Duchaud E, Rusniok C, Frangeul L, Buchrieser C, Givaudan A, Taourit S, Bocs S, Boursaux-Eude C, Chandler M, Charles JF, Dassa E, Derose R, Derzelle S, Freyssinet G, Gaudriault S, Medigue C, Lanois A, Powell K, Siguier P, Vincent R, Wingate V, Zouine M, Glaser P, Boemare N, Danchin A, Kunst F.** 2003. The genome sequence of the entomopathogenic bacterium *Photorhabdus luminescens*. *Nature biotechnology* **21**:1307-1313.
65. **Wilkinson P, Waterfield NR, Crossman L, Corton C, Sanchez-Contreras M, Vlisidou I, Barron A, Bignell A, Clark L, Ormond D, Mayho M, Bason N, Smith F, Simmonds M, Churcher C, Harris D, Thompson NR, Quail M, Parkhill J, French-Constant RH.** 2009. Comparative genomics of the emerging human pathogen *Photorhabdus asymbiotica* with the insect pathogen *Photorhabdus luminescens*. *BMC genomics* **10**:302.
66. **Ciche T.** 2007. The biology and genome of *Heterorhabditis bacteriophora*. *WormBook* : the online review of *C elegans* biology doi:10.1895/wormbook.1.135.1:1-9.
67. **Jami E, Israel A, Kotser A, Mizrahi I.** 2013. Exploring the bovine rumen bacterial community from birth to adulthood. *ISME J* **7**:1069-1079.
68. **Lee MM, Stock SP.** 2010. A multilocus approach to assessing co-evolutionary relationships between *Steinernema* spp. (Nematoda: Steinernematidae) and their bacterial symbionts *Xenorhabdus* spp. (gamma-Proteobacteria: Enterobacteriaceae). *Syst Parasitol* **77**:1-12.
69. **Goodrich-Blair H, Clarke DJ.** 2007. Mutualism and pathogenesis in *Xenorhabdus* and *Photorhabdus*: two roads to the same destination. *Mol Microbiol* **64**:260-268.
70. **Easom CA, Joyce SA, Clarke DJ.** 2010. Identification of genes involved in the mutualistic colonization of the nematode *Heterorhabditis bacteriophora* by the bacterium *Photorhabdus luminescens*. *BMC Microbiol* **10**:45.
71. **Somvanshi VS, Kaufmann-Daszczuk B, Kim KS, Mallon S, Ciche TA.** 2010. *Photorhabdus* phase variants express a novel fimbrial locus, *mad*, essential for symbiosis. *Mol Microbiol* **77**:1021-1038.
72. **Cowles CE, Goodrich-Blair H.** 2008. The *Xenorhabdus nematophila* *nilABC* genes confer the ability of *Xenorhabdus* spp. to colonize *Steinernema carpocapsae* nematodes. *J Bacteriol* **190**:4121-4128.
73. **Bhasin A, Chaston JM, Goodrich-Blair H.** 2012. Mutational analyses reveal overall topology and functional regions of NilB, a bacterial outer membrane protein required for host-association in a model animal-bacterial mutualism. *J Bacteriol* **194**:1763-1776.
74. **McFall-Ngai M, Nyholm SV, Castillo MG.** 2010. The role of the immune system in the initiation and persistence of the *Euprymna scolopes*--*Vibrio fischeri* symbiosis. *Seminars in immunology* **22**:48-53.
75. **Easom CA, Clarke DJ.** 2011. HdfR is a regulator in *Photorhabdus luminescens* that modulates metabolism and symbiosis with the nematode *Heterorhabditis*. *Environmental microbiology* doi:10.1111/j.1462-2920.2011.02669.x.

76. **An R, Grewal PS.** 2010. Molecular mechanisms of persistence of mutualistic bacteria *Photorhabdus* in the entomopathogenic nematode host. PLoS one **5**:e13154.
77. **Peters A, Ehlers RU.** 1997. Encapsulation of the entomopathogenic nematode *Steinernema feltiae* in *Tipula oleracea*. J Invertebr Pathol **69**:218-222.
78. **Brivio MF, Moro M, Mastore M.** 2006. Down-regulation of antibacterial peptide synthesis in an insect model induced by the body-surface of an entomoparasite (*Steinernema feltiae*). Dev Comp Immunol **30**:627-638.
79. **Ehlers RU, Wulff A, Peters A.** 1997. Pathogenicity of axenic *Steinernema feltiae*, *Xenorhabdus bovienii*, and the bacto-helminthic complex to larvae of *Tipula oleracea* (Diptera) and *Galleria mellonella* (Lepidoptera). J Invertebr Pathol **69**:212-217.
80. **Proschak A, Zhou Q, Schoner T, Thanwisai A, Kresovic D, Dowling A, ffrench-Constant R, Proschak E, Bode HB.** 2014. Biosynthesis of the insecticidal xenocycloins in *Xenorhabdus bovienii*. Chembiochem **15**:369-372.
81. **Sergeant M, Baxter L, Jarrett P, Shaw E, Ousley M, Winstanley C, Morgan JA.** 2006. Identification, typing, and insecticidal activity of *Xenorhabdus* isolates from entomopathogenic nematodes in United Kingdom soil and characterization of the *xpt* toxin loci. Appl Environ Microbiol **72**:5895-5907.
82. **Fang XL, Han LR, Cao XQ, Zhu MX, Zhang X, Wang YH.** 2012. Statistical optimization of process variables for antibiotic activity of *Xenorhabdus bovienii*. PLoS One **7**:e38421.
83. **Fang XL, Li ZZ, Wang YH, Zhang X.** 2011. In vitro and in vivo antimicrobial activity of *Xenorhabdus bovienii* YL002 against *Phytophthora capsici* and *Botrytis cinerea*. J Appl Microbiol **111**:145-154.
84. **Morales-Soto N, Gaudriault S, Ogier JC, Thappeta KR, Forst S.** 2012. Comparative analysis of P2-type remnant prophage loci in *Xenorhabdus bovienii* and *Xenorhabdus nematophila* required for xenorhabdycin production. FEMS Microbiol Lett **333**:69-76.
85. **Lee MM, Stock SP.** 2010. A multigene approach for assessing evolutionary relationships of *Xenorhabdus* spp. (gamma-Proteobacteria), the bacterial symbionts of entomopathogenic *Steinernema* nematodes. J Invertebr Pathol **104**:67-74.

CHAPTER 2

***Xenorhabdus bovienii* interactions with *Steinernema* spp. nematodes**

Generation of hypotheses, analysis of data, and construction of figures for this chapter was done in collaboration with Dr. Darby Sugar, Dr. John Chaston, and Dr. Heidi Goodrich-Blair. All data presented in this chapter were generated by Kristen E. Murfin.

Sections of this work have been published as:

Sugar DR, **Murfin KE**, Chaston JM, Andersen AW, Richards GR, Deléon L, Baum JA, Clinton WP, Forst S, Goldman BS, Krasomil-Osterfeld KC, Slater S, Stock SP, and Goodrich-Blair H. 2011. "Phenotypic variation and host interactions of *Xenorhabdus bovienii* SS-2004, the entomopathogenic symbiont of *Steinernema jolietii* nematodes." *Environ Microbiol.* 2012 Apr;14(4):924-39. doi: 10.1111/j.1462-2920.2011.02663.x

Murfin KE, Chaston J, and Goodrich-Blair, H. "Visualizing bacteria in nematodes using fluorescence microscopy." *J Vis Exp.* 2012 Oct 19;(68). doi: 10.3791/4298.

Chaston J, **Murfin KE**, Heath-Heckman, EA, and Goodrich-Blair, H. "Previously unrecognized stages of species-specific colonization in the *Xenorhabdus-Steinernema* mutualism" *Cell Microbiol.* 2013 Sep;15(9):1545-59. doi: 10.1111/cmi.12134

ABSTRACT

Commonly, bacterial symbionts are able to form mutually beneficial symbiotic associations with several different host species or populations (i.e. broad host-range mutualisms). Although these associations are integrally important to our understanding of host and symbiont interactions, many basic questions remain about partner recognition, host switching, and evolutionary maintenance of these associations. Furthermore, little is known about the impact of bacterial symbiont strain variability on these associations. In this thesis chapter, I describe the fundamental characteristics of the association between *Xenorhabdus bovienii* bacterial strains and their various *Steinernema* spp. nematode hosts, providing the basis for further investigations of this broad-host range mutualism. The study includes isolation and phenotypic and phylogenetic characterization of nine *X. bovienii* bacterial isolates from six different nematode host species. Using one particular *X. bovienii* – *Steinernema* pair we investigated cellular processes underlying colonization and transmission of the bacterial symbiont by the nematode host. In addition, this work established a suite of *X. bovienii* strains and nematode hosts and experimental tools that facilitated subsequent work investigating host range and evolution of the *X. bovienii* – nematode symbiosis.

INTRODUCTION

In many beneficial symbioses (i.e. mutualisms), particularly those involving bacterial symbionts, a single symbiont species can associate with many different host species. This type of broad host-range symbiosis is common in nature. For example, different bifidobacteria species (e.g. *Bifidobacterium pseudolongum*) and nitrogen-fixing bacteria (e.g. *Rhizobium etli*) each associate with several different animal and plant hosts respectively (1, 2). However, little is known about how partner recognition and maintenance occurs in such associations or the impact that bacterial strain variability can have on the fitness of the symbiotic holobiont. To begin to address such questions we developed tools and resources to investigate the broad-host range bacterium *Xenorhabdus bovienii* and its various *Steinernema* nematode host species.

All members of the genus *Xenorhabdus* associate with *Steinernema* nematodes, and vice versa. Together these bacterium-nematode associates undergo a complex life cycle that includes both environmental stages and reproductive stages (Figure 2.1). The environmental stage nematodes, known as infective juveniles (IJs), carry bacteria within a specialized extracellular pocket within the intestine, known as the receptacle (3-5). The IJs migrate through the soil in search of insect hosts, which they invade through natural openings. Once inside the insect host, the nematodes release the bacterial symbiont through defecation (6, 7), and the nematodes and bacteria kill the insect host. The nematodes then grow into adults that mate and lay eggs. These eggs hatch into juvenile nematodes that grow and develop into adults. Growth and reproduction of the nematodes continues for 2 or 3 generations (8), until conditions in the cadaver induce the formation of progeny IJs (9-11). Juvenile nematodes then undergo an alternate developmental pathway to become pre-IJs and then IJs, which are distinguished by several morphological changes: constriction of the nematode intestine, closing of the mouth and

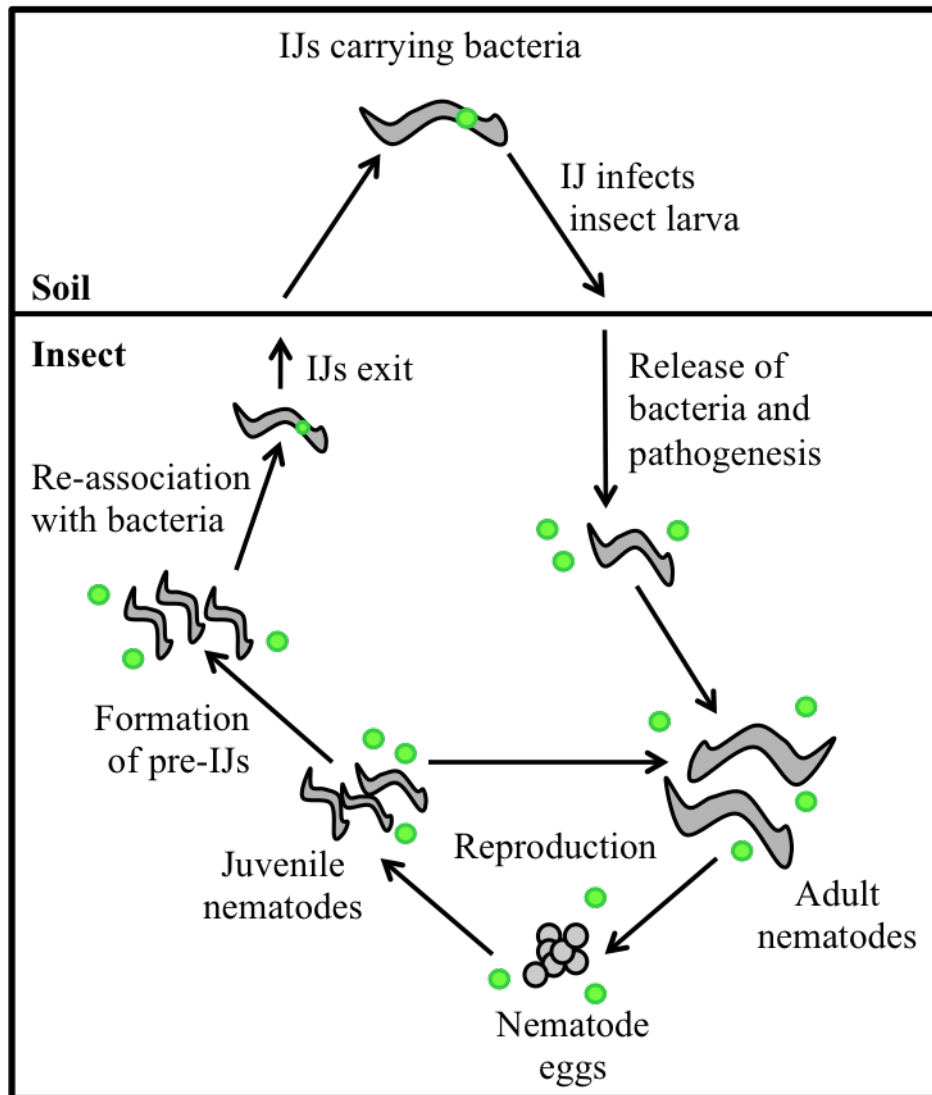


Figure 2.1 *Steinernema* nematode and *Xenorhabdus* bacteria life cycle. Schematic shows the life cycle of nematodes (grey) and bacteria (green). Infective juvenile (IJ) nematodes carry the bacterial symbiont through the soil in search of insect hosts. The IJ invades the insect host and releases the bacterial symbiont. The nematodes and bacteria then kill the insect and reproduce within the insect cadaver. When conditions signal the end of reproduction, the nematodes develop into pre-IJs, which re-associate with the bacterial symbiont as they develop into IJs. The new progeny IJs then exit the insect cadaver in search of new insect hosts.

anus, formation of the IJ cuticle, and formation of the receptacle and its colonization by a specific *Xenorhabdus* bacterial symbiont (7, 12).

Xenorhabdus – *Steinernema* associations have been developed to study binary interactions (i.e. one symbiont and one host). For example the association between *X. nematophila* and *S. carpocapsae* has been studied in detail and provide a basis for development of the system as a model for mutualism. Overall, these studies have revealed that the nematode host facilitates transmission of the bacterial symbiont between insect hosts (4, 13) and contributes to virulence towards the insect host (14, 15). In turn, the bacterial symbiont also contributes to virulence toward the insect host (5, 16), provides nutrients to the nematode host for growth and development (17, 18), and plays a defensive role by producing antibiotics (19, 20) and anti-predatory compounds (21, 22) that deter microbes and scavengers from consuming the insect cadaver. In *Xenorhabdus* bacteria, regulation of many of these symbiotic factors are under the control of phenotypic variation. *Xenorhabdus* species undergo reversible phenotypic switching between primary and secondary form cells (23, 24). Primary form cells are always isolated from nematode IJs and can be identified through the binding of bromothymol blue dye (23, 24). In general, primary form cells are associated with the production of potential virulence factors, such as hemagglutinins and hemolysins, while secondary form cells do not bind dye and are associated with increased motility and production of compounds related to nutrition, such as lipase. Although it is not entirely clear what genetic factors are responsible for the switch, long-term growth in stationary phase and repeated passage of the bacteria through laboratory media can induce the formation of secondary form cells from primary form.

In the insect environment, *Xenorhabdus* bacteria are acquired by the nematode IJs horizontally using a selective process. Nematode eggs are aposymbiotic, and maternal transmission of bacterial symbionts has not been observed in *Steinernema* nematodes (3, 4, 12, 25), making it unlikely that vertical transmission occurs. However, the bacteria are seeded into

the insect cadaver environment by the IJs that invade the insect host and grow to a very high density (6, 7), which likely increases the probability that developing pre-IJs will encounter the bacterial symbiont. Bacterial symbiont acquisition by pre-IJs is a selective process where only 1-2 bacterial cells initiate colonization then grow to fill the nematode receptacle (4, 5). In the *S. carpocapsae* – *X. nematophila* association, the selective colonization initiation event requires specific bacterial genetic factors. *X. nematophila nil* (nematode intestinal localization) genes are required for the bacteria to colonize the IJ receptacle, as removal of these genes reduced nematode colonization below the level of detection (3, 26-28). Furthermore, addition of these genes to non-native, non-colonizing *Xenorhabdus* spp. increased colonization to a detectable level (3, 28, 29). Taken together these studies have led to the model that colonization of a *Steinernema* nematode host is a specific process in which the nematode selects the bacterial symbiont based on the presence of specific colonization factors.

To build upon these studies for the development of a broad host-range mutualism model, we have utilized the interaction between *X. bovienii* bacteria and *Steinernema* spp. hosts. To define features of the *X. bovienii* – *Steinernema* spp. association, we isolated and identified nine *X. bovienii* strains from nematodes known to harbor *X. bovienii*. We utilized these strains to assess phenotypic diversity among the bacterial strains, including phenotypic variation, and the processes involved in colonization of the nematode host. These experiments formed the basis for subsequent investigations on the symbiotic fitness and evolutionary processes of the *X. bovienii* – *Steinernema* spp. association.

RESULTS

Isolation and identification of *X. bovienii* bacterial strains from *Steinernema* species.

A primary goal of future experiments is to assess the contribution of *X. bovienii* symbionts to nematode host fitness in a phylogenetic context. To study such topics, a suite of *X. bovienii* strains isolated from divergent hosts is necessary. Therefore, we obtained nine isolates of six different nematode host species known to harbor *X. bovienii* and isolated the bacterial strains associated with them (Table 2.1). Bacteria were confirmed to be *X. bovienii* through 16S rRNA sequencing and alignment to known *X. bovienii* sequences (data not shown). Additionally, BLAST analysis confirmed that the top hit for each 16S sequence was *X. bovienii* (data not shown). Further preliminary characterization was done on the strain isolated from *S. jollieti* nematodes (Xb-Sj), as this strain has a fully sequenced genome. Secondary form Xb-Sj (Xb-Sj-2°) was isolated from the primary form through long-term growth in laboratory culture and confirmed lack of dye binding (23, 24). Specifically, the primary and secondary form isolates displayed differences in cell morphology and the production of compounds, such as pigments. Primary, but not secondary, bacteria produced a strong yellow-orange pigment in culture (Figure 2.2 a, b). Primary form cells were also larger (Figure 2.2 c, d), and some primary form cells became extremely elongated (Figure 2.2 c, inset). Other *X. bovienii* strains also underwent phenotypic variation (Chapter 4), and displayed similar phenotypes with regards to pigment production and cell morphology (data not shown).

Additionally, it was determined that phenotypic variation can impact the success of symbiotic interactions. Co-injections of aposymbiotic nematodes with primary form, but not secondary form, Xb-Sj in *Galleria mellonella* insects resulted in the production of progeny IJs (Figure 2.3). To determine if nematodes failed to grow in secondary form infected insect cadavers, co-injected *G. mellonella* insect cadavers were dissected for observation of

Table 2.1. Bacterial strains and plasmids used in this study^a

Strain or Plasmid Name ^a	Relevant Features ^b	Source or Reference
<i>Bacterial Strains</i>		
Xb-Sf-FL	Wild type from <i>Steinernema feltiae</i> isolated in Florida, USA	(30, 31)
Xb-Sf-FR	Wild type from <i>Steinernema feltiae</i> isolated in France	(30, 31)
Xb-Sf-MD	Wild type from <i>Steinernema feltiae</i> isolated in Moldova	(30, 31)
Xb-Sp	Wild type from <i>Steinernema punctauvense</i> isolated in Costa Rica	(30, 31)
Xb-Sj	Wild type from <i>Steinernema jolietii</i> supplied by Monsanto	(30, 31)
Xb-So	Wild type <i>Steinernema oregonense</i> isolated in Oregon, USA	(30, 31)
Xb-Sk-BU	Wild type <i>Steinernema kraussei</i> supplied by Becker Underwood	(30, 31)
Xb-Sk-Q	Wild type <i>Steinernema kraussei</i> isolated in Quebec, CA	(30, 31)
Xb-Si	Wild type <i>Steinernema intermedium</i> isolated in North Carolina, USA	(30, 31)
Xb-Sj-2°	Xb-Sj in secondary form	(5)
Xb-Sf-FL-GFP	Xb-Sf-FL with GFP expression (pMini-Tn7-KSGFP)	(3)
Xb-Sf-FR-GFP	Xb-Sf-FR with GFP expression (pMini-Tn7-KSGFP)	This Study
Xb-Sp-GFP	Xb-Sp with GFP expression (pMini-Tn7-KSGFP)	This Study
BW29427	<i>Escherichia coli</i> donor strain for conjugation, requires diaminopimelic acid (DAP)	
<i>Plasmids</i>		
pMini-Tn7-KSGFP	Tn7 delivery vector carrying GFP	(32)
pUX-BF13	Helper plasmid for insertion of Tn7 plasmid	(33)

^aTable of bacterial strains that were used in this study.

^bRelevant features of the strain, including nematode host, expression changes, and mutations.

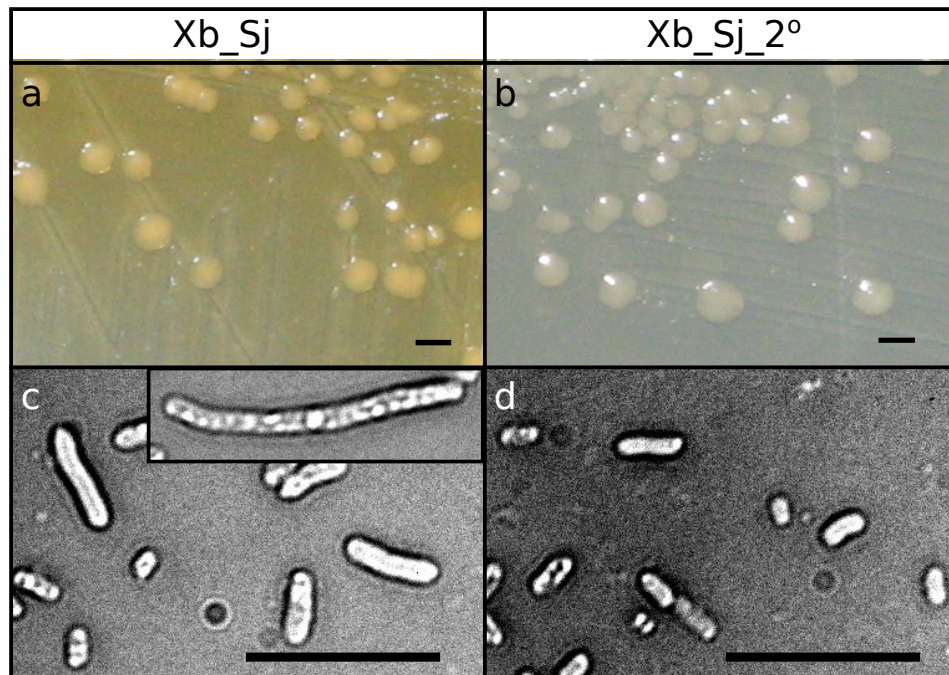


Figure 2.2 Morphological differences in primary and secondary form *X. bovienii*. Primary (Xb-Sj) and secondary (Xb-Sj-2°) form *X. bovienii* from *S. jolietii* nematodes was assessed for morphological differences due to phenotypic variation. Primary form bacteria grown on solid medium (a) produced a yellow-orange pigment that was not produced by secondary form (b). Scale bars represent 2mM. Primary form cells also appeared larger (c) than secondary form cells (d). The inset (c) shows a very elongated primary form cell. Scale bars represent 10μM. Images were used in Sugar *et. al* 2012 (5) and are reproduced here with permission.

resulting nematodes (Figure 2.3 a-d). In co-injections with either primary or secondary form, injected IJs recovered and developed into adult nematodes that reproduced. However, in co-injections with secondary form, nematodes failed to develop into IJs, even after 14 days of incubation. Nematodes harvested from these co-injections showed body morphology consistent with juvenile nematodes (Figure 2.3 a), including an open mouth (Figure 2.3 c). This is in contrast to co-injections with Xb-Sj primary form, which resulted in progeny nematodes with body morphology resembling IJ nematodes (b), and progeny had closed mouths consistent with IJ development (d). In addition, cadavers injected with nematodes and primary form Xb-Sj became soft and flaccid, but cadavers injected with nematodes and secondary form Xb-Sj remained hard and rigid, similar to bacterial only injections (Figure 2.3 e-h). It also should be noted that cadavers injected with primary and secondary form strains turned different colors, supporting that the differences in bacterial product production are likely also occurring within insects in addition to *in vitro* conditions previously measured. Differences in nematode life cycle production and cadaver consistency were not due to a lack of growth of either bacterial strain, as *in vivo* imaging analysis of injections revealed that primary and secondary form Xb-Sj expressing GFP are both able to grow within the insect cadaver (Figure 2.3 i-j).

Colonization of *Steinernema* spp. IJs by *X. bovienii* bacterial strains. To assess to what extent *X. bovienii* bacterial strains colonize the IJ stage of their *Steinernema* spp. nematode hosts, we performed a series of colonization assays with different *X. bovienii* strains and their cognate hosts under *in vivo* (in *G. mellonella* larvae) and *in vitro* conditions. *X. bovienii* strains were engineered to express GFP (Table 2.1), so that colonization could be assessed by microscopy (25). Microscopic analysis of colonization measures the percentage of nematodes within the population that carry the GFP-expressing bacterial symbiont. Strains for these

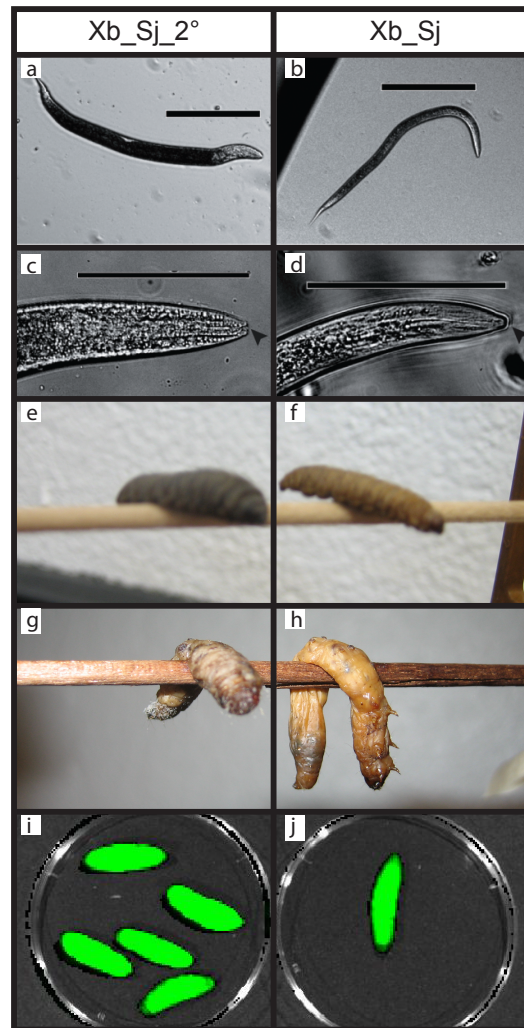


Figure 2.3 Phenotypic variation affects progeny IJ development. Nematodes from co-injections were harvested by dissection (a-d). Panels a and b show full body morphology, scale bars represent 200 μ M. Panels c-d show the anterior end of the harvested nematodes, and the arrowhead points out location of the mouth. Scale bars represent 100 μ M. Co-injections produced different nematode cadaver consistencies (e-h). Bacterial only injections of secondary (e) and primary (f) form cells became rigid. Injections of secondary form bacteria with nematodes (g) remained rigid, where injections of primary form bacteria with nematodes (h) became soft and flaccid. Imaging of cadavers injected with secondary (i) and primary (j) form bacteria expressing GFP. Images were used in Sugar *et. al* 2012 (5) and are reproduced here with permission.

experiments were chosen based on their ability to be genetically manipulated and the availability of the nematode host. Colonization of *S. feltiae* FL, *S. feltiae* FR, and *S. punctauvese* was assessed using Xb-Sf-FL-GFP, Xb-Sf-FR-GFP, and Xb-Sp-GFP respectively. Colonization rates were assessed in two common *in vitro* conditions as well as *in vivo* to compare the success of *in vitro* assays relative to ecologically relevant conditions (Figure 2.4). Bacterial symbionts showed the highest rate of colonization when nematodes and bacteria were reared *in vivo*. However, colonization rates were not significantly different when nematodes and bacteria were reared on liver kidney agar (LKA). This in contrast to nematodes and bacteria reared on lipid agar, which showed a significantly lower rate of colonization ($p < 0.01$). Based on these data, all subsequent *in vitro* nematode rearing assays were performed using LKA conditions.

***X. bovienii* strains colonize *Steinernema* nematode non-IJ life stages.** Previous studies, demonstrated that *X. nematophila* colonizes non-IJ life stages of the nematode host (Appendix 3). To determine if this is a phenomenon that is conserved among other *Xenorhabdus* – *Steinernema* associations, we assessed colonization of *S. feltiae* nematodes by its cognate *X. bovienii* bacterial symbiont strain. Colonization was assessed with GFP-expressing symbiont (Xb-Sf-FL-GFP) on all life stages of the nematode host (25). Colonization was assessed in LKA conditions (Figure 2.5, 2.6) as well as *in insecta* (data not shown).

Colonization assays demonstrated that *X. bovienii* also colonizes specific locations within different *S. feltiae* nematode life stages (Figure 2.5). In all life stages, *X. bovienii* colonizes sites that are close to the junction between the esophagus and the intestine, and in this area are several major features, including the esophagus, basal bulb (swallowing organ), pharyngeal intestinal valve (ring of cells that opens and closes the junction), and the intestine

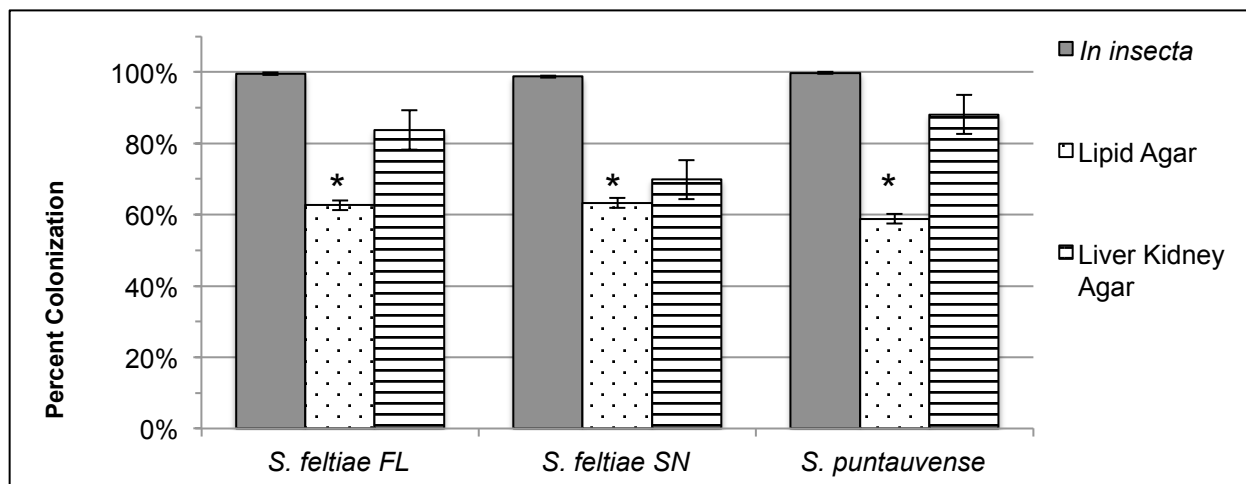


Figure 2.4 Colonization percentage of *Steinerinema* nematode hosts by *X. bovienii* strains in various nutritional conditions. The colonization of GFP-expressing *X. bovienii* strains was assessed in cognate hosts *in vivo* (in *G. mellonella* larvae) and *in vitro* (lipid agar and liver kidney agar). The percentage of nematodes within the population that are colonized was determined by microscopy. * indicates significant differences from the *in vivo* condition using ANOVA, $p < 0.05$.

(Figure 2.5 a). Within adult and juvenile nematodes *X. bovienii* colonizes an area within the intestine that is adjacent to the junction between the nematode esophagus and the intestine termed the anterior intestinal cecum (AIC) (Figure 2.5 b, c). Within juvenile nematodes, the bacteria can also colonize the pharyngeal intestinal valve (PIV) (Figure 2.5 d). PIV colonization by the bacterium also occurs in juvenile nematodes as they morphologically change into IJs (Figure 2.5 e, f). Within this transitional period the nematode intestine constricts and closes along with the mouth and anus (Figure 2.5 e). The IJ cuticle then forms and the nematodes further constrict to change shape into IJs. IJs can be visualized that have bacteria in a location similar to PIV, although it is difficult to determine the exact location of the bacteria as nematode tissues are compacted (Figure 2.5 f). IJs were also seen that show colonization characteristic of IJs, as has been previously described (Figure 2.5 g) (4, 5, 12). In this colonization state, bacteria are localized to an intercellular space within the nematode intestine, known as the receptacle (4, 12). In *X. bovienii* hosts there is also a structure within the receptacle, referred to as a vesicle (5). The vesicle is a non-cellular, clear envelope or membrane structure that appears to contain the bacteria within the receptacle.

To determine if colonization of nematodes within the insect host is similar to what we described *in vitro*, we co-injected nematodes with GFP-expressing symbiont into *G. mellonella*. Nematodes were harvested from the insect environment by dissection and were assessed for colonization state. As in the *in vitro* assays, we observed the nematode life stages colonized in the same locations (data not shown).

Colonization of *S. feltiae* life stages is likely a sequential process. To determine timing of bacterial colonization during the nematode life cycle, we assessed colonization of *S. feltiae* nematodes over time (Figure 2.6). Infective juvenile nematodes were added to lawns of GFP-

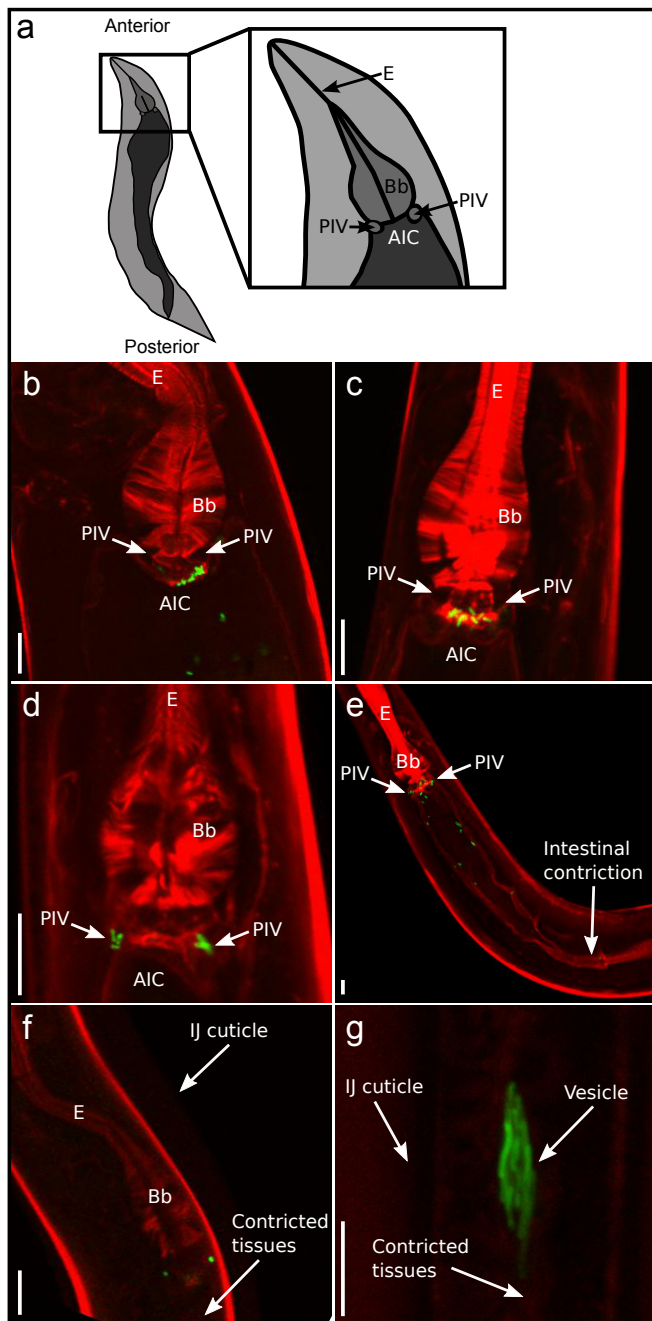


Figure 2.5 Colonization of *S. feltiae* life stages. Nematodes reared on lawns of GFP symbiont in LKA conditions were assessed for localization of the symbiont using confocal microscopy. (a) Schematic showing nematode morphological features: esophagus (E), basal bulb (Bb), pharyngeal intestinal valve (PIV), and anterior intestinal cecum (AIC). Symbionts localize to the AIC of adults (b) and most juvenile (c) nematodes. Some juveniles are colonized by symbionts in the PIV (d). PIV colonization persists in nematodes undergoing morphological changes into IJs, including intestinal constriction (e) and cuticle formation (f). Mature IJs show bacterial colonization in the vesicle (g).

expressing cognate symbiont (Xb-Sf-FL-GFP) in LKA conditions. Life stage and colonization state was assessed for nematodes every day for at least five days starting at day seven post-addition to bacterial lawns. This was determined to be sufficient to capture the progression of the nematode life cycle from adults to IJs (data not shown).

We observed a colonization of >85% of all nematode life stages at all time points and a clear progression of nematode life stages over time from adults to juveniles to IJs (Figure 2.6). At time points prior to day five the majority of the nematode population is adults (data not shown). Starting at day seven the majority of the nematode population is juveniles and PIV colonization in juveniles starts occurring. At time points prior to day seven, only AIC colonization is present in juveniles and adults. Beginning at day eight, juvenile nematodes start showing characteristics that they will become IJs, such as a constricting intestine. All nematodes showing this transitional stage are colonized in the PIV. Nematodes showing characteristics of IJs become part of the population starting at day eight as well. These first IJs are mono-colonized or non-colonized, and later IJs start showing the full-colonization typically seen in emerged IJs. At time points past day thirteen, IJs begin to make up the majority of the population (data not shown).

These data are consistent with colonization being a sequential process based on nematode life stages, as AIC colonization occurs prior to PIV colonization, which is prior to IJ receptacle colonization. However, it is unclear if the bacteria colonizing the nematode host migrate between colonization sites within the nematode host or if new bacterial cells are acquired from the environment to occupy these colonization locations.

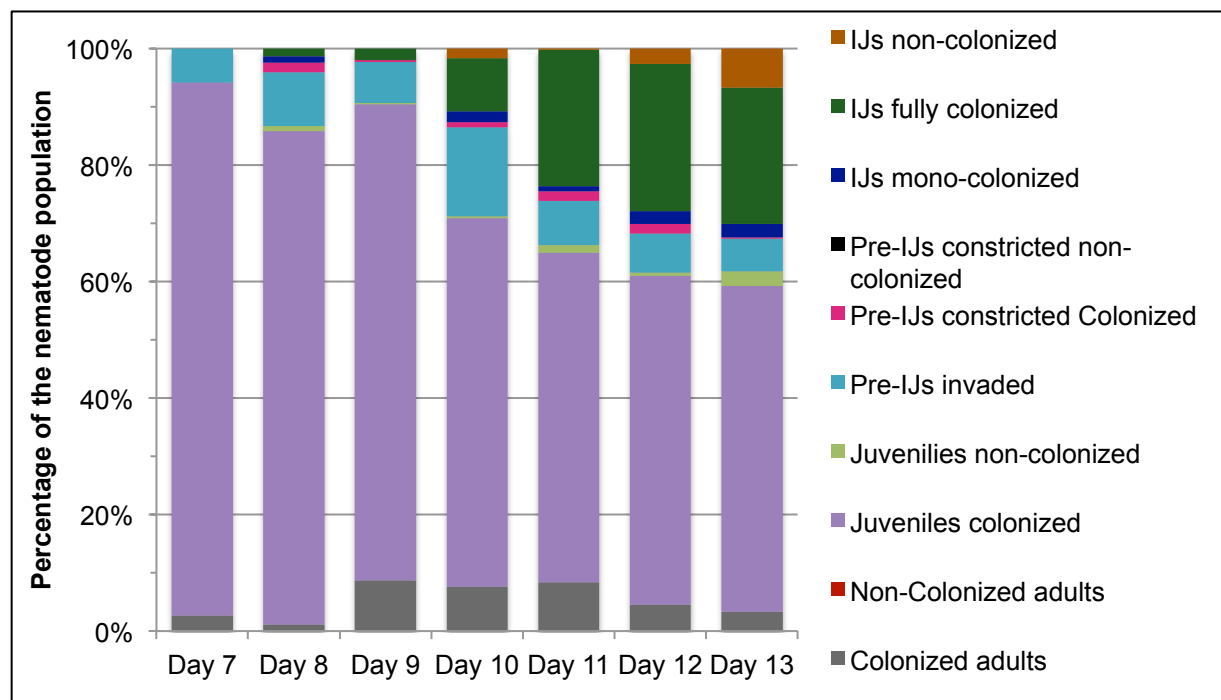


Figure 2.6 Progression of colonization in *S. feltiae* life cycle. Colonization and life stage was scored for at least 100 nematodes for 7 days starting at Day 7 post-addition of nematodes to bacterial lawns. Proportions of the nematode population within each category are shown in the stacked bar graph above.

CONCLUSIONS

Our data characterize many aspects of the interaction between *X. bovienii* bacteria and their *Steinernema* spp. hosts. Specifically we identified that *X. bovienii* undergoes phenotypic variation that causes differential production of compounds and cell morphology (Figure 2.3). Interestingly we also identified that phenotypic variation affects the ability of the bacteria to support production of IJ nematodes *in insecta* (Figure 2.3). Our work also demonstrates that *X. bovienii* colonizes specific locations within the nematode host in a sequential process (Figure 2.5, 2.6). This information provides insights that will form the framework for future studies in this system. For example, when assessing *X. bovienii* bacterial strains for the production of compounds it will be important to analyze both primary and secondary form isolates, and when assessing bacterial factors contributing to colonization, it will be useful to monitor multiple nematode life stages.

The lack of IJ development in primary and secondary form co-injections is likely due to the absence of a bacterially derived signal or lack of bacterial developmental support. Previously identified cues known to stimulate IJ development are based on nematode growth processes, including the accumulation of waste products, such as ammonia, and physical crowding of the nematodes. However, these cues are likely not defective in secondary co-injections, as the nematodes within co-injected cadavers grew to a high density (data not shown). Therefore differences in nematode host support by primary and secondary form *X. bovienii* are likely due to the change in products produced between the bacterial isolates. Bacterially derived products could be molecules that signal to the nematode to undergo IJ development. Such inter-kingdom signaling has been observed in *Rhizobium*-legume symbioses (34). Alternatively, the lack of IJ development could be due to deficiency of an essential nutrient for the developmental process that is derived from the bacterial symbiont. It is known that *Xenorhabdus* bacteria nutritionally support nematode reproduction (17). Within these

co-injections, inappropriate production of a particular nutrient provisioning gene product (e.g. lipase, lecithinase or protease) could cause a developmental delay due to the absence or presence of a particular nutrient. It is also possible that the instead of indirect nutrient provisioning through production of breakdown enzymes, the bacterial symbiont is inappropriately providing a nutrient produced by the bacterium, such as amino acids or vitamins.

Another, mutually inclusive possibility, is that physical degradation of the cadaver may be necessary to stimulate IJ development and exit from the insect cadaver. The cadavers injected with nematodes and secondary form cells did not become flaccid to the same extent as those co-injected with primary form. Soft and flaccid cadaver phenotypes indicative of physical degradation, only occurred when primary form bacteria were co-injected with nematodes, in contrast to secondary form co-injections and bacteria only injections (Figure 2.3 e-h). This indicates that the nematode host either contributes to degradation or stimulates production of particular compounds in the primary form bacterium that cause degradation. Candidate bacterial genes contributing to degradation include chitinases and proteases, which could degrade the insect tissues, or makes catepillars floppy genes (*mcf*). In *Photorhabdus luminescens*, *mcf1* and *mcf2* likely contribute to toxicity and loss of caterpillar body turgor (35). Xb-Sj has a homolog of *mcf1* (data not shown). Further testing, including transcriptional and mutational analysis will be necessary to determine the bacterial mechanisms responsible for differences in IJ production between primary and secondary form *X. bovienii*.

Colonization assays demonstrated that nutritional conditions can greatly affect the colonization rate of nematode hosts (Figure 2.4). Within our study, we found that the highest colonization rates were *in insecta*, as compared to *in vitro* conditions. This is similar to what was previously observed for *X. nematophila* colonization of *S. carpocapsae* (36). The nutritional differences in these conditions could be influencing several variables that could impact colonization rate, such as bacterial density, production of bacterial factors facilitating

colonization, or nematode health. Regardless of the cause of colonization rate differences, these data suggest that colonization studies with *X. bovienii* should be conducted *in insecta* or on LKA to most similarly model ecologically relevant phenotypes. This finding is in contrast to other systems, where there is only small differences in the colonization rate between nematodes reared *in insecta* or *in vitro* (3).

Our colonization studies also revealed temporal changes (Figure 2.6) in the specific nematode tissues colonized by *X. bovienii* (Figure 2.5) during association with the *S. feltiae* nematode host. During the first two generations of reproduction most adults and juveniles are AIC colonized. Because adults and juveniles that will never become IJs are colonized, this suggests that AIC colonization may have a function other than, or in addition to, transmission of the bacterium. Exposure to bacteria could facilitate functions that are seen in other symbioses, such as immune education (37), development (38-40), exclusion of pathogens (41), or nutrition (42, 43). It is also possible that AIC colonization serves the function of facilitating PIV colonization in juveniles, as AIC colonization occurs prior to PIV colonization. PIV colonization only occurs and persists in nematodes that are morphologically changing into IJs, and AIC colonization or localization to other sites was not observed in these nematodes. After intestinal constriction and closure of the mouth and anus, it is unlikely that bacteria could enter the nematode body. Therefore, bacteria colonizing the PIV most likely form the basis of the bacteria that colonize the IJ receptacle. We also only observed one or a few cells within the PIV, which is consistent with previous observations that only one or two bacterial cells initiate colonization of the IJ receptacle (4). This suggests that PIV colonization may be the bottleneck step in the colonization process that selects for the few cells that will be the transmitted population. However, we did not directly observe migration of the bacterial cells from the PIV to the IJ receptacle. Therefore, further studies, such as time-lapse experiments, will be needed to confirm this.

In total our data describe specific functions within *X. bovienii* – *Steinernema* spp. associations that will provide the basis for further mechanistic studies. These data highlight certain features of the system that will need to be considered in future studies, such as the impact of phenotypic variation and nutritional conditions on symbiotic interactions. These data also provide the framework for future studies to identify bacterial mechanisms and the distribution of these mechanisms among *X. bovienii* associations through providing a suite of nematode hosts and bacterial strains, experimental conditions and genetic manipulation techniques.

ACKNOWLEDGEMENTS

The authors wish to thank Elizabeth A. Hussa for help with the *in vivo* imaging system. The authors would also like to thank Sergei Spiridonov, Maurice Moens, and Kurt Heungens for the *S. jollieti* nematode isolate, Adler Dillman, John Chaston, Michael Gebre and Byron Adams for the *S. feltiae* MD nematode isolate, Lorena Uribe-Lorío for the *S. puntauense* nematode isolate, and S. Patricia Stock for all other nematode isolates. This work was supported by collaborative grants from the National Science Foundation awarded to H.G.B. (NSF IBN-0416783; IOS-0920631), Steve Forst (NSF IOB-0416747; IOS-0919912), and S. Patricia Stock (NSF IOB-0146644; IOS-0919565), an Investigators in Pathogenesis of Infectious Disease Award from the Burroughs Welcome Fund (H.G.B.), and the National Institutes of Health Grant GM59776 (H.G.B.). KEM also was supported by the National Institutes of Health (NIH) National Research Service Award T32 AI55397 and a Louis and Elsa Thomsen Distinguished Predoctoral Fellowship.

MATERIALS AND METHODS

***X. bovienii* bacterial strains and nematode hosts.** Bacterial strains (Table 2.1) were obtained by sonication of nematode hosts after surface sterilization. *X. bovienii* bacterial strain species identity was confirmed by analysis of 16S rRNA (Figure 2.1) (31, 44). Storage of bacterial strains was done in Lysogeny Broth (LB) supplemented with 20% glycerol frozen at -80°C. Bacterial strains were grown at 30°C in LB with aeration in the dark or on LB agar supplemented with 0.1% pyruvate, unless otherwise noted (45). Nematode isolates were verified through sequencing of the 12S and 28S genes (data not shown) (30). Nematodes were propagated through *Galleria mellonella* larvae as previously described (4). Nematodes were stored at 25°C in 250 ml tissue culture flasks (BD Falcon, Franklin Lakes, NJ, USA) at a density of 5-10 IJs/ μ l and a volume less than 60 ml.

Characterization of *X. bovienii* bacterial strains. Secondary form bacterial isolates were generated from primary form bacterial isolates through daily subculturing in LB and testing for dye binding (23). Colony color and morphology was observed after growth of 24-36 hours on LB agar plates. Cell morphology was determined by microscopy after overnight growth in LB.

Genetic manipulation of bacterial strains. GFP-expression was inserted in the Tn7 site of *X. bovienii* strains using pMini-Tn7-KSGFP (32) and helper plasmid pUX-BF13 (33) using conjugation, similar to previously described methods (4, 25). For conjugation, *Escherichia coli* donor and helper strains (Table 2.1) was grown at 37°C with aeration in LB supplemented with diaminopimelic acid (DAP). Overnight cultures of donor, helper and recipient were subcultured and grown for four hours at 30°C with aeration in LB supplemented with DAP not exposed to the light. *X. bovienii* was subcultured 1:50 and *E. coli* was subcultured 1:100 into 2mL. 1mL of each donor, helper and recipient were combined, pelleted, and spotted onto LB agar supplemented

with DAP and pyruvate. Plates were grown at 30°C for 24 hours. Bacteria were then collected and struck out using a sterile stick on LB agar supplemented with pyruvate and Kanamycin. Plates were grown at 30°C until colonies formed, up to 2 days. Bacteria were then struck for isolation onto fresh LB agar supplemented with pyruvate and Kanamycin. Bacterial colonies were confirmed as GFP positive by viewing using florescent microscopy at 4x magnification on a Nikon Eclipse TE300 inverted microscope.

Co-injections and colonization assays. For both co-injections and colonization assays, axenic IJs were produced *in vitro* as previously described (12, 46). For co-injections, nematodes were surface sterilized and mixed with log-phase bacterial culture in order to inject 50 IJ nematodes with 100 CFU of bacteria. *In vitro* nematode growth was done on lipid agar or liver kidney agar (12, 46) as previously described (25). Nematodes were visualized by microscopy for observation of morphology and colonization state. For colonization assays, two technical replicates of at least 100 nematodes were counted per condition and scored for colonization state. Three biological replicates were performed and averaged.

Photography. Photography for colony morphology and insect cadavers was done using a Canon Powershot camera. Scale bars were inserted using Metamorph version 4.5r6 software (Universal Imaging Corporation, West Chester, PA).

Microscopy. Phase-contrast, differential interference contrast (DIC), and florescent microscopy was performed using a Nikon Eclipse TE300 inverted microscope. Florescence microscopy was performed using fluorescein isothiocyanate, tetramethyl rhodamin isocyanate (FITC). Images were taken using an ORCA digital camera (Hamamatsu, Hamatsu City, Japan) and Metamorph software. For cell morphology, bacterial cells were immobilized on 3% agarose

pads and viewed under DIC at 100X magnification. For visualization of nematode IJs, whole nematodes were paralyzed with 1% levamisole and placed on agar pads. Nematodes were viewed using phase contrast or fluorescent settings at 20X or 40X magnification.

For assessment of nematode colonization sites and population counting, nematodes and bacteria were viewed as stated above for whole nematode. Imaging of nematode tissues with bacterial cells was done using confocal microscopy on a Zeiss LSM 510 confocal microscope. Specimens were first stained with 6.6 mM rhodamine phalloidin (Sigma) or 0.125 mg ml⁻¹ Alexa Fluor 633 concanavalin A (Invitrogen; dissolved in 0.1 M sodium bicarbonate) (gifts from M. McFall-Ngai). To prevent photobleaching of fluorophores, samples were prepared in the dark. Nematode cultures were resuspended in PBS + 4% final concentration paraformaldehyde and fixed for at least 18 h. Samples were washed at least three times in PBS, permeabilized in PBS-T (1% final volume Triton X-100) for at least 18 h, and infiltrated with stains + 1% Triton X-100 for at least 18 h prior to visualization.

In vivo imaging. Imaging of insect cadavers injected with GFP-expressing symbiont was done seven days post injection. Analysis was done using an IVIS Imaging System 200 (Xenogen, Alameda, CA). Fluorescence was quantified by using Living Image software v2.6 (Xenogen). One to ten insects were imaged per biological replicate and three biological replicates were performed.

REFERENCES

1. **D'Aimmo MR, Modesto M, Mattarelli P, Biavati B, Andlid T.** 2014. Biosynthesis and cellular content of folate in bifidobacteria across host species with different diets. *Anaerobe* **30**:169-177.
2. **Rogel MA, Bustos P, Santamaria RI, Gonzalez V, Romero D, Cevallos MA, Lozano L, Castro-Mondragon J, Martinez-Romero J, Ormeno-Orrillo E, Martinez-Romero E.** 2014. Genomic basis of symbiovar mimosae in *Rhizobium etli*. *BMC Genomics* **15**:575.
3. **Chaston JM, Murfin KE, Heath-Heckman EA, Goodrich-Blair H.** 2013. Previously unrecognized stages of species-specific colonization in the mutualism between *Xenorhabdus bacteria* and *Steinernema* nematodes. *Cell Microbiol* **15**:1545-1559.
4. **Martens EC, Heungens K, Goodrich-Blair H.** 2003. Early colonization events in the mutualistic association between *Steinernema carpocapsae* nematodes and *Xenorhabdus nematophila* bacteria. *J Bacteriol* **185**:3147-3154.
5. **Sugar DR, Murfin KE, Chaston JM, Andersen AW, Richards GR, deLeon L, Baum JA, Clinton WP, Forst S, Goldman BS, Krasomil-Osterfeld KC, Slater S, Stock SP, Goodrich-Blair H.** 2012. Phenotypic variation and host interactions of *Xenorhabdus bovienii* SS-2004, the entomopathogenic symbiont of *Steinernema jolietii* nematodes. *Environ Microbiol* **14**:924-939.
6. **Poinar GOJ, Thomas GM.** 1966. Significance of *Achromobacter nematophilus* Poinar and Thomas (Achromobacteraceae: Eubacteriales) in the development of the nematode, DD-136 (*Neoaplectana* sp. Steinernematidae). *Parasitology* **56**:385-390.
7. **Snyder H, Stock SP, Kim SK, Flores-Lara Y, Forst S.** 2007. New insights into the colonization and release processes of *Xenorhabdus nematophila* and the morphology and ultrastructure of the bacterial receptacle of its nematode host, *Steinernema carpocapsae*. *Appl Environ Microbiol* **73**:5338-5346.
8. **Wang J, Bedding RA.** 1996. Population development of *Heterorhabditis bacteriophora* and *Steinernema carpocapsae* in the larvae of *Galleria mellonella*. *Fundamental and Applied Nematology* **19**:363-367.
9. **Kaplan F, Alborn HT, von Reuss SH, Ajredini R, Ali JG, Akyazi F, Stelinski LL, Edison AS, Schroeder FC, Teal PE.** 2012. Interspecific nematode signals regulate dispersal behavior. *PLoS One* **7**:e38735.
10. **San-Blas E, Gowen SR, Pembroke B.** 2008. *Steinernema feltiae*: ammonia triggers the emergence of their infective juveniles. *Exp Parasitol* **119**:180-185.
11. **San-Blas E, Pirela D, Garcia D, Portillo E.** 2014. Ammonia concentration at emergence and its effects on the recovery of different species of entomopathogenic nematodes. *Exp Parasitol* **144**:1-5.
12. **Martens EC, Goodrich-Blair H.** 2005. The *Steinernema carpocapsae* intestinal vesicle contains a subcellular structure with which *Xenorhabdus nematophila* associates during colonization initiation. *Cellular microbiology* **7**:1723-1735.

13. **Sicard M, Brugirard-Ricaud K, Pages S, Lanois A, Boemare NE, Brehelin M, Givaudan A.** 2004. Stages of infection during the tripartite interaction between *Xenorhabdus nematophila*, its nematode vector, and insect hosts. *Appl Environ Microbiol* **70**:6473-6480.
14. **Ehlers RU, Wulff A, Peters A.** 1997. Pathogenicity of axenic *Steinernema feltiae*, *Xenorhabdus bovienii*, and the bacto-helminthic complex to larvae of *Tipula oleracea* (Diptera) and *Galleria mellonella* (Lepidoptera). *J Invertebr Pathol* **69**:212-217.
15. **Brivio MF, Moro M, Mastore M.** 2006. Down-regulation of antibacterial peptide synthesis in an insect model induced by the body-surface of an entomoparasite (*Steinernema feltiae*). *Dev Comp Immunol* **30**:627-638.
16. **Orchard SS, Goodrich-Blair H.** 2004. Identification and functional characterization of a *Xenorhabdus nematophila* oligopeptide permease. *Appl Environ Microbiol* **70**:5621-5627.
17. **Richards GR, Goodrich-Blair H.** 2010. Examination of *Xenorhabdus nematophila* lipases in pathogenic and mutualistic host interactions reveals a role for *xlpA* in nematode progeny production. *Appl Environ Microbiol* **76**:221-229.
18. **Chapuis E, Emelianoff V, Paulmier V, Le Brun N, Pages S, Sicard M, Ferdy JB.** 2009. Manifold aspects of specificity in a nematode-bacterium mutualism. *J Evol Biol* **22**:2104-2117.
19. **Morales-Soto N, Forst SA.** 2011. The *xnp1* P2-like tail synthesis gene cluster encodes xenorhabdycin and is required for interspecies competition. *J Bacteriol* **193**:3624-3632.
20. **Bode HB.** 2009. Entomopathogenic bacteria as a source of secondary metabolites. *Curr Opin Chem Biol* **13**:224-230.
21. **Gulcu B, Hazir S, Kaya HK.** 2012. Scavenger deterrent factor (SDF) from symbiotic bacteria of entomopathogenic nematodes. *J Invertebr Pathol* **110**:326-333.
22. **Zhou X, Kaya HK, Heungens K, Goodrich-Blair H.** 2002. Response of ants to a deterrent factor(s) produced by the symbiotic bacteria of entomopathogenic nematodes. *Appl Environ Microbiol* **68**:6202-6209.
23. **Boemare NE, Akhurst RJ.** 1988. Biochemical and physiological characterization of colony form variants in *Xenorhabdus* spp. (Enterobacteriaceae). *J Gen Microbiol* **134**:751-761.
24. **Volgyi A, Fodor A, Szentirmai A, Forst S.** 1998. Phase Variation in *Xenorhabdus nematophilus*. *Appl Environ Microbiol* **64**:1188-1193.
25. **Murfin KE, Chaston J, Goodrich-Blair H.** 2012. Visualizing bacteria in nematodes using fluorescent microscopy. *J Vis Exp* doi:10.3791/4298.
26. **Bhasin A, Chaston JM, Goodrich-Blair H.** 2012. Mutational analyses reveal overall topology and functional regions of NilB, a bacterial outer membrane protein required for host association in a model of animal-microbe mutualism. *J Bacteriol* **194**:1763-1776.

27. **Heungens K, Cowles CE, Goodrich-Blair H.** 2002. Identification of *Xenorhabdus nematophila* genes required for mutualistic colonization of *Steinernema carpocapsae* nematodes. *Mol Microbiol* **45**:1337-1353.
28. **Veesenmeyer JL, Andersen AW, Lu X, Hussa EA, Murfin KE, Chaston JM, Dillman AR, Wassarman KM, Sternberg PW, Goodrich-Blair H.** 2014. NiID CRISPR RNA contributes to *Xenorhabdus nematophila* colonization of symbiotic host nematodes. *Mol Microbiol* **93**:1026-1042.
29. **Cowles CE, Goodrich-Blair H.** 2008. The *Xenorhabdus nematophila* *niABC* genes confer the ability of *Xenorhabdus* spp. to colonize *Steinernema carpocapsae* nematodes. *J Bacteriol* **190**:4121-4128.
30. **Lee MM, Stock SP.** 2010. A multilocus approach to assessing co-evolutionary relationships between *Steinernema* spp. (Nematoda: Steinernematidae) and their bacterial symbionts *Xenorhabdus* spp. (gamma-Proteobacteria: Enterobacteriaceae). *Syst Parasitol* **77**:1-12.
31. **Lee MM, Stock SP.** 2010. A multigene approach for assessing evolutionary relationships of *Xenorhabdus* spp. (gamma-Proteobacteria), the bacterial symbionts of entomopathogenic *Steinernema* nematodes. *J Invertebr Pathol* **104**:67-74.
32. **Teal TK, Lies DP, Wold BJ, Newman DK.** 2006. Spatiometabolic stratification of *Shewanella oneidensis* biofilms. *Appl Environ Microbiol* **72**:7324-7330.
33. **Bao Y, Lies DP, Fu H, Roberts GP.** 1991. An improved Tn7-based system for the single-copy insertion of cloned genes into chromosomes of gram-negative bacteria. *Gene* **109**:167-168.
34. **Okazaki S, Kaneko T, Sato S, Saeki K.** 2013. Hijacking of leguminous nodulation signaling by the rhizobial type III secretion system. *Proc Natl Acad Sci U S A* **110**:17131-17136.
35. **Daborn PJ, Waterfield N, Silva CP, Au CP, Sharma S, Ffrench-Constant RH.** 2002. A single *Photorhabdus* gene, makes caterpillars floppy (*mcf*), allows *Escherichia coli* to persist within and kill insects. *Proc Natl Acad Sci U S A* **99**:10742-10747.
36. **Goetsch M, Owen H, Goldman B, Forst S.** 2006. Analysis of the PixA inclusion body protein of *Xenorhabdus nematophila*. *J Bacteriol* **188**:2706-2710.
37. **Kandasamy S, Chattha KS, Vlasova AN, Rajashekara G, Saif LJ.** 2014. Lactobacilli and Bifidobacteria enhance mucosal B cell responses and differentially modulate systemic antibody responses to an oral human rotavirus vaccine in a neonatal gnotobiotic pig disease model. *Gut Microbes* doi:10.4161/19490976.2014.969972:0.
38. **Bennuru S, Meng Z, Ribeiro JM, Semnani RT, Ghedin E, Chan K, Lucas DA, Veenstra TD, Nutman TB.** 2011. Stage-specific proteomic expression patterns of the human filarial parasite *Brugia malayi* and its endosymbiont *Wolbachia*. *Proceedings of the National Academy of Sciences of the United States of America* **108**:9649-9654.

39. **Bouskra D, Brezillon C, Berard M, Werts C, Varona R, Boneca IG, Eberl G.** 2008. Lymphoid tissue genesis induced by commensals through NOD1 regulates intestinal homeostasis. *Nature* **456**:507-510.
40. **Chaston J, Goodrich-Blair H.** 2010. Common trends in mutualism revealed by model associations between invertebrates and bacteria. *FEMS Microbiol Rev* **34**:41-58.
41. **Reid G, Bruce AW, McGroarty JA, Cheng KJ, Costerton JW.** 1990. Is there a role for lactobacilli in prevention of urogenital and intestinal infections? *Clin Microbiol Rev* **3**:335-344.
42. **Prell J, Bourdes A, Kumar S, Ludwig E, Hosie A, Kinghorn S, White J, Poole P.** 2010. Role of symbiotic auxotrophy in the *Rhizobium*-legume symbioses. *PLoS One* **5**:e13933.
43. **Salem H, Bauer E, Strauss AS, Vogel H, Marz M, Kaltenpoth M.** 2014. Vitamin supplementation by gut symbionts ensures metabolic homeostasis in an insect host. *Proc Biol Sci* **281**.
44. **Chaston JM, Suen G, Tucker SL, Andersen AW, Bhasin A, Bode E, Bode HB, Brachmann AO, Cowles CE, Cowles KN, Darby C, de Leon L, Drace K, Du Z, Givaudan A, Herbert Tran EE, Jewell KA, Knack JJ, Krasomil-Osterfeld KC, Kukor R, Lanois A, Latreille P, Leimgruber NK, Lipke CM, Liu R, Lu X, Martens EC, Marri PR, Medigue C, Menard ML, Miller NM, Morales-Soto N, Norton S, Ogier JC, Orchard SS, Park D, Park Y, Qurollo BA, Sugar DR, Richards GR, Rouy Z, Slominski B, Slominski K, Snyder H, Tjaden BC, van der Hoeven R, Welch RD, Wheeler C, Xiang B, Barbazuk B, et al.** 2011. The entomopathogenic bacterial endosymbionts *Xenorhabdus* and *Photorhabdus*: convergent lifestyles from divergent genomes. *PLoS One* **6**:e27909.
45. **Xu J, Hurlbert RE.** 1990. Toxicity of Irradiated Media for *Xenorhabdus* spp. *Appl Environ Microbiol* **56**:815-818.
46. **Sicard M, Le Brun N, Pages S, Godelle B, Boemare N, Moulia C.** 2003. Effect of native *Xenorhabdus* on the fitness of their *Steinernema* hosts: contrasting types of interaction. *Parasitol Res* **91**:520-524.

CHAPTER 3

***Xenorhabdus bovienii* bacterial strain diversity impacts coevolution and symbiotic maintenance with *Steinernema spp.* nematode hosts**

This chapter is in press as:

Murfin KE, Lee MM, Klassen J, McDonald BR, Stock SP, Forst S, Currie CR, and Goodrich-Blair H. "*Xenorhabdus bovienii* bacterial strain diversity impacts coevolution and symbiotic maintenance with *Steinernema spp.* nematode hosts" mBio. 2015

ABSTRACT

Microbial symbionts provide benefits that contribute to the ecology and fitness of host plants and animals. Therefore, the evolutionary success of plants and animals fundamentally depends on long-term maintenance of beneficial associations. Most work investigating coevolution and symbiotic maintenance has focused on species level associations, and studies are lacking that assess the impact of bacterial strain diversity on symbiotic associations within a coevolutionary framework. Here, we demonstrate that fitness in mutualism varies depending on bacterial strain identity, and this is consistent with variation shaping phylogenetic patterns and maintenance through fitness benefits. Through genome sequencing of nine bacterial symbiont strains and co-phylogenetic analysis, we demonstrate diversity among *Xenorhabdus bovienii* bacteria. Further, we identified co-cladogenesis between *Steinernema feltiae* nematode hosts and their corresponding *X. bovienii* symbiont strains, indicating potential specificity within the association. To test specificity, we performed laboratory crosses of nematode hosts with native and non-native symbiont strains, which revealed that combinations with the native bacterial symbiont and closely related strains performed significantly better than those with more divergent symbionts. Through genomic analyses we also define potential factors contributing to specificity between nematode hosts and bacterial symbionts. These results suggest that strain-level diversity (e.g. subspecies-level differences) in microbial symbionts can drive variation in the success of host-microbe associations, and this suggests that these differences in symbiotic success could contribute to maintenance of the symbiosis over an evolutionary time scale.

IMPORTANCE

Beneficial symbioses between microbes and plant or animal hosts are ubiquitous, and in these associations, microbial symbionts provide key benefits to their hosts. As such, host success is fundamentally dependent on long-term maintenance of beneficial associations. Prolonged association between partners in evolutionary time is expected to result in interactions in which only specific partners can fully support symbiosis. The contribution of bacterial strain diversity on specificity and coevolution in beneficial symbiosis remains unclear. In this study, we demonstrate that strain-level differences in fitness benefits occur in beneficial host-microbe interactions, and this variation likely shapes phylogenetic patterns and symbiotic maintenance. This highlights that symbiont contributions to host biology can vary significantly based on very fine scale differences among members of a microbial species. Further, this work emphasizes the need for greater phylogenetic resolution when considering the causes and consequences of host-microbial interactions.

INTRODUCTION

Mutually beneficial symbiosis (i.e. mutualism) occurs in all domains of life and ecosystems, and its maintenance is critical to plant and animal ecology (1), evolution (2), and health (3-5). Coevolution (reciprocal evolution) and co-adaptation (coordinated mutual change of traits) between partner pairs shapes long-term maintenance of mutualisms and leads to specificity between hosts and symbionts, in that only particular potential partners can fulfill the needs of the symbiosis. Significant insights into mutualism have been gained by studying specificity and coevolution at the species-level or higher (6-8). However, animal- and plant-associated bacterial strains (members of a bacterial species as defined by molecular methods) can exhibit dramatic genomic and functional differences (9, 10). Also, host genotype x symbiont genotype x environment interactions likely influence coevolution, according to geographic mosaic theory (11). Indeed, within host-microbe associations, host genotype x symbiont genotype differences in mutualistic success have been identified (12-14). Furthermore, experimental studies have demonstrated coevolution between bacterial symbionts and nonnative hosts such that they better engage in symbiosis (15), as well as the influence of coevolution on competition among symbionts (16). However, lacking are studies that experimentally examine the influence of symbiont strain variation on specificity within a coevolutionary context. Such studies are necessary to better understand how symbiont diversity impacts co-adaptation, coevolution, and mutualism maintenance. In this study, we assessed the influence of bacterial strain diversity on specificity and coevolution in the association between *Xenorhabdus bovienii* bacterial symbiont strains and *Steinernema* spp. nematodes (Nematoda: Panagrolaimomorpha).

The life cycle of *Steinernema* nematodes and their proteobacterial symbionts of the genus *Xenorhabdus* (17) includes reproductive stages that requisitely occur within an insect host and an environmental nematode stage, the infective juvenile (IJ) (Figure 3.1) (18). IJs seek

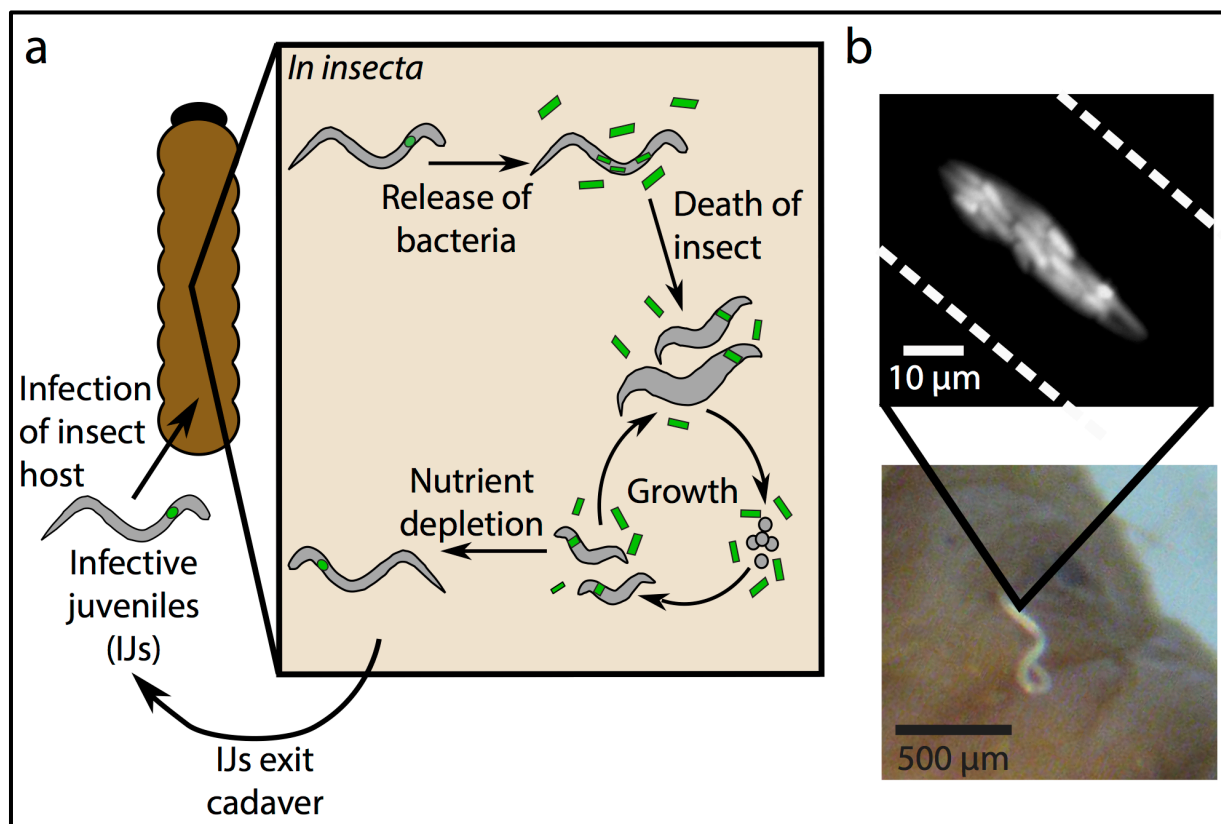


Figure 3.1 *X. bovienii* bacteria – *Steinernema* spp. nematode – *Galleria mellonella* insect interactions. (a) Schematic diagram of the nematode (grey) – bacterial (green) life cycle. All the events shown within the box occur within the insect host. (b) Image of interactions provided to show actual scale. The photograph shows an infective juvenile nematode newly emerged from a *G. mellonella* cadaver. Inset depicts a micrograph of bacteria within the nematode receptacle. Scale bar is 10 μm .

and invade the insect host, and the nematodes and bacteria kill the insect and reproduce within the cadaver (18, 19). When nutrients are depleted, the nematode progeny form the next generation of IJs (20). Previous studies on a selection of *Steinernema-Xenorhabdus* pairs have shown that the bacteria can contribute to virulence toward the insect host (21, 22) and support of nematode reproduction (19), but it is not known if these bacterial contributions occur in other nematode-bacterial pairs. This interaction is an obligate mutualism in some associations (17), where the nematodes cannot reproduce without the bacterial symbiont (Figure 3.1 a) and bacteria rely on the nematode host for transmission between insect hosts (Figure 3.1 b).

Xenorhabdus bovienii bacterial strains are broad host-range symbionts that associate with at least nine *Steinernema* nematode species from two phylogenetic sub-clades. Conversely, each of the nematode host species harbors only *X. bovienii* (23). This suggests that symbiotic maintenance and coevolution may depend on the bacterial sub-species (strain)-level diversity. To assess the impact of bacterial strain diversity within an evolutionary context, we integrated phylogenetic analysis and experimental crossing of symbionts to analyze the coevolutionary relationship and specificity between *X. bovienii* bacterial strains and their associated nematode hosts.

RESULTS

Genetic diversity of *X. bovienii* strains. Genetic variation among possible partner pairs is a pre-requisite for specificity in bacterial-host associations. To begin to understand the extent of genetic variation among *X. bovienii* strains, we conducted genomic comparisons of nine bacterial strains, identified as *X. bovienii* through 16S rRNA sequencing (Table 3.S1), isolated from six different nematode host species (24, 25). We sequenced and annotated the genomes, and the conserved homologs were compared for average nucleotide identity (ANI). All *X. bovienii* strains had ANI greater than 96% (Table 3.S2), further supporting that they belong to a

single species according to current standard criteria in microbial systematics (26).

To discern conservation and variation in gene content in the nine *X. bovienii* strains, we conducted gene content analyses using the MaGe platform (27, 28). We found that approximately 55% of the genome content is shared by all strains, and approximately 94% is shared with at least one other strain, with a range of <1% to 9% of genes being unique to an individual strain (Table 3.S3). Since these unique genes may represent specificity determinants, we analyzed their possible functions suggested by annotation (Table 3.S3). Within each strain, the most highly represented gene category was that of unknown function. Additionally, unique genes in some strains are predicted to encode membrane or secreted proteins (e.g. putative toxins), which might be expected to interact with nematode or insect hosts (Table 3.S3). Other genes identified in this analysis included those of predicted metabolic or cellular function and mobile genetic elements (Table 3.S3). Although examination of the flexible gene content of the *X. bovienii* strains awaits a more detailed analysis, in total these data indicate a large spectrum of genetic diversity, and therefore differences in functional potential among *X. bovienii* bacterial strains. These results strengthen the idea that specificity and coevolution among partner pairs may be occurring between *Steinernema* spp. hosts and their native *X. bovienii* partners.

Co-phylogenetic analysis. Specificity between partner pairs is expected to arise through coevolution occurring during long-term maintenance of symbioses. Therefore, to focus our attention on those partner pairs most likely to exhibit specificity, we used phylogenetic analyses to assess the potential for coevolution, as evidenced by co-cladogenesis (identical topologies) between symbiont and host phylogenetic trees. A previous phylogenetic study using a multi-locus approach revealed instances of co-diversification (similar but not identical tree topologies) in some but not all *X. bovienii* – *Steinernema* spp. associations, suggesting that fine scale specificity between hosts and symbionts may occur (24). To generate more refined phylogenetic

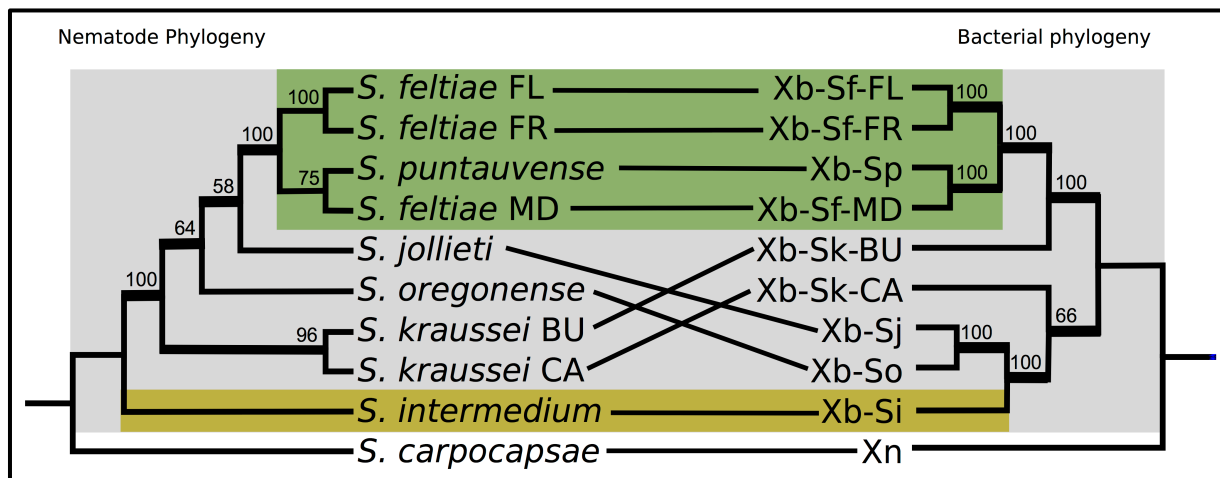


Figure 3.2 Co-phylogeny of nematode spp. hosts and bacterial symbiont strains. Numbers indicate bootstrap values and thicker lines indicate posterior probabilities greater than 0.9. All posterior probabilities were greater than 0.8. Shaded boxes indicate clades of nematodes with their respective symbionts: *X. bovienii* nematode hosts (grey), *S. feltiae* and *S. punctauvense* nematodes (green), and the distantly related nematode *S. intermedium* (yellow).

inferences we used conserved homologs from whole bacterial genome content to construct the bacterial phylogeny. Co-phylogenetic analyses (Figure 3.2) revealed congruencies between the *X. bovienii* phylogeny (Figure 3.S1a) and the *Steinernema* host phylogeny (Figure 3.S1b). Specifically, the co-phylogeny provides robust support for co-cladogenesis between the group of *S. feltiae* and *S. punctauvense* bacterial symbiont strains, which is supported by statistical evidence. For the nine *X. bovienii* strain genomes, there are 2,027,025 possible rooted trees. Of these, only 14,175 (0.7% of the total) contain a monophyletic clade consisting of the four bacterial strains from the *S. feltiae* and *S. punctauvense* nematode isolates. Furthermore, in only 945 of the possible trees (0.05% of the total) does the topology of the bacterial tree match identically with the nematode tree, indicating that the bacterial monophyletic clade is unlikely to occur by random chance. This statistical permutation test provides strong evidence that the *S. feltiae* and *S. punctauvense* nematode isolates and their bacterial symbiont strains share a common evolutionary history, and it is likely that specificity is occurring between these partner pairs. In contrast, among other nematode isolates and bacterial strains, host switching has occurred, including one bacterial strain, Xb-Si, which associates with a nematode of another clade, *S. intermedium*. Host switching within some but not all parts of the nematode-bacterial phylogeny indicates that not all pairings are strictly maintained. Therefore, there are likely divergent maintenance pressures impacting the different nematode-bacterial pairings.

Experimental testing of mutualistic interactions. As an experimental test of specificity and coevolution, we examined the ability of nematode-bacterial pairs to engage in mutualism through experimental co-injections of three *S. feltiae* nematode isolates and nine *X. bovienii* bacterial strains (Fig. S2). Nematodes and bacteria were reared separately, mixed, and co-injected into *Galleria mellonella* (Lepidoptera: Pyralidae) larvae. The progression of the life cycle (Figure 3.1 a, Fig. S2) was then monitored for virulence (percent mortality of the co-

injected insects), productive infection (percent of insect cadavers that produced progeny), progeny number (average number of progeny per productive infection), progeny infective potential (ability of the progeny IJs to seek, invade and kill an insect host), and bacterial carriage (average colony forming units per IJ). To assess these traits within a phylogenetic framework, we used linear regression to compare the measurements to bacterial and nematode phylogenetic distance, Bayesian tree distance (i.e. branch lengths from the consensus Bayesian tree between the native pair and the tested bacterial strain or its host). This analysis enables the comparison of the experimental data to the strongest phylogenetic trend within the bacterial strains to link performance in mutualism with evolutionary history. Certain nematode-bacterial combinations displayed a large amount of trial-to-trial variability, possibly due to seasonal fluctuations or the use of outbred insect and nematode lines. Due to the lack of an inbred insect line, we controlled for differences among insect hosts by limiting insect size variation and randomizing insects among treatments. To address genetic differences between biological replicates and to control for seasonal fluctuations, data were normalized relative to the native combination within each experiment. While variation remains large in some cases, trends (e.g. slope of the linear regression lines) were similar across trials.

With respect to virulence, some combinations showed significant differences when compared by log-rank analysis, measuring the overall trends within a survival curve (Table 3.S4). However, linear regression analysis did not show significant correlations between the phylogenetic framework and individual measurements of virulence, such as LT50 values (e.g. the time at which half the insects have died), which suggests the differences do not reflect coevolution (Table 3.S5). As expected, *S. feltiae* FL and *S. feltiae* FR nematodes alone killed fewer insects than nematode-bacterial combinations, indicating *X. bovienii* bacteria contribute to virulence (Table 3.S4, $p < 0.05$). Similarly, *S. feltiae* MD nematodes were significantly more virulent by log-rank test when associated with six of the bacterial strains (Table 3.S4, $p < 0.05$),

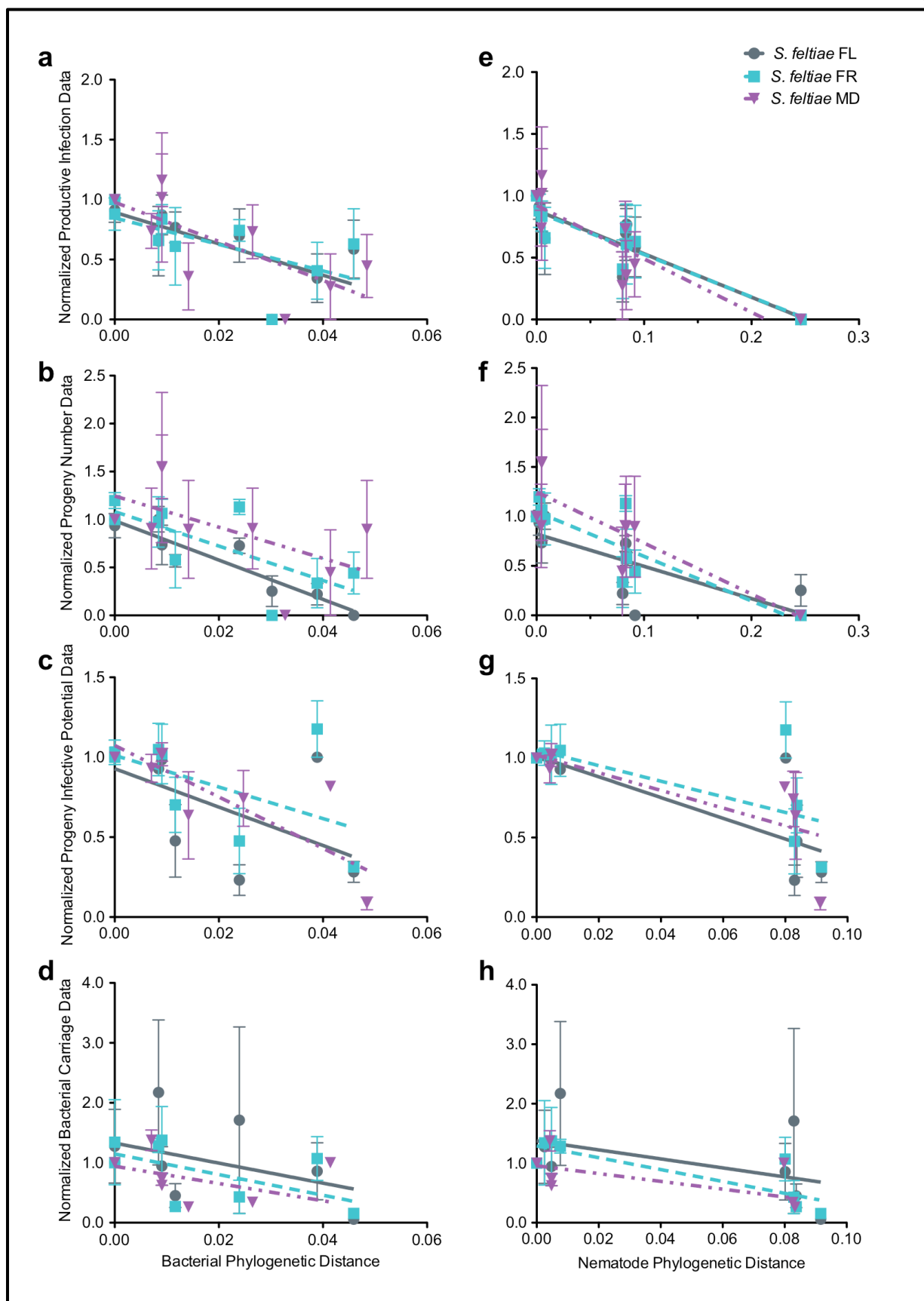


Figure 3.3 Measurement of mutualistic interaction parameters. Individual parameters of the progression of the nematode-bacterial life cycle were measured with respect to bacterial and nematode phylogenetic distance, including (a, e) productive infection percentage, (b, f) progeny number (c, g), progeny infective potential and, (d, h) bacterial carriage. Phylogenetic distance was taken as Bayesian tree distance from the native combination. Data points represent averages of the measurements for each set of data (n=3), and error bars represent standard error. Lines show linear regression for each set of data points (Table 3.S5). All regressions display a significant negative correlation (r -squared > 0.2 , $p < 0.01$) for productive infection percentage, progeny number, and progeny infective potential, except for progeny number of *S. feltiae* MD (r -squared = 0.11, $p = 0.089$). The correlation of bacterial carriage for *S. feltiae* FR and *S. feltiae* MD with respect to nematode phylogenetic distance was also significant.

though there was no significant difference when combined with the three other strains (Table 3.S4). This suggests that *S. feltiae* MD is less reliant than the other nematodes on its bacterial symbiont for virulence. By seven days post injection, there were no significant differences among the nematode-bacterial combinations in the percentages of insects they killed (Table 3.S4). Therefore, minor differences in virulence among the nematode-bacterial combinations likely do not significantly impact the mutualism.

With regard to nematode progeny characteristics, significant differences were identified among different nematode-bacterial pairings relative to bacterial phylogenetic distance, or divergence from the native symbiont. Injections of nematodes alone resulted in no production of progeny, supporting that bacterial symbionts contribute to *S. feltiae* nematode reproduction (data not shown). Both the ability to produce progeny (productive infection percentage and progeny number) and the infective potential of those progeny correlated with the bacterial phylogenetic distance; as bacterial strain divergence increased the success of the interaction decreased (with one exception, the number of *S. feltiae* MD progeny) (Figure 3.3 a-c, Table 3.S5). Although bacterial carriage in nematode progeny also shows a negative trend with respect to phylogenetic distance (Figure 3.3 d), this was not significant (Table 3.S5). Productive infection percentage, progeny number, and progeny infective potential also strongly correlate with nematode host phylogenetic distance (Figure 3.3 e-g, Table 3.S5), indicating that bacteria from hosts more closely related to the *S. feltiae* nematodes are better able to engage in symbiosis than bacteria from more distantly related hosts.

Because the infective potential of the nematode progeny is integral to subsequent nematode reproduction and therefore evolutionary success, we examined potential causes of defects in nematode progeny infective potential. However, we found no significant correlation between bacterial phylogenetic distance and progeny IJ longevity (Figure 3.S3 a) or IJ

development as assessed by morphology (Fig. S3b, c), indicating these parameters do not affect progeny infective potential.

Nematode and bacterial strain fitness. Experimental testing suggests that interactions between the nematode host and bacterial strains closely related to its native symbiont are more efficacious than those with divergent symbionts. We evaluated this trend using linear regression analysis of nematode reproductive fitness (i.e. total number of progeny, the product of productive infection percentage and progeny number) relative to bacterial (Figure 3.4 a, Table 3.S5) and nematode (Table 3.S5) phylogenetic distance. There was a significant negative relationship for each nematode isolate (Table 3.S5), demonstrating that nematode fitness is highest with strains closest to its native bacterial partner or isolated from closely related hosts.

To measure bacterial fitness within each combination, we calculated the total number of bacteria that are transmitted to the next generation. Because bacteria are only transmitted through the IJ progeny, this is defined as the product of nematode reproductive fitness and bacterial carriage. Using linear regression, a significant negative trend was observed between bacterial fitness and either bacterial phylogenetic distance (Figure 3.4 b, Table 3.S5) or nematode phylogenetic distance (Table 3.S5), indicating that bacterial fitness when associating with *S. feltiae* is proportional to how similar the bacterium is to the native symbiont and how similar its native host is to *S. feltiae*. Although absolute bacterial carriage per IJ showed a negative trend observed among strain combinations, the correlation was not significant (Figure 3.3 dh, Table 3.S5), indicating nematode reproductive fitness contributes more than carriage rate to bacterial fitness.

The data show a clear trend that strains within the same phylogenetic clade as the natural symbiont provide greater benefits than those from different clades (Figure 3.4 c). This indicates that closely related strains (those that fall within the same clade as the native

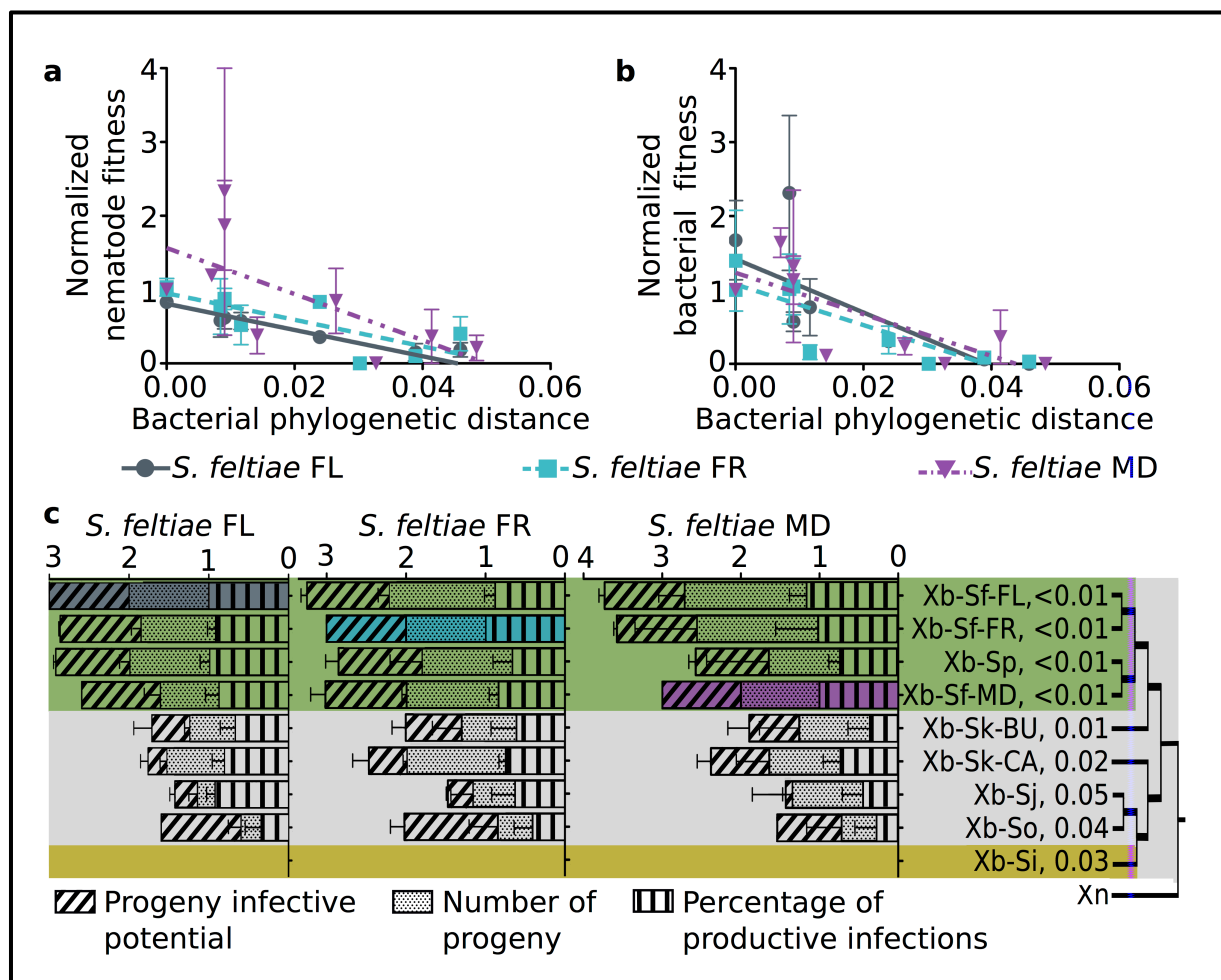


Figure 3.4 Nematode and bacterial combinations show measurements consistent with coadaptation. Graphs show linear regression analyses of normalized values of (a) nematode and (b) bacterial fitness relative to bacterial phylogenetic distance. Data points represent averages of the measurements for each set of data ($n=3$), and error bars represent standard error. Lines show linear regression for each set of data points (Table 3.S5). Both linear regressions had a significant negative correlation ($r\text{-squared} > 0.16$, $p < 0.04$). In the stacked bar graph (c), the differing mutualistic interaction parameters are compared to the bacterial phylogeny with coloring from Figure 3.2. Filled bars indicate the natural combination, and values next to terminal branches indicate Bayesian tree distance from Xb-Sf symbionts.

symbiont) may be functionally redundant in hosts, which in turn suggests that *S. feltiae* and *S. puntauvense* nematode isolates require the same goods and services from their symbiont. In contrast, more distantly related strains were defective in varying parameters of mutualistic support of nematode fitness (e.g. Xb-Sj has more of a defect in progeny infective potential than Xb-So, which has a greater defect in productive infection percentage), suggesting not all *X. bovienii* bacterial strains are functionally redundant within nematode hosts (Figure 3.3 , 4c).

The observed negative trends might be caused by bimodal or distributed variations in strain contributions to fitness. Distributed variation is supported by the fact that negative trends remained similar (e.g. negative slope of the same magnitude) when only the symbionts outside of the native clade were considered (data not shown). To examine this further, the effects of the native clade data points on the linear negative trends relative to bacterial phylogenetic distance (Figure 3.3, Table 3.S5) were analyzed by computing Cook's distance (29). Linear regressions for each trend containing all 5 strains outside the native clade and one data point representing the average of all symbionts from the native clade were constructed and used for the analyses. In all trends tested but one, the Cook's distance of the point representing the native symbiont clade was less than one, indicating that this data point was not influential on the overall trend (Table 3.S6). Therefore, the observed trends depend on the varying results from all bacterial strains, not just a gross difference between bacteria that fall within the clade versus those outside of the clade. The one trend that was dependent on inclusion of the native symbiont clade in the analyzed data was bacterial carriage by *S. feltiae* MD. However, the high variability of the data underlying this particular trend likely caused dramatic impacts on regression curves when individual data points were removed.

X. *bovienii* bacterial genes contributing to specificity. Fitness benefit differences among the bacterial strains is unexpected in light of their close phylogenetic relationship: One explanation

for the observed fitness advantages of *X. bovienii* within the *S. feltiae* and *S. punctauvense* clade symbionts is variation in shared bacterial genes which could alter functionality and/or cause incompatibility between hosts and symbionts. Such genes are expected to be under positive selection across all bacterial symbionts or within specific group, such as the *S. feltiae* and *S. punctauvense* clade. However, due to the close similarities of the bacterial strains we were unable to reliably detect positive selection through dN/dS analysis.

Another explanation is that *S. feltiae* and *S. punctauvense* symbionts as a group uniquely encode or lack genes that impact fitness. The increased fitness of these symbionts relative to other strains may be due to the presence of genes that are absent in other bacterial strains that increase their ability to support symbiotic interactions or the absence of genes that are present in other bacterial strains that have deleterious effects on the nematode host. To assess which genes follow this pattern, we identified genes, based on sequence identity and clustering, that were significantly overrepresented or underrepresented in the symbionts of *S. feltiae* and *S. punctauvense* compared to the other *X. bovienii* strains (Fig. S4). Among the identified families, the most common were of unknown function, representing 80% of overrepresented genes and 54% of underrepresented families. Families of mobile genetic elements were the second most abundant, comprising 4% of overrepresented genes and 38% of underrepresented genes. Other families were those predicted to be involved in primary and secondary metabolism, toxins, and toxin/antitoxin systems. Genes involved in metabolism are potentially important in the symbiosis due to their possible nutritional role. Among the overrepresented metabolic genes (Fig. S4) were two (*azlC* and *azlD*) predicted to encode components of a branched chain amino-acid transporter and one predicted to encode an associated transcriptional regulator (*rhaR*). Genes from these three families, as well as another of unknown function (listed in the metabolism group), are clustered together in a putative operon that is only present in the *S. feltiae* and *S. punctauvense* symbionts. Toxins may also be involved in symbiosis specificity due to their

potential role in defensive symbiosis. Additionally, toxin-antitoxin modules have been implicated in ensuring symbiont transmission through regulation of symbiosis genes (30). However, elucidation of the role of these gene families awaits further functional analyses.

The presence or absence of specific genes within the *S. feltiae* and *S. puntauvense* clade symbionts likely reflects the coevolution between these symbionts and their specific hosts. It is possible that the symbionts within the clade have gained or lost certain genes due to the requirements of the nematode host. However, it is also possible that the nematode host has evolved to in response to the bacterial products (e.g. now the host requires nutrients because the bacterium could produce them). In either case, the partners are a coevolved unit.

CONCLUSIONS

The observed negative correlation between symbiotic success and the phylogenetic framework supports two overarching ideas. First, the correlation suggests that in the *S. feltiae*-*X. bovienii* symbiosis, specificity likely is due to coadaptation between symbionts and hosts, with the bacterial symbiont and/or the host being coevolved to fill the needs of the other partner. Additionally, the fact that the observed fitness trends are inversely correlated with nematode host phylogenetic distance, in some cases more strongly than with bacterial phylogenetic distance (Table 3.S5), provides compelling evidence that the nematode host with which a symbiont associates is a contributing factor to the correlation. This idea is further supported by our finding that the bacterial strain that associates with the most phylogenetically distant nematode host, Xb-Si, is unable to engage in any aspect of mutualism with *S. feltiae*, even though it is not the most distantly related bacterium from the native symbiont (Figure 3.4 c). Xb-Sj is the most distantly related symbiont, but it is able to engage in symbiotic interactions (Figure 3.3, 4c).

The second fundamental concept supported by our experimental data is that animal hosts can receive significantly different fitness benefits when associating with divergent bacterial symbiont strains, and such variation could contribute to the evolution of specificity within a symbiosis. Coevolution and coadaptation may be caused by nematode adaptation to unique provisions of particular bacterial strains or by bacterial strain adaptation to fulfilling the specialized needs of a nematode host. In either case, the nematode-bacterial pairings are coevolved units; their life histories are intertwined, and the fitness of each depends on their combined success. The two overarching ideas supported by our data are likely true within other symbioses. Indeed, recent studies have revealed that strain level symbiont variability impacts the success of the squid-*Vibrio* (14) and legume-*Rhizobium* (12, 13) symbioses, although these studies did not assess the impact of variability with relation to coevolution.

Our data are based on experimental laboratory crosses, but the findings are likely to be ecologically relevant, as mixed infections with multiple nematode hosts and symbionts can occur (31). In fact, nematode isolates of three of the host species relevant to our study (*S. feltiae*, *S. kraussei*, and *S. intermedium*) have been isolated in close proximity (32), although the isolates used here were not. Because mixed infections can lead to non-native crosses of nematode hosts and bacterial symbionts, variations in benefits could play a significant role in driving maintenance of partner pairs. Greater benefits of some associations relative to others could provide positive feedback for the evolutionary maintenance of the mutualism (i.e. increased evolutionary success) and therefore selective pressure that results in the observed phylogenetic patterns (Figure 3.5). This is consistent with the theory of partner fidelity feedback, where linkages in host and symbiont fitness provide positive reinforcement that stabilizes the mutualism(2). A partner fidelity feedback mechanism is further supported by the fact that *S. feltiae* nematodes and *X. bovienii* bacteria cannot separately complete their life cycles (Figure

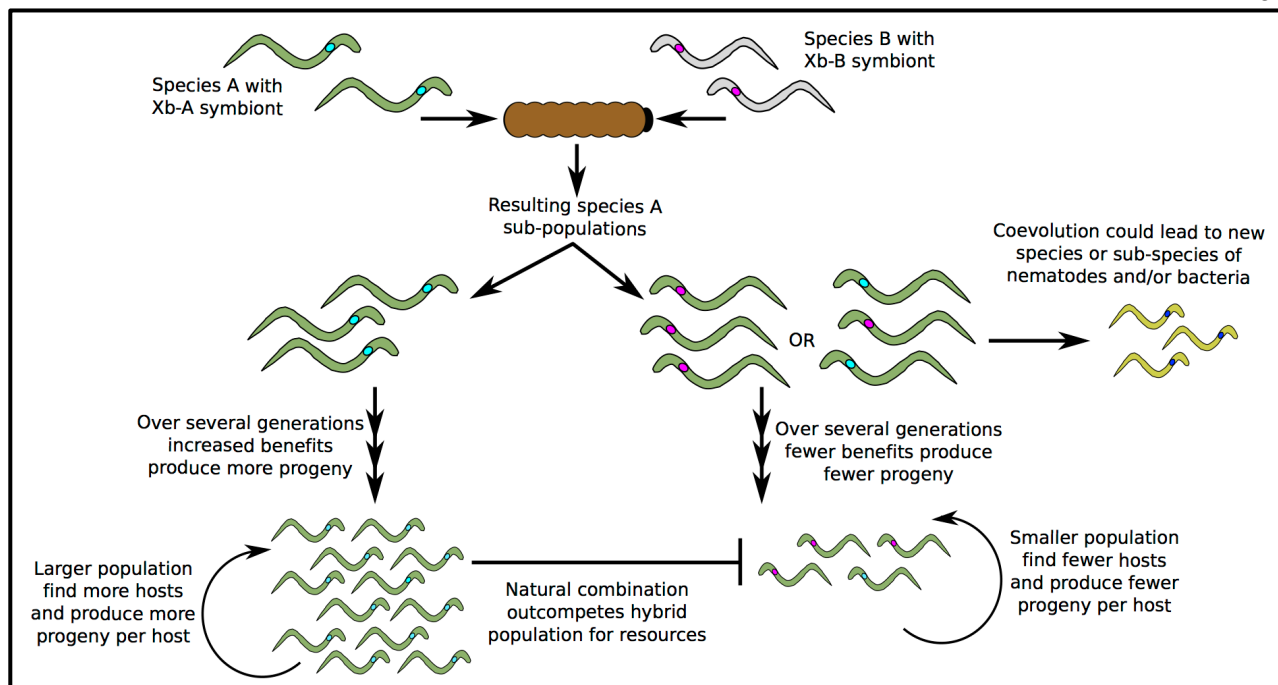


Figure 3.5 Contribution of increased benefits in maintenance of symbiosis. The schematic above describes how increased benefits of the native pairing could serve to reinforce partner fidelity within a symbiosis and therefore contribute to symbiotic maintenance. The different colors represent divergent nematode species or bacterial strains.

3.1 b, data not shown). Our data extend current theory by demonstrating that bacterial strain diversity can drive partner fidelity feedback for maintenance of mutualisms.

Diversity in the goods and services that are integral to symbiotic function are likely responsible for variations in symbiotic success. One mutualistic role that bacterial symbionts can perform is defensive, where the symbiont provides protection of the host against specific pathogens, competitors, or predators. For example, this type of function can be conferred by secondary symbionts of aphids, where the bacterial symbiont contributes to protection against a parasitoid wasp predator of the aphid host. In some of these associations protection is conferred by a phage-encoded toxin, but this mechanism is not conserved among all secondary symbionts (33). Similarly, specialized toxins or secondary metabolites produced by some but not all *X. bovienii* may contribute to nematode host defense against organisms within the insect host, as is true for *X. nematophila* (34, 35). In the absence of the defensive compound, the nematode host may be killed before establishing a new infection or suffer from population losses that result in fewer progeny. Alternatively, since some classes of *Xenorhabdus* toxins are insecticidal (36), variations in symbiont-encoded toxins could influence the efficiency of insect host killing, as well as the insect host range of the nematode. Finally, symbiont-derived toxins may have nematocidal effects, to which the native nematode host is resistant. In a non-native pairing, such a nematocidal activity obviously would have a detrimental impact.

Many of the genes identified as unique (Table 3.S3) or enriched (Fig. S4) within the *X. bovienii* bacterial strains could encode defensive factors. For example, unique and enriched genes included those encoding exported proteins of unknown function, non-ribosomal peptide synthetases (NRPS), polyketide synthetases (PKS), and a predicted Shiga toxin. NRPS-PKS gene clusters are of particular interest as they synthesize small molecules (secondary metabolites) that have a variety of biological activities, such as antimicrobial (37-39), hemolytic (39), and immunosuppressive (40) effects, which could serve as defensive factors. Indeed, a

fungal endosymbiont NRPS gene cluster provides plants protection from insect feeding (41). Also of interest is the putative Shiga toxin that among the tested *X. bovienii* strains is uniquely encoded by Xb-Si. Shiga toxins affect lipid bi-layers and have cytotoxic activities that allow bacterial pathogens to cause disease within eukaryotic hosts (42). Such a toxin could be involved in pathogenesis towards the insect host or in defense. Indeed, the presence of this toxin may be responsible for the inability of Xb-Si to support symbiosis with *S. feltiae* nematodes (Figure 3.4 c), as it could have a cytotoxic affect in the *S. feltiae* nematodes.

Another basis for many symbiotic relationships is the mutually beneficial exchange of nutrients between host and symbiont, and integration of nutritional requirements could influence co-adaptation. It has been proposed that *Xenorhabdus* bacteria provide nutritional support to the nematode host, and lack of this support leads to decreased ability to produce progeny(19, 43). Consistent with this, *S. feltiae* nematodes are unable to reproduce within the insect host without their bacterial symbionts (data not shown), possibly due to a lack of specific nutrients. Further corroborating this idea, we observed that among the *S. feltiae/S. puntauvense* symbionts there was an over-representation of genes predicted to encode branched-chain amino acid transporter systems, which could contribute to nutritional support of nematode reproduction or infective potential. Branched chain amino acid transport influences *Rhizobia* nodulation on plants, with varying phenotypes depending on the plant host (44). Thus, variability in symbiont amino acid transport capability, coupled with variation in nematode host requirements for certain amino acids, could help explain some fitness differences.

There is increasing recognition that beneficial microbes profoundly impacted the origin and evolution of animals (4), and studies have implicated symbiosis in host speciation through reproductive isolation (8). These phenomena depend on symbioses being maintained throughout the evolutionary history of the host organism. We show this maintenance is shaped by bacterial strain diversity, highlighting that the contributions of symbionts to host biology can

vary significantly based on differences among members of a microbial species. Furthermore, this finding suggests that in addition to current studies of microbiota that identify microbes by the species or phylum level, a comprehensive understanding of the causes and consequences of host-microbial interactions will require the use of greater phylogenetic resolution and classification through evolutionary and functional characterization.

ACKNOWLEDGMENTS

The authors thank Adler Dillman, John Chaston, Michael Gebre and Byron Adams (Brigham Young University), for the *S. feltiae* MD nematode isolate and Lorena Uribe-Lorío (ICBCM, Universidad de Costa Rica) for the *S. puntauvense* nematode isolate. The authors also acknowledge the College of Agriculture and Life Sciences Statistical Consulting Group for support in statistical analyses and MaGe for genome annotation and analysis. This study was supported by a collaborative grant from the National Science Foundation to HGB (IOS-0920631), SF (IOS-0919912) and SPS (IOS-0919565). KEM also was supported by the National Institutes of Health (NIH) National Research Service Award T32 AI55397 and a Louis and Elsa Thomsen Distinguished Predoctoral Fellowship. BRM was supported by the NIH National Research Service Award T32 GM07215 and the Department of Energy Great Lakes Bioenergy Research Center (DOE Office of Science BER DE-FC02-07ER64494). JLK was supported by the National Science and Engineering Research Council of Canada (NSERC Canada) Postdoctoral Fellowship.

MATERIALS AND METHODS

Bacterial Strains and Nematode Isolates. Bacterial strains were obtained by sonication of nematode hosts after surface sterilization. Strain identity was confirmed by analysis of 16S rRNA from whole genome sequence (25, 43) and average nucleotide identity (26). Bacterial strains were stored in Lysogeny Broth (LB) supplemented with 20% glycerol frozen at -80°C. Bacterial cultures were grown at 30°C in LB that had not been exposed to light with aeration or on LB agar with 0.1% pyruvate (45). *S. feltiae* nematode isolates used were obtained from the laboratories of Dr. Patricia Stock or Dr. Byron Adams (via Adler Dillman) and were verified through sequencing of the 12S and 28S genes (24). Nematodes were propagated through *Galleria mellonella* larvae (46). Axenic IJs were produced *in vitro* as previously described (47, 48). Nematodes were stored at 25°C in 250 ml tissue culture flasks (BD Falcon, Franklin Lakes, NJ, USA) at a density of 5-10 IJs/ μ l and a volume less than 60 ml.

Gene and Genome Sequencing and Assembly. Nematode 12S and 28S rRNA genes were sequenced as previously described (49), and sequences were submitted to NCBI. Bacterial genomes were sequenced using Illumina paired-end libraries (mean insert length = 300bp) and quality trimmed using DynamicTrim.pl v.1.10 in the solexQC package. Dynamic trimming was according to TrimAl's, v1.2rev59 (50) default settings. After excluding reads <20 bp and lacking barcode sequences, genomes were assembled with VELVET v.1.1.06 (51, 52) using automatic determination of sequencing coverage and a series of kmer values. Draft genomes were annotated using MaGe (27, 28) and submitted to EMBL. 16S rRNA sequences from draft genomes were assessed using BLASTn (<http://blast.ncbi.nlm.nih.gov>) and were submitted to GenBank (Table 3.S1).

Phylogenetic Analysis. For bacterial phylogenies, MaGe was used to identify homologs (genes with conserved synteny with $\geq 30\%$ nucleotide identity over $\geq 80\%$ of the length) present in the *X. bovienii* and *X. nematophila* genomes, yielding 2,166 gene sets. Sets were excluded if any genome possessed multiple homologs (putative paralogs), resulting in 1,893 ortholog sets. Nematode genes and ortholog sets were corrected using ORFcor v1.02 (53). The corrected sets were aligned using MUSCLE v3.7 (54, 55), and poorly aligned regions were excluded using TrimAl v1.2rev59 (50). Genes were concatenated into a single alignment (1,867,725 bp total). Maximum likelihood analyses were performed in RAxML v7.2.8(56) using the GTRGAMMA substitution model with rapid bootstrapping of 1000 bootstrapping replicates, as optimized by jModelTest v2.1.4 (57). Bayesian analyses were done using Mr Bayes v3.2.1(58). For the nematode tree, posterior probabilities were sampled from 4,000,000 MCMC replicates, with the first 1,000,000 discarded as burn-in. Using the GTR+Gamma substitution model, the final standard deviation of split frequencies was 0.0081. For the bacterial tree, posterior probabilities were sampled from 1,000,000 MCMC replicates, with the first 250,000 discarded as burn-in. The GTR+Gamma substitution model was used, as were the following non-standard parameters to optimize MCMC sampling: 2 runs, each 5 heated + 1 cold chain, Multiplier(V) $\lambda = 0.05$ and TLMultiplier(V) $\lambda = 0.05$. Topologies of nematode and of bacterial phylogenies were identical from both methods. Distance trees were viewed and drawn in iTol (59).

Testing of mutualistic interactions. Virulence assays: Fifth instar *G. mellonella* larvae (Grubco, Hamilton, OH) were used for injections. Overnight cultures of bacteria were subcultured 1:100 into LB, grown to $OD_{600} \sim 0.65$, and diluted in Grace's Insect Medium (Sigma, St. Louis, MO) to inject 200 CFUs in 10 μ l. Prior to injections, test OD measurements and CFU counting by dilution plating were done to ensure that equal CFU counts were used for all strains. Axenic nematodes were surface sterilized and diluted in Grace's medium to inject 50 IJs in 10

µl. For co-injections, bacteria and nematodes were prepared as above and combined for injection with 200 CFU of bacteria and 50 IJs in 10 µl. Virulence was measured as percent survival, with assessment every 24 hours for 7 days. Insects were considered dead when they no longer responded to gentle prodding. Twelve insects were injected per treatment, and three experimental replicates were performed.

Productive infection percentage: Insect cadavers obtained from injection assays were placed individually in a modified White Trap (60) at day 7 post injection and observed for progeny emergence daily for up to one month. Cadavers producing at least 100 IJs were scored as productive, and productive infection percentage was calculated as the number of cadavers producing progeny out of the total number. Three experimental replicates were performed.

Progeny Number: The numbers of IJs produced from each insect cadaver was determined by removing and measuring water from each white trap and counting the number of IJs/ml. IJs were counted every other day for 16 days and on day 28, and the total number of IJs was calculated. Three biological replicates were performed. IJ progeny were collected for 10 days from the average first day of emergence, pooled together, and stored for use.

Progeny Infective Potential: Progeny infective potential was determined through a modified sand trap assay (61), using 50 IJs in 100 µl of water. Two technical replicates of 12 *G. mellonella* larva were used per pool of progeny. Mortality was monitored every 8 h for 96 h. Three biological replicates were performed. For linear regression, percent mortality at 48 hours was used, as it showed the largest difference between combinations.

Bacterial Carriage: Bacterial symbiont carriage was determined similarly to a previously described method (62) through surface sterilization, grinding of progeny nematodes, and dilution plating. Two technical replicates and three biological replicates were performed.

Progeny IJ Longevity: Progeny IJs were stored for 6 months post emergence and then examined at 3x magnification. Dead nematodes were straight and/or showed no movement,

whereas live nematodes had a curved appearance or were moving. IJs were confirmed as dead by gentle prodding. Two technical replicates of at least 100 IJs were counted, and three biological replicates were performed.

Morphometric Analysis: 10 mL progeny IJs were heat killed in M9 buffer at 60°. Heat-killed IJs were fixed in triethanolamine formalin (TAF) at 60°C (63) and mounted on glass slides for morphometric analysis. Quantitative measurements (length and width) were made using an Olympus BX51 microscope with Olympus Microsuite software (Soft Imaging System Corp., Ca., USA).

Comparative genomics. dN/dS analysis: Analysis was done using PAML v4.7 (64). Protein sequences of bacterial homologs (see phylogenetic analysis) were aligned using the e-nsi-i algorithm implemented in MAFFT v7.029 (65) and converted to codon alignments. The branch model was used to test for positive selection in the *X. bovienii* clade, and a dN/dS cutoff of 1-6 with at least 2% amino acid divergence was used (66).

Overrepresented and underrepresented gene sets: Protein sequences were downloaded from MaGe and annotated using HMMer models for KEGG (<http://nar.oxfordjournals.org/cgi/pmidlookup?view=long&pmid=24214961>) and PFAM (67). Sequences were clustered *de-novo*, based on amino acid sequence identity (25% sequence identity and 50% coverage), using proteinortho5 (<http://www.biomedcentral.com/1471-2105/12/124>). Fisher's exact test, implemented by python package scipy (<http://www.scipy.org>), was used to identify gene families or domains that were over or under represented in a particular clade. A cutoff of $p < 0.05$ was used to determine significance.

Statistics. The co-phylogeny was statistically measured by a permutation test. The total number of possible *X. bovienii* trees was compared to number of possible trees that contained

the monophyletic group of *S. feltiae* and *S. puntauvense* symbionts and to the number of possible trees with identical topology in bacterial monophyletic group (68). The number of trees with a given split is the product of rooted trees for each half.

Statistical analyses for experimental testing were performed in R (69) or Prism (GraphPad). For virulence assays, log rank test and LT50 calculation was done. In log-rank analysis, all data points from the three experimental replicates were combined. Each experimental block was also analyzed separately, and trends remained the same. For experimental testing of mutualistic interactions, linear regression analyses was done to determine R-squared values, and p-values of trends. The data was normalized to the native combination (all values were divided by the value of the natural combination). Technical replicates were averaged and plotted versus the phylogenetic distance of the bacterial symbiont or nematode host of the bacterial symbiont, Bayesian tree distance from the native combination. The data was also compared to ANI and maximum likelihood tree distance with similar results. Cook's distance for each trend was computed using a linear regression constructed from all symbionts outside the native clade (i.e. Xb-Si, Xb-Sj, Xb-Sk-BU, Xb-Sk-CA, Xb-So) plus one data point of the average of the native clade (i.e. Xb-Sf-FL, Xb-Sf-FR, Xb-Sf-MD, Xb-Sp). A Cook's distance >1 was considered influential.

REFERENCES

1. **Saavedra S, Stouffer DB, Uzzi B, Bascompte J.** 2011. Strong contributors to network persistence are the most vulnerable to extinction. *Nature* **478**:233-235.
2. **Weyl EG, Frederickson ME, Yu DW, Pierce NE.** 2010. Economic contract theory tests models of mutualism. *Proc Natl Acad Sci U S A* **107**:15712-15716.
3. **Berg G.** 2009. Plant-microbe interactions promoting plant growth and health: perspectives for controlled use of microorganisms in agriculture. *Appl Microbiol Biotechnol* **84**:11-18.
4. **McFall-Ngai M, Hadfield MG, Bosch TC, Carey HV, Domazet-Lošo T, Douglas AE, Dübilier N, Eberl G, Fukami T, Gilbert SF, Hentschel U, King N, Kjelleberg S, Knoll AH, Kremer N, Mazmanian SK, Metcalf JL, Nealson K, Pierce NE, Rawls JF, Reid A, Ruby EG, Rumpho M, Sanders JG, Tautz D, Wernegreen JJ.** 2013. Animals in a bacterial world, a new imperative for the life sciences. *Proc Natl Acad Sci U S A* **110**:3229-3236.
5. **Nicholson JK, Holmes E, Kinross J, Burcelin R, Gibson G, Jia W, Pettersson S.** 2012. Host-gut microbiota metabolic interactions. *Science* **336**:1262-1267.
6. **Tianero MD, Kwan JC, Wyche TP, Presson AP, Koch M, Barrows LR, Bugni TS, Schmidt EW.** 2014. Species specificity of symbiosis and secondary metabolism in ascidians. *ISME J* doi:10.1038/ismej.2014.152.
7. **Muegge BD, Kuczynski J, Knights D, Clemente JC, Gonzalez A, Fontana L, Henrissat B, Knight R, Gordon JI.** 2011. Diet drives convergence in gut microbiome functions across mammalian phylogeny and within humans. *Science* **332**:970-974.
8. **Brucker RM, Bordenstein SR.** 2013. The hologenomic basis of speciation: gut bacteria cause hybrid lethality in the genus *Nasonia*. *Science* **341**:667-669.
9. **Galardini M, Mengoni A, Brilli M, Pini F, Fioravanti A, Lucas S, Lapidus A, Cheng JF, Goodwin L, Pitluck S, Land M, Hauser L, Woyke T, Mikhailova N, Ivanova N, Daligault H, Bruce D, Detter C, Tapia R, Han C, Teshima H, Mocali S, Bazzicalupo M, Biondi EG.** 2011. Exploring the symbiotic pangenome of the nitrogen-fixing bacterium *Sinorhizobium meliloti*. *BMC Genomics* **12**:235.
10. **Hansen EE, Lozupone CA, Rey FE, Wu M, Guruge JL, Narra A, Goodfellow J, Zaneveld JR, McDonald DT, Goodrich JA, Heath AC, Knight R, Gordon JI.** 2011. Pan-genome of the dominant human gut-associated archaeon, *Methanobrevibacter smithii*, studied in twins. *Proc Natl Acad Sci U S A* **108 Suppl 1**:4599-4606.
11. **Thompson J.** 2005. The geographic mosaic of coevolution. The University of Chicago Press, Chicago, IL.
12. **Heath KD.** 2010. Intergenomic epistasis and coevolutionary constraint in plants and rhizobia. *Evolution* **64**:1446-1458.

13. **Thrall PH, Laine AL, Broadhurst LM, Bagnall DJ, Brockwell J.** 2011. Symbiotic effectiveness of rhizobial mutualists varies in interactions with native Australian legume genera. *PLoS One* **6**:e23545.
14. **Chavez-Dozal AA, Gorman C, Lostroh CP, Nishiguchi MK.** 2014. Gene-swapping mediates host specificity among symbiotic bacteria in a beneficial symbiosis. *PLoS One* **9**:e101691.
15. **Soto W, Punke EB, Nishiguchi MK.** 2012. Evolutionary perspectives in a mutualism of sepiolid squid and bioluminescent bacteria: combined usage of microbial experimental evolution and temporal population genetics. *Evolution* **66**:1308-1321.
16. **Nishiguchi MK, Ruby EG, McFall-Ngai MJ.** 1998. Competitive dominance among strains of luminous bacteria provides an unusual form of evidence for parallel evolution in Sepiolid squid-*Vibrio* symbioses. *Appl Environ Microbiol* **64**:3209-3213.
17. **Poinar GOJ, Thomas GM.** 1966. Significance of *Achromobacter nematophilus* Poinar and Thomas (Achromobacteraceae: Eubacteriales) in the development of the nematode, DD-136 (*Neoaplectana* sp. Steinernematidae). *Parasitology* **56**:385-390.
18. **Herbert EE, Goodrich-Blair H.** 2007. Friend and foe: the two faces of *Xenorhabdus nematophila*. *Nat Rev Microbiol* **5**:634-646.
19. **Richards GR, Goodrich-Blair H.** 2010. Examination of *Xenorhabdus nematophila* lipases in pathogenic and mutualistic host interactions reveals a role for *xlpA* in nematode progeny production. *Appl Environ Microbiol* **76**:221-229.
20. **Popiel I, Grove DL, Friedman MJ.** 1989. Infective juvenile formation in the insect parasitic nematode *Steinernema feltiae*. *Parasitology* **99**:77-81.
21. **Sugar DR, Murfin KE, Chaston JM, Andersen AW, Richards GR, deLeon L, Baum JA, Clinton WP, Forst S, Goldman BS, Krasomil-Osterfeld KC, Slater S, Stock SP, Goodrich-Blair H.** 2012. Phenotypic variation and host interactions of *Xenorhabdus bovienii* SS-2004, the entomopathogenic symbiont of *Steinernema jolietii* nematodes. *Environ Microbiol* **14**:924-939.
22. **Orchard SS, Goodrich-Blair H.** 2004. Identification and functional characterization of a *Xenorhabdus nematophila* oligopeptide permease. *Appl Environ Microbiol* **70**:5621-5627.
23. **Stock SP, Goodrich-Blair H.** 2008. Nematode-bacterium symbioses: crossing kingdom and disciplinary boundaries. *Symbiosis* **46**:61-64.
24. **Lee MM, Stock SP.** 2010. A multilocus approach to assessing co-evolutionary relationships between *Steinernema* spp. (Nematoda: Steinernematidae) and their bacterial symbionts *Xenorhabdus* spp. (gamma-Proteobacteria: Enterobacteriaceae). *Syst Parasitol* **77**:1-12.
25. **Lee MM, Stock SP.** 2010. A multigene approach for assessing evolutionary relationships of *Xenorhabdus* spp. (gamma-Proteobacteria), the bacterial symbionts of entomopathogenic *Steinernema* nematodes. *J Invertebr Pathol* **104**:67-74.

26. **Konstantinidis KT, Tiedje JM.** 2005. Genomic insights that advance the species definition for prokaryotes. *Proc Natl Acad Sci U S A* **102**:2567-2572.
27. **Vallenet D, Belda E, Calteau A, Cruveiller S, Engelen S, Lajus A, Le Fevre F, Longin C, Mornico D, Roche D, Rouy Z, Salvignol G, Scarpelli C, Thil Smith AA, Weiman M, Medigue C.** 2013. MicroScope--an integrated microbial resource for the curation and comparative analysis of genomic and metabolic data. *Nucleic Acids Res* **41**:D636-647.
28. **Vallenet D, Labarre L, Rouy Z, Barbe V, Bocs S, Cruveiller S, Lajus A, Pascal G, Scarpelli C, Medigue C.** 2006. MaGe: a microbial genome annotation system supported by synteny results. *Nucleic Acids Res* **34**:53-65.
29. **Cook RD.** 1977. Detection of influential observation in linear regression. *Technometrics* **19**:15-18.
30. **Nor I, Engelstadter J, Duron O, Reuter M, Sagot MF, Charlat S.** 2013. On the genetic architecture of cytoplasmic incompatibility: inference from phenotypic data. *Am Nat* **182**:E15-24.
31. **Koppenhofer AM, Kaya HK.** 1996. Coexistence of two steinernematid nematode species (Rhabditida:Steinernematidae) in the presence of two host species. *Appl Soil Ecol* **4**:221-230.
32. **Valadas V, Mracek Z, Oliveira S, Mota M.** 2011. Three species of entomopathogenic nematodes of the family Steinernematidae (Nematoda: Rhabditida) new to continental Portugal. *Nematologia Mediterranea* **39**:169-178.
33. **Oliver KM, Russell JA, Moran NA, Hunter MS.** 2003. Facultative bacterial symbionts in aphids confer resistance to parasitic wasps. *Proc Natl Acad Sci U S A* **100**:1803-1807.
34. **Singh S, Reese JM, Casanova-Torres AM, Goodrich-Blair H, Forst S.** 2014. Microbial population dynamics in the hemolymph of *Manduca sexta* infected with *Xenorhabdus nematophila* and the entomopathogenic nematode *Steinernema carpocapsae*. *Appl Environ Microbiol* **80**:4277-4285.
35. **Morales-Soto N, Forst SA.** 2011. The xnp1 P2-like tail synthesis gene cluster encodes xenorhabdicolin and is required for interspecies competition. *J Bacteriol* **193**:3624-3632.
36. **Park JM, Kim M, Min J, Lee SM, Shin KS, Oh SD, Oh SJ, Kim YH.** 2012. Proteomic identification of a novel toxin protein (Txp40) from *Xenorhabdus nematophila* and its insecticidal activity against larvae of *Plutella xylostella*. *J Agric Food Chem* **60**:4053-4059.
37. **Garcia-Gonzalez E, Muller S, Ensle P, Sussmuth RD, Genersch E.** 2014. Elucidation of sevadicin, a novel non-ribosomal peptide secondary metabolite produced by the honey bee pathogenic bacterium *Paenibacillus larvae*. *Environ Microbiol* **16**:1297-1309.
38. **Cochrane SA, Vederas JC.** 2014. Lipopeptides from *Bacillus* and *Paenibacillus* spp.: A gold mine of antibiotic candidates. *Med Res Rev* doi:10.1002/med.21321.

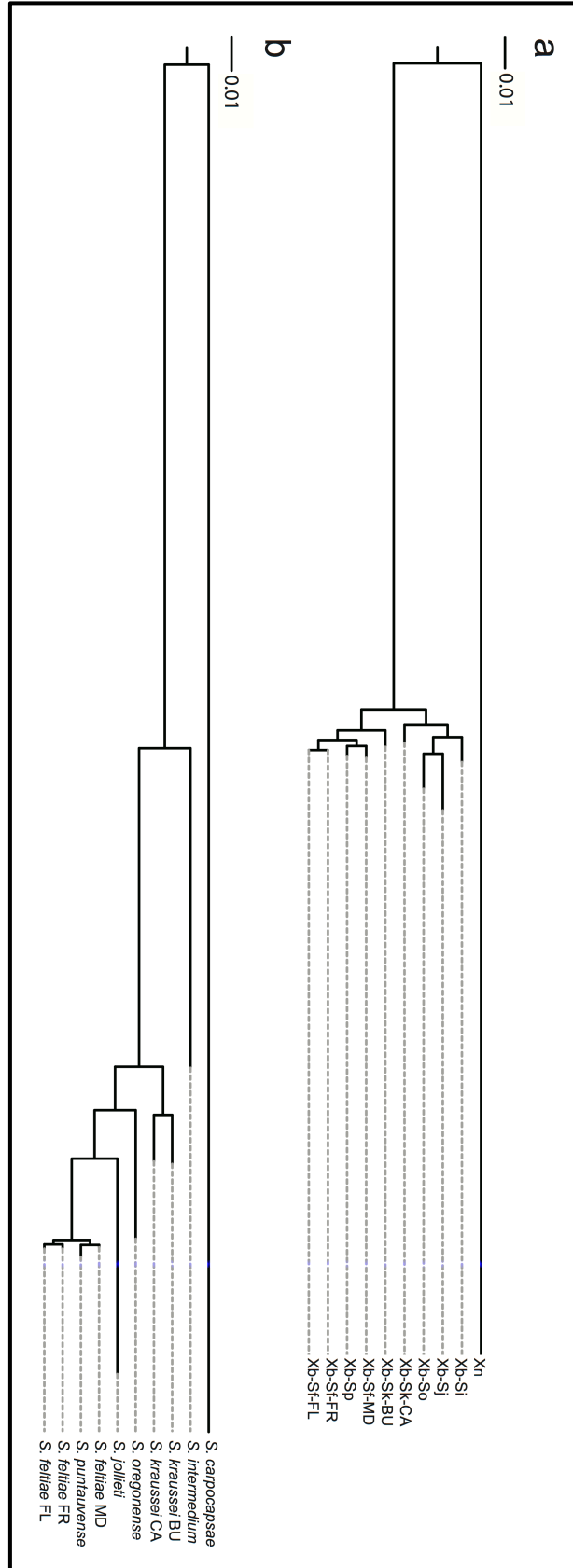
39. **Luo C, Liu X, Zhou H, Wang X, Chen Z.** 2014. Identification of four NRPS gene clusters in *Bacillus subtilis* 916 for four families of lipopeptides biosynthesis and evaluation of their intricate functions to the typical phenotypic features. *Appl Environ Microbiol* doi:10.1128/AEM.02921-14.
40. **Schwecke T, Aparicio JF, Molnar I, Konig A, Khaw LE, Haydock SF, Oliynyk M, Caffrey P, Cortes J, Lester JB, et al.** 1995. The biosynthetic gene cluster for the polyketide immunosuppressant rapamycin. *Proc Natl Acad Sci U S A* **92**:7839-7843.
41. **Tanaka A, Tapper BA, Popay A, Parker EJ, Scott B.** 2005. A symbiosis expressed non-ribosomal peptide synthetase from a mutualistic fungal endophyte of perennial ryegrass confers protection to the symbiotum from insect herbivory. *Mol Microbiol* **57**:1036-1050.
42. **Obrig TG, Karpman D.** 2012. Shiga toxin pathogenesis: kidney complications and renal failure. *Curr Top Microbiol Immunol* **357**:105-136.
43. **Chaston JM, Suen G, Tucker SL, Andersen AW, Bhasin A, Bode E, Bode HB, Brachmann AO, Cowles CE, Cowles KN, Darby C, de Leon L, Drace K, Du Z, Givaudan A, Herbert Tran EE, Jewell KA, Knack JJ, Krasomil-Osterfeld KC, Kukor R, Lanois A, Latreille P, Leimgruber NK, Lipke CM, Liu R, Lu X, Martens EC, Marri PR, Medigue C, Menard ML, Miller NM, Morales-Soto N, Norton S, Ogier JC, Orchard SS, Park D, Park Y, Qurollo BA, Sugar DR, Richards GR, Rouy Z, Slominski B, Slominski K, Snyder H, Tjaden BC, van der Hoeven R, Welch RD, Wheeler C, Xiang B, Barbazuk B, et al.** 2011. The entomopathogenic bacterial endosymbionts *Xenorhabdus* and *Photorhabdus*: convergent lifestyles from divergent genomes. *PLoS One* **6**:e27909.
44. **Prell J, Bourdes A, Kumar S, Ludwig E, Hosie A, Kinghorn S, White J, Poole P.** 2010. Role of symbiotic auxotrophy in the *Rhizobium*-legume symbioses. *PLoS One* **5**:e13933.
45. **Xu J, Hurlbert RE.** 1990. Toxicity of Irradiated Media for *Xenorhabdus* spp. *Appl Environ Microbiol* **56**:815-818.
46. **Martens EC, Heungens K, Goodrich-Blair H.** 2003. Early colonization events in the mutualistic association between *Steinernema carpocapsae* nematodes and *Xenorhabdus nematophila* bacteria. *J Bacteriol* **185**:3147-3154.
47. **Martens EC, Goodrich-Blair H.** 2005. The *Steinernema carpocapsae* intestinal vesicle contains a subcellular structure with which *Xenorhabdus nematophila* associates during colonization initiation. *Cellular microbiology* **7**:1723-1735.
48. **Sicard M, Le Brun N, Pages S, Godelle B, Boemare N, Moulia C.** 2003. Effect of native *Xenorhabdus* on the fitness of their *Steinernema* hosts: contrasting types of interaction. *Parasitol Res* **91**:520-524.
49. **Nadler S, Bolotin E, Stock S.** 2006. Phylogenetic relationships of *Steinernema* (Cephalobina, Steinernematidae) based on nuclear, mitochondrial, and morphological data. *Systematic Parasitology* **64**:159-179.

50. **Capella-Gutierrez S, Silla-Martinez JM, Gabaldon T.** 2009. trimAl: a tool for automated alignment trimming in large-scale phylogenetic analyses. *Bioinformatics* **25**:1972-1973.
51. **Zerbino DR.** 2010. Using the Velvet de novo assembler for short-read sequencing technologies. *Curr Protoc Bioinformatics* **Chapter 11**:Unit 11 15.
52. **Zerbino DR, Birney E.** 2008. Velvet: algorithms for de novo short read assembly using de Bruijn graphs. *Genome Res* **18**:821-829.
53. **Klassen JL, Currie CR.** 2013. ORFcor: Identifying and Accommodating ORF Prediction Inconsistencies for Phylogenetic Analysis. *PLoS One* **8**:e58387.
54. **Edgar RC.** 2004. MUSCLE: a multiple sequence alignment method with reduced time and space complexity. *BMC Bioinformatics* **5**:113.
55. **Edgar RC.** 2004. MUSCLE: multiple sequence alignment with high accuracy and high throughput. *Nucleic Acids Res* **32**:1792-1797.
56. **Rokas A.** 2011. Phylogenetic analysis of protein sequence data using the Randomized Accelerated Maximum Likelihood (RAXML) Program. *Curr Protoc Mol Biol* **Chapter 19**:Unit19 11.
57. **Posada D.** 2008. jModelTest: phylogenetic model averaging. *Mol Biol Evol* **25**:1253-1256.
58. **Ronquist F, Huelsenbeck JP.** 2003. MrBayes 3: Bayesian phylogenetic inference under mixed models. *Bioinformatics* **19**:1572-1574.
59. **Letunic I, Bork P.** 2011. Interactive Tree Of Life v2: online annotation and display of phylogenetic trees made easy. *Nucleic Acids Res* **39**:W475-478.
60. **Kaya HK, Stock SP.** 1997. *Techniques in insect nematology*. Academic Press, London.
61. **Grewal PS, Selvan S, Gaugler R.** 1994. Thermal adaptation of entomopathogenic nematodes: niche breadth for infection, establishment, and reproduction. *Journal of Thermal Biology* **19**:245-253.
62. **Goetsch M, Owen H, Goldman B, Forst S.** 2006. Analysis of the PixA inclusion body protein of *Xenorhabdus nematophila*. *J Bacteriol* **188**:2706-2710.
63. **Courtney W, Polley D, Miller V.** 1955. TAF, an improved fixative in nematode techniques. *Plant Disease Reporter* **39**:570-571.
64. **Yang Z.** 1997. PAML: a program package for phylogenetic analysis by maximum likelihood. *Comput Appl Biosci* **13**:555-556.
65. **Katoh K, Standley DM.** 2014. MAFFT: iterative refinement and additional methods. *Methods Mol Biol* **1079**:131-146.

66. **Rocha EP, Smith JM, Hurst LD, Holden MT, Cooper JE, Smith NH, Feil EJ.** 2006. Comparisons of dN/dS are time dependent for closely related bacterial genomes. *J Theor Biol* **239**:226-235.
67. **Finn RD, Bateman A, Clements J, Coggill P, Eberhardt RY, Eddy SR, Heger A, Hetherington K, Holm L, Mistry J, Sonnhammer EL, Tate J, Punta M.** 2014. Pfam: the protein families database. *Nucleic Acids Res* **42**:D222-230.
68. **Felsenstein J.** 1978. The number of evolutionary trees. *Syst Zool* **27**:27-33.
69. **R Core Team.** 2013. R: A language and environment for statistical computing, *on R Foundation for Statistical Computing*. <http://www.R-project.org/>.

SUPPLEMENTAL MATERIALS

Figure 3.S1 Bayesian distance phylogenies. Bacterial (a) and nematode (b) distance trees are shown. The trees were constructed using Bayesian methods and had the same topology and similar distances as those constructed using maximum likelihood.



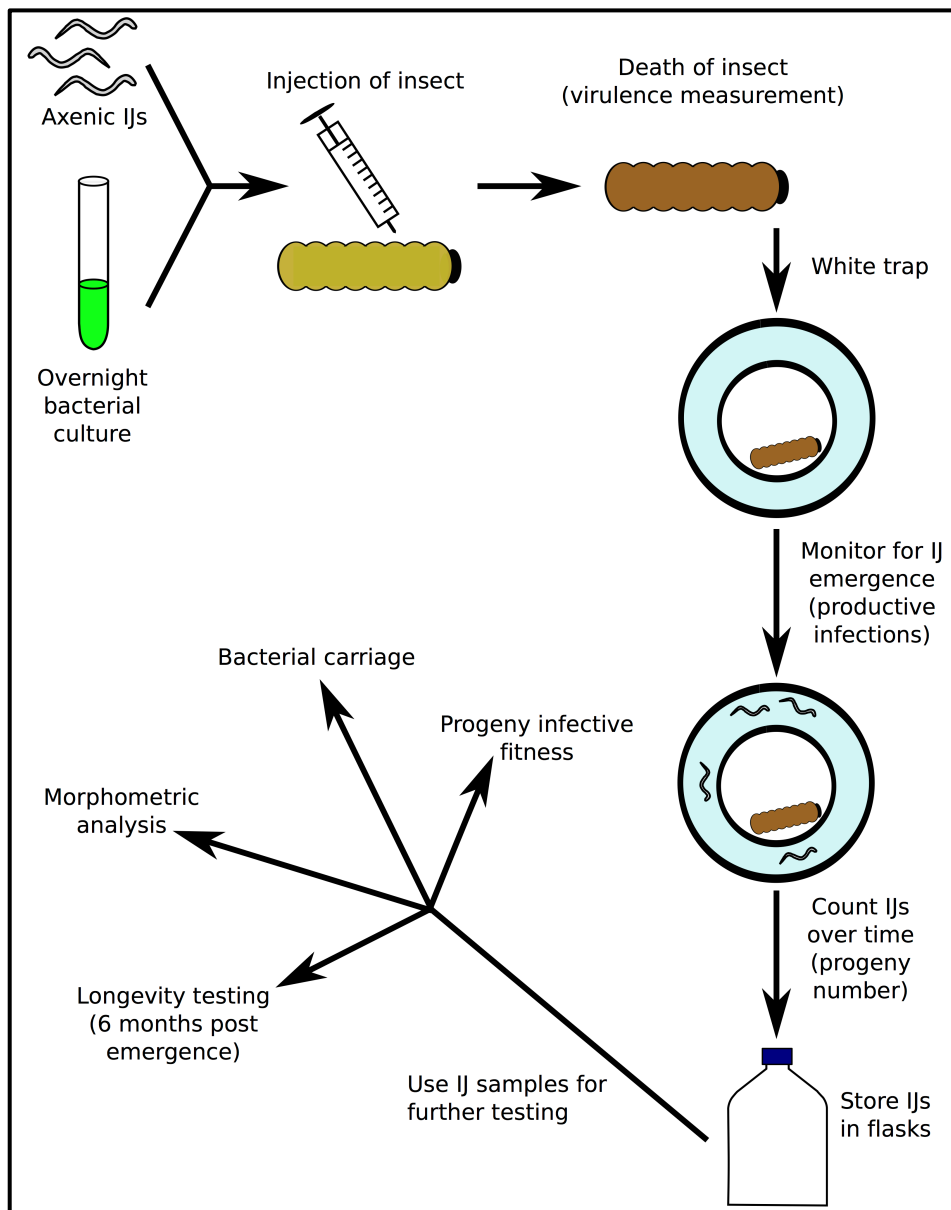


Figure 3.S2 Schematic diagram of mutualistic testing. The diagram depicts the progression of experimental testing. Axenic IJs (nematodes not exposed to bacteria) and the bacterial symbionts were reared separately, and each combination was mixed and co-injected into the insect host. Insects were monitored for percent mortality (virulence of combination) and progeny nematode IJ emergence (productive infections and progeny number). Progeny IJs were stored in flasks and then used for progeny measurements: progeny infective potential, bacterial carriage, morphometric analysis, and longevity.

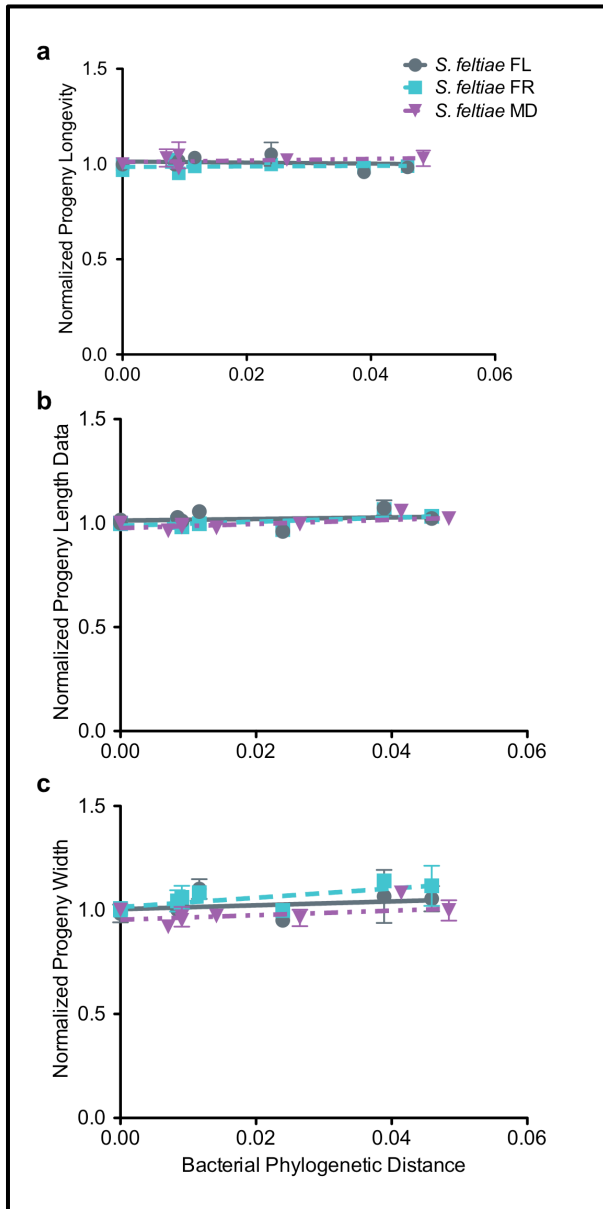


Figure 3.S3 Possible causes of progeny infective fitness defects. Causes of progeny infective fitness defects were analyzed using linear regression relative to bacterial phylogenetic distance (Bayesian tree distance): nematode progeny longevity (a), or morphometric analyses (b, c). For morphometric analyses, both length (b) and width (c) were taken into consideration as measurements of nematode progeny health. No significant correlations were found with adequate r-squared values. Data points represent averages of the measurements for each set of data (n=3), and error bars represent standard error.

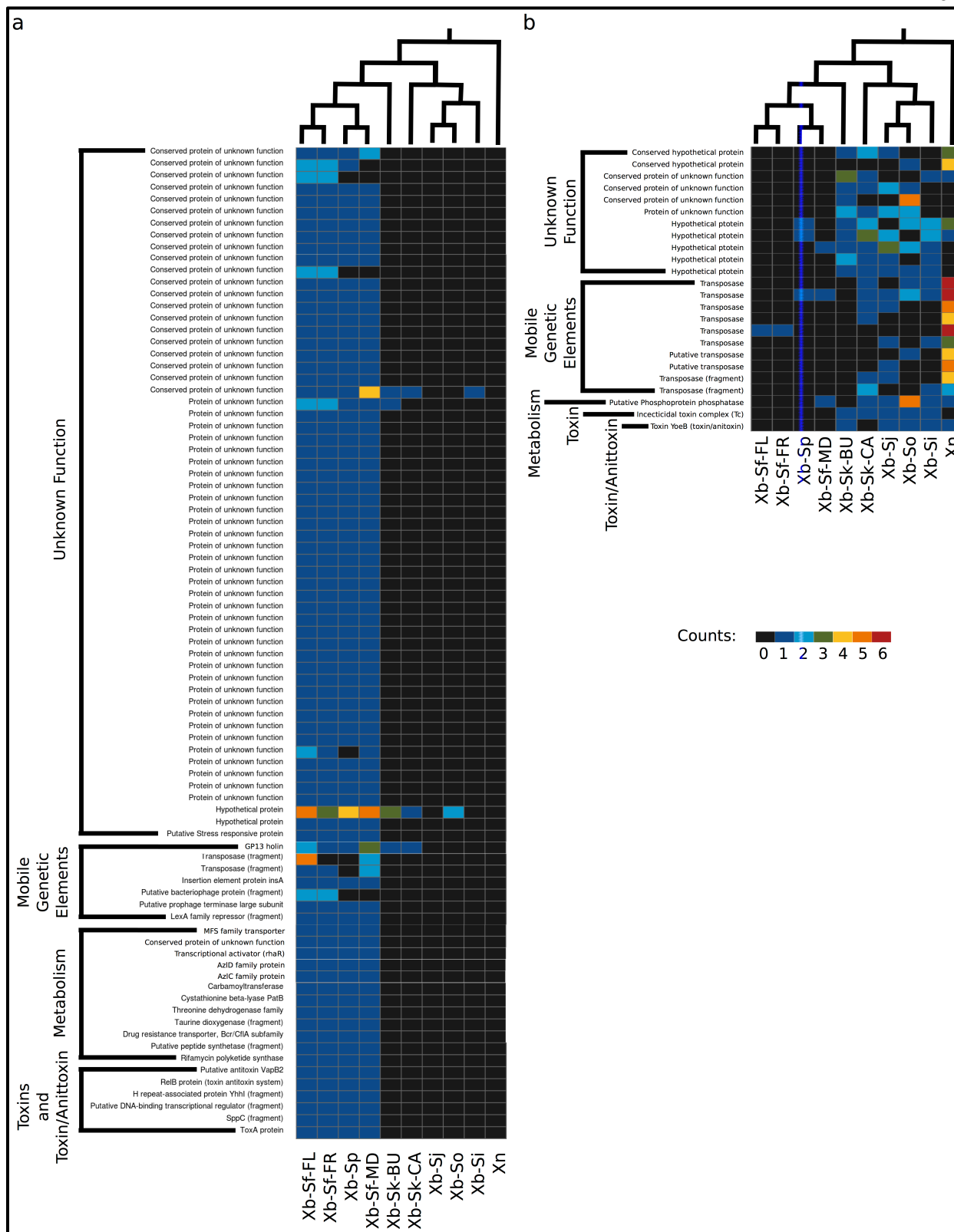


Figure 3.S4 Heatmap of overrepresented and underrepresented genes. To identify non-conserved gene sets potentially involved in the nematode-bacterial mutualism, genes from all *X. bovienii* genomes were analyzed for overrepresentation (a) or underrepresentation (b) within the monophyletic clade of *S. feltiae* and *S. punctauvense* bacterial symbiont strains. Total gene number per symbiont genome is shown in the heatmap relative to the phylogeny of bacterial symbionts. Each gene family is listed in a separate row, and the predicted function is shown to the left of each row of counts.

Table 3.S1 Bacterial strains and nematode host species used in this study.

Bacterial strains ^a	<i>Xenorhabdus</i> bacterial species designation ^b	<i>Steinernema</i> nematode host species ^c	Source or isolation location ^d	Bacterial 16S rRNA accession number ^e	Bacterial genome accession number ^f	Nematode 12S rRNA accession number ^g	Nematode 28S rRNA accession number ^h
Xn	<i>nematophila</i>	<i>carpocapsae</i>	USA	GU480972*	FN887742**	AY944007*	AF331900*
Xb-Sf-FL	<i>bovieni</i>	<i>feltiae</i>	Florida, USA	KF437819	PRJEB4320	GU569030*	GU569049*
Xb-Sf-FR	<i>bovieni</i>	<i>feltiae</i>	France	KF437820	PRJEB4319	GU569031*	GU569050*
Xb-Sp	<i>bovieni</i>	<i>puntauvense</i>	Costa Rica	KF437827	PRJEB4322	GU569037*	GU569056*
Xb-Sf-MD	<i>bovieni</i>	<i>feltiae</i>	Moldova	KF437821	PRJEB4321	KF437815	KF437816
Xb-Sk-BU	<i>bovieni</i>	<i>kraussei</i>	Becker Underwood	KF437824	PRJEB4325	KF437817	KF437818
Xb-Sk-CA	<i>bovieni</i>	<i>kraussei</i>	Quebec, CA	KF437825	PRJEB4324	GU569034*	GU569053*
Xb-Si	<i>bovieni</i>	<i>intermedium</i>	North Carolina, USA	KF437822	PRJEB4327	AY944013*	AY598358*
Xb-So	<i>bovieni</i>	<i>oregonense</i>	Oregon, USA	KF437826	PRJEB4323	GU569036*	GU569055*
Xb-Sj	<i>bovieni</i>	<i>jolietii</i>	Monsanto	KF437823	PRJEB4326	GU569032*	GU569051*

^aStrain abbreviation used in the main text

^bBacterial species designation as determined by 16S rRNA and ANI

^cSpecies designation of the nematode host from which the bacterium was isolated

^dThe source company or location of nematode isolation

^eThe accession number for the 16s rRNA sequence of the bacterial strain in NCBI GenBank

^fAccession number for the full draft genome sequence of the bacterial strain in the EMBL database

^gThe accession number for the nematode host 12s rRNA sequence in NCBI GenBank

^hThe accession number for the nematode host 28s rRNA sequence in NCBI GenBank

*From Lee and Stock 2010b(24)

** From Chaston *et al.* 2011(43), submission to GenBank

Table 3.S2 Average nucleotide identity of *X. bovienii* strains used in these experiments^a

	Xn^b	Xb-Sf-FL	Xb-Sf-FR	Xb-Sp	Xb-Sf-MD	Xb-Sk-BU	Xb-Sk-CA	Xb-Si	Xb-So	Xb-Sj
Xn^b	100%	85%	85%	85%	85%	85%	85%	86%	86%	86%
Xb-Sf-FL	85%	100%	100%	99%	99%	99%	98%	97%	97%	96%
Xb-Sf-FR	85%	100%	100%	99%	99%	99%	98%	97%	97%	96%
Xb-Sp	85%	99%	99%	100%	99%	98%	98%	97%	97%	96%
Xb-Sf-MD	85%	99%	99%	99%	100%	99%	98%	97%	97%	96%
Xb-Sk-BU	85%	99%	99%	98%	99%	100%	98%	97%	97%	96%
Xb-Sk-CA	85%	98%	98%	98%	98%	98%	100%	98%	98%	97%
Xb-Si	86%	97%	97%	97%	97%	97%	98%	100%	97%	97%
Xb-So	86%	97%	97%	97%	97%	97%	98%	97%	100%	97%
Xb-Sj	86%	96%	96%	96%	96%	96%	97%	97%	97%	100%

^aGray boxes indicate comparisons of the bacterial strains to themselves.

^bOne strain of *X. nematophila* (ATCC19061) is shown as an out-group.

Table 3.S3 Unique genomic content differences between *X. bovienii* strains^a.

Bacterial Strain	Percent Unique^b	Protein of unknown function^c	Conserved protein of unknown function^d	Membrane or exported protein^e	Metabolism or cellular function protein^f	Mobile genetic elements^g
Xb-Sf-FL	1%	25	1	0	0	0
Xb-Sf-FR	0%	19	0	0	0	0
Xb-Sf-MD	5%	151	51	12	22	6
Xb-Sp	6%	125	41	7	19	4
Xb-Sj	8%	215	44	20	27	18
Xb-Sk-CA	6%	169	40	7	36	2
Xb-Sk-BU	9%	211	126	26	60	19
Xb-So	6%	69	216	18	35	15
Xb-Si	7%	233	39	20	24	8

^aPercentage and categorization of unique genome content within each *X. bovienii* strain.

^bPercentage of the coding sequences identified within the genome that are not found in any other *X. bovienii* strain.

^cNumber of unique genes that do not have a predicted function.

^dNumber of unique genes that do not have a predicted function and are conserved within other bacterial species.

^eNumber of unique genes that are predicted to be membrane bound or exported.

^fNumber of unique genes that are predicted to be involved in metabolic or cellular functions (e.g. cell division).

^gNumber of unique genes that are predicted to be mobile genetic elements, such as phage regions, transposable elements, or insertion elements.

Table 3.S4 Virulence of *S. feltiae* nematodes alone and *X. bovienii* co-injections.

Bacterial Strain	<i>S. feltiae</i> FL Nematodes			<i>S. feltiae</i> FR Nematodes			<i>S. feltiae</i> MD Nematodes		
	LT50 ^a	Percent Survival ^b	Log-rank test ^c	LT50 ^a	Percent Survival ^b	Log-rank test ^c	LT50 ^a	Percent Survival ^b	Log-rank test ^c
None	104*	42%*	e	72*	39%*	d	32	0%	b
Xb-Sf-FL	40	0%	bc	43	0%	a	40	0%	a
Xb-Sf-FR	48	0%	cd	48	0%	bc	44	0%	b
Xb-Sf-MD	48	0%	cd	48	0%	c	44	0%	b
Xb-Sp	43	0%	ab	40	0%	a	36	0%	a
Xb-Sj	36	0%	a	40	0%	a	36	0%	a
Xb-Sk-CA	48	0%	d	56	5.6%	d	44	2.8%	b
Xb-Sk-BU	36	0%	cd	40	0%	b	36	0%	a
Xb-So	36	0%	cd	36	0%	a	36	0%	a
Xb-Si	36	0%	ab	36	0%	a	36	0%	a

^aAverage LT50 of condition (time required to kill 50% of the insects); *indicates differences from all other conditions ($p < 0.05$).

^bAverage percent survival of insects at 7 days post injection; *indicates differences from all other conditions ($p < 0.05$).

^cLog-rank test on survival curves for statistical differences. Letters indicate differences with $p < 0.05$.

Table 3.S5 Table of statistical analysis of linear regression analyses of data shown in Table 3.S4, Figure 3.3, and Figure 3.4 relative to bacterial phylogenetic distance.

	<i>S. feltiae</i> FL nematodes			<i>S. feltiae</i> FR nematodes			<i>S. feltiae</i> MD nematodes		
	Slope	R-squared	P-value	Slope	R-squared	P-value	Slope	R-squared	P-value
Virulence	-3.4	0.07	0.186	-4.3	0.14	0.067	-3.9	0.14	0.07
	-3.0	0.03	0.39	-2.5	0.01	0.28	-3.0	0.08	0.19
Productive Infection Percentage	-13	0.29	0.004	-11	0.20	0.021	-16	0.25	0.009
	-5.1	0.45	<0.001	-5.1	0.42	<0.001	-6.7	0.37	<0.001
Progeny Number	-21	0.71	<0.001	-18	0.36	<0.001	-16	0.11	0.089
	-4.9	0.39	<0.001	-6.4	0.50	<0.001	-8.9	0.24	0.010
Progeny Infective Potential	-12	0.27	0.013	-10	0.20	0.042	-16	0.567	<0.001
	-9.1	0.58	<0.001	-8.2	0.34	0.006	-8.3	0.50	<0.001
Bacterial Carriage	-17	0.05	0.3131	-17	0.14	0.088	-14	0.15	0.107
	-20	0.08	0.223	-16	0.33	0.005	-11	0.38	0.006
Nematode Fitness	-18	0.65	<0.001	-18	0.41	<0.001	-31	0.16	0.040
	-4.8	0.53	<0.001	-5.9	0.45	<0.001	-13	0.19	0.021
Bacterial Fitness	-36	0.36	<0.001	-28	0.42	<0.001	-28	0.31	0.003
	-11	0.26	0.007	-8.5	0.36	0.001	-10	0.33	0.002
Overall Success	-52	0.66	<0.001	-47	0.35	0.001	-54	0.33	0.002
	-15	0.79	<0.001	-18	0.57	<0.001	-20	0.47	<0.001

The table shows the slope, r-squared, and p-value measurements for each linear regression calculated for the nematode isolates. The values are shown for each experimental measurement with respect to bacterial (top row) and nematode (bottom row) phylogenetic distance. Gray shading indicates values of a non-significant trend.

Table 3.S6 Cook's distance of native symbiont clade average point derived from from linear regression analyses of parameters from Table 3.S5 and Figure 3.3^a

	<i>S. feltiae</i> FL nematodes		<i>S. feltiae</i> FR nematodes		<i>S. feltiae</i> MD nematodes	
	Cook's Distance ^b	Data point Influence ^c	Cook's Distance ^b	Data point Influence ^c	Cook's Distance ^b	Data point Influence ^c
Productive Infection Percentage	0.073	Not influential	0.155	Not influential	0.298	Not influential
Progeny Number	0.032	Not influential	0.022	Not influential	0.012	Not influential
Progeny Infective Potential	0.470	Not influential	0.155	Not influential	9.30x10 ⁻⁵	Not influential
Bacterial Carriage	1.67x10 ⁻⁵	Not influential	0.415	Not influential	2.83	Influential
Nematode Fitness	0.550	Not influential	0.111	Not influential	0.099	Not influential
Bacterial Fitness	4.23x10 ⁻⁵	Not influential	0.452	Not influential	0.678	Not influential
Overall Success	0.427	Not influential	0.095	Not influential	0.112	Not influential

^aA linear regression of data from the non-native symbiont clade and an average point of the native symbiont clade was constructed, and the Cook's distance of the average point was calculated.

^bCook's distance of the average native symbiont clade point.

^cInfluence of the average data point based on Cook's distance. We considered Cook's distance >1 as influential within the data set, indicating that the native clade average data point greatly influences the trend of the linear regression.

CHAPTER 4

Comparison of *Xenorhabdus bovienii* bacterial strain genomes reveals diversity in secondary metabolism and symbiotic functions

This chapter will be submitted for publication as:

Murfin KE, Whooley AC, Klassen JL, and Goodrich-Blair H. "Comparison of *Xenorhabdus bovienii* bacterial strain genomes reveals diversity in secondary metabolism and symbiotic functions"

ABSTRACT

Background: *Xenorhabdus* bacteria engage in a beneficial symbiosis with *Steinernema* nematodes, in part by providing activities that help kill and degrade insect hosts that these two organisms utilize for nutrition. *Xenorhabdus* strains (members of a single species) can display wide variation in host-interaction phenotypes and genetic potential, raising the likely possibility that they differ in their encoded symbiosis factors, including secreted metabolites. To discern strain-level variation among symbiosis factors, and facilitate the identification of novel compounds, we performed a comparative analysis of the genomes of 10 *X. bovienii* bacterial strains.

Results: The analyzed *X. bovienii* genomes are broadly similar in structure (e.g. size, GC content, number of coding sequences), but the draft genomes are at least partially incomplete. Genome content analysis revealed that general classes of putative host-microbe interaction functions, such as secretion systems and toxin classes, were identified in all bacterial strains. In contrast, we observed diversity of individual genes within families (e.g. non-ribosomal peptide synthetase clusters and insecticidal TC toxin components), indicating the specific molecules secreted by each strain can vary. Additionally, phenotypic analysis indicates that regulation of activities (e.g. enzymes and motility) differs among strains.

Conclusions: The analyses presented here demonstrate that while there are general mechanisms by which *X. bovienii* bacterial strains interact with their invertebrate hosts are similar, the specific molecules mediating these interactions differ. Our data support the idea that adaptation of individual bacterial strains to distinct hosts or niches has occurred. For example, diverse metabolic profiles among bacterial symbionts may have been selected in evolutionary time by dissimilarities in nutritional requirements of their different nematode hosts. Similarly, factors involved in parasitism (e.g. immune suppression and microbial competition factors), likely differ based on evolution in response to naturally encountered organisms, such as insect

hosts, competitors, predators or pathogens. This study provides insight into effectors of a symbiotic lifestyle, and also highlights that when mining *Xenorhabdus* species for novel natural products, including antibiotics and insecticidal toxins, analysis of multiple bacterial strains likely will increase the potential for the discovery of novel molecules.

INTRODUCTION

Xenorhabdus bacteria are beneficial symbionts of entomopathogenic (insect-parasitic) *Steinernema* nematodes. In addition to the *Xenorhabdus* – *Steinernema* complexes being effective biocontrol agents for a variety of insect pests (1, 2), they are tractable laboratory systems that facilitate investigation of ecological (3), evolutionary (4) (Chapter 3), and symbiotic (5, 6) processes. The integrated life cycle of *Xenorhabdus* bacteria and *Steinernema* nematodes comprises the alternating environments of the soil and insect hosts infected by the pair (Figure 4.1) (5). The infective juvenile (IJ) is the soil dwelling, environmental stage of the nematode that carries bacteria and infects insect hosts. Once within the blood cavity of an insect host, the nematodes and bacteria kill the insect and reproduce using the nutrients derived from the cadaver. During reproduction, the nematodes and bacteria are vulnerable to predation by scavenger insects (7, 8) and to competition from other opportunistic microbes, such as other nematodes, bacteria, or fungi (9-12). After nutrients within the insect cadaver are consumed, and nematode density is high, the nematodes develop into the next generation of progeny IJs that exit the cadaver to repeat the cycle (13). In the united nematode-bacterium association, the bacterial symbiont contributes to virulence against the insect (14, 15) (Chapter 3), support of nematode reproduction within the insect cadaver (4, 16) (Chapter 3), and defense against insect predators (7, 8) and microbial competitors (9, 17). In turn, the nematode partner serves as a vector to transmit bacteria between insect hosts (18, 19) and augments bacterial virulence against insects (20, 21) (Chapter 3).

To accomplish symbiotic functions, *Xenorhabdus* bacteria encode a wide array of bioactive molecules that can function as virulence factors (22-26), degradative enzymes for nutritional support (16), anti-predatory compounds (7, 8), and anti-microbial compounds (9, 10, 17). Because of this large repertoire of biological activities, *Xenorhabdus* spp. have been proposed as a rich source of secondary metabolites (17, 27, 28) that have potential applications

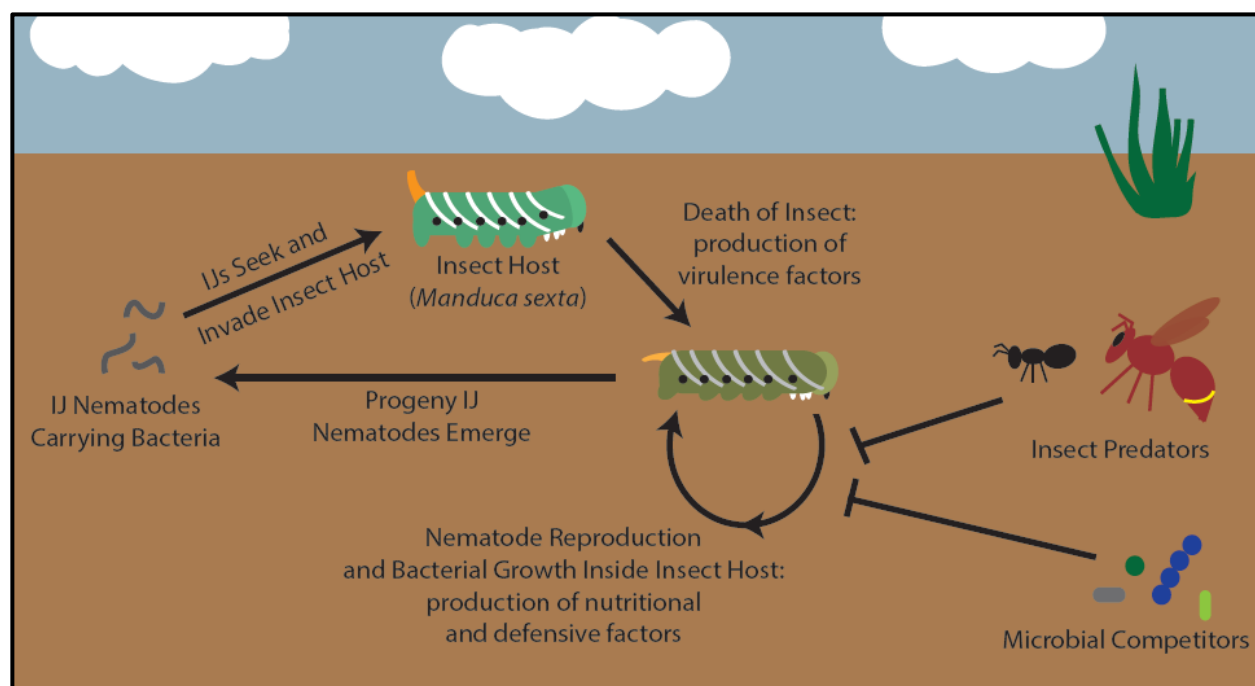


Figure 4.1 *Xenorhabdus* bacteria and *Steinernema* nematode life cycle. In the soil, *Steinernema* infective juvenile (IJ) nematodes, containing their *Xenorhabdus* symbionts, seek out and invade insect hosts. Once in the insect blood cavity, the nematodes and bacteria produce virulence factors and kill the insect host. The nematodes and bacteria then grow and reproduce within the insect cadaver utilizing nutritional factors produced by the bacterial symbiont. During reproduction, the growing nematodes and bacteria are vulnerable to insect predators and microbial competitors, and therefore, defensive compounds are produced during reproduction. Once all nutrients within the cadaver are consumed, the nematodes form the next generation of IJs (progeny) that then exit the insect cadaver to seek new insect hosts.

as insecticides, nematicides, and antimicrobials. This idea prompted successful genome mining of diverse *Xenorhabdus* species to identify novel metabolites with useful pharmaceutical properties (17, 27, 28). Our recent work has revealed intra-species variation in the ability of *X. bovienii* to engage in symbiosis with *S. feltiae* nematode hosts (Murfin *et al.*, 2015), indicating the strong likelihood that examination of multiple strains within a species has the potential to expose additional diversity of bioactive metabolites. Indeed, pan-genomic analysis of *X. bovienii* strains revealed the core genome to be approximately 55% of total coding content, with 1-9% of the coding content being unique to an individual strain (Chapter 3). The remaining 44-36% therefore is shared among some, but not all, bacterial strains studied. However, it is unclear how the genes encoding specific bioactive molecules, such as those mentioned above are distributed among the strains and if variability in activity of conserved loci occurs. To address these questions, we performed a comparative genomic analysis on 10 previously published bacterial genomes (29, 30) (Chapter 3) that were isolated from 6 different *Steinernema* spp. nematodes hosts (Table 4.1), focusing on compounds likely to be involved in symbiotic interactions.

RESULTS AND DISCUSSION

General genomic features of *Xenorhabdus bovienii*. We recently reported a brief description of draft genomes of 9 *X. bovienii* strains, but did not provide an in depth comparison of the general genomic features relative to the finished *X. bovienii* genome (Chapter 3) (29, 30). Here we present a more thorough analysis, which indicated that all the examined *X. bovienii* genomes are similar to each other in genome in size, GC content, number of coding sequences and coding density (Table 4.1). On average the genomes are 4.4 Mbp, with 4451 coding sequences. No plasmids were detected in any of these strains through sequencing or common preparation methods (data not shown).

Table 4.1 *Xenorhabdus bovienii* genomes used in this study^a.

Genome ^a	<i>Steinernema</i> nematode host ^b	Source ^c	Genome Accession Number ^d	Study ^e	Genome Size (Mb) ^f	G + C content (%) ^g	Number of CDS ^h	Coding Density (%) ⁱ
Xb-Sf-FL	<i>S. feltiae</i>	Florida, USA	PRJEB4320	(Chapter 3)	4.47	44.89	4508	83.43
Xb-Sf-FR	<i>S. feltiae</i>	France	PRJEB4319	(Chapter 3)	4.41	44.75	4441	84.06
Xb-Sf-MD	<i>S. feltiae</i>	Moldova	PRJEB4321	(Chapter 3)	4.66	44.36	4695	83.82
Xb-Si	<i>S. intermedium</i>	North Carolina, USA	PRJEB4327	(Chapter 3)	4.71	44.89	4719	83.39
Xb-Sj	<i>S. jolietii</i>	Monsanto	PRJEB4326	(Chapter 3)	3.93	44.48	3939	83.20
Xb-Sj-2004	<i>S. jolietii</i>	Monsanto	FN667741	(30)	4.23	44.97	4406	84.07
Xb-Sk-BU	<i>S. kraussei</i>	Becker Underwood	PRJEB4325	(Chapter 3)	4.72	44.75	4860	83.10
Xb-Sk-CA	<i>S. kraussei</i>	Quebec, CA	PRJEB4324	(Chapter 3)	4.21	44.18	4097	83.96
Xb-So	<i>S. oregonense</i>	Oregon, USA	PRJEB4323	(Chapter 3)	4.13	44.90	4261	84.30
Xb-Sp	<i>S. puntauvense</i>	Costa Rica	PRJEB4322	(Chapter 3)	4.48	44.32	4584	84.34

^aAbbreviation used for bacterial genomes.

^bThe *Steinernema* nematode host species from which the *X. bovienii* bacterial strain was isolated from.

^cThe location or company from which the nematode was obtained from.

^dThe accession number for the bacterial genome in EMBL.

^eStudy the genome was sequenced in.

^fSize of the genome in megabases.

^gGC content percentage of the genome.

^hTotal number of coding sequences in the genome.

ⁱAmount of the genome that is coding sequences.

To assess completeness of the draft genomes, we assessed the number and size of contigs. All of the draft genomes have ~400 contigs, with an N50 value between 30-55 megabasepairs (Table 1), indicating that the assembly is fragmented. Additionally, the draft genome sequence of the *S. jollieti* symbiont (Xb-Sj) shows genome-wide synteny to the finished genome sequence (Xb-Sj-2004), but the draft genome lacks portions found within the complete genome (Figure 4.2). Synteny differences are likely not due to contig order, as the contigs within the draft genomes were aligned using progressive MAUVE (Chapter 3). Synteny differences are likely due to missassembly of the draft genome, as all breaks in the draft genome sequence (except two) are within 1000bp of contig ends. However, not all contig ends result in breaks in the genome, so not all contig breaks contribute to lack of synteny. Xb-Sj and Xb-Sj-2004 are bacterial strains that came from the same nematode host strain but were isolated seven years apart (14). Therefore it is expected that these two genomes should be almost identical. This comparison therefore indicates that the assembly of the Xb-Sj draft genome, and presumably the other draft genomes as well, may not be complete. It is also possible that differences in the size of Xb-Sj and Xb-Sj-2004 genomes could be due to genome reduction in the symbiont associated with the host for a longer period of time. Additionally, Xb-Sj contains 76 predicted open reading frames not present in Xb-Sj-2004, which supports that genome content has changed between these two strains. However, all unique predicted open reading frames are proteins of unknown function.

Secretion systems are conserved among *X. bovienii* strains. For our comparative genomic analyses we chose to focus on factors likely to contribute to *X. bovienii* interaction with its hosts. Bacterial products that directly interact with host tissues and cells must be exported out of the bacterial cell through secretion systems. Indeed, disruption of secretion systems in bacterial symbionts can cause defects in pathogenesis (31, 32) and mutualism (33, 34). To determine if secretion system types are present among *X. bovienii* genomes we searched for gene clusters

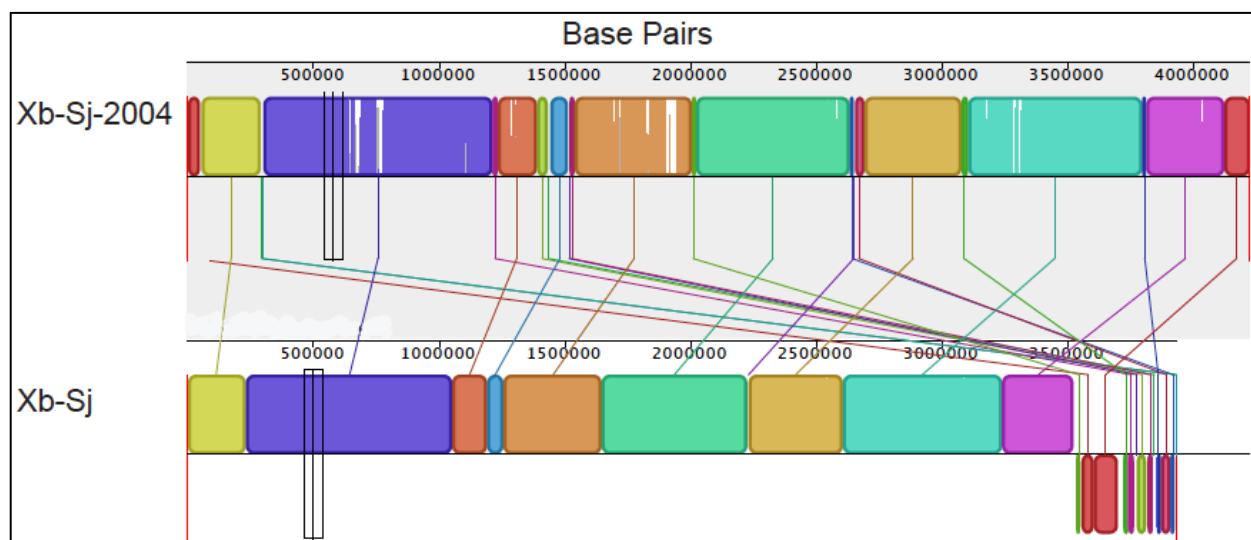


Figure 4.2 Genome synteny between finished and draft *X. bovienii* genomes. Genomes were aligned with progressive MAUVE to assess the large-scale synteny among the draft *X. bovienii* genome (Xb-Sj) and the finished *X. bovienii* genome (Xb-Sj-2004). The names of each genome are reprinted on the left for ease of viewing, and the scale is shown in base pairs. Colored boxes indicate regions of synteny, and colored lines connect alike regions. The Xb-Sj draft genome shares large-scale synteny with the Xb-Sj-2004 finished genome, but is not identical.

known to encode systems responsible for secretion of host-interacting factors in various bacteria. Further, none of the *X. bovienii* strains encoded a complete Type IV secretion system (35), although various genes encoding Type IV-system-related proteins were present in the Xb-Sf-FL and the Xb-Sf-FR genomes. Other secretion systems involved in host interactions include the flagellar export apparatus, which is evolutionarily related to Type III, for secretion of certain substrates, such as xenocin and virulence factors (36-38). Type II secretion systems are responsible for transporting folded proteins (e.g. toxins and degradative enzymes) from the periplasm to the extracellular environment in Gram-negative bacteria(39). Also, Type VI secretion systems transfer effectors (e.g. hemolysins) directly from the bacterial cell into the target host through injection (40, 41) and the alkaline protease secretion system secretes the protease PrtA (42). Examination of the *X. bovienii* strain genomes revealed each has single intact flagellar, type II, and type VI secretion systems as well as an alkaline protease secretion system. In each case, all the required structural genes were present in a single copy (Table 4.S1). However, there are additional type VI structural genes are present in the genome, such as multiple *vgrG* genes, which were present in all strains (data not shown). Overall, the types and numbers of intact secretion systems of *X. bovienii* appear to be conserved, in that each bacterial strain has a single syntenous region containing all required secretion system components.

The presence of the same secretion systems in all *X. bovienii* strains likely reflects their similar symbiotic lifestyles interacting with nematode and insect hosts. However, in nature, the bacterial strains associate with divergent nematode host species and likely encounter different insect host species. Therefore, the secreted effector proteins delivered by the secretion systems are expected to vary. To address this idea, we further investigated bacterial factors, or putative secreted effector molecules, that may be involved in symbiotic interactions.

Phenotypic testing of *X. bovienii* bacterial strains. Some *Xenorhabdus* factors that are likely to be secreted and involved in symbiosis have readily monitored activities. For example, lipase activity in *X. nematophila* contributes to nutritional support of its nematode host, *Steinernema carpocapsae*, and is secreted through the flagellar apparatus (43). To assess the diversity of phenotypes associated with symbiosis among the *X. bovienii* strains, we measured activities implicated in bacterial or nematode nutrition, including siderophores that mediate iron acquisition (44, 45) and lipase (16, 38), lecithinase (16), and protease (16, 42) activities that likely degrade insect tissues. In addition, we monitored hemolytic activity (24) and motility (43), which are associated with virulence towards the insect host or subsequent degradation (46-48). Finally, we assessed antibiotic activity, which likely plays a defensive role in removing competitor or nematode-pathogenic microbes from the insect cadaver (10).

In *Xenorhabdus* species, including *X. bovienii*, assessment of the activities listed above is complicated by phenotypic variation. All *Xenorhabdus* spp. studied to date undergo phenotypic variation between primary and secondary form cells that can alter the levels of some activities, such as lipase and antibiotics (14, 28). In the laboratory, primary form cells give rise to secondary form cells after long-term cultivation in liquid media. However, it remains unclear if or when phenotypic variation occurs within the natural life cycle. To ensure that we accurately determined the production potential of activities in *X. bovienii* strains, we generated secondary form bacterial isolates from primary form isolates and used both for phenotypic testing (Table 4.2).

Almost all strains had swimming motility, lipase, lecithinase, protease, siderophore hemolysin, and antibiotic activities in at least one form, except that Xb-Sk-Bu lacked protease activity, and Xb-Sp lacked hemolysin activity (Table 4.2). Several strains (i.e. Xb-Sf-MD, Xb-Sk-BU, Xb-Sj, Xb-Sj-2004, and Xb-Sp) lacked swarming motility (Table 4.2). Some activities, such as lecithinase and siderophore production, were not affected by phenotypic variation in any of the bacterial strains. Other activities, such as lipase and hemolysin production, did differ

Table 4.2 Phenotypes of *X. bovienii* bacterial strains^a.

Strain ^b	Swimming Motility ^c	Swarming Motility ^d	Lipase ^e	Lecithinase ^f	Protease ^g	Siderophore ^h	Horse Hemolysin ⁱ	Rabbit Hemolysin ^l	Antibiotic Activity ^k
Xb_Sf_FL	Both	Both	Primary	Both	Both	Both	Both	Both	Both
Xb_Sf_FR	Both	Both	Primary	Both	Both	Both	Primary	Primary	Both
Xb_Sf_MD	Both	None	Secondary	Both	Both	Both	Primary	None	Both
Xb_Si	Both	Both	Both	Both	Both	Both	Both	Both	Both
Xb_Sk_CA	Both	Both	Primary	Both	Primary	Both	Both	Both	Both
Xb_Sk_BU	Both	None	Primary	Both	None	Both	Primary	Primary	Both
Xb_Si	Both	None	Secondary	Both	Both	Both	Both	Both	Both
Xb_Si_2004	Both	None	Secondary	Both	Both	Both	Both	Both	Both
Xb_So	Both	Both	Secondary	Both	Both	Both	Both	Primary	Both
Xb_Sp	Both	None	Primary	Both	Both	Both	None	None	Both

^aPhenotypic testing of primary and secondary form *X. bovienii* bacterial strains. Each result is given as the form that produces that activity: Primary – activity in primary form only (blue), Secondary – activity in secondary form only (pink), Both – activity in primary and secondary forms (purple), or None – no activity in either form (no fill).

^bThe bacterial strain tested.

^cSwimming motility detected as motility through soft agar (0.5% LB agar).

^dSwarming motility detected as motility on top of semi-solid agar (0.7% LB agar).

^eLipase activity as detected on Tween 20 agar.

^fLecithinase activity as detected on egg yolk agar.

^gProtease activity as detected on milk agar.

^hSiderophore activity as detected activity on CAS plates.

ⁱHemolysin activity as detected on horse blood agar.

^lHemolysin activity as detected on rabbit blood agar.

^kAntibiotic activity as detected by antibiotic overlay assays.

between the two forms, and which form produces the activity was inconsistent among the strains. These differences could be due to variations in coding potential among the strains or differences in regulatory control of the genes encoding the activities tested.

To assess if activity differences are due to variation in the coding potential, we examined the *X. bovienii* genomes for relevant genes (Table 4.S2) such as lipase (*xlpA*) (16), lecithinase (*estA*) (16), protease (*prtA*) (42), and motility (flagellar operons, motility regulators) (49). All of the strains, including those strains that lacked detectable activities, encode intact homologs of these genes (Table 4.S2). This indicates that differences in activity phenotypes are more likely due to regulatory differences among the strains.

Among *Xenorhabdus* species, the regulatory pathways of *X. nematophila* are the best characterized. In this species, the leucine-responsive regulatory protein (Lrp) (50), two-component signal transduction systems CpxRA (51) and OmpR-EnvZ (52), LysR like homolog A (LrhA) (38), flagellar transcriptional regulators (FlhDC) (43, 46, 47), and nematode intestinal localization repressor (NilR) (16) regulatory proteins have been implicated in controlling the expression of the phenotypic activities listed in Table 2. Each *X. bovienii* strain encodes homologs of all these regulators except NilR (Table 4.S3). Interestingly, in *X. nematophila*, NilR functions synergistically to negatively regulate the *nilA*, *B*, and *C* genes, which are nematode-host range specificity determinants that not present in the *X. bovienii* genomes (16, 29, 53).

LysR type transcriptional regulators, of which LrhA is a member, are broadly distributed among bacteria, and can respond to specific signals to regulate narrow and broad regulons that can include genes involved in virulence, metabolism, and other behaviors (54). We assessed putative LysR type regulators encoded by *X. bovienii* and identified 19 *lysR*-type genes that are present within all *X. bovienii* strains and 7 with homologs in one or more strains (Table 4.S4). While our inability to identify certain homologs may be due to their absence in draft assemblies, we did identify a *lysR*-type gene within several draft genomes that was absent in the complete

Xb-Sj genome. This gene co-occurs with genes encoding a putative aspartate racemase and a putative glutamate symporter. This analysis indicates that distinctive LysR-type transcription factor regulation of specific metabolic pathways could occur in some strains relative to others.

An additional class of regulators common in bacteria is the two-component regulatory systems (TCSs), which perceive signals, often from the extracellular environment, and cause transcriptional changes. In canonical TCSs, the histidine kinase (HK) protein recognizes a stimulus, such as an antimicrobial peptide or quorum sensing molecule, and transmits this signal to the response regulator (RR), which then either directly or indirectly influences transcription (55). These transcriptional changes can affect bacterial phenotypic variation (56) and the production of virulence factors (57, 58) and degradative enzymes, such as lipase (59). We assessed the distribution of TCSs among the *X. bovienii* strains, and identified 23 TCSs and 2 orphan RRs which are present in all the strains, and 1 orphan HK and 4 orphan RRs that are within some but not all bacterial strains (Table 4.S5), suggesting differences in TCS-dependent regulation may occur among *X. bovienii* strains.

Our analysis indicates broad conservation of coding potential for transcriptional regulators, and the limited observed variation in the presence or absence of encoded regulators is unlikely to explain the breadth of observed phenotypic differences. Instead, phenotypic differences among strains are more likely due to variation in the expression or activity modulation of regulatory factors. The transcription factor Lrp is of particular interest in this regard as there is an established link between Lrp-dependent regulation and phenotypic variation (50). However, a detailed understanding of the basis of observed phenotype differences among strains awaits further experimentation examining their individual regulatory hierarchies. The identification of distinct signals to which regulators respond, as well as variations in the constituents of their regulons likely will provide further insights into niche diversification among these bacteria.

Annotated toxins encoded by *X. bovienii* bacterial strains. Bacteria encode a wide range of toxins that are exported by various secretions systems (60). In symbioses, these toxins can be involved in defensive mutualism (i.e. protection against predators, pathogens, or competitors) or in pathogenesis. For example, lysogenic-phage-encoded toxins expressed by the bacterial secondary symbionts of aphids protect the aphid host from parasitism by parasitoid wasps (61), while lysogenic-phage-encoded Cholera toxin (62) and Shiga toxin (63) are produced during human infection by the bacteria *Vibrio cholerae* and *Escherichia coli* respectively. In the case of *X. bovienii* bacterial strains, bacterially derived toxins could play a defensive role in protecting the insect cadaver from predators and competitors or could aid in killing the insect host. Genome analyses indicated that all *X. bovienii* bacterial strains contain annotated genes for makes caterpillars floppy toxin 1 (*mcf1*), metalloprotease RTX toxin similar to MARTX toxins (*rtxA*), zinc alkaline metalloprotease similar to RTX toxins (*prtA*), and hemolysins *Xenorhabdus* alpha-xenorhabdolysin (*xaxAB*) and one or two homologs of *Xenorhabdus* hemolysin (*xhIA* and *xhIA2*) (Additional File 6) .

The Mcf1 toxin protein from *P. luminescens* induces apoptosis in both the insect's midgut and hemocytes (64), and a Mcf1 homolog was previously identified in the finished *X. bovienii* genome (14). To determine if the annotated Mcf1 toxins from *X. bovienii* varied among the strains, we aligned the Mcf1 amino acids from all *X. bovienii* strains to that of *P. luminescens* and Xb-Sj-2004. The amino acid sequences of Mcf1 from all *X. bovienii* strains, including the Mcf1 from the finished genome, were very similar (average 3.2 PAM₁), and assessment of protein domains demonstrated that all were predicted to contain the same three domains. Similar to the previous study, we found that two of these three domains are found also in the *P. luminescens* Mcf1 protein (Figure 4.3A) (14). All of the *X. bovienii* Mcf1 toxins contain a C-terminal RTX toxin like domain predicted to be involved in export, and a middle toxin-B like domain involved in gut destruction (64). Whereas, the Mcf1 proteins from *P. luminescens* and *P.*

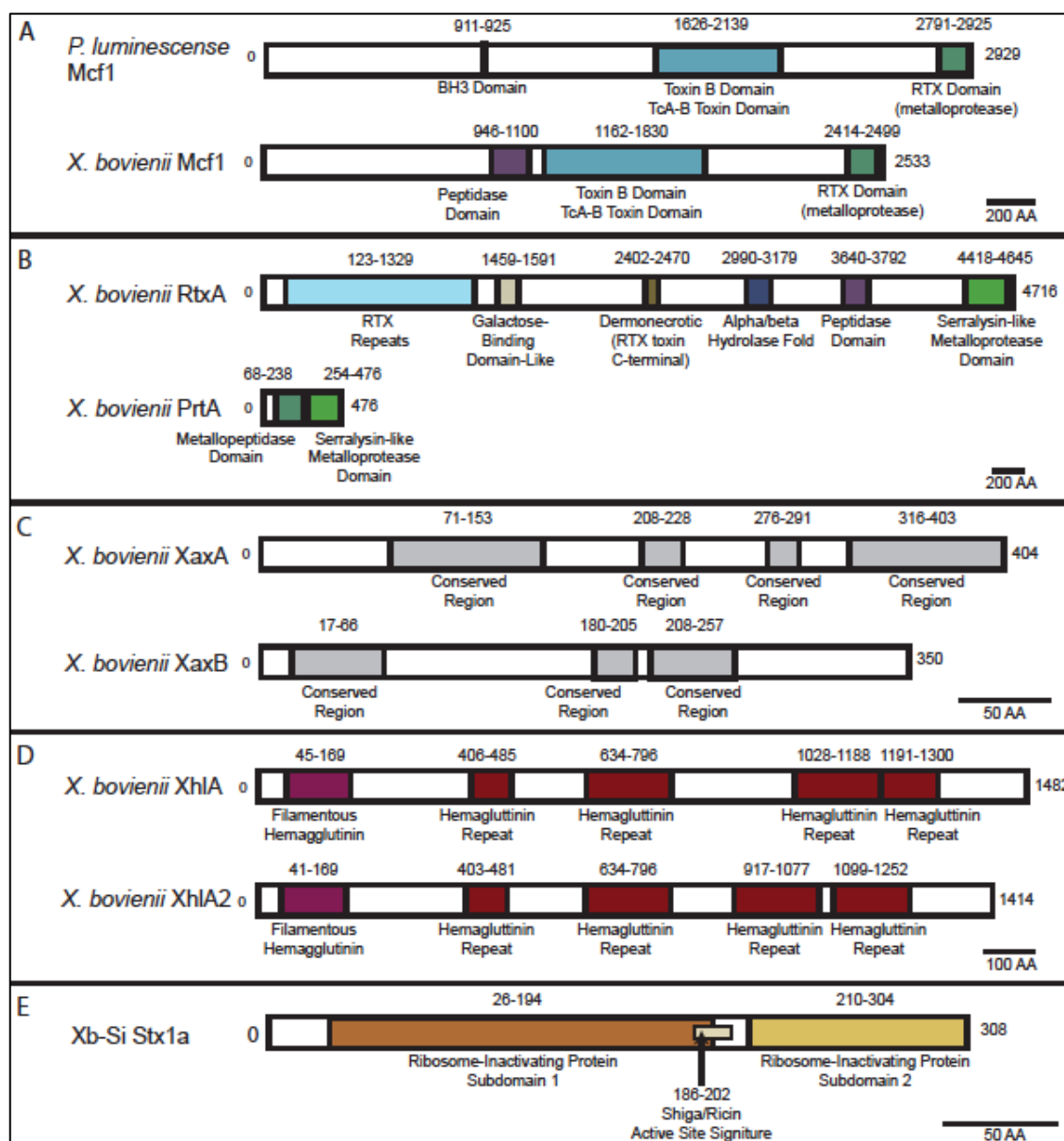


Figure 4.3 Annotated toxin genes in *X. bovienii* genomes. Schematics represent the domains identified in the proteins Mcf1 (A), RtxA and PrtA (B), XaxA and XaxB (C), XhIA and XhIA2 (D), and Stx1a (E). Names of the bacteria encoding the protein and the protein name are listed to the left of each schematic. Colored boxes represent different protein domains, and similar domains are colored the same. The predicted type of domain is listed below, and the amino acids spanning each domain are labeled above. Scale bars represent the amino acid number per distance for each panel.

asymbiotica have an N-terminal BH3-like domain that is predicted to be proapoptotic (64), the Mcf1 proteins from *X. bovienii* strains have a putative peptidase domain similar to that identified in RTX toxins that activate toxins via cleavage (Figure 4.3A) (65). Among the conserved domains, substitutions in *X. bovienii* strains Mcf1 proteins appear to be evenly distributed, with no one area showing more diversity than others (Figure 4.S1A). This indicates that no one region of the protein is under different selective pressure. To further assess if the Mcf1 proteins likely perform similar functions we assessed the possibility of horizontal gene transfer (HGT) to distinguish between putative orthologs (same function) and paralogs (potentially divergent function). Recombination testing of the nucleotide sequence indicated no sites of recombination, so trees of the genes were built using the full-length sequence (Figure 4.S2 A). All strongly supported splits in the tree match that of the previously published bacterial phylogeny, indicating that *mcf1* genes are likely orthologs and encode similar function. Additionally, testing for selection provided evidence for stabilizing selection ($dN/dS=0.3$), indicating that function is likely being maintained. In total our analyses indicates that the function of Mcf1 proteins is likely conserved among *X. bovienii* strains, but they differ in function from Mcf1 in *P. luminescens*.

Analysis of the annotated metalloprotease proteins RtxA and PrtA from all *X. bovienii* strains revealed homologs to RTX metalloproteases (Figure 4.3B) (66). Among *X. bovienii* strains there is a general conservation of amino acid sequence for both the RtxA (average 4.1 PAM) and PrtA (average 3.0 PAM). The RtxA toxin protein from Xb-Sj-2004 has been previously identified as a MARTX toxin, large RTX toxins containing >40 repeats (67). Many MARTX proteins are pathogenesis factors, including the cytotoxic RtxA from *Vibrio vulnificus* (68) to which *X. bovienii* RtxA is most similar to (Figure 4.3B). Among the *X. bovienii* strains, the amino acid sequence of RtxA proteins from those bacteria that associate with *S. feltiae* or *S. punctauvense* nematodes is very similar (average 0.8 PAM), while other pairs or groups of RtxA proteins have more diverse amino acid sequences (e.g. RtxA from the two *S. krausseii*

symbionts have a distance of 3.8 PAM). This may indicate that function of these proteins is important for the *S. feltiae* and *S. punctauvense* symbiotic life cycle and therefore they are under selective pressure to be conserved. Substitutions in the RtxA amino acid sequence were concentrated in regions between identified functional domains (e.g. amino acids 1675-1700, Figure 4.3 B, Figure 4.S1 B). These areas are known to experience weaker selection because of their lesser contribution to protein structure and function. Therefore this indicates that activity is likely conserved among *X. bovienii* RtxA homologs. The *X. bovienii* PrtA proteins show similar domains and homology to previously identified PrtA proteins from entomopathogenic bacterial symbionts *P. luminescens* (42) and *X. nematophila* (69) that associate with *Heterorhabditis bacteriophora* and *S. carpocapsae* nematodes respectively. These PrtA proteins cleave insect hemolymph proteins and are most likely involved in immunosuppression (70). Among the PrtA proteins in *X. bovienii* strains, substitutions are distributed evenly throughout the protein, indicating that no portion is highly diversified (Figure 4.S1 C). Further analyses of HGT using full-length nucleotide sequence (recombination was not detected) demonstrated that *rtxA* and *prtA* genes likely underwent HGT, as not all strongly supported splits in the gene trees match that of the bacterial phylogeny (Figure 4.S2 B,C). This indicates that some groups of genes may be paralogs. However, testing of selection indicated stabilizing selection in portions of the *rtxA* and *prtA* genes ($dN/dS=0.2$ and $dN/dS=0.3$ respectively), indicating that paralogs may have conserved function. It should also be noted that in all strains the operons encoding RtxA and PrtA include genes responsible for regulation and secretion machinery.

The *X. bovienii* strains also encode several putative hemolysins. All strains encode an annotated XaxAB protein homologous to the XaxAB binary toxin proteins in *X. nematophila* (23, 71) and *P. luminescens* (72). Among the *X. bovienii* strains, XaxA amino acid sequences are more conserved than XaxB (average 2.2 PAM and 3.5 PAM respectively). Relative to the proteins in *X. nematophila*, the XaxA proteins from *X. bovienii* strains have an average of 75%

identity over 98% of the length, and the XaxB proteins from *X. bovienii* strains have an average of 68% identity over 100% of the length. As previously reported for XaxAB from *X. nematophila* and *P. luminescens*, we were unable to identify homology to known binary toxins or any known toxin domains. Analysis of variation among the XaxAB proteins from *X. bovienii* strains revealed four portions of XaxA and three portions of XaxB that had low amino acid sequence diversity (i.e. 100% identity) (Figure 3C), divided by stretches of amino acids that have lower similarity (i.e. higher frequency of amino acid substitutions) (Figure 4.S1 D,E). When comparing the amino acid sequence of XaxAB proteins from the *X. bovienii* to proteins from *X. nematophila* and *P. luminescens*, the regions with high similarity among the *X. bovienii* proteins are also more similar between *X. nematophila* and *P. luminescens*, indicating that they may be under selection to be maintained. This suggests that some of these areas may be important for function of the protein, an idea that awaits experimental investigation. Additionally, no recombination was detected. Analyses indicate that HGT occurred for *xaxA* genes but not *xaxB* genes, as *xaxA* trees do not match the bacterial phylogeny and *xaxB* genes do (Figure 4.S2 D,E). However, *xaxA* and *xaxB* gene portions are under stabilizing selection ($dN/dS < 0.3$), indicating that function of both XaxA and XaxB is likely conserved. In addition to XaxAB, all *X. bovienii* strains contain one or two homologs of XhIA that, in *X. nematophila*, functions as a hemolysin (24) (Table 4.S6). One homolog (XhIA) is present in all of the *X. bovienii* strains (average 2.9 PAM), while the other (XhIA2) is within a subset of strains (i.e. Xb-Sf-FL, Xb-Sf-FR, Xb-Sf-MD, Xb-Sp and Xb-Si) (average 4.8 PAM). Both the XhIA and XhIA2 proteins are of a similar size (1400 amino acids) and have similar filamentous hemolysin and hemagglutinin repeat domains (Figure 4.3D). The XhIA and XhIA2 proteins represent probable paralogs, with very little conservation of amino acid sequence (average 72.3 PAM), and with diversity distributed throughout the length of the proteins (Figure 4.S1 F). Assessment of HGT supports this, as *xhIA* and *xhIA2* form separate clades but branching within the clade matches the

bacterial phylogeny (Figure 4.S2 F). Additionally, no recombination among the genes in each clade or between clades was identified. Interestingly, XhIA is more similar to the hemolysin XhIA from *X. nematophila* (24) (average 3.0 PAM) than to XhIA2 in *X. bovienii* strains. This indicates that XhIA may have similar function to the previously identified XhIA, while XhIA2 may have a divergent function.

In addition to the toxins identified in all strains that are described above, the symbiont from *S. intermedium*, Xb-Si, also encodes a putative Shiga toxin chain A (Table 4.S6). This gene was previously identified through analyses of proteins unique to each *X. bovienii* strain (73). The top hits for this protein from BLAST indicate that it is most similar to Shiga toxin 1 variant A from *Escherichia coli* (Table 4.S7), and analysis of the protein domains indicate that both active domains and the conserved active site are present (Figure 4.3E) (74). Examination of the surrounding proteins and total genome content did not reveal an obvious Shiga toxin B chain homolog. The B chain associated with other Shiga toxins is responsible for targeting the toxin complex to the correct cell type by binding globotriaosylceramide, a cell-surface ganglioside in humans (75). It seems plausible that, if functional, the Shiga toxin from Xb-Si uses a different targeting protein than do the Shiga toxins present in human-pathogenic bacteria because *Xenorhabdus* species are not human pathogens and it is unlikely that the bacterium encounters mammals during its lifecycle. Instead, we predict that the Xb-Si Shiga toxin utilizes a targeting factor that recognizes the cell-surface receptor of insect hemocytes, or those on the surfaces of other competitors or predators encountered by *X. bovienii*. The genes surrounding the Xb-Si Shiga toxin are of unknown function or are phage associated (i.e. holin and transposase). This suggests that the toxin may have been transferred in with a phage, similar to Shiga toxin producing *E. coli* or *Vibrio cholerae* (76). Analysis of the predicted holin and transposase did not conclusively identify the type of phage from which they were derived, and no other phage genes were detected in the region, since the locus is represented on a small

contig.

Insecticidal toxin complexes are diverse among *X. bovienii* bacterial strains. In addition to the annotated toxins described in the previous section, *Xenorhabdus* and *Photorhabdus* bacteria encode insecticidal toxin complex (Tc) proteins (77, 78). Tc toxins are large molecular weight toxins comprised of three subunits: A, B, and C. For each subunit, there are multiple genes that can encode a similar function (e.g. *xptA2* and *tccA2* both encode A subunit proteins that have similar features but may not function identically) (77, 78). Recent literature suggests that all three protein subunits function together for secretion from the cell, binding of the target membrane, and translocation into the cell to deliver the C-terminal end of the C subunit, which is the functional toxin. The C-terminal ends of two C-subunit proteins (TccC3 and TccC5) have ADP-ribosylating activity that results in actin polymerization and consequent toxicity (79, 80). The N-terminal end of one C subunit (TccC5), in combination with the N-terminal end of one B subunit (TcdB1), has been implicated in secretion of the toxin complex from the bacterial cell (81). The B subunit has also been proposed to function in linking the A and C subunits. The A subunit functions in targeting the toxin complex through membrane receptor binding of insect intestinal cells (80), and A subunits provide specificity of the toxin for different insect hosts (78, 82). Additionally, some A subunit proteins (*XptA1* and *XptA2*) have oral toxicity against insects (78, 82).

The finished genome of *X. bovienii* (Sj-2004) encodes Tc toxin genes (29), including three intact A subunits, two intact B subunits, and two intact C subunits. To determine if Tc toxin subunit coding regions have diversified within different strains of *X. bovienii* we conducted a keyword search of genome annotations and used BLASTp against the 9 draft genomes to identify all Tc toxin subunits encoded in these genomes (Table 4.S8). We identified 118 potential A, B, and C subunit genes within the *X. bovienii* bacterial genomes with 4-20 genes in

each genome, but analysis of the genes and their protein products revealed that many of the genes did not encode full length protein subunits (i.e. were truncated versions of the proteins identified in other *X. bovienii* strains) (Table 4.S6). Although it is possible that the truncated genes are a result of poor assembly in these genes due to the large repeats found within Tc toxin genes, this is unlikely as there was only one gene found within the finished genome, Xb-Sj-2004, that was not found within the draft Xb-Sj genome. Further supporting this, the non-full-length genes are located in the middle of contigs and in similar locations to intact homologs within other genomes and are often close to intact genes. When considering only full length coding regions, all of the *X. bovienii* strains encoded at least one of three potential A subunits (XptA2, TccA2, TccB2), five strains encoded an intact B subunit (TcaC), and four strains encoded an intact C subunit (TccC) (Table 4.S8). To determine the most likely subtype of the TccC proteins, we used BLASTp analysis and found that each TccC protein showed the highest similarity to one of four potential subtypes (TccC1, TccC4, TccC5, TccC7) (Table 4.S8). However, each of the TccC proteins were similar to several of these four potential types with different portions of the protein aligning to each subtype, indicating that the highest similarity may not be the correct subtype call for the whole protein, which also suggest recombination of these proteins. Only three (Xb-Sk-Q, Xb-Sj, Xb-Si) of the nine draft genomes encode at least one intact protein of each subunit type. However, all genomes had fragmented open reading frames corresponding to each subunit. It is unclear if these fragments would be able to function as a complete protein when combined.

To assess the variability among intact Tc protein sequences, we compared full-length amino acid sequences of *X. bovienii*, *P. luminescens*, and *X. nematophila* subunit proteins and constructed phylogenetic trees. Separate analysis of the three A subunit types (i.e. XptA2, TccA2, TccB2) revealed that substitutions in amino acid sequences among the homologs are distributed evenly throughout the amino acid sequence (i.e. no regions of the protein showed

greater number of substitutions than others) (Figure 4.S1 G-I). Other than XptA2 from Xb-Sp, the *X. bovienii* XptA2 subunit proteins were similar in amino acid sequence (average 13.7 PAM). Additionally, XptA2 from Xb-Sp also clustered away from other *X. bovienii* XptA2 proteins indicating it may have a different evolutionary history when assessing the full-length amino acid sequence (Figure 4.4A). When testing recombination, there are 5 distinct portions of the nucleotide sequence, each with a distinct phylogenetic tree that was not the same as the bacterial phylogenetic tree (Figure 4.S2 I). This indicates that HGT and recombination are occurring among these genes, which may indicate functional diversification. Selection analysis of the sections of the genes with different phylogenetic history indicate that stabilizing selection is occurring in all portions ($dN/dS < 0.3$), which suggests function of paralogs may be conserved. In contrast, all TccA2 and TccB2 proteins from *X. bovienii* had greater conservation of amino acid sequence (average 4.2 and 3.1 PAM respectively) and clustered away from *P. luminescens* and *X. nematophila* A subunits based on full-length amino acid sequence (Figure 4.4B-C), indicating the potential for conservation of function among these proteins. This was confirmed through HGT analysis of nucleotide sequence, which showed branching patterns consistent with the bacterial phylogeny (Figure 4.S2 G,H). Selection analysis of TccA2 and TccB2 also showed stabilizing selection ($dN/dS = 0.2$ and $dN/dS = 0.1$ respectively), further supporting conservation of function. Analysis of the B subunit proteins (TcaC) showed a greater amount of variability than A subunit proteins (average 42.2 PAM) and clustered into two groups by full-length amino acid sequence (Figure 4.4D), indicating the potential for divergent functions among the proteins. The substitutions in these proteins were also distributed across the length of the protein (Figure 4.S1 J). We identified that recombination was occurring and identified that portions were undergoing HGT as the phylogenies do not match the bacterial phylogeny (Figure 4.S2 J). However, the portions of the proteins are under stabilizing selections ($dN/dS < 0.3$), suggesting that function

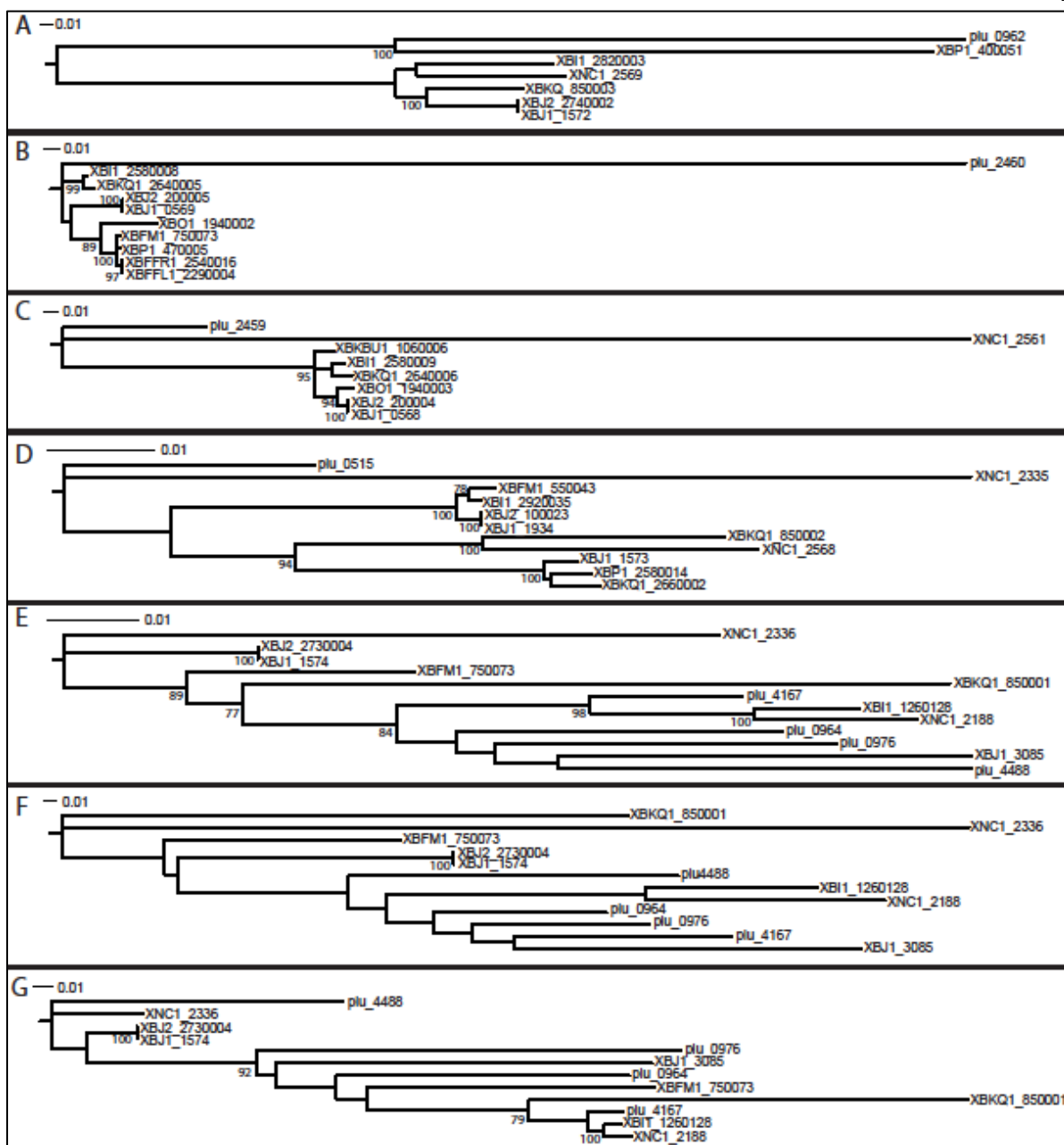


Figure 4.4 Tc toxin protein phylogenetic analyses. Analysis of Tc toxin subunit protein similarity was conducted through construction of trees using maximum likelihood methods. Subunits were grouped by type of protein: XptA (a), TccA2 (b), TccB2 (c), TcaC (d), and TccC (e). The TccC proteins were further divided into the N (f) and C (g) termini for analysis and these regions showed differing amounts of variability. Scale bars indicate 1% change in amino acid sequence for each panel.

may be conserved. To assess the diversity and evolutionary history of C subunits, we compared of all TccC subunit proteins together to identify if there were any subtypes that showed a similar evolutionary history. As expected, analysis of the amino acid sequences indicated the C subunits were more variable than A and B subunits (average 78.9 PAM). Similar to previous reports, we found that much of the diversity was concentrated in the C-terminal region (last 300 amino acids) of the proteins (Figure 4.S1 K). To account for the differences in variability, we constructed phylogenetic trees of the total protein (Figure 4.4E), the C-terminus alone (Figure 4.4F), and the N-terminus alone (Figure 4.4G). Each of these trees had distinct topologies. Additionally, we identified no patterns in clustering in any tree consistent with the subunit subtypes (Figure 4.4E-G). Further analysis of recombination indicated that the nucleotide sequence is recombining at the same place as diversity increases (Figure 4.S2 K). Surprisingly, assessment of selection indicated that portions of the gene are under stabilizing selection ($dN/dS < 0.3$). Together these data indicate that the TccC proteins are quite varied, but are under selective pressure to be maintained.

The data presented above indicate that there are considerable differences in the coding potential for Tc toxins among *X. bovienii* strains and each of the three subunits gave distinct conservation patterns, raising the idea that the selective pressures for each subunit type are different. In total, *X. bovienii* strains encode three different subunit A proteins, which may target toxin complexes to different host cell types or different insect species. However, within each A subunit protein type (i.e. all of the TccA2 proteins from *X. bovienii*) the amino acid sequences are highly similar, indicating a likely conservation of function across proteins. Therefore, variation in A subunits occur between protein types not among the proteins from different *X. bovienii* strains. For the B subunit proteins, although they are all the same type (i.e. TcaC), there is much less conservation among the proteins. This suggests that linking and secretion functions may require less conservation than the targeting function or that these proteins are

under more selective pressure to diversify. The most variation was observed among the C subunit proteins, specifically in the C-terminal domain. This is the active domain of the complex, conferring toxicity. Diversity of this domain likely reflects differences in C subunit activities. This is supported by the fact that TccC3 and TccC5 both have ADP ribosylating activity, but target different substrates. The differences in conservation level between the C- and N-terminal also indicates that these regions may have been inherited separately through horizontal gene transfer, have undergone recombination, or are under different selective pressures.

Some *X. nematophila* and *P. luminescens* Tc toxins (XptA, XptC, TccC3, TccC5) are insecticidal and *X. bovienii* homologs may function similarly. However, there is considerable divergence among the characterized Tc toxin proteins and those identified in *X. bovienii*, indicating that *X. bovienii* toxin proteins may target different insects or have different effects on the target. As insecticidal toxins, these proteins may function in the symbiosis to aid in killing the insect host or to protect the insect cadaver against insect scavengers. Therefore, variation in the Tc toxins among *X. bovienii* strains likely reflects differences in the insect hosts or scavengers encountered during their lifecycle.

Non-ribosomal peptide synthetase and polyketide synthetase cluster variation. Another class of molecules likely involved in symbiotic interactions is that produced by non-ribosomal peptide synthetase (NRPS) and polyketide synthetase (PKS) systems: multi-gene, modular enzymes that synthesize small molecules with a variety of biological functions. Prior studies have reported extensive diversity in NRPS and PKS clusters among entomopathogenic nematode symbiont species, such as *X. nematophila* and *P. luminescens* (17, 29). Among *X. bovienii* bacterial strains, variation in NRPS and PKS coding potential also occurs (Table 4.3). A total of 29 distinct NRPS and PKS clusters were identified among all the analyzed strains combined. Of these clusters, six were identified in all of the strains (conserved) and seven were

found within only one strain (unique). The remaining sixteen clusters were found in a subset of some, but not all, strains (shared).

One of the conserved clusters, one of the unique clusters, and four shared clusters have known siderophore (i.e. metal scavenging compounds) or antibiotic products (Table 4.3). The remaining clusters (5 conserved, 6 unique, and 12 shared clusters) do not have a known product. When compared to published genomes of *X. nematophila* and *P. luminescens* (29, 30) we found that of the 29 identified clusters, 6 (2 conserved, 1 unique, and 3 shared clusters) were also shared by *X. nematophila* and none were shared by *P. luminescens* (Table 4.3). This indicates that while the entomopathogenic symbiont species all have a large number of NRPS and PKS clusters, it is likely that the majority of the products produced are different among species. This also suggests that many of the identified *X. bovienii* clusters may produce novel compounds, as very closely related species lack them.

The function of NRPS and PKS products are diverse, and can have an equally diverse range of functions including anti-microbial (10, 17, 83-85), anti-predation (7, 8, 86), immunosuppressive (87), hemolytic (85), and metal acquisition (88) activities. Several of these functions have the potential to provide symbiotic benefits. Products that provide anti-microbial or anti-predation activity could play a defensive role within the symbiosis by protecting the insect cadaver, and therefore the developing nematodes and bacteria, from invasion by pathogens, competitors, or predators. Additionally, products that provide immunosuppressive or hemolytic activity could aid in the killing of the insect host, thereby providing nutrition to the nematodes and bacteria. Although it is possible that the predicted NRPS and PKS cluster products provide these benefits, defining the activities and role of the molecules awaits further experimental testing and functional characterization.

Table 4.3 NRPS and PKS clusters^a.

Type	Predicted Product	Xb_Sf_FL	Xb_Sf_FR	Xb_Sf_MD	Xb_Sp	Xb_Sk_BU	Xb_Sk_Q	Xb_Sj_SS2004	Xb_Sj	Xb_So	Xb_Si	Xn
NRPS	Rhizobactin siderophore	140051	80052	820008	2430008	240012	180016	3246	1680051	140008	120011	
NRPS	Vibrobactin siderophore									2570021		
NRPS	Enterobactin siderophore	2380017	310119	750018	930044	570012	1280020	1435	2690027		1870125	
NRPS		310016	1840016	1540002	2990118	3020004	23500301	0310	130005	850003	1570007	
NRPS		850036	2390016	900015	2380011	1920022	1200019	0543	170017	290109	2060012	0646
NRPS		980025	1830002	530035	2230045	1810023	850099	2153	1190003	1300223	200022	2152
NRPS		1440021	630020	1510028	400023	2960007	850017	2367	1260017	1300059	1260106	
NRPS		80002		40001						20001	60001	
NRPS		2690021	310123	750012	930038	570003	1280024	1439	2690021		1870129	
NRPS		1160033	1760003	1310046	1340054	1720001	1190001				1940050	
NRPS		2270014	1140008	1950014	930013	1370008						
NRPS						3890002		1967				
NRPS		350018	50002	2380002							1450002	
NRPS		70001										2713
NRPS				20001								
NRPS											2990001	
NRPS											40001	
NRPS						9400034						
NRPS						3150001						
NRPS										1400001		
NRPS - t1 PKS		350012	1030011	2380008	2940097	3440004	2890014				1450014	
NRPS - t1 PKS		1860006	2330006	670005	950007	420004	150005	2690	2870029	480093	1220007	
NRPS - t1 PKS		350015	1030008	2380005	2940010	3440001	2890017				1450011	
NRPS - t1 PKS	Xenocomaucin antibiotic (<i>xncL</i>)	2670005	2570004	1900004	2630007	4010035	2820032				1920001	1700
NRPS - t1 PKS	Xenocomaucin antibiotic (<i>xncA</i>)	1870004	2350004	700004	960004	430004	160004	2695	2870024	480088	1230006	1711
NRPS - t1 PKS	Clauvimate antibiotic	1750009	850008	1990007	2300008		1080012					2156
PKS	Rifamycin antibiotic	1430002	270007	2350005	1910006							
Trans AT PKS - NRPS				2060004						980004		
Trans AT PKS - NRPS							2930021				2660058	

^aDistribution of NRPS and PKS clusters among the *X. bovienii* genomes listed as the first biosynthesis gene of the cluster. The number designation for each gene is given without the prefixes: Xb-Sf-FL (XBFFL1), Xb-Sf-FR (XBFFR1), Xb-Sf-MD (XBFMD1), Xb-Sp (XBP1), Xb-Sk-BU (XBKB1), Xb-Sk-Q (XBKQ1), Xb-Sj-2004 (XBJ1), Xb-Sj (XBJ2), Xb-So (XBO1), Xb-Si (XBI1), and Xn (XNC1). Green shading highlights distribution among the strains.

^bTypes of clusters: NRPS (non-ribosomal peptide synthetase), PKS (polyketide synthetase), T1 PKS (type 1 PKS), or Trans AT PKS (trans-acyltransferase PKS).

^cPredicted product from the NRPS and PKS clusters, if known.

CONCLUSIONS

Overall, the presented analyses highlight that there is conservation among *X. bovienii* strains in fundamental processes underlying symbiotic interactions (e.g. secretion systems and degradative activities). However, phenotypic testing indicates that despite conservation in coding potential, strain-level differences in expression of symbiosis factors could contribute to varying fitness in selective environments. Further, we observed notable variation in certain classes of genes, such as those encoding NRPS and PKS clusters and Tc toxins, indicating that the factors contributing to host interactions likely differ.

Variation in the ability of the bacterial strains to engage in symbiosis with the nematode likely results from coevolution, and therefore co-adaptation, between nematode host species and bacterial symbiont strains (4, 73). However, it is also possible that differences in the ability of symbionts to engage in symbiosis could be due to differential gene loss or access to gene pools, not necessarily dependent on coevolution. A corollary to this is that changes in coding potential or regulation that confer relative increases in fitness will be selected within individual bacteria-nematode complexes. Activities predicted to diversify in this way are those that benefit the nematode host, such as those involved in nutrient acquisition. Our data indicate that while the many of the nutritional factors do not differ among strains the regulation does (e.g. lipase). This indicates that while overall nutritional requirements may not vastly differ between nematode hosts, the necessary timing of nutrient production varies and is likely important for optimal symbiotic benefits. In contrast, bacterial factors that contribute to virulence towards the insect host or to defense against predators are more likely to vary based on selective pressures of environmental differences encountered by the bacterial strains, such as the insect host species, endogenous bacterial competitors within these insects, or the predators, competitors, and pathogens naturally encountered. Our genomics analyses demonstrate diversity in many of these types of compounds (e.g. NRPS encoded molecules, Tc toxins, and hemolysins),

indicating that the nematode – bacterial pairs likely encounter different insect hosts and competitors, as some of these have been demonstrated to function differently against divergent insect hosts (82). However, many of the large molecular weight toxins (e.g. Mcf1, RTX toxin, and XaxAB) are conserved, as homologs are present in all strains, indicating that these toxins may not be specific to particular insect host ranges and instead functional against many insect hosts. Together, our comparative genomics and phenotypic analyses suggest that symbiotic functions of the *X. bovienii* bacterial strains differ due to the diversity of effectors and their regulation rather than the utilization of different mechanisms for interacting with hosts.

In addition to providing insight into the diversity of potential symbiotic functions, the data presented here highlight that strain variability is an important consideration when exploiting *Xenorhabdus* bacteria for discovery of compounds for application purposes. For the discovery of novel antibiotics or other NRPS- and PKS-derived compounds from *Xenorhabdus* spp., it will be useful to assess multiple bacterial strains, as we observed large strain-level diversity in coding potential for these systems. This is also the case when assessing Tc toxin clusters. However, for the application of many other large molecular weight toxins (e.g. XaxAB, Mcf1, RtxA), the activities determined from a single bacterial strain likely will be similar among the members of that species, although this might not be the case across *Xenorhabdus* spp.

In summary, the comparative genomic analysis presented here provides an assessment of *X. bovienii* bacterial strain variation in factors that could be involved in symbiotic interactions and may be utilized for applications. This analysis provides a foundation for understanding how bacterial strain variability affects symbiosis and for the discovery of novel compounds within *Xenorhabdus* spp.

AUTHOR CONTRIBUTIONS

KEM did all comparative genomics analyses. ACW and KEM completed phenotypic experiments. KEM, JLK, and HGB analyzed data and wrote the manuscript. All authors read and approved the final manuscript. The authors declare that they have no competing interests.

ACKNOWLEDGEMENTS

This study was supported by grants from the National Science Foundation to HGB (IOS-0920631 and IOS-1353674). KEM also was supported by the National Institutes of Health (NIH) National Research Service Award T32 AI55397, a Louis and Elsa Thomsen Distinguished Predoctoral Fellowship, and a Betley-Allen Predoctoral Fellowship. The authors wish to thank Thomas Sorenson for his contributions to the analysis presented in Table 4.S2.

MATERIALS AND METHODS

Genome Features. Genomes were submitted to MaGe (89, 90) for annotation and analysis.

The genomes were analyzed for size, GC content, number of coding sequences, and the percentage of the genome covered by coding content. The genomes were assessed for synteny using MAUVE (91) relative to the finished genome of *X. bovienii* (Table 4.1) (30).

Secretion systems. The secretion systems were found through keyword searching for secretion system components. The intactness of the secretion systems was determined by assessing the genomes for homologs to known structural components in the secretion systems. For a secretion system to be called intact, it must have had all known necessary secretion system genes (31, 32, 36, 39-41, 92, 93). Absence of other secretion systems was determined through comparing known necessary secretion system components to the genomes using BLASTp (94).

NRPS and PKS clusters. NRPS and PKS clusters were found by assessing each genome with antiSMASH (95) for all potential clusters. Clusters were confirmed as intact by assessing that each cluster has at least one adenylation domain, one condensation domain, and one thioesterase domain. The NRPS and PKS clusters were compared to one another to determine their distribution among the *X. bovienii* genomes through assessing the cluster proteins for local synteny within the genomes, using MaGE and MAUVE alignments. The presence or absence of the *X. bovienii* NRPS and PKS clusters in *X. nematophila* and *P. lumenescens* was determined by searching for the gene clusters in the finished genomes using MaGE synteny mapping.

Toxins. Genes for putative toxin proteins were revealed by searching for genes annotated as toxins by the MaGe platform. Annotations were further supported by BLASTp, Interpro 51.0

(96), and Swiss Prot (89, 90) analyses. Toxin domains were analyzed using Interpro, and in the case of Mcf1, comparison to known protein domains in homologs. Assessment of toxin subtypes (i.e. Shiga toxin and Tc toxin) was performed based on BLASTp results (94). For assessing similarities among *X. bovienii*, amino acid sequences were aligned using MUSCLE 3.7 (97, 98), and protein distances were calculated using Phylip 3.695 with the Jones-Taylor-Thornton model in Protdist (99). Protein distances are given in point accepted mutation (PAM), representing the number of point mutation events in 100 amino acids. Protein trees were built using Maximum Likelihood and bootstrapped in Phylip (99), and trees were visualized in iTol (100). For visualization of amino acid differences along the length of the proteins, the alignment was visualized in MegAlign Pro from DNASTAR 11.0 (www.dnastar.com). Regions of dissimilarity were considered when at least 4 amino acids in a row were different among at least 50% of the homologs.

Testing of Recombination, Horizontal Gene Transfer, and Selection. Nucleotide sequences were aligned in MEGA v6.0 (101). Analyses of nucleotide sequences was done in Topali v2 (102). Assessment of recombination was done using DSS and the sequence was partitioned. Horizontal gene transfer was done through comparison of gene phylogenies to the bacterial whole genome phylogeny (73). Phylogenetic trees were built from partitioned sequences and bootstrapped using maximum likelihood. Bootstrap values were used to determine strongly supported splits (>75). Selection was determined using PAML in Topali to calculation dN/dS ratios (103).

Phenotypic Testing. Stable secondary form bacterial isolates were made from stable primary form bacterial strains through repeated passage. Briefly, bacterial strains were grown at 30°C in lysogeny broth with aeration in the dark. Bacterial strains were grown approximately 24 hours

and sub-cultured into fresh media. Sub-culturing occurred for a period of 2-4 weeks, until bacteria spread on NBTA agar (104) no longer bound bromothymol blue dye and was red in color with repeated restreaking. Phenotypic tests were done similar to previously described for swimming (105) and swarming (47) motility on LB agar, lipase on tween 20 agar (106), lecithinase on egg yolk agar (107), protease on milk agar (107), siderophore on CAS agar (45), and hemolysin on horse and rabbit blood agar plates (108). For all assays, 5 μ L of overnight bacterial culture was spotted onto the agar plate and dried, and the plates were incubated at 30°C in the dark for 48 hours prior to reading. Antibiotic activity was determined through overlay assays using *Escherichia coli*, *Micrococcus luteus*, and *Bacillus subtilis* as the overlaid test strains (109). For antibiotic activity, 5 μ L of overnight *X. bovienii* bacterial culture was spotted onto LB agar plates supplemented with pyruvate and dried, and the plates were incubated for at 30°C in the dark for 24 hours prior to overlaying with the test bacterial strain. After overlay, the plates were incubated for at 37°C for 24 hours prior to reading. For these experiments, all test strains were inhibited.

Assessment of *X. bovienii* genes contributing to phenotypic activity. Homologs of genes known to contribute to the identified activity were assessed through BLAST P analysis of the homologs in each *X. bovienii* bacterial strain. For multifactorial activities, assessment was done as mentioned in NRPS and PKS clusters.

REFERENCES

1. **Grewal PS, Ehlers RU, Shapiro-Ilan DI (ed).** 2005. Nematodes as Biocontrol Agents. CABI Publishing, Wallingford, UK.
2. **Griffin CT.** 2012. Perspectives on the behavior of entomopathogenic nematodes from dispersal to reproduction: traits contributing to nematode fitness and biocontrol efficacy. *J Nematol* **44**:177-184.
3. **Campos-Herrera R, Barbercheck M, Hoy CW, Stock SP.** 2012. Entomopathogenic nematodes as a model system for advancing the frontiers of ecology. *J Nematol* **44**:162-176.
4. **Chapuis E, Emelianoff V, Paulmier V, Le Brun N, Pages S, Sicard M, Ferdy JB.** 2009. Manifold aspects of specificity in a nematode-bacterium mutualism. *J Evol Biol* **22**:2104-2117.
5. **Herbert EE, Goodrich-Blair H.** 2007. Friend and foe: the two faces of *Xenorhabdus nematophila*. *Nat Rev Microbiol* **5**:634-646.
6. **Richards GR, Goodrich-Blair H.** 2009. Masters of conquest and pillage: *Xenorhabdus nematophila* global regulators control transitions from virulence to nutrient acquisition. *Cell Microbiol* **11**:1025-1033.
7. **Gulcu B, Hazir S, Kaya HK.** 2012. Scavenger deterrent factor (SDF) from symbiotic bacteria of entomopathogenic nematodes. *J Invertebr Pathol* **110**:326-333.
8. **Zhou X, Kaya HK, Heungens K, Goodrich-Blair H.** 2002. Response of ants to a deterrent factor(s) produced by the symbiotic bacteria of entomopathogenic nematodes. *Appl Environ Microbiol* **68**:6202-6209.
9. **Morales-Soto N, Forst SA.** 2011. The xnp1 P2-like tail synthesis gene cluster encodes xenorhabdicolin and is required for interspecies competition. *J Bacteriol* **193**:3624-3632.
10. **Singh S, Orr D, Divinagracia E, McGraw J, Dorff K, Forst S.** 2015. Role of secondary metabolites in establishment of the mutualistic partnership between *Xenorhabdus nematophila* and the entomopathogenic nematode *Steinernema carpocapsae*. *Appl Environ Microbiol* **81**:754-764.
11. **Singh S, Reese JM, Casanova-Torres AM, Goodrich-Blair H, Forst S.** 2014. Microbial population dynamics in the hemolymph of *Manduca sexta* infected with *Xenorhabdus nematophila* and the entomopathogenic nematode *Steinernema carpocapsae*. *Appl Environ Microbiol* **80**:4277-4285.
12. **Koppenhofer AM, Kaya HK.** 1996. Coexistence of two steinernematid nematode species (Rhabditida:Steinernematidae) in the presence of two host species. *Appl Soil Ecol* **4**:221-230.
13. **Popiel I, Grove DL, Friedman MJ.** 1989. Infective juvenile formation in the insect parasitic nematode *Steinernema feltiae*. *Parasitology* **99**:77-81.

14. **Sugar DR, Murfin KE, Chaston JM, Andersen AW, Richards GR, deLeon L, Baum JA, Clinton WP, Forst S, Goldman BS, Krasomil-Osterfeld KC, Slater S, Stock SP, Goodrich-Blair H.** 2012. Phenotypic variation and host interactions of *Xenorhabdus bovienii* SS-2004, the entomopathogenic symbiont of *Steinernema jolietii* nematodes. *Environ Microbiol* **14**:924-939.
15. **Orchard SS, Goodrich-Blair H.** 2004. Identification and functional characterization of a *Xenorhabdus nematophila* oligopeptide permease. *Appl Environ Microbiol* **70**:5621-5627.
16. **Richards GR, Goodrich-Blair H.** 2010. Examination of *Xenorhabdus nematophila* lipases in pathogenic and mutualistic host interactions reveals a role for *xlpA* in nematode progeny production. *Appl Environ Microbiol* **76**:221-229.
17. **Bode HB.** 2009. Entomopathogenic bacteria as a source of secondary metabolites. *Curr Opin Chem Biol* **13**:224-230.
18. **Martens EC, Heungens K, Goodrich-Blair H.** 2003. Early colonization events in the mutualistic association between *Steinernema carpocapsae* nematodes and *Xenorhabdus nematophila* bacteria. *J Bacteriol* **185**:3147-3154.
19. **Sicard M, Brugirard-Ricaud K, Pages S, Lanois A, Boemare NE, Brehelin M, Givaudan A.** 2004. Stages of infection during the tripartite interaction between *Xenorhabdus nematophila*, its nematode vector, and insect hosts. *Appl Environ Microbiol* **70**:6473-6480.
20. **Ehlers RU, Wulff A, Peters A.** 1997. Pathogenicity of axenic *Steinernema feltiae*, *Xenorhabdus bovienii*, and the bacto-helminthic complex to larvae of *Tipula oleracea* (Diptera) and *Galleria mellonella* (Lepidoptera). *J Invertebr Pathol* **69**:212-217.
21. **Brivio MF, Moro M, Mastore M.** 2006. Down-regulation of antibacterial peptide synthesis in an insect model induced by the body-surface of an entomoparasite (*Steinernema feltiae*). *Dev Comp Immunol* **30**:627-638.
22. **Sheets JJ, Hey TD, Fencil KJ, Burton SL, Ni W, Lang AE, Benz R, Aktories K.** 2011. Insecticidal toxin complex proteins from *Xenorhabdus nematophilus*: structure and pore formation. *J Biol Chem* **286**:22742-22749.
23. **Vigneux F, Zumbihl R, Jubelin G, Ribeiro C, Poncet J, Baghdiguian S, Givaudan A, Brehelin M.** 2007. The *xaxAB* genes encoding a new apoptotic toxin from the insect pathogen *Xenorhabdus nematophila* are present in plant and human pathogens. *J Biol Chem* **282**:9571-9580.
24. **Cowles KN, Goodrich-Blair H.** 2005. Expression and activity of a *Xenorhabdus nematophila* haemolysin required for full virulence towards *Manduca sexta* insects. *Cell Microbiol* **7**:209-219.
25. **Eom S, Park Y, Kim Y.** 2014. Sequential immunosuppressive activities of bacterial secondary metabolites from the entomopathogenic bacterium *Xenorhabdus nematophila*. *J Microbiol* **52**:161-168.

26. **Reimer D, Cowles KN, Proschak A, Nollmann FI, Dowling AJ, Kaiser M, ffrench-Constant R, Goodrich-Blair H, Bode HB.** 2013. Rhabdopeptides as insect-specific virulence factors from entomopathogenic bacteria. *Chembiochem* **14**:1991-1997.
27. **Pidot SJ, Coyne S, Kloss F, Hertweck C.** 2014. Antibiotics from neglected bacterial sources. *Int J Med Microbiol* **304**:14-22.
28. **Vizcaino MI, Guo X, Crawford JM.** 2014. Merging chemical ecology with bacterial genome mining for secondary metabolite discovery. *J Ind Microbiol Biotechnol* **41**:285-299.
29. **Chaston JM, Suen G, Tucker SL, Andersen AW, Bhasin A, Bode E, Bode HB, Brachmann AO, Cowles CE, Cowles KN, Darby C, de Leon L, Drace K, Du Z, Givaudan A, Herbert Tran EE, Jewell KA, Knack JJ, Krasomil-Osterfeld KC, Kukor R, Lanois A, Latreille P, Leimgruber NK, Lipke CM, Liu R, Lu X, Martens EC, Marri PR, Medigue C, Menard ML, Miller NM, Morales-Soto N, Norton S, Ogier JC, Orchard SS, Park D, Park Y, Qurollo BA, Sugar DR, Richards GR, Rouy Z, Slominski B, Slominski K, Snyder H, Tjaden BC, van der Hoeven R, Welch RD, Wheeler C, Xiang B, Barbazuk B, et al.** 2011. The entomopathogenic bacterial endosymbionts *Xenorhabdus* and *Photorhabdus*: convergent lifestyles from divergent genomes. *PLoS One* **6**:e27909.
30. **Latreille P, Norton S, Goldman BS, Henkhaus J, Miller N, Barbazuk B, Bode HB, Darby C, Du Z, Forst S, Gaudriault S, Goodner B, Goodrich-Blair H, Slater S.** 2007. Optical mapping as a routine tool in bacterial genome sequencing. *BMC Genomics* **8**:321.
31. **Coulthurst SJ.** 2013. The Type VI secretion system - a widespread and versatile cell targeting system. *Res Microbiol* **164**:640-654.
32. **Cianciotto NP.** 2013. Type II secretion and *Legionella* virulence. *Curr Top Microbiol Immunol* **376**:81-102.
33. **Jani AJ, Cotter PA.** 2010. Type VI secretion: not just for pathogenesis anymore. *Cell Host Microbe* **8**:2-6.
34. **Okazaki S, Kaneko T, Sato S, Saeki K.** 2013. Hijacking of leguminous nodulation signaling by the rhizobial type III secretion system. *Proc Natl Acad Sci U S A* **110**:17131-17136.
35. **Christie PJ, Whitaker N, Gonzalez-Rivera C.** 2014. Mechanism and structure of the bacterial type IV secretion systems. *Biochim Biophys Acta* **1843**:1578-1591.
36. **Singh P, Park D, Forst S, Banerjee N.** 2013. Xenocin export by the flagellar type III pathway in *Xenorhabdus nematophila*. *J Bacteriol* **195**:1400-1410.
37. **Barrero-Tobon AM, Hendrixson DR.** 2014. Flagellar biosynthesis exerts temporal regulation of secretion of specific *Campylobacter jejuni* colonization and virulence determinants. *Mol Microbiol* **93**:957-974.

38. **Richards GR, Herbert EE, Park Y, Goodrich-Blair H.** 2008. *Xenorhabdus nematophila* *lrhA* is necessary for motility, lipase activity, toxin expression, and virulence in *Manduca sexta* insects. *J Bacteriol* **190**:4870-4879.
39. **Nivaskumar M, Francetic O.** 2014. Type II secretion system: a magic beanstalk or a protein escalator. *Biochim Biophys Acta* **1843**:1568-1577.
40. **Cascales E.** 2008. The type VI secretion toolkit. *EMBO Rep* **9**:735-741.
41. **Silverman JM, Brunet YR, Cascales E, Mougous JD.** 2012. Structure and regulation of the type VI secretion system. *Annu Rev Microbiol* **66**:453-472.
42. **Bowen DJ, Rocheleau TA, Grutzmacher CK, Meslet L, Valens M, Marble D, Dowling A, Ffrench-Constant R, Blight MA.** 2003. Genetic and biochemical characterization of PrtA, an RTX-like metalloprotease from *Photorhabdus*. *Microbiology* **149**:1581-1591.
43. **Givaudan A, Lanois A.** 2000. *flhDC*, the flagellar master operon of *Xenorhabdus nematophilus*: requirement for motility, lipolysis, extracellular hemolysis, and full virulence in insects. *J Bacteriol* **182**:107-115.
44. **An R, Sreevatsan S, Grewal PS.** 2009. Comparative *in vivo* gene expression of the closely related bacteria *Photorhabdus temperata* and *Xenorhabdus koppenhoeferi* upon infection of the same insect host, *Rhizotrogus majalis*. *BMC Genomics* **10**:433.
45. **Schwyn B, Neilands JB.** 1987. Universal chemical assay for the detection and determination of siderophores. *Anal Biochem* **160**:47-56.
46. **Jubelin G, Pages S, Lanois A, Boyer MH, Gaudriault S, Ferdy JB, Givaudan A.** 2011. Studies of the dynamic expression of the *Xenorhabdus* FliAZ regulon reveal atypical iron-dependent regulation of the flagellin and haemolysin genes during insect infection. *Environ Microbiol* **13**:1271-1284.
47. **Kim DJ, Boylan B, George N, Forst S.** 2003. Inactivation of *ompR* promotes precocious swarming and *flhDC* expression in *Xenorhabdus nematophila*. *J Bacteriol* **185**:5290-5294.
48. **Chapuis E, Arnal A, Ferdy JB.** 2012. Trade-offs shape the evolution of the vector-borne insect pathogen *Xenorhabdus nematophila*. *Proc Biol Sci* **279**:2672-2680.
49. **Macnab RM.** 1992. Genetics and biogenesis of bacterial flagella. *Annu Rev Genet* **26**:131-158.
50. **Cowles KN, Cowles CE, Richards GR, Martens EC, Goodrich-Blair H.** 2007. The global regulator Lrp contributes to mutualism, pathogenesis and phenotypic variation in the bacterium *Xenorhabdus nematophila*. *Cell Microbiol* **9**:1311-1323.
51. **Herbert EE, Cowles KN, Goodrich-Blair H.** 2007. CpxRA regulates mutualism and pathogenesis in *Xenorhabdus nematophila*. *Appl Environ Microbiol* **73**:7826-7836.
52. **Park D, Forst S.** 2006. Co-regulation of motility, exoenzyme and antibiotic production by the EnvZ-OmpR-FlhDC-FliA pathway in *Xenorhabdus nematophila*. *Mol Microbiol* **61**:1397-1412.

53. **Bhasin A, Chaston JM, Goodrich-Blair H.** 2012. Mutational analyses reveal overall topology and functional regions of NilB, a bacterial outer membrane protein required for host association in a model of animal-microbe mutualism. *J Bacteriol* **194**:1763-1776.
54. **Maddocks SE, Oyston PC.** 2008. Structure and function of the LysR-type transcriptional regulator (LTTR) family proteins. *Microbiology* **154**:3609-3623.
55. **Jung K, Fried L, Behr S, Heermann R.** 2012. Histidine kinases and response regulators in networks. *Curr Opin Microbiol* **15**:118-124.
56. **Derzelle S, Ngo S, Turlin E, Duchaud E, Namane A, Kunst F, Danchin A, Bertin P, Charles JF.** 2004. AstR-AstS, a new two-component signal transduction system, mediates swarming, adaptation to stationary phase and phenotypic variation in *Photothabdus luminescens*. *Microbiology* **150**:897-910.
57. **Derzelle S, Turlin E, Duchaud E, Pages S, Kunst F, Givaudan A, Danchin A.** 2004. The PhoP-PhoQ two-component regulatory system of *Photothabdus luminescens* is essential for virulence in insects. *Journal of bacteriology* **186**:1270-1279.
58. **Reboul A, Lemaitre N, Titecat M, Merchez M, Deloison G, Ricard I, Pradel E, Marceau M, Sebbane F.** 2014. *Yersinia pestis* requires the 2-component regulatory system OmpR-EnvZ to resist innate immunity during the early and late stages of plague. *J Infect Dis* **210**:1367-1375.
59. **Krzeslak J, Gerritse G, van Merkerk R, Cool RH, Quax WJ.** 2008. Lipase expression in *Pseudomonas alcaligenes* is under the control of a two-component regulatory system. *Appl Environ Microbiol* **74**:1402-1411.
60. **Zhang D, de Souza RF, Anantharaman V, Iyer LM, Aravind L.** 2012. Polymorphic toxin systems: Comprehensive characterization of trafficking modes, processing, mechanisms of action, immunity and ecology using comparative genomics. *Biol Direct* **7**:18.
61. **Oliver KM, Russell JA, Moran NA, Hunter MS.** 2003. Facultative bacterial symbionts in aphids confer resistance to parasitic wasps. *Proc Natl Acad Sci U S A* **100**:1803-1807.
62. **Jobling MG, Holmes RK.** 2000. Identification of motifs in cholera toxin A1 polypeptide that are required for its interaction with human ADP-ribosylation factor 6 in a bacterial two-hybrid system. *Proc Natl Acad Sci U S A* **97**:14662-14667.
63. **Obrig TG, Karpman D.** 2012. Shiga toxin pathogenesis: kidney complications and renal failure. *Curr Top Microbiol Immunol* **357**:105-136.
64. **Daborn PJ, Waterfield N, Silva CP, Au CP, Sharma S, Ffrench-Constant RH.** 2002. A single *Photothabdus* gene, makes caterpillars floppy (*mcf*), allows *Escherichia coli* to persist within and kill insects. *Proc Natl Acad Sci U S A* **99**:10742-10747.
65. **Sheahan KL, Cordero CL, Satchell KJ.** 2007. Autoprocessing of the *Vibrio cholerae* RTX toxin by the cysteine protease domain. *EMBO J* **26**:2552-2561.

66. **Linhartova I, Bumba L, Masin J, Basler M, Osicka R, Kamanova J, Prochazkova K, Adkins I, Hejnova-Holubova J, Sadilkova L, Morova J, Sebo P.** 2010. RTX proteins: a highly diverse family secreted by a common mechanism. *FEMS Microbiol Rev* **34**:1076-1112.
67. **Satchell KJ.** 2007. MARTX, multifunctional autoprocessing repeats-in-toxin toxins. *Infect Immun* **75**:5079-5084.
68. **Lee JH, Kim MW, Kim BS, Kim SM, Lee BC, Kim TS, Choi SH.** 2007. Identification and characterization of the *Vibrio vulnificus rtxA* essential for cytotoxicity *in vitro* and virulence in mice. *J Microbiol* **45**:146-152.
69. **Caldas C, Cherqui A, Pereira A, Simoes N.** 2002. Purification and characterization of an extracellular protease from *Xenorhabdus nematophila* involved in insect immunosuppression. *Appl Environ Microbiol* **68**:1297-1304.
70. **Massaoud MK, Marokhazi J, Fodor A, Venekei I.** 2010. Proteolytic enzyme production by strains of the insect pathogen *Xenorhabdus* and characterization of an early-log-phase-secreted protease as a potential virulence factor. *Appl Environ Microbiol* **76**:6901-6909.
71. **Brillard J, Ribeiro C, Boemare N, Brehelin M, Givaudan A.** 2001. Two distinct hemolytic activities in *Xenorhabdus nematophila* are active against immunocompetent insect cells. *Appl Environ Microbiol* **67**:2515-2525.
72. **Zhang X, Hu X, Li Y, Ding X, Yang Q, Sun Y, Yu Z, Xia L, Hu S.** 2014. XaxAB-like binary toxin from *Photorhabdus luminescens* exhibits both insecticidal activity and cytotoxicity. *FEMS Microbiol Lett* **350**:48-56.
73. **Murfin KE, Lee MM, Klassen JL, McDonald BR, Larget B, Forst S, Stock SP, Currie CR, Goodrich-Blair H.** in press 2015. *Xenorhabdus bovienii* bacterial strain diversity impacts coevolution and symbiotic maintenance with *Steinernema* spp. nematode hosts. *mBio*.
74. **Hovde CJ, Calderwood SB, Mekalanos JJ, Collier RJ.** 1988. Evidence that glutamic acid 167 is an active-site residue of Shiga-like toxin I. *Proc Natl Acad Sci U S A* **85**:2568-2572.
75. **Stein PE, Boodhoo A, Tyrrell GJ, Brunton JL, Read RJ.** 1992. Crystal structure of the cell-binding B oligomer of verotoxin-1 from *E. coli*. *Nature* **355**:748-750.
76. **Brussow H, Canchaya C, Hardt WD.** 2004. Phages and the evolution of bacterial pathogens: from genomic rearrangements to lysogenic conversion. *Microbiol Mol Biol Rev* **68**:560-602, table of contents.
77. **Ffrench-Constant R, Waterfield N.** 2006. An ABC guide to the bacterial toxin complexes. *Adv Appl Microbiol* **58**:169-183.
78. **Waterfield N, Hares M, Yang G, Dowling A, ffrench-Constant R.** 2005. Potentiation and cellular phenotypes of the insecticidal toxin complexes of *Photorhabdus bacteria*. *Cell Microbiol* **7**:373-382.

79. **Lang AE, Ernst K, Lee H, Papatheodorou P, Schwan C, Barth H, Aktories K.** 2014. The chaperone Hsp90 and PPIases of the cyclophilin and FKBP families facilitate membrane translocation of *Photorhabdus luminescens* ADP-ribosyltransferases. *Cell Microbiol* **16**:490-503.
80. **Lang AE, Schmidt G, Schlosser A, Hey TD, Larrinua IM, Sheets JJ, Mannherz HG, Aktories K.** 2010. *Photorhabdus luminescens* toxins ADP-ribosylate actin and RhoA to force actin clustering. *Science* **327**:1139-1142.
81. **Yang G, Waterfield NR.** 2013. The role of TcdB and TccC subunits in secretion of the *Photorhabdus* Tcd toxin complex. *PLoS Pathog* **9**:e1003644.
82. **Sergeant M, Jarrett P, Ousley M, Morgan JA.** 2003. Interactions of insecticidal toxin gene products from *Xenorhabdus nematophilus* PMFI296. *Appl Environ Microbiol* **69**:3344-3349.
83. **Garcia-Gonzalez E, Muller S, Ensle P, Sussmuth RD, Genersch E.** 2014. Elucidation of sevadicin, a novel non-ribosomal peptide secondary metabolite produced by the honey bee pathogenic bacterium *Paenibacillus larvae*. *Environ Microbiol* **16**:1297-1309.
84. **Cochrane SA, Vederas JC.** 2014. Lipopeptides from *Bacillus* and *Paenibacillus* spp.: A gold mine of antibiotic candidates. *Med Res Rev* doi:10.1002/med.21321.
85. **Luo C, Liu X, Zhou H, Wang X, Chen Z.** 2014. Identification of four NRPS gene clusters in *Bacillus subtilis* 916 for four families of lipopeptides biosynthesis and evaluation of their intricate functions to the typical phenotypic features. *Appl Environ Microbiol* doi:10.1128/AEM.02921-14.
86. **Tanaka A, Tapper BA, Popay A, Parker EJ, Scott B.** 2005. A symbiosis expressed non-ribosomal peptide synthetase from a mutualistic fungal endophyte of perennial ryegrass confers protection to the symbiotum from insect herbivory. *Mol Microbiol* **57**:1036-1050.
87. **Schwecke T, Aparicio JF, Molnar I, Konig A, Khaw LE, Haydock SF, Oliynyk M, Caffrey P, Cortes J, Lester JB, et al.** 1995. The biosynthetic gene cluster for the polyketide immunosuppressant rapamycin. *Proc Natl Acad Sci U S A* **92**:7839-7843.
88. **Raymond KN, Dertz EA, Kim SS.** 2003. Enterobactin: an archetype for microbial iron transport. *Proc Natl Acad Sci U S A* **100**:3584-3588.
89. **Vallenet D, Belda E, Calteau A, Cruveiller S, Engelen S, Lajus A, Le Fevre F, Longin C, Mornico D, Roche D, Rouy Z, Salvignol G, Scarpelli C, Thil Smith AA, Weiman M, Medigue C.** 2013. MicroScope--an integrated microbial resource for the curation and comparative analysis of genomic and metabolic data. *Nucleic Acids Res* **41**:D636-647.
90. **Vallenet D, Labarre L, Rouy Z, Barbe V, Bocs S, Cruveiller S, Lajus A, Pascal G, Scarpelli C, Medigue C.** 2006. MaGe: a microbial genome annotation system supported by synteny results. *Nucleic Acids Res* **34**:53-65.

91. **Darling AC, Mau B, Blattner FR, Perna NT.** 2004. Mauve: multiple alignment of conserved genomic sequence with rearrangements. *Genome Res* **14**:1394-1403.
92. **Abrusci P, McDowell MA, Lea SM, Johnson S.** 2014. Building a secreting nanomachine: a structural overview of the T3SS. *Curr Opin Struct Biol* **25**:111-117.
93. **Brugirard-Ricaud K, Givaudan A, Parkhill J, Boemare N, Kunst F, Zumbihl R, Duchaud E.** 2004. Variation in the effectors of the type III secretion system among *Phototrhobdus* species as revealed by genomic analysis. *J Bacteriol* **186**:4376-4381.
94. **Altschul SF, Gish W, Miller W, Myers EW, Lipman DJ.** 1990. Basic local alignment search tool. *J Mol Biol* **215**:403-410.
95. **Blin K, Medema MH, Kazempour D, Fischbach MA, Breitling R, Takano E, Weber T.** 2013. antiSMASH 2.0--a versatile platform for genome mining of secondary metabolite producers. *Nucleic Acids Res* **41**:W204-212.
96. **Mitchell A, Chang HY, Daugherty L, Fraser M, Hunter S, Lopez R, McAnulla C, McMenamin C, Nuka G, Pesseat S, Sangrador-Vegas A, Scheremetjew M, Rato C, Yong SY, Bateman A, Punta M, Attwood TK, Sigrist CJ, Redaschi N, Rivoire C, Xenarios I, Kahn D, Guyot D, Bork P, Letunic I, Gough J, Oates M, Haft D, Huang H, Natale DA, Wu CH, Orengo C, Sillitoe I, Mi H, Thomas PD, Finn RD.** 2015. The InterPro protein families database: the classification resource after 15 years. *Nucleic Acids Res* **43**:D213-221.
97. **Edgar RC.** 2004. MUSCLE: a multiple sequence alignment method with reduced time and space complexity. *BMC Bioinformatics* **5**:113.
98. **Edgar RC.** 2004. MUSCLE: multiple sequence alignment with high accuracy and high throughput. *Nucleic Acids Res* **32**:1792-1797.
99. **Retief JD.** 2000. Phylogenetic analysis using PHYLIP. *Methods Mol Biol* **132**:243-258.
100. **Letunic I, Bork P.** 2011. Interactive Tree Of Life v2: online annotation and display of phylogenetic trees made easy. *Nucleic Acids Res* **39**:W475-478.
101. **Tamura K, Stecher G, Peterson D, Filipski A, Kumar S.** 2013. MEGA6: Molecular Evolutionary Genetics Analysis version 6.0. *Mol Biol Evol* **30**:2725-2729.
102. **Milne I, Lindner D, Bayer M, Husmeier D, McGuire G, Marshall DF, Wright F.** 2009. TOPALi v2: a rich graphical interface for evolutionary analyses of multiple alignments on HPC clusters and multi-core desktops. *Bioinformatics* **25**:126-127.
103. **Hurst LD.** 2002. The Ka/Ks ratio: diagnosing the form of sequence evolution. *Trends Genet* **18**:486.
104. **Boemare NE, Akhurst RJ.** 1988. Biochemical and physiological characterization of colony form variants in *Xenorhabdus* spp. (Enterobacteriaceae). *J Gen Microbiol* **134**:751-761.

105. **Vivas EI, Goodrich-Blair H.** 2001. *Xenorhabdus nematophilus* as a model for host-bacterium interactions: *rpoS* is necessary for mutualism with nematodes. *J Bacteriol* **183**:4687-4693.
106. **Sierra G.** 1957. A simple method for the detection of lipolytic activity of micro-organisms and some observations on the influence of the contact between cells and fatty substrates. *Antonie Van Leeuwenhoek* **23**:15-22.
107. **Boemare N, Thaler JO, Lanois A.** 1997. Simple bacteriological tests for phenotypic characterization of *Xenorhabdus* and *Photorhabdus* phase variants. *Symbiosis* **22**.
108. **Rowe GE, Welch RA.** 1994. Assays of hemolytic toxins. *Methods Enzymol* **235**:657-667.
109. **Akhurst RJ.** 1982. Antibiotic activity of *Xenorhabdus* spp., bacteria symbiotically associated with insect pathogenic nematodes of the families Heterorhabditidae and Steinernematidae. *J Gen Microbiol* **128**:3061-3065.

SUPPLEMENTAL MATERIALS

Table 4.S1. Secretion system genes.

Secretion System ^a	Gene Name ^b	Gene Annotation ^c
Type II	<i>ffh</i>	XBJ1_3270
Type II	<i>ftsY</i>	XBJ1_0553
Type II	<i>lepB</i>	XBJ1_3149
Type II	<i>lexA</i>	XBJ1_3997
Type II	<i>lspA</i>	XBJ1_1725
Type II	<i>secA</i>	XBJ1_3467
Type II	<i>secB</i>	XBJ1_4332
Type II	<i>secD</i>	XBJ1_1677
Type II	<i>secE</i>	XBJ1_4060
Type II	<i>secF</i>	XBJ1_1676
Type II	<i>secG</i>	XBJ1_0365
Type II	<i>secM</i>	XBJ1_3468
Type II	<i>secY</i>	XBJ1_4221
Type II	<i>sppA</i>	XBJ1_2447
Type II	<i>yajC</i>	XBJ1_1678
Type II	<i>yidC</i>	XBJ1_4410
Type VI	<i>clpV</i>	XBJ1_0271
Type VI	<i>icmF</i>	XBJ1_0275
Type VI	<i>impA</i>	XBJ1_0274
Type VI	<i>impB</i>	XBJ1_0262
Type VI	<i>impC</i>	XBJ1_0263
Type VI	<i>impG/vasA</i>	XBJ1_0265
Type VI	<i>impH/vasB</i>	XBJ1_0266
Type VI	<i>impJ/vasE</i>	XBJ1_0269
Type VI	<i>impK/vasF</i>	XBJ1_0270
Type VI	<i>hcp/tssD</i>	XBJ1_0261
Type VI	<i>vasD</i>	XBJ1_0268
Type VI	<i>vasI</i>	XBJ1_0273
Type VI	<i>vgrG</i>	XBJ1_0277
Type VI	<i>vgrG</i>	XBJ1_0302
Flagellar	<i>dsbB</i>	XBJ1_2460
Flagellar	<i>flgA/flaU</i>	XBJ1_1949
Flagellar	<i>flgB/flbA</i>	XBJ1_1950
Flagellar	<i>flgC/flaW</i>	XBJ1_1951
Flagellar	<i>flgD/claV</i>	XBJ1_1952
Flagellar	<i>flgE/flaK</i>	XBJ1_1953
Flagellar	<i>flgF/flaX</i>	XBJ1_1954
Flagellar	<i>flgG/flaL</i>	XBJ1_1955
Flagellar	<i>flgH/flaY</i>	XBJ1_1957
Flagellar	<i>flgI/flaM</i>	XBJ1_1959
Flagellar	<i>flgJ/flaZ</i>	XBJ1_1960
Flagellar	<i>flgK/flaS</i>	XBJ1_1961
Flagellar	<i>flgL/flaT</i>	XBJ1_1962
Flagellar	<i>flgN</i>	XBJ1_1947
Flagellar	<i>flhA/flaH</i>	XBJ1_1939
Flagellar	<i>flhB/flaG</i>	XBJ1_1938
Flagellar	<i>flhC/flaI</i>	XBJ1_1918

Flagellar	<i>flhD/flbB</i>	XBJ1_1917
Flagellar	<i>fliA/flaD</i>	XBJ1_1996
Flagellar	<i>fliD/flbC</i>	XBJ1_1994
Flagellar	<i>fliE/flaN/flaAI</i>	XBJ1_2703
Flagellar	<i>fliF/flaBI</i>	XBJ1_2704
Flagellar	<i>fliG</i>	XBJ1_2705
Flagellar	<i>fliH</i>	XBJ1_2706
Flagellar	<i>fliJ/flaO</i>	XBJ1_2708
Flagellar	<i>fliK/flaE</i>	XBJ1_2709
Flagellar	<i>fliS</i>	XBJ1_1993
Flagellar	<i>fliT</i>	XBJ1_1992
Flagellar	<i>motA/flaJ</i>	XBJ1_1919
Flagellar	<i>motB/flaJ</i>	XBJ1_1920
Protease Secretion	<i>arpD</i>	XBJ1_0489
Protease Secretion	<i>arpE</i>	XBJ1_0488
Protease Secretion	<i>arpF</i>	XBJ1_0487

^aSecretion system that the gene is part of.

^bGene annotation.

^cNumber designation for the gene in the Xb_Sj_2004 genome. All genomes encode these genes, although only Xb-Sj-2004 designations are shown.

Table 4.S2. Bacterial genes predicted to encode select symbiotic activities^a

Activity^b	Predicted gene product(s)^c	Predicted gene(s)^d
Swimming and Swarming motility	Flagellar structural components and regulators	<i>flgA-M, flhA-D, fliAE-TY, flaA-CENP-R, ompR/envZ</i>
Lipase	Phospholipase A1	<i>xlpA</i>
Lecithinase	Thioesterase	<i>estA</i>
Protease	alkaline protease	<i>prtA</i>
Siderophore	small molecule siderophore	<i>xhbF</i> , several NRPS/PKS clusters
Horse and rabbit hemolysin	secreted hemolysin	<i>xhIAB, xhIA2B2, xaxAB</i> , several NRPS/PKS clusters
Antibiotic activity	small molecules	several NRPS/PKS clusters

^aList of genes and gene products predicted to encode the activities measured in Table 4.

^bActivity measured as listed in Table 4.

^cGene product that would likely produce the measured activity.

^dAnnotated genes from *X. bovienii* genomes that could produce the measured activity.

Table 4.S3. Regulatory proteins found within *X. bovienii* strains.

Gene	Xb-Sf-FL (XBFFL1 v2_)	Xb-Sf-FR (XBFFR1 v2_)	Xb-Sf-MD (XBFM1v 2_)	Xb-Si (XBI1v 2_)	Xb-Sj (XBJ2v 2_)	Xb-Sj- 2004 (XBJ1_)	Xb-Sk- BU (XBKB1 v2_)	Xb-Sk-Q (XBKQ1 v2_)	Xb-So (XBO1 v2_)	Xb-Sp (XBP1 v2_)
<i>Irp</i>	90006	20006	2680044	238004 9	430007	0890	80006	2220007	600065	10006
<i>cpxR</i> <i>A</i>	1090026 1090027	1130027 1130028	1910032 1910033	186000 3 186000 4	239006 2 239006 3	4311 4312	4140046 4140047	2880005 2880006	253002 1 253002 2	620048 620049
<i>omp</i> <i>R</i> – <i>envZ</i>	2170097 2170107	2050016 2050006	2050020 2050010	281008 3 281007 3	60035 60046	0186 0197	1240066 NA	1840014 NA	251005 3 255002 0	220002 8 145003 0
<i>lrhA</i>	1190023	2070078	1740082	301008 1	156001 6	2926	440019	1850085	970022	301005 8
<i>flhDC</i>	2770014 2770015	1260014 1260015	2140014 2140013	292005 0 292004 9	100001 0 100001 1	1917 1918	3820015 3820014	2240014 2240013	480012 480013	308001 3 308001 4
<i>niIR</i>	NA	NA	NA	NA	NA	NA	NA	NA	NA	NA

Table of genes annotated as homologs to regulatory proteins in *X. bovienii* genomes as determined by MaGe and listed as the annotated gene. The number designation for each gene(s) is given without the prefixes, which are listed at the top of each column. HK in gene column designates unknown histidine kinase, while RR designates an unknown response regulator.

Table 4.S4. *Xenorhabdus bovienii* genes predicted to encode LysR family transcription factors.

Gene	Xb-Sf-FL (XBFL1v2_)	Xb-Sf-FR (XBFRR1v2_)	Xb-Sf-MD (XBFM1v2_)	Xb-SI (XB11v2_)	Xb-SJ (XB12v2_)	Xb-SJ-2004 (XBJ1_)	Xb-Sk-BU (XBKB1v2_)	Xb-Sk-Q (XBKQ1v2_)	Xb-So (XBO1v2_)	Xb-Sp (XBP1v2_)
<i>gcVA</i>	910075	2140057	810058	1730051	160014	0494	1200046	2900026	2250006	720057
<i>meIR</i>	2560025	900025	990009	2260025	160018	0498	40005	350025	1960011	1770006
<i>nhaR</i>	2360049	1490049	2600062	1420042	880022	1730	4190052	580020	2390037	650067
<i>cysB</i>	2210009	2290025	2480042	1260022	1240064	2290	3970002	120021	1300149	1210023
<i>ynfL</i>	2490048	560048	2480013	1260049	1250025	2320	2370001	120048	1300122	2830026
<i>ydhB</i>	2260041	1870037	50033	3080053	1300068	2497	3950022	2150005	1040057	2480041
<i>yeiE</i>	2760007	2090038	2120013	840088	1550053	2880	440059	1850050	2000028	270151
<i>lrrHA</i>	1190023	2070078	1740082	3010081	1560016	2926	440019	1850085	970022	3010058
<i>lysR</i>	2510040	2220040	520040	3050018	1730005	3332	270002	2140017	2260030	2940057
<i>argP</i>	930010	2420055	1100076	2960034	1810030	3446	2990031	1060031	1820025	1760025
<i>leuO</i>	920011	2420011	1100030	2290030	1810074	3490	3000039	1990024	2270001	520040
<i>yhaJ</i>	170045	110045	1310050	1940055	1930049	3863	300046	790006	290073	1340046
<i>malT</i>	190024	130024	80023	1740023	2650022	4039	370012	220023	170022	110024
<i>ilvY</i>	2550011	2130052	90031	1560010	2110046	4190	390040	2340011	180002	740011
<i>oxyR</i>	480007	1280007	2550007	1860044	2140007	4266	4140007	1110036	2530064	620007
-	1640023	1990058	2750024	2810025	80013	0253	10009	2780038	1800039	1450059
-	310095	1840097	1260056	1570088	130075	0382	1550004	760003	1300098	2990040
-	2310008	1350008	1100011	2310004	2690011	1451	3000058	430004	2100015	520023
-	910017	2150053	890006	700016	1900017	3766	2020009	1660001	1300098	2990114
-	2380059	310077	750061	1870083	480014	1128	1120007	1280065	930085	
-	1540002	400002	140007	2510012	1480005	2773		2360005	1530003	1100004
-	2160021	260016	1190031	1090041		0157		2740008		1620011
-					60009	4397				
-					2370007	2330				

Table of genes annotated as toxins in *X. bovienii* genomes as determined by MaGe, listed as the annotated gene. The number designation for each gene is given without the prefixes, which are listed at the top of each column. Dashes in the gene column indicate an unnamed regulator.

Table 4.S5 *Xenorhabdus bovienii* genes predicted to encode two-component regulatory systems^a.

Gene ^b	Xb-Sf-FL (XBFL1v2)	Xb-Sf-FR (XBFR1v2)	Xb-Sf-MD (XBFM1v2)	Xb-SI (XB1v2)	Xb-SJ (XB2v2)	Xb-SI-2004 (XB1)	Xb-SK-BU (XBKB1v2)	Xb-SK-Q (XBKQ1v2)	Xb-So (XB01v2)	Xb-Sp (XBPIv2)
<i>malT</i>	190024	130024	80023	1740023	2050022	4039	370012	220023	170022	110024
<i>cpvRA</i>	1090026	1130027	1910032	1860003	2390062	4311	4140046	2880005	2530021	620048
	1090027	1130028	1910033	1860004	2390063	4312	4140047	2880006	2530022	620049
<i>ctd</i>	1190069	2070032	1740029	3010036	1570002	2972	210015	2570004	2030031	3010002
	1190070	2070033	1740030	3010037	1570003	2973	210016	2570005	2030032	3010003
<i>yfhAK</i>	1310005	1550023	2390005	2040060	1570065	3037	2770012	2600046	2110040	2040012
	1310007	1550025	2390007	2040062	1570067	3039	2770014	2600048	2110042	2040014
<i>phoBR</i>	1610004	550015	600062	2280004	870102	1687	150026	580065	90020	650013
	1610005	550016	600063	2280005	870103	1688	150027	580066	90021	650014
<i>glnL G</i>	1640068	1990012	160005	2810057	60058	209	1240043	2780002	2550007	1450016
	1640069	1990013	160006	2810058	60059	210	1240044	2780003	2550008	1450017
<i>arcAB</i>	170036	110036	1310059	1420070	1820017	3517	300037	2630003	290064	1340037
	2370012	1490080	2600024	1940064	1930040	3853	4190083	2860030	2340008	2930050
<i>kdpED</i>	1900070	1900025	820104	1150047	440138	1070	100007	70005	1370022	2520010
	1900071	1900026	820105	1150048	440139	1071	100008	70006	1370023	2520011
<i>uvrY/b</i>	330008	650009	860008	2310026	1420014	2676	870037	2280010	460002	520002
	1930009	1190008	1800008	2510006	1860060	3656	890002	2360011	1710072	1260008
<i>ompR/</i>	2170097	2050015	2050019	2810082	60035	0186	1240005	1840013	2510053	2200028
	2170098	2050016	2050020	2810083	60036	0187	1240006	1840014	2510054	2200029
<i>envZ</i>	2400037	720037	320022	840044	1550012	2835	1420013	1850008	2630035	270105
	2400038	720038	320023	840045	1550013	2836	1420014	1850009	2630036	270106
<i>rssB</i>	2660011	2300019	2420035	2660028	1300007	2436	180007	2150063	1300192	2720025
<i>cheAB</i>	2770018	1260018	2140004	2920041	1000014	1921	3820006	2240005	480016	3080017
	2770023	1260023	2140009	2920046	1000019	1926	3820011	2240010	480021	3080022
<i>cheY</i>	2770024	1260024	2140003	2920040	1000020	1927	3820005	2240004	480022	3080023
<i>yehTU</i>	310086	1840086	1260065	1570080	130067	0375	20062	760012	1780003	2990047
	310087	1840087	1260066	1570081	130068	0376	20063	760013	1780004	2990048
<i>luxR</i>	310116	1840117	1260037	1570114	130092	402	800002	2320025	280014	2990021
<i>uphAB</i>	660003	2320005	2330007	1870173	1140029	2122	1660007	2730004	1230039	3060021
	660004	2320007	2330008	1870174	1610030	3090	1660008	2730005	1230044	3060022
<i>pprP</i>	740010	1560010	2730010	410002	630004	1343	3980004	300043	2270020	1080006
<i>narP</i>	770041	1910056	320086	2640032	1330010	2592	1420078	2750012	2380011	270043
	770074	1910023	320054	840009	1450010	2733	1420046	2690006	2380039	270074
<i>baeRS</i>	770075	1910024	320055	840010	1450011	2734	1420047	2690007	2380040	270075
<i>rcsBC</i>	940012	2470012	2280037	400030	330015	0731	1510026	280007	2360012	1120032
	940013	2470013	2280038	400031	330016	0732	1510027	280008	2360013	1120033
<i>rcsD</i>	940014	2470014	2280039	400032	330017	733	1510028	280009	2360014	1120034
<i>RR-1</i>	550002	830002	2100010	2920064	990005	1898	3580004	740003	470001	3020002
<i>RR-2</i>	2380032	310104	750033	1870110	480007	1121	570034	1280035	2660005	930060
<i>HK-1</i>	2610007	2550013	2670003	770008	1140030	2123	1930003	1950007		1950015
<i>RR-3</i>	2500011	220007					2970021			
<i>RR-4</i>				1620001	2740004	1569		2660004	2420016	
<i>RR-5</i>					2820006	3941				

Table of genes annotated as toxins in *X. bovienii* genomes as determined by MaGe, listed as the annotated gene. The number designation for each gene(s) is given in numerical order without the prefixes, which are listed at the top of each column. HK in gene column designates and unknown histidine kinase, while RR designates an unknown response regulator.

Table 4.S6. Annotated toxin genes^a

Genes ^b	Gene Products ^c	Xb_Sf_FL	Xb_Sf_FR	Xb_Sf_MD	Xb_Si	Xb_Sj	Xb_Sj_2004	Xb_Sk_BU	Xb_Sk_Q	Xb_So	Xb_Sp
<i>mcf1</i>	Putative Mcf toxin	1530001	1740002	2420009	2660002	1290015	2410	3530004	130003	1300170	510006
<i>rtxA</i>	RTX toxin	1910012	1900014	820092	1150035	440015	1089	110001	2030002	1370016	990035
<i>prtA</i>	RTX-like metalloprotease	910078	2140054	810055	1730048	160011	0491	1200049	2900029	2250009	720054
<i>xaxAB</i>	cytotoxin XaxA and transporter XaxB	2360019 2360018	1490019 1490018	2600093 2600094	1420016 1420015	880002 880001	1711 1710	4190021 4190020	580043 580044	2390017 2390016	650034 650033
<i>xnlA</i>	Hemolysin	1640017	1990063	2750030	2810020	80018	0258	10018	2780047	1800045	1450065
<i>shlA</i>	Hemolysin	360004	1030003	290005	2350006						1130006
<i>stxA1</i>	Shiga toxin A-chain				2730004						

^aTable of genes annotated as toxins in *X. bovienii* genomes as determined by MaGe, listed as the annotated gene. The number designation for each gene is given without the prefixes: Xb-Sf-FL (XBFFL1), Xb-Sf-FR (XBFFR1), Xb-Sf-MD (XBFMD1), Xb-Sp (XBP1), Xb-Sk-BU (XKBKBU1), Xb-Sk-Q (XKBKQ1), Xb-Sj (XBSJ1), Xb-Sj_2004 (XBSJ1), Xb-Sj (XBSJ2), Xb-So (XBO1), Xb-Si (XBI1), and Xn (XNC1).

^bGene annotation for toxin.

^cPredicted gene product.

Table 4.S7 Best BlastP hits of Xb-Si putative Shiga toxin^a.

GenBank Accession Number^b	Description^c	Coverage^d	Identity^e	E-value^f
WP_006035658.1	Shiga toxin A-chain from <i>Rickettsiella grylli</i>	89%	35%	1.0E-37
CAA85366.1	Shiga-like toxin 1 A-chain from <i>Escherichia coli</i>	98%	29%	2.0E-23
WP_001365506.1	Shig toxin A-chain from <i>Escherichia coli</i>	98%	29%	3.0E-23
CAA85368.1	Shiga-like toxin 1 A-chain from <i>Escherichia coli</i>	98%	29%	3.0E-23
BAC78639.1	Shiga toxin 1 variant A (<i>stx1a</i> in <i>Escherichia coli</i>)	98%	29%	3.0E-23

^aTable of BlastP results of the top five hits for Xbl1v2_2730004 (Xb-Si putative Shiga Toxin), excluding itself.

^bThe GenBank accession number for each hit.

^cA short description of the hit based on the provided information in GenBank.

^dThe percentage of the query amino acid sequence that is covered by the hit.

^eThe percentage of the amino acid sequence that is identical between the hit and the query.

^fExpect (E) value is the number of sequences that you would expect to obtain from the database that match equally well based on chance.

Table 4.S8 Tc subunit genes from *X. bovienii* genomes^a.

Genome	ORF ^b	Gene Annotation ^c	Subunit Type ^d
Xb-Sf-FL	XBFFL1_1440001	<i>xptA/tcdA</i>	A'
Xb-Sf-FL	XBFFL1_1440006	<i>xptA/tcdA</i>	A'
Xb-Sf-FL	XBFFL1_1440007	<i>xptA/tcdA</i>	A'
Xb-Sf-FL	XBFFL1_1440008	<i>xptA/tcdA</i>	A'
Xb-Sf-FL	XBFFL1_2490001	<i>xptA/tcdA</i>	A'
Xb-Sf-FL	XBFFL1_2490003	<i>xptA/tcdA</i>	A'
Xb-Sf-FL	XBFFL1_2290004	<i>tccA</i>	A
Xb-Sf-FL	XBFFL1_2290002	<i>tccB/xptD</i>	A'
Xb-Sf-FL	XBFFL1_2290003	<i>tccB/xptD</i>	A'
Xb-Sf-FL	XBFFL1_1440004	<i>xptC/tcaC</i>	B'
Xb-Sf-FL	XBFFL1_1440005	<i>xptC/tcaC</i>	B'
Xb-Sf-FL	XBFFL1_2380073	<i>tccC6</i>	C'
Xb-Sf-FR	XBFFR1_560001	<i>xptA/tcdA</i>	A'
Xb-Sf-FR	XBFFR1_560003	<i>xptA/tcdA</i>	A'
Xb-Sf-FR	XBFFR1_630033	<i>xptA/tcdA</i>	A'
Xb-Sf-FR	XBFFR1_630034	<i>xptA/tcdA</i>	A'
Xb-Sf-FR	XBFFR1_630035	<i>xptA/tcdA</i>	A'
Xb-Sf-FR	XBFFR1_630040	<i>xptA/tcdA</i>	A'
Xb-Sf-FR	XBFFR1_2540016	<i>tccA</i>	A
Xb-Sf-FR	XBFFR1_2540017	<i>tccB/xptD</i>	A'
Xb-Sf-FR	XBFFR1_2540018	<i>tccB/xptD</i>	A'
Xb-Sf-FR	XBFFR1_630036	<i>xptC/tcaC</i>	B'
Xb-Sf-FR	XBFFR1_630037	<i>xptC/tcaC</i>	B'
Xb-Sf-FR	XBFFR1_630039	<i>tccC1</i>	C
Xb-Sf-MD	XBFM1_1510009	<i>xptA/tcdA</i>	A'
Xb-Sf-MD	XBFM1_1510010	<i>xptA/tcdA</i>	A'
Xb-Sf-MD	XBFM1_1510014	<i>xptA/tcdA</i>	A'
Xb-Sf-MD	XBFM1_1510015	<i>xptA/tcdA</i>	A'
Xb-Sf-MD	XBFM1_1510016	<i>xptA/tcdA</i>	A'
Xb-Sf-MD	XBFM1_900054	<i>tccA</i>	A
Xb-Sf-MD	XBFM1_900052	<i>tccB/xptD</i>	A'
Xb-Sf-MD	XBFM1_900053	<i>tccB/xptD</i>	A'
Xb-Sf-MD	XBFM1_1510012	<i>xptC/tcaC</i>	B'
Xb-Sf-MD	XBFM1_1510013	<i>xptC/tcaC</i>	B'
Xb-Sf-MD	XBFM1_550043	<i>xptC/tcaC</i>	B
Xb-Sf-MD	XBFM1_550044	<i>xptC/tcaC</i>	B'
Xb-Sf-MD	XBFM1_750073	<i>tccC4</i>	C
Xb-Sf-MD	XBFM1_2330011	<i>tccC5</i>	C'
Xb-Sf-MD	XBFM1_2330012	<i>tccC5</i>	C'
Xb-Si	XBI1_2820003	<i>xptA/tcdA</i>	A
Xb-Si	XBI1_2580008	<i>tccA</i>	A
Xb-Si	XBI1_2580009	<i>tccB/xptD</i>	A
Xb-Si	XBI1_1670005	<i>xptC/tcaC</i>	B'
Xb-Si	XBI1_1680001	<i>xptC/tcaC</i>	B'
Xb-Si	XBI1_1690001	<i>xptC/tcaC</i>	B'
Xb-Si	XBI1_2830001	<i>xptC/tcaC</i>	B'
Xb-Si	XBI1_2840001	<i>xptC/tcaC</i>	B'
Xb-Si	XBI1_2920035	<i>xptC/tcaC</i>	B
Xb-Si	XBI1_2050001	<i>xptC/tcaC</i>	B'
Xb-Si	XBI1_1120001	<i>tccC4</i>	C'
Xb-Si	XBI1_1260128	<i>tccC1</i>	C
Xb-Si	XBI1_2050001	<i>tccC6</i>	C'
Xb-Sj	XBJ2_2740002	<i>xptA/tcdA</i>	A
Xb-Sj	XBJ2_200005	<i>tccA</i>	A
Xb-Sj	XBJ2_200004	<i>tccB/xptD</i>	A
Xb-Sj	XBJ2_2730005	<i>xptC/tcaC</i>	B'
Xb-Sj	XBJ2_2740001	<i>xptC/tcaC</i>	B'
Xb-Sj	XBJ2_1000023	<i>xptC/tcaC</i>	B
Xb-Sj	XBJ2_1610026	<i>tccC5</i>	C'
Xb-Sj	XBJ2_2730004	<i>tccC7</i>	C
Xb-Sj-2004	XBJ1_1572	<i>xptA/tcdA</i>	A
Xb-Sj-2004	XBJ1_1932	<i>xptA/tcdA</i>	A'
Xb-Sj-2004	XBJ1_1933	<i>xptA/tcdA</i>	A'
Xb-Sj-2004	XBJ1_0569	<i>tccA</i>	A
Xb-Sj-2004	XBJ1_0568	<i>tccB/xptD</i>	A
Xb-Sj-2004	XBJ1_1573	<i>xptC/tcaC</i>	B
Xb-Sj-2004	XBJ1_1934	<i>xptC/tcaC</i>	B
Xb-Sj-2004	XBJ1_2397	<i>tcdB</i>	B'

Xb-Sj-2004	XBj1_1574	<i>tccC5</i>	C
Xb-Sj-2004	XBj1_3085	<i>tccC7</i>	C
Xb-Sk-BU	XBKB1_700008	<i>xptA/tcdA</i>	A'
Xb-Sk-BU	XBKB1_700009	<i>xptA/tcdA</i>	A'
Xb-Sk-BU	XBKB1_700011	<i>xptA/tcdA</i>	A'
Xb-Sk-BU	XBKB1_700013	<i>xptA/tcdA</i>	A'
Xb-Sk-BU	XBKB1_700014	<i>xptA/tcdA</i>	A'
Xb-Sk-BU	XBKB1_700015	<i>xptA/tcdA</i>	A'
Xb-Sk-BU	XBKB1_1060007	<i>tccA</i>	A'
Xb-Sk-BU	XBKB1_1060008	<i>tccA</i>	A'
Xb-Sk-BU	XBKB1_1060009	<i>tccA</i>	A'
Xb-Sk-BU	XBKB1_1060006	<i>tccB/xptD</i>	A
Xb-Sk-BU	XBKB1_2960024	<i>tccC2</i>	C'
Xb-Sk-BU	XBKB1_2960025	<i>tccC1</i>	C'
Xb-Sk-Q	XBKQ1_420007	<i>xptA/tcdA</i>	A'
Xb-Sk-Q	XBKQ1_420008	<i>xptA/tcdA</i>	A'
Xb-Sk-Q	XBKQ1_420009	<i>xptA/tcdA</i>	A'
Xb-Sk-Q	XBKQ1_850003	<i>xptA/tcdA</i>	A
Xb-Sk-Q	XBKQ1_2640005	<i>tccA</i>	A
Xb-Sk-Q	XBKQ1_2640006	<i>tccB/xptD</i>	A
Xb-Sk-Q	XBKQ1_2660002	<i>xptC/tcaC</i>	B
Xb-Sk-Q	XBKQ1_850002	<i>xptC/tcaC</i>	B
Xb-Sk-Q	XBKQ1_850001	<i>tccC1</i>	C
Xb-Sk-Q	XBKQ1_850035	<i>tccC1</i>	C'
Xb-Sk-Q	XBKQ1_1280067	<i>tccC5</i>	C'
Xb-Sk-Q	XBKQ1_2730001	<i>tccC5</i>	C'
Xb-So	XBO1_1940002	<i>tccA</i>	A
Xb-So	XBO1_1940003	<i>tccB/xptD</i>	A
Xb-So	XBO1_480026	<i>xptC/tcaC</i>	B'
Xb-So	XBO1_1300030	<i>tccC1</i>	C'
Xb-Sp	XBP1_400038	<i>xptA/tcdA</i>	A'
Xb-Sp	XBP1_400039	<i>xptA/tcdA</i>	A'
Xb-Sp	XBP1_400040	<i>xptA/tcdA</i>	A'
Xb-Sp	XBP1_400041	<i>xptA/tcdA</i>	A'
Xb-Sp	XBP1_400042	<i>xptA/tcdA</i>	A'
Xb-Sp	XBP1_400051	<i>xptA/tcdA</i>	A
Xb-Sp	XBP1_470005	<i>tccA</i>	A
Xb-Sp	XBP1_470002	<i>tccB/xptD</i>	A'
Xb-Sp	XBP1_470003	<i>tccB/xptD</i>	A'
Xb-Sp	XBP1_470004	<i>tccB/xptD</i>	A'
Xb-Sp	XBP1_400044	<i>xptC/tcaC</i>	B'
Xb-Sp	XBP1_400045	<i>xptC/tcaC</i>	B'
Xb-Sp	XBP1_400046	<i>xptC/tcaC</i>	B'
Xb-Sp	XBP1_2580014	<i>xptC/tcaC</i>	B
Xb-Sp	XBP1_400047	<i>tccC5</i>	C'
Xb-Sp	XBP1_400048	<i>tccC1</i>	C'
Xb-Sp	XBP1_930099	<i>tccC2</i>	C'
Xb-Sp	XBP1_2950001	<i>tccC4</i>	C'
Xb-Sp	XBP1_3060016	<i>tccC5</i>	C'
Xb-Sp	XBP1_3060017	<i>tccC5</i>	C'

^aTable of all annotated Tc toxin subunit genes in all *X. bovienii* genomes (i.e. all 9 draft genomes and finished genome). Grey shading highlights intact genes. Heavier dotted lines delineate different subunits, while full lines delineate different genomes.

^bOpen reading frame (ORF) as labeled in EMBL and GenBank.

^cAnnotation of gene from MaGe. For genes that can have multiple labels both are listed (e.g. *xptC* and *tcaC* are the same genes that were annotated in *X. nematophila* and *P. luminescens* respectively.)

^dSubunit types that are intact (A, B, or C) or fragments (A', B', B').

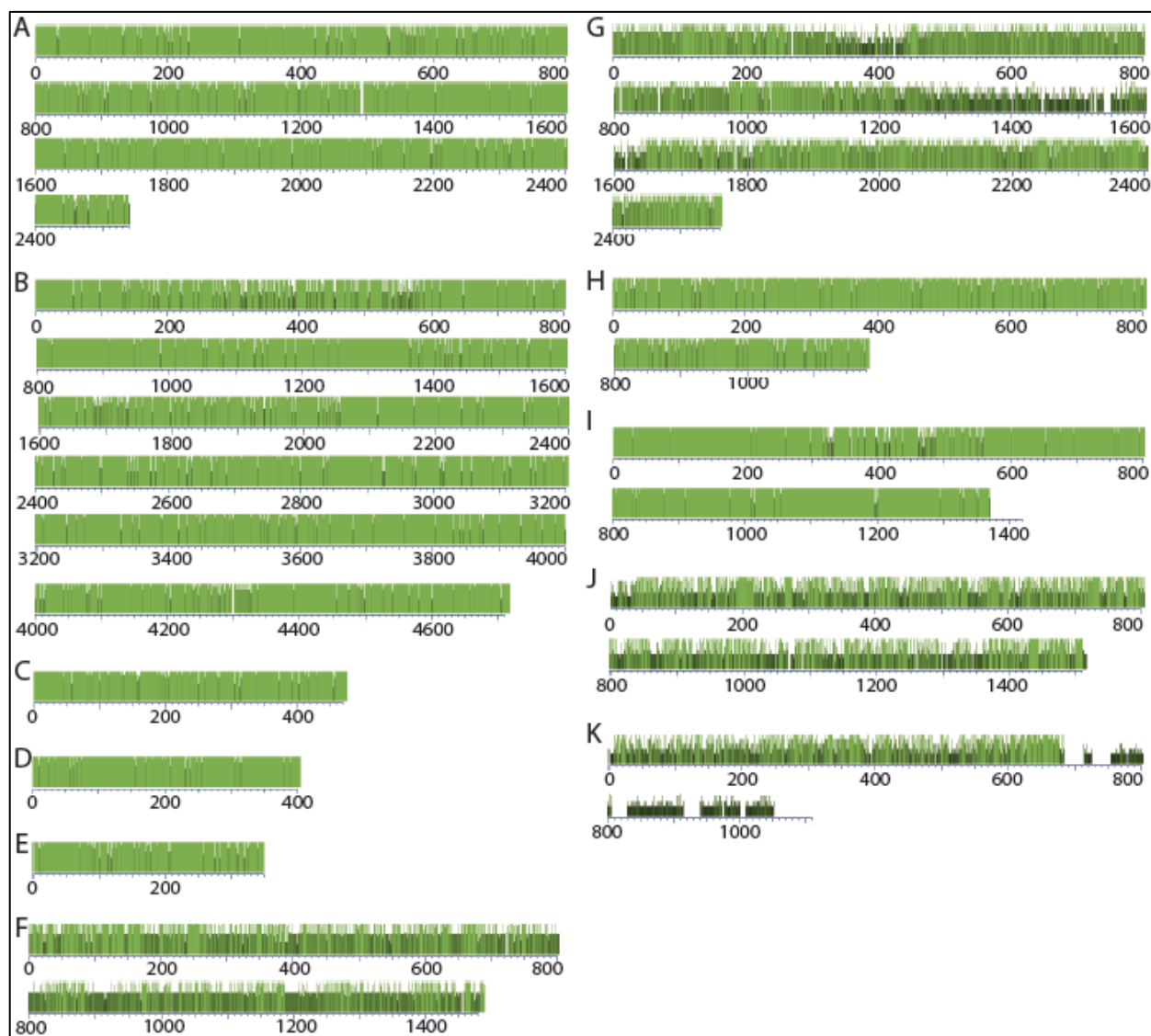


Figure S1. Distribution of amino acid sequence divergence in proteins. The amino acid sequence divergence of *X. bovienii* proteins for Mcf1 (A), RtxA (B), PrtA (C), XaxA (D), XaxB (E), XhIA (F), XptA2 (G), TccA2 (H), TccB2 (I), TcaC (J), and TccC (K) is shown. Green bar graph indicates the percent of amino acids that match the consensus sequence at the positions in the protein, and the amino acid numbers are given below the graph. Light green bars have 100% identity, and darker colors indicate lower percent matching to the consensus.

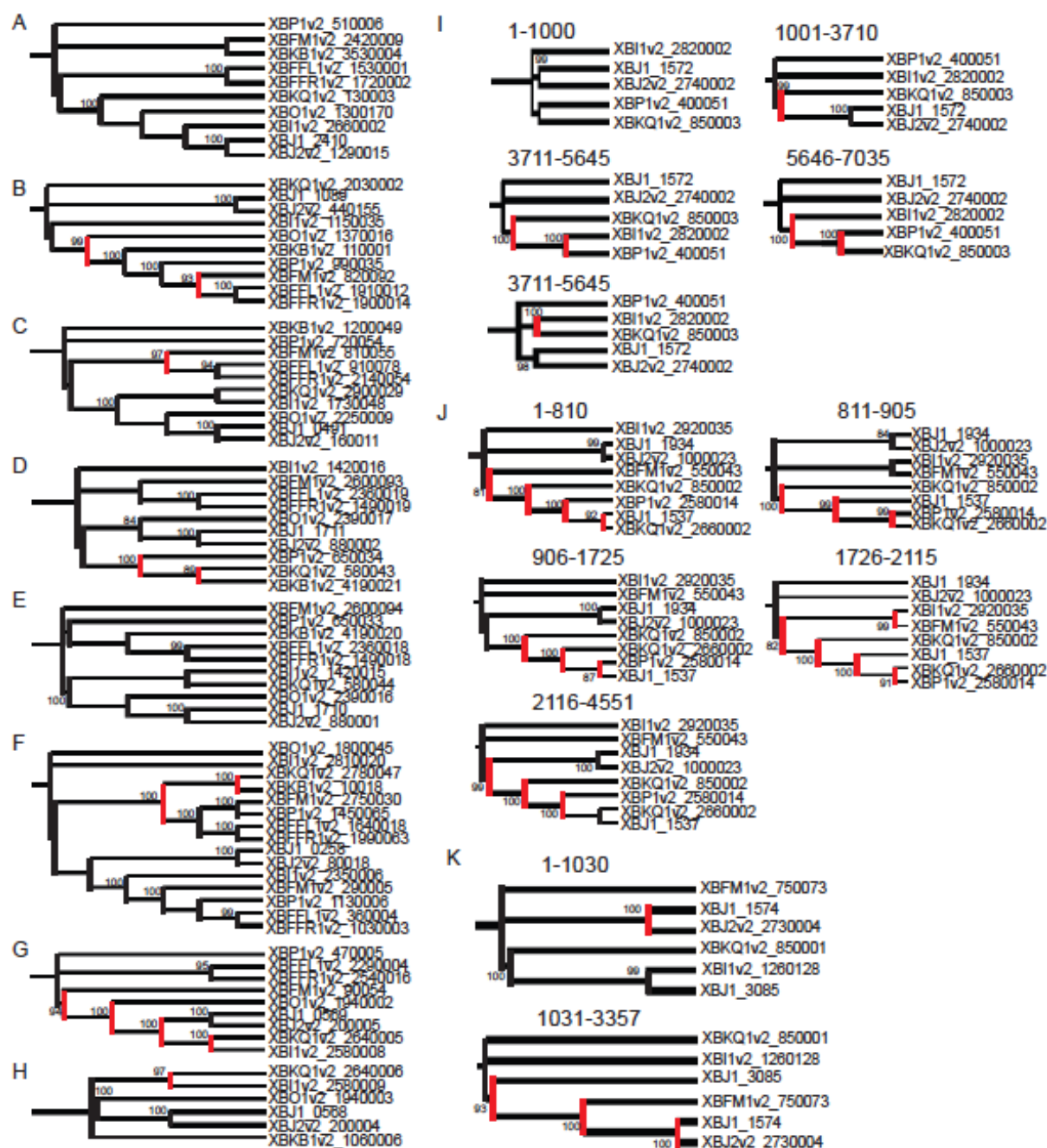


Figure S2. Nucleotide phylogenies. The nucleic acid sequences of genes were analyzed for recombination, and for each piece, phylogenies were built. Shown above are the trees for *X. bovienii* genes *mcf1* (A), *rtxA* (B), *prtA* (C), *xaxA* (D), *xaxB* (E), *xhIA* (F), *xptA2* (G), *tccA2* (H), *tccB2* (I), *tcaC* (J), and *tccC* (K). Values next to branches indicate bootstrap values and above trees denote the nucleotides used. Red highlighting indicates strongly supported branches in the gene tree that do not match the previously reported bacterial phylogeny (5).

CHAPTER 5

Xenorhabdus bovienii symbionts provide an advantage to their *Steinernema affine* nematode hosts by killing competitor *Steinernema feltiae* nematodes

This chapter will be submitted as:

Murfin KE, Bashey-Visser F, and Goodrich-Blair H. “*Xenorhabdus bovienii* symbionts provide an advantage to their *Steinernema affine* nematode hosts by killing competitor *Steinernema feltiae* nematodes”

ABSTRACT

Parasites can engage in mutualism with bacterial symbionts that contribute to parasitic success. When parasitizing insects, nematodes in the genus *Steinernema* utilize *Xenorhabdus* bacterial symbionts for insect host killing and nutritional bioconversion. In this study we establish that the *Xenorhabdus bovienii* bacterial symbiont of *Steinernema affine* nematodes (Xb-Sa) can impact the competition between *S. affine* and *S. feltiae*. Through co-injection and natural infection assays we demonstrate that Xb-Sa is both necessary and sufficient to inhibit *S. feltiae* nematodes during competition, which provides a competitive advantage to *S. affine*. Survival assays revealed that Xb-Sa bacteria inhibit *S. feltiae* nematodes by killing the reproductive life stages. Microscopy and timed infection assays indicate that Xb-Sa bacteria colonize *S. feltiae* nematode intestines, ultimately leading to an altered morphology of the intestinal epithelium. These data suggest that Xb-Sa may be an intestinal pathogen of the non-native *S. feltiae* nematode, although it is a beneficial and non-harmful colonizer of its native nematode host *S. affine*.

INTRODUCTION

In natural environments with mixed populations of microbes, nutrient availability is typically limiting, making competition a key driver in the ecology and evolution of microorganisms. For example, parasitic organisms can compete with each other to successfully infect a limited number of available hosts. Once within a host, mixed infections can develop, giving rise to competition for host-derived nutrients. These types of competition occur between sympatric insect-parasitic *Steinernema* nematode species. Previous studies identified a variety of competitive outcomes among *Steinernema* species during co-infections, including equal reproduction of both species (1, 2), suppression of reproduction by one species (1, 2), and improved reproduction of one species (3). However, mechanisms underlying the competitive differences among *Steinernema* nematodes have not been explored in detail. In this study, we assess a competitive interaction that occurs between *S. affine* and *S. feltiae* nematodes that is modulated by the beneficial bacterial symbionts of these nematodes.

Steinernema nematodes have been extensively studied due to their use for biological control of agricultural insect pests (4), as well as a model of beneficial symbiosis (5). Insect parasitic *Steinernema* nematodes engage in mutually beneficial symbiosis (mutualism) with *Xenorhabdus* γ -proteobacteria (Figure 5.1). In the soil environment, the nematodes exist as a non-feeding 3rd stage juvenile, known as the infective juvenile (IJ). IJ nematodes are resistant to environmental stresses and have a thick chitin cuticle layer, closed mouth, and closed anus. The IJs house bacterial symbionts within a specialized portion of the intestine in order to carry them between insects (5-7). IJs infect an insect through natural openings and migrate into the insect blood cavity, the hemocoel (8). Once inside the hemocoel, the nematodes undergo a recovery process to become J3 juveniles, where the chitin cuticle is shed, the mouth and anus open, the bacterial symbionts are released, and the nematode begins feeding (9). The nematodes and bacteria then kill the insect host and grow within the cadaver (5, 10). Several

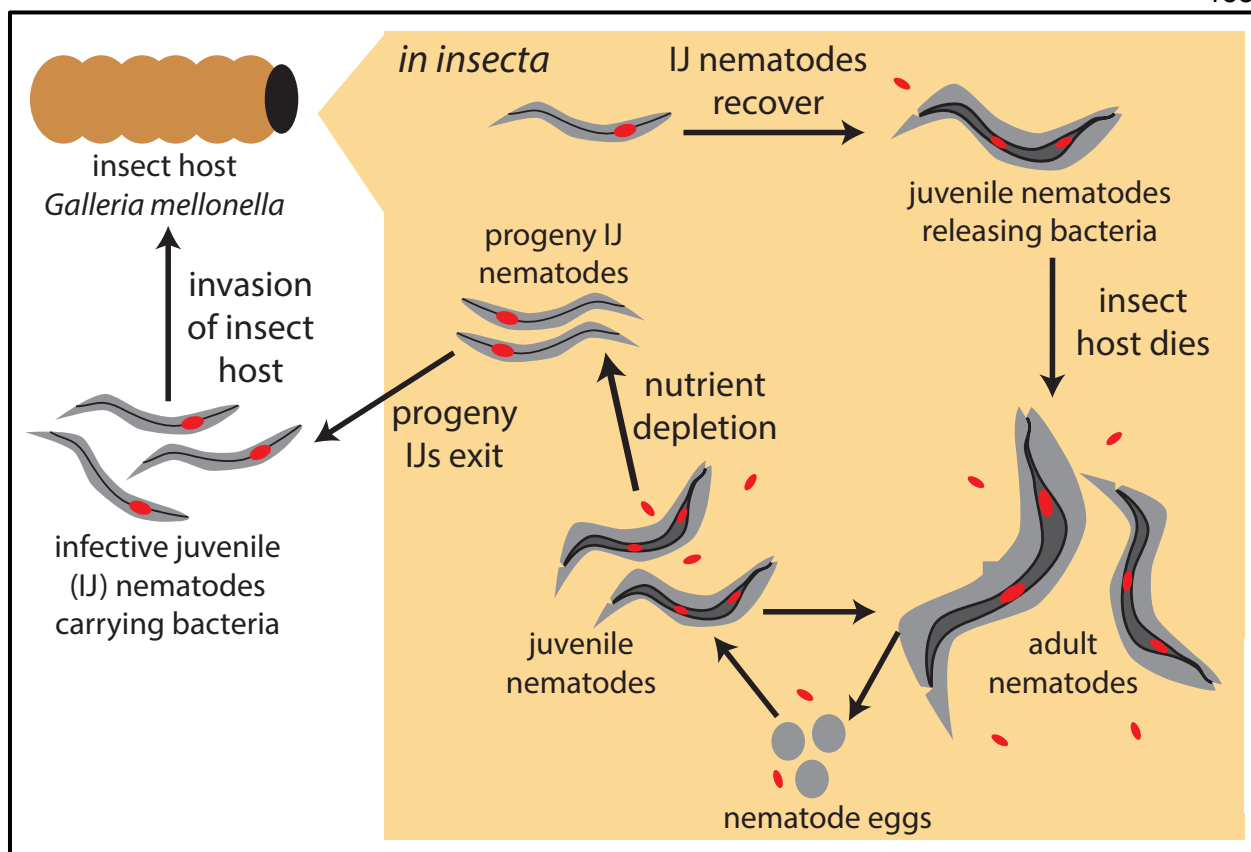


Figure 5.1 *Steinerinema* nematodes and *Xenorhabdus* bacteria lifecycle. The schematic above shows the combined life cycle of the nematodes (grey) and bacteria (red) in the insect host (tan). In the soil environment, IJ nematodes carry the bacteria in their intestine as they seek and invade insect hosts. Once inside the insect host environment, IJ nematodes recover into juveniles with open mouths and anuses and release their bacterial symbiont. The nematodes also begin consuming bacteria and nutrients. The nematodes and bacteria then kill the insect host and reproduce within the cadaver, including adult, egg, and juvenile stages. Once nutrients are limiting the nematodes form the next generation of progeny IJs that exit the cadaver.

rounds of nematode reproduction occur within the cadaver, in which the nematodes go through adult, egg, and juvenile (J1-4) life stages (10, 11). Once nutrients in the insect become limiting, the nematodes undergo an alternate developmental pathway to form the next generation of progeny IJs carrying the bacterial symbiont that will exit the insect cadaver to seek new hosts (12).

Several studies indicate that bacteria can modulate parasitic success and competition between parasites. For example, mutualists of a parasitized host can reduce parasitic infections, such as tsetse fly mutualists that induce the tsetse immune system to kill trypanosome parasites (13). Additionally, mutualistic bacteria of the parasite itself can positively influence its parasitic success, such as the *X nematophila* symbiont of *S. carpocapsae* that inhibits competing *Photorhabdus* bacteria (14). In previous work we observed that the *S. intermedium* nematode bacterial symbiont, *X. bovienii* (hereafter referred to as Xb-Si) has an incompatible interaction with *S. feltiae* nematodes that associate with a different *X. bovienii* bacterial strain (Xb-Sf) (Table 5.1). Specifically, when *S. feltiae* nematodes are co-injected into insects with Xb-Si, no *S. feltiae* progeny are produced, although several other *X. bovienii* bacterial strains are able to support progeny development in insects (Chapter 3). Similarly, we discovered an incompatible interaction when *S. feltiae* is co-injected with the symbiont of *S. affine*, a nematode closely related to *S. intermedium*, (data not shown). Incompatible interactions such as these are likely to influence the competition between the nematode species infecting the same insect host.

The goal of this study was to characterize incompatibility between the *S. affine* bacterial symbiont and *S. feltiae* nematodes and how this incompatibility impacts competition between nematode hosts. We utilized *S. affine* and *S. feltiae* nematodes along with their *X. bovienii* bacterial symbionts (Xb-Sa and Xb-Sf) (Table 5.1) to investigate the occurrence of inhibition of non-native hosts, assess the impact of inhibition on competition, and identify the mechanism likely contributing to observed incompatibility.

Table 5.1 Bacterial strains and plasmids used in this study.

Abbreviation^a	Comments^b	Study^c
Bacterial Strains		
Xb-Sf	Native symbiont of <i>S. feltiae</i> nematodes, isolated in Florida	Lee 2010
Xb-Sf-GFP	GFP-expressing Xb-Sf	Chaston 2013
Xb-Si	Native symbiont of <i>S. intermedium</i> nematodes	Lee 2010
Xb-Sa	Native symbiont of <i>S. affine</i> nematodes, isolate #78	This study
Xb-Sa-GFP	GFP-expressing Xb-Sa	This study
Xb-Sk	Native symbiont of <i>S. kraussei</i> nematodes, isolated in Quebec, CA	Lee 2010
Xn	ATCC19069, native symbiont of <i>S. carpocapsae</i> nematodes	Lee 2010
Plasmids		
pURR25 mini Tn7KS-GFP	Tn7 GFP donor plasmid	Teal 2006
pUX-BF 13	Conjugation helper plasmid	Bao 1991

^aAbbreviation used to refer to the strain or plasmid.

^bDescription of the strain genotype or the function of the plasmid.

^cStudy where the strain or plasmid was first published.

RESULTS

***S. feltiae* is inhibited by incompatible *X. bovienii* symbiont strains.** There are two potential explanations for the incompatibility between *S. feltiae* and Xb-Si or Xb-Sa: within an insect host these bacterial strains are insufficient to support nematode growth and reproduction, or they inhibit nematode growth and reproduction. To distinguish between these possibilities we grew bacteria and nematodes together in permissive conditions (liver kidney agar - LKA). In these conditions, nematodes can grow with or without bacteria. Addition of IJs to plain LKA plates or LKA lawns of Xb-Sf resulted in growth and development of the nematodes into adults by five days post addition, and nematode reproduction to the next generation of progeny IJs occurred by day 14 (Table 5.2). In contrast, addition of nematodes to Xb-Si or Xb-Sa bacterial lawns resulted in no growth or development of IJ nematodes into adults or progeny, indicating that lack of growth of *S. feltiae* nematodes is due to inhibition rather than lack of nutritional support (Table 5.2). Due to the availability of the *S. affine* nematode host and the ability to genetically manipulate the bacterial symbiont, we chose to pursue interactions occurring between Xb-Sa bacteria and *S. feltiae* nematodes.

Inhibition by Xb-Sa influences competition between *S. feltiae* and *S. affine*. Because *S. feltiae* and *S. affine* co-occur geographically (15, 16) and inhibition occurs *in vivo*, we considered the possibility that Xb-Sa symbiont inhibition of non-native *S. feltiae* nematodes could provide a competitive advantage to its native nematode host *S. affine*. Symbiont inhibition could provide *S. affine* nematodes an advantage during co-infection with *S. feltiae* nematodes, or it could allow *S. affine* to superinfect an insect cadaver previously infected by *S. feltiae*. Also, inhibition might prevent *S. feltiae* from superinfecting an insect cadaver previously infected by *S. affine*.

Table 5.2. Development of *S. feltiae* nematodes on *X. bovienii* bacterial strains.

Bacterial Strain^a	<i>S. feltiae</i> Nematodes^b	Adult Nematodes^c	Progeny IJ Nematodes^d
None	Conventional IJs	Yes	Yes
None	Axenic IJs	Yes	Yes
Xb-Sf	Conventional IJs	Yes	Yes
Xb-Sf	Axenic IJs	Yes	Yes
Xb-Si	Conventional IJs	No	No
Xb-Si	Axenic IJs	No	No
Xb-Sa	Conventional IJs	No	No
Xb-Sa	Axenic IJs	No	No

^aBacterial strain tested.

^bType of nematode tested. Bacterial lawns were seeded with nematode IJs. Conventional IJs contain the native symbiont and were harvested from insect infections. Axenic IJs contain no bacterial symbiont and were grown *in vitro* (on LKA).

^cPresence of visible adult nematodes by five days post addition.

^dPresence of visible progeny IJs by 14 days post addition.

To assess competition phenotypes between *S. affine* or *S. feltiae* we performed co-injection assays (Figure 5.2). When equal numbers of conventionally reared nematodes (i.e. carrying symbiont) were injected at the same time, all of the resulting progeny IJs were *S. affine*, indicating this nematode has a competitive advantage in direct competition. To confirm that Xb-Sa is mediating this competitive advantage, we performed co-injections assays of axenic nematodes hosts (i.e. nematodes reared without bacteria) with and without the symbionts (Figure 5.2). As expected, co-injections of both nematode hosts with both symbionts or both nematode hosts with only Xb-Sa resulted in all *S. affine* progeny. However, co-injections of both nematode hosts with only Xb-Sf resulted in the production of only *S. feltiae* progeny. These data support that the symbiont of Xb-Sa is necessary for *S. affine* to have a competitive advantage over *S. feltiae*.

Under natural environmental conditions, simultaneous infection by two parasites, while possible, is less likely than sequential infection, in which a secondary parasite attempts to superinfect an insect previously infected by another species. To assess if the competitive advantage of *S. affine* occurs during superinfection by one or the other species, we performed sequential injections of conventionally reared nematodes (Figure 5.2). When *S. affine* was injected before *S. feltiae*, all resulting nematode progeny were *S. affine*, and when *S. feltiae* was injected before *S. affine*, almost all resulting progeny were *S. feltiae*. Trends were the same when Xb-Sa was used in injections in place of *S. affine* (data not shown). This indicates that inhibition of *S. feltiae* by Xb-Sa most likely functions to protect *S. affine* infected insect cadavers from a successful superinfection by *S. feltiae*.

In the assays described above, nematodes and bacteria were directly injected into insects. To assess competition during superinfection in a more natural infection, we provided conventionally-reared nematodes to insects in a sand trap assay, which requires that the nematodes locate and infect the insect host (Figure 5.S1). As expected, when the insect

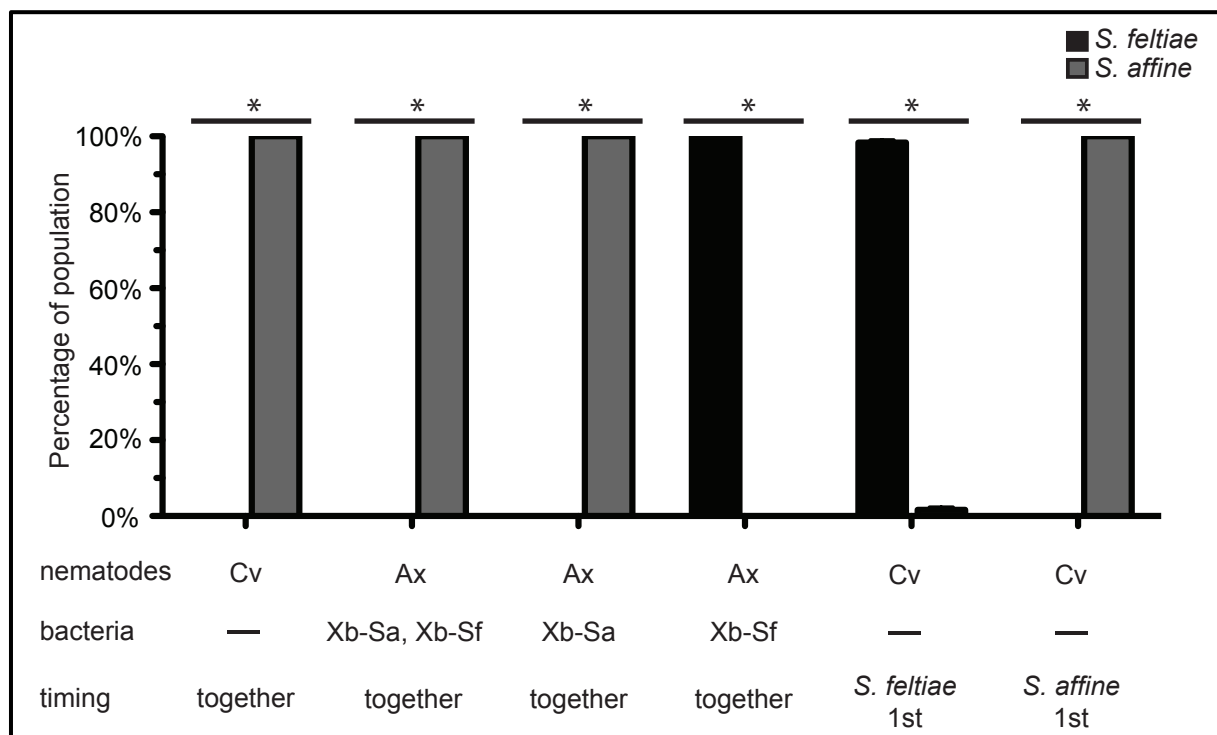


Figure 5.2 *S. feltiae* and *S. affine* competition experiments. Conventional (Cv), reared with symbiont, or axenic (Ax), reared with no bacteria, *S. feltiae* and *S. affine* nematodes were co-injected with and without their symbionts (Xb-Sa or Xb-Sf), either at the same time (together) or sequentially (*S. feltiae* 1st or *S. affine* 1st). The bar graph shows the percentage of the progeny population that was *S. feltiae* (black) or *S. affine* (grey). Measurements are an average of three blocks with at least 4 technical replicates. *indicate bars significantly indicate different percentages of the population, representing a competitive advantage for one species ($p < 0.05$).

host was exposed to *S. affine* prior to *S. feltiae*, all resulting progeny were *S. affine*, and when the insect host was exposed to *S. feltiae* prior to *S. affine*, all resulting progeny were *S. feltiae*. The same results were observed when injection of Xb-Sa was used instead of infection of *S. affine* (data not shown). These data support that infection by *S. affine* prevents successful superinfection by *S. feltiae* in a natural setting. However, when *S. affine* and *S. feltiae* were allowed to infect at the same time, all resulting progeny were *S. feltiae* (Figure 5.S1). One possible explanation is that *S. feltiae* may be able to infect insects faster than *S. affine* and prevent superinfection.

To assess if failure of *S. feltiae* nematode superinfection under natural conditions is due to prevention of infection (i.e. the nematodes don't invade the insect cadaver) or inhibition of nematodes in the insect cadaver, we monitored the invasion of *S. feltiae* nematodes within insects using their GFP-expressing symbiont as a proxy (Figure 5.S2). Insects that were alive, freeze-killed, or injected with *S. affine* or *S. feltiae* nematodes were exposed to *S. feltiae* nematodes carrying GFP-expressing symbiont and monitored for fluorescence. In all insect cadavers exposed to *S. feltiae* nematodes, fluorescence was detected by four days post exposure, indicating that *S. feltiae* nematodes invade previously-infected insect hosts. Therefore, Xb-Sa prevention of superinfection through inhibition of *S. feltiae* nematodes is likely an ecologically relevant phenomenon.

Previous reports of competition among bacterial symbionts demonstrate that bacterial-bacterial competition can influence the outcome of host reproduction, where a bacterial symbiont can remove competing microbes through the production of antimicrobials (14). To assess if bacterial-bacterial competition occurred between Xb-Sf and Xb-Sa and is influencing competition, we performed several bacterial competition experiments, including cross streaking, overlays, bacteriocin assays, and co-injections in insects. All of these experiments showed that the bacterial strains were able to grow together and did not inhibit one another (data not shown).

This indicates that bacterial-bacterial competition is likely not significantly affecting the competitive outcome.

Xb-Sa kills *S. feltiae* through an infection-mediated process. The observed phenotypes of Xb-Sa preventing nematode adult and progeny production could be a result of the bacteria inhibiting nematode growth and development or killing the nematodes. To distinguish between the possibilities, we first assessed if *S. feltiae* IJ nematodes recovered into J3 nematodes when exposed to GFP-expressing Xb-Sf (Xb-Sf-GFP) and Xb-Sa (Xb-Sa-GFP). By 6 h post-exposure, nematodes on both symbiont lawns had morphology consistent with initiation of recovery (i.e. open mouths and GFP-expressing bacteria present within the esophagus and intestine) (Figure 5.3 A-C). By 24 hours post-addition to bacterial lawns, the majority of nematodes on Xb-Sa-GFP were dead, while the majority of nematodes on Xb-Sf-GFP were alive. However, the nematodes that were alive on both lawns showed development indicative of full recovery (i.e. GFP-expressing bacteria were present in the intestine and nematodes had an open mouth, anus, and intestine) (Figure 5.3 D, E). These data are consistent with Xb-Sa not impairing recovery and development of IJ nematodes but rather killing nematodes during or after recovery. To confirm that Xb-Sa can kill *S. feltiae* nematodes, we performed survival assays using young adult *S. feltiae* nematodes transferred to lawns of Xb-Sf and Xb-Sa. All nematodes transferred to Xb-Sa lawns were dead within 24 hours, whereas nematodes transferred to lawns of native symbiont survived, confirming that *S. feltiae* nematodes are killed by Xb-Sa (Figure 5.3 F).

The timing of Xb-Sa-mediated *S. feltiae* death falls between previously defined fast and slow killing phenotypes of bacterial pathogens on *Caenorhabditis elegans*, which correspond to toxin-mediated and infection-mediated killing respectively (17). To determine if the killing of *S. feltiae* by Xb-Sa is due to Xb-Sa changing the environment such that *S. feltiae* cannot survive

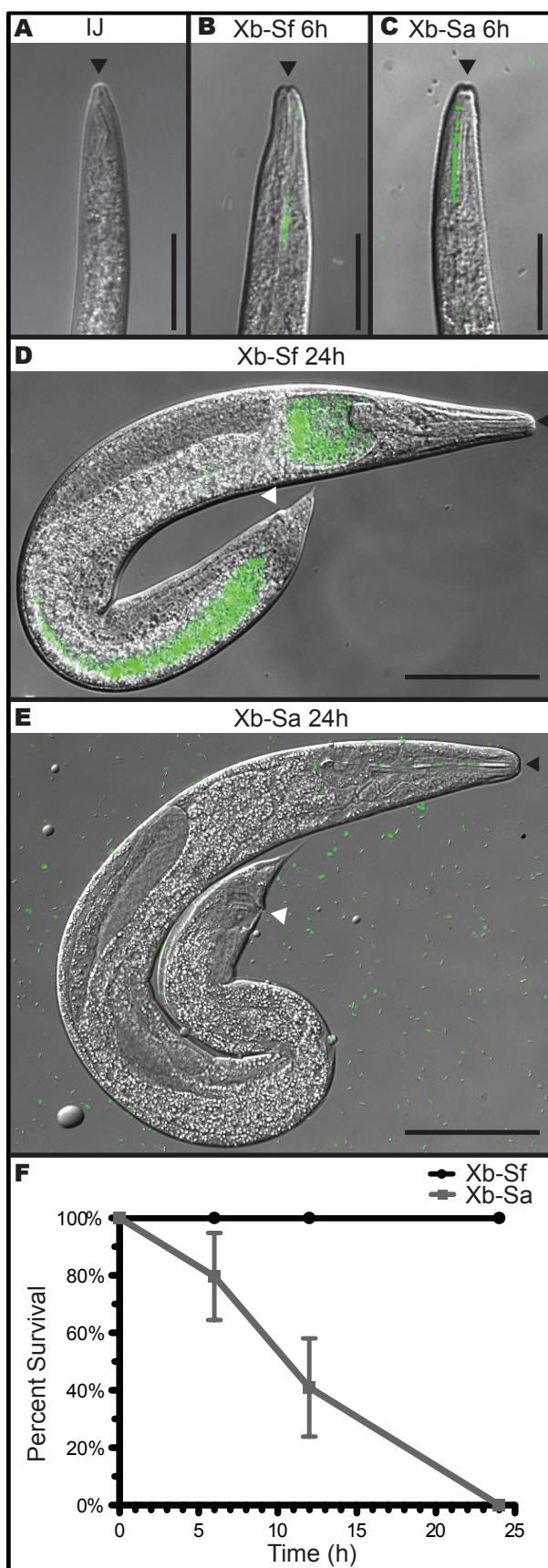


Figure 5.3 Xb-Sa kills *S. feltiae* nematodes rather than inhibiting development. IJ

nematodes (A) were assessed for recovery at 6 hours (B, C) and 24 hours (D, E) post-addition to bacterial lawns of the GFP-expressing symbionts Xb-Sf-GFP (B, D) or Xb-Sa-GFP (C, E). For both strains, nematodes showed morphology consistent with recovery (i.e. shedding of the chitin cuticle, opening of the mouth and anus, and bacteria present within the esophagus and intestine). Bacteria are in green and overlaid on nematode phase contrast images. The black arrowheads point to the nematode mouths, and the white arrowheads point to anuses. The scale bars represent 25 μm in A-C and 50 μm in D-E. To confirm nematode killing, a survival curve of *S. feltiae* nematodes was done on both bacterial strains (F), and the lines were significantly different using log-rank analysis ($p < 0.05$).

(e.g. production of toxins), we performed survival assays of nematodes on plates pre-conditioned by Xb-Sf and Xb-Sa (Table 5.S1). All nematodes transferred onto each of these plates survived, indicating that the inhibition of *S. feltiae* by Xb-Sa is not due to the bacteria changing the media environment. To assess if the killing is due to an infection-mediated process, we performed nematode shifting assays, where adult nematodes were exposed to the bacterial strains (Xb-Sf-GFP and Xb-Sa-GFP) for 1, 4, or 8 hours, transferred onto plain agar plates, and monitored for percent survival over time (Figure 5.4). Nematodes exposed to Xb-Sa-GFP for as little as 1 h showed significantly decreased survival compared to nematodes exposed to Xb-Sf-GFP (Figure 5.4 A), supporting an infection-mediated killing mechanism.

Both bacterial strains were visible in the nematode intestine at the time of transfer (Figure 5.4 B-D, H-J). By 24 h post transfer, no Xb-Sf-GFP cells were visible within the nematode intestine (Figure 5.4 E-G). However, Xb-Sa-GFP cells persisted within the nematode intestine (Figure 5.4 K-M). It should also be noted that Xb-Sf-GFP-exposed nematodes had obvious empty spaces in their intestines by 24 hours (either representing air bubbles or lipid granules), where the majority of Xb-Sa-GFP exposed nematodes lacked these (Figure 5.4). This could be explained by a difference in feeding or pumping of the basal bulb (swallowing organ) between the two conditions.

During shifting assays, bacteria were observed primarily in the intestine of the nematodes prior to nematode death, the only exception being gravid female nematodes. Occasionally these nematodes could be observed with Xb-Sa-GFP bacteria localized to the area surrounding the eggs (Figure 5.S3). During the exposure of the nematodes to Xb-Sa-GFP, the nematode intestinal morphology of the nematode appears to change (Figure 5.4 B-M). To further characterize the morphological differences in the nematode intestine and intestinal localization of the bacteria, we performed confocal microscopy on adult nematodes exposed to Xb-Sf-GFP or Xb-Sa-GFP for 8 hours (Figure 5.5 A). Nematodes exposed to Xb-Sf-GFP

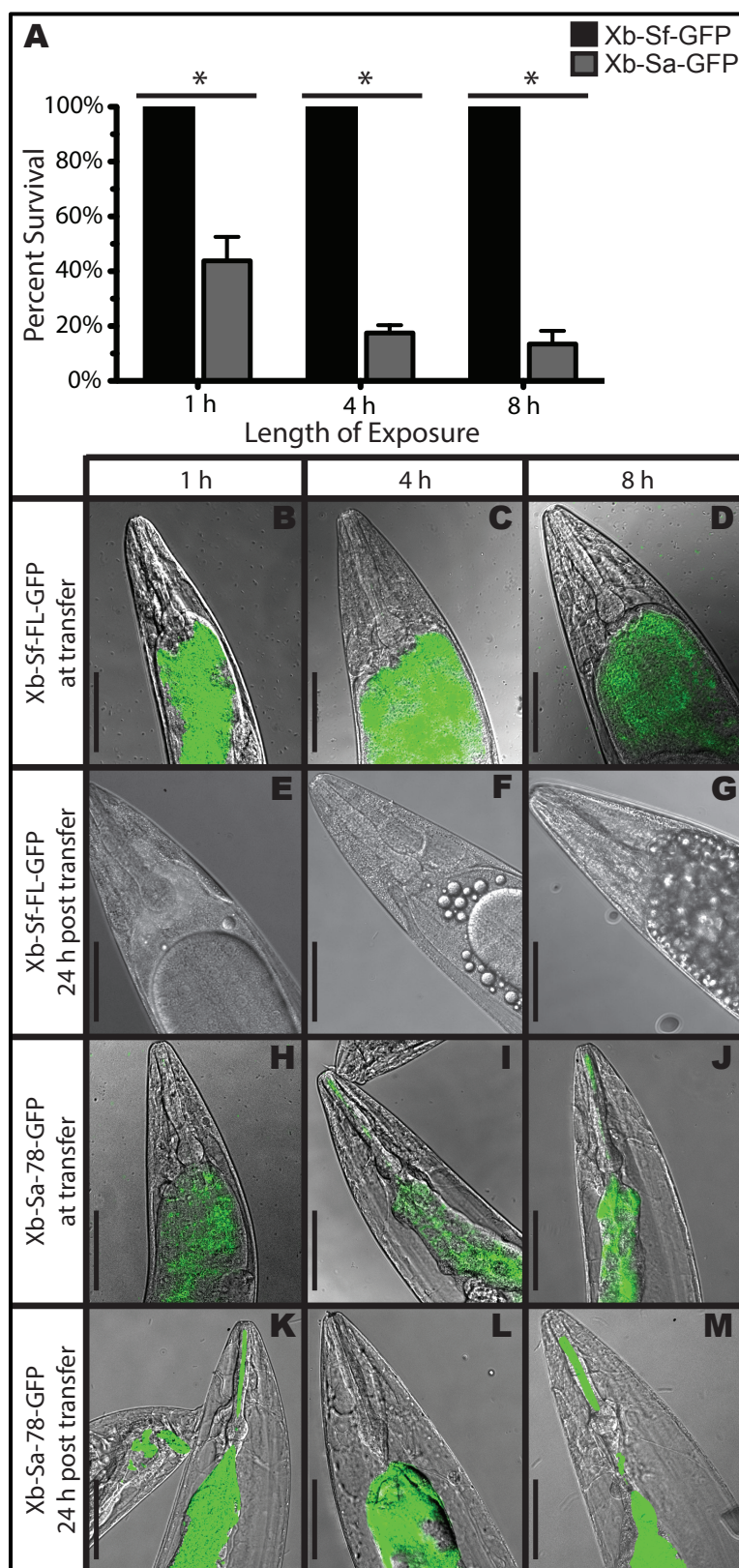


Figure 5.4 Xb-Sa killing of *S. feltiae* is infection mediated. *S. feltiae* adult nematodes were transferred from native symbiont bacterial lawns onto GFP-expressing native symbiont (Xb-Sf-GFP) or the symbiont of *S. affine* (Xb-Sa-GFP) and exposed for 1 (B, E, H, K), 4(C, F, I, L), or 8 (D, G, J, M) hours. The nematodes were then collected and transferred onto blank agar plates. Nematodes were monitored for survival at 32 hours post initial exposure (A), and nematodes exposed to Xb-Sa-GFP showed significantly less survival than nematodes exposed to Xb-Sf ($p < 0.05$). Graphs show averages of 3 blocks of 100 nematodes. Nematodes were also visually inspected at that time of transfer (B-D, H-J) and at 24 hours post transfer (E-G, K-M) for the localization, presence, and persistence of bacteria. Scale bars indicate 50 μm .

displayed normal intestinal morphology (i.e. open, smooth intestines) throughout the total length of their body (Figure 5.5 B). However, nematodes exposed to Xb-Sa-GFP had frequent narrow spots along the entire length of the intestine and a constricted, ruffled appearance (Figure 5.5 C). Localization of the bacteria to the intestine and altered intestinal morphology suggests that killing of *S. feltiae* is likely due to an intestinal infection by Xb-Sa-GFP.

CONCLUSIONS

In this study we describe a competitive interaction that occurs between *S. affine* and *S. feltiae* nematodes that is modulated by the *X. bovienii* bacterial symbiont associated with *S. affine*, Xb-Sa. To our knowledge, this is the first study to identify bacterial symbionts affecting the outcome of parasitic success through infection and direct inhibition of the competing parasite. Previous work has shown that bacterial symbionts can affect parasitic success and competition through indirect methods, such stimulating the host immune system to overcome parasitic infection (13, 18) or inhibiting the bacterial symbiont of the parasite (14). These studies, along with our work, highlight that the interactions between hosts, parasites and symbionts are complex and likely vary in mechanism and function between and within particular types of associations. Our study also demonstrates that these differences can occur at the isolate level, as the two *X. bovienii* bacterial isolates studied here (Xb-Sa and Xb-Sf), although the same species, have very different impacts on *S. feltiae* nematodes.

In competitive interactions between *S. affine* and *S. feltiae*, the outcome of the competition (i.e. which nematode is able to produce progeny) depends on the presence or absence of Xb-Sa (Figure 5.2). Our data also support that Xb-Sa is both necessary and sufficient for *S. affine* to outcompete *S. feltiae* (Figure 5.2, data not shown), and that this competitive advantage likely functions to prevent successful *S. feltiae* superinfection of *S. affine* infected cadavers (Figure 5.2, S1, S2). These data are in contrast to a previous study that

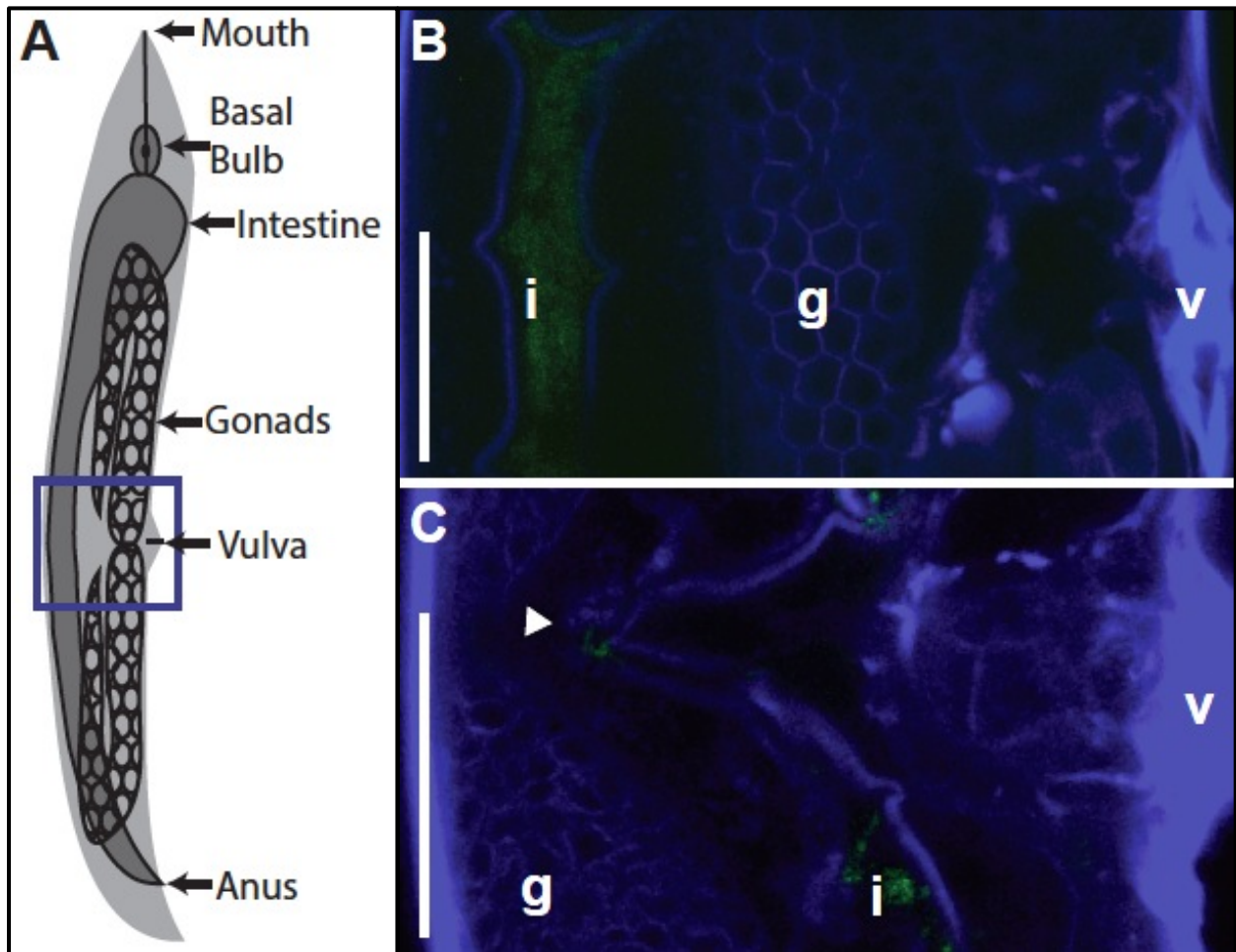


Figure 5.5 *S. feltiae* nematodes have narrowed intestines when exposed to Xb-Sa.

Schematic depicts whole nematode to show the tissues viewed on the microscope, with arrows pointing to the nematode tissues (A). The area designated by the purple box in the schematic (A) is the area seen in the micrographs (B, C). Nematodes exposed to Xb-Sf-GFP (B) or Xb-Sa-GFP (C) were stained and viewed using confocal microscopy. In the micrographs above nematode tissues are colored blue-purple and bacteria are colored green. Scale bars represent 50 μm , and the white arrowhead points to an area of intestinal narrowing. Lettering labels the nematode morphological features: intestine (i), vulva (v), and gonad (g). Nematodes exposed to Xb-Sa-GFP had places of narrowing of the intestine, where nematodes reared on Xb-Sf-GFP did not show intestinal narrowing.

demonstrated *S. affine* successfully superinfects and suppresses progeny production of *S. kraussei* (3). Taken together, these studies highlight that competition outcomes depend on many variables, including symbiont strain and nematode isolate identity. However, it is possible that mechanisms of inhibition on the competitor nematodes are similar.

Steinernema nematodes fall into five distinct phylogenetic clades, and *X. bovienii* strains associate with at least ten different nematode host species in two clades (clade I and clade III) (19). From this study, we determined that the symbiont of *S. affine* (clade I) inhibits *S. feltiae* (clade III) to provide a competitive advantage. Additionally, we identified that the symbiont of *S. intermedium* (clade I) does not support *S. feltiae* (clade III) (Chapter 3), and we have confirmed that this is also due to inhibition (Table 5.1). Likewise, Půža and Mracek found that *S. affine* (clade I) outcompetes *S. kraussei* (clade III) (3). Similarly, a study by Chapuis *et al.* identified that *S. feltiae* (clade III) did not reproduce well when reared with the *X. bovienii* symbionts of *S. sichuanense*, *S. intermedium* or *S. affine* (clade I) (20). Together, these data demonstrate that *X. bovienii* symbionts from clade I nematodes are incompatible with clade III nematodes, and this suggests that symbiont-derived inhibition may be a conserved phenomenon among *X. bovienii* strains of clade I nematodes for a competitive advantage against clade III nematodes.

Even though clade I nematodes appear to consistently outcompete clade III nematodes, clade I and clade III nematode species have been isolated in close proximity to one another (15, 16). This indicates that there must be mechanisms in play that stabilize their coexistence. Our study supports that differences in the ability of the nematode species to infect may contribute to coexistence, as *S. feltiae* nematodes seem to be able to overcome the competitive advantage of *S. affine* by infecting at a faster rate (Figure 5.S1). Such differences in infection rate may be due to differing ability to move through the sand or differences in hunting strategy. In addition to differences in infection rate other factors may facilitate coexistence of the species. For example, the infection index (number of parasites per host) of both species would need to be relatively

high in the same area to result in a high number of coinfections, so a species may be stabilized when the number of nematodes per potential host is low. Additionally, it was previously proposed that differing natural insect range or insect hunting behavior may facilitate the coexistence of competing nematodes (2). In total, these mechanisms would work to reduce the frequency of *S. affine* and *S. feltiae* co-infection, thereby allowing *S. feltiae* to exist in the same environment with *S. affine*.

Within natural systems, parasites are likely to come in contact with bacterial symbionts, either of the host or other parasites. Therefore, interactions between bacteria and symbionts, such as symbiont-mediated killing, may be important in parasite success within the environment. As parasites can have a profound impact on the ecology of host populations (21), affect predator – prey relationships (22), and play a significant role in host evolution (23, 24), understanding competition between parasites how it is modulated by microbial symbionts is important for our understanding of the ecology and evolution of natural systems.

ACKNOWLEDGEMENTS

The authors would like to thank Mengyi Cao for assistance in confocal microscopy and S. P. Stock (University of Arizona) and S. Forst (UW-Milwaukee) for collaborations that led to the current work. This work was funded by grants from the National Science Foundation: an NSF Doctoral Dissertation Improvement Grant (DEB-1310985) and an award to HGB (IOS-1353674). KEM was supported by the National Institutes of Health (NIH) National Research Service Award T32 AI55397, a Louis and Elsa Thomsen Distinguished Predoctoral Fellowship, and a Betley-Allen Bacteriology Departmental Fellowship.

MATERIALS AND METHODS

Nematode and bacterial strains. Bacterial strains were isolated through sonication of surface sterilized nematode hosts, and species identity was confirmed by analysis of 16S rRNA (Table 5.1) (19, 25). Bacterial strains were stored in Lysogeny Broth (LB) supplemented with 20% glycerol frozen at -80°C. Unless otherwise noted, bacterial strains were grown in LB with aeration or on LB agar supplemented with 0.1% pyruvate at 30°C in the dark (26). Nematode isolates were obtained from the laboratories of Dr. S. Patricia Stock or Dr. Farrah Bashey-Visser, and species identity of the nematodes were verified through sequencing of the 12S and 28S genes (Table 5.1) (27). Nematodes were propagated through *Galleria mellonella* larvae at 25°C as previously described (6). Nematodes were stored at 25°C at a density less than 5 IJs/ μ l at a volume less than 60 in 250 ml tissue culture flasks (BD Falcon, Franklin Lakes, NJ, USA). These IJ nematodes are used directly from storage as the conventional nematodes for testing.

Axenic IJs were produced *in vitro* on liver kidney agar (LKA) similar to previously described methods (28, 29). The protocol was modified to produce axenic *S. affine*. Instead of direct addition of nematodes eggs to LKA, nematode eggs were incubated in LB supplemented with 150 μ M kanamycin for three days. Additionally LKA plates were also supplemented with 150 μ M kanamycin and 100 μ M ampicillin.

Genetic modification of the bacterial strains to express GFP was performed as previously described (11, 30). Briefly, the pURR25 Tn7 delivery vector including the gene encoding GFP was transferred from *Escherichia coli* into recipient *Xenorhabdus* strains using tri-parental mating conjugations (31) and a helper plasmid (32). GFP-expressing exconjugants in which the Tn7 had inserted into the *attTn7* site were selected using LB supplemented with pyruvate and 50 μ M kanamycin.

Assays to assess inhibition of *S. feltiae* nematodes. To test inhibition, conventional or axenic IJ nematodes were added directly to test bacterial strain lawns on lipid agar (LA) plates. Briefly, 600 μ L of overnight bacterial culture of the native symbiont was spread on 6 cm lipid agar (LA) plates and allowed to grow at 25°C. Approximately 2,000 surface sterilized nematodes in 200 μ L LB was added to the bacterial lawn, and the nematodes were allowed to develop at 25°C. Plates were viewed under 4x magnification daily to assess the production of adults and juvenile progeny. At least three blocks of two technical replicates were performed.

Injections in *Galleria mellonella*. Axenic or conventional nematodes were surface sterilized and mixed with log-phase bacterial culture in order to inject 50 IJ nematodes. For injections of bacteria, overnight cultures were subcultured, grown to \sim 0.6 OD, and diluted to inject 100 CFU of log phase bacterial cells. In co-injections, bacteria were grown separately and combined prior to injection in order to inject 100 CFU of log phase bacterial cells for each strain. For competition injections, nematodes were mixed and 50 IJs of each species were co-injected. For sequential injections, 50 IJs of the first species were injected, and 50 IJs of the second species were injected after 72 h. At 7 d post-1st-injection, the insect cadavers were placed in a water trap, and nematodes emerged within 10 d post-trapping. For co-injections that did not display nematode emergence, cadavers were dissected to confirm that no nematodes were present. For quantification of progeny populations, 100 nematodes from each water trap were scored for species identify based on size. For each treatment, five insects were injected and scored as technical replicates and averaged. Three blocks were performed. In all injections, at least four insect cadavers produced progeny.

Natural infections. Sand traps were performed similarly to previously described (Chapter 3). Briefly, 1 g of sand was added to wells of a 12-well plate. Approximately 50 IJs in 100 μ L of water were added to the well and allowed to equilibrate for one hour. For direct competition, 50 IJs of each species in 100 μ L of water was added together in one well. One *G. mellonella* larva was added to each well and allowed to infect for 7 days. For sequential natural infections, the first species was allowed to infect for 3.5 days, and then insect cadavers were transferred to new sand trap wells with the second species for an additional 3.5 days. 7 days post-initial infection, the insect cadavers were placed in a water trap, and nematodes emerged within 10 days of trapping. For infections from which no nematodes emerged, cadavers were dissected to confirm that no nematodes were present. For quantification of progeny populations, 100 nematodes from each water trap were scored for species identify based on size. For each treatment, 5 insects were infected and scored as technical replicates. Three blocks were performed and averaged. At least 4 insect cadavers per treatment produced progeny.

Nematode recovery assays. Conventional IJ nematodes were added to LA plates with bacterial lawns, grown as described in inhibition assays. Nematodes were rinsed off of LA plates at various time points using 1 mL of PBS and collected in microfuge tubes. Nematodes were rinsed three times in PBS: nematodes were allowed to settle, PBS was removed and replaced with fresh PBS. Nematodes and GFP-expressing bacteria were viewed by microscopy using a Nikon Eclipse TE300 inverted microscope under 10x, 20x, and 40x magnification. Images were taken using a Hamamatsu digital camera (Hamamatsu City, Japan; model C4742-95-10NR) and analyzed using the Metamorph software v4.5r6 (Universal Imaging Corporation, West Chester, Pa.). Three blocks of two technical replicates were performed, and at least 25 nematodes were observed per technical replicate.

***In vitro* nematode growth and survival assays.** *In vitro* growth screening and testing was performed by transferring adult nematodes from native symbiont growth plates onto test bacterial strains. Briefly, 600 μ L of overnight bacterial culture of the native symbiont was spread on 6 cm lipid agar (LA) plates and allowed to grow at 25°C for 48 hours. Approximately 5,000 IJ nematodes in 500 μ L of LB was added to the bacterial lawn on LA, and the nematodes were allowed to grow at 25°C for 48 h. During nematode growth, test plates were set up by adding 600 μ L of overnight bacterial culture of test strains to LKA or LA and allowing growth at 25°C for 48 h (28, 29). After growth was complete, adult nematodes were transferred from growth plates to test plates. Nematodes were collected in PBS and rinsed 3 times. Approximately 200 rinsed nematodes in 200 μ L of PBS were added to each test plate and air dried in a hood. For growth assays, nematodes were monitored every 24 h for seven days. For growth assays on plates pre-conditioned by bacterial growth, a sterile filter paper was added to the surface of the test plate prior to addition of the test bacterial strain. Before nematode addition, the filter paper containing the bacterial lawn was removed. Two technical replicates of transfer plates were observed for qualitative growth for each condition, and three blocks were performed.

Survival assays were set up the same way as growth assays using the transfer method of adult nematodes. Nematode survival was monitored every 6 h for 24 h, and 20-25 nematodes were scored at each time point. Nematodes were scored as dead when they no longer moved or responded to gentle prodding with a thin wire. Two technical replicates from separate transfer plates were counted per condition and averaged, and three blocks were performed.

Testing of bacterial localization was done using *in vitro* transfer methods as described for growth assays. *S. feltiae* adult nematodes were transferred from native symbiont LA plates onto test LKA or LA plates with GFP-expressing bacterial cultures. Nematodes were collected in PBS

after 4, 8, 12, and 24 h post-transfer. Nematodes were rinsed in PBS three times and observed using epifluorescent and phase contrast microscopy on a Nikon Eclipse TE300 inverted microscope. Three blocks of two technical replicates were performed, and at least 25 nematodes were observed per technical replicate.

Confocal imaging of nematodes. Fixing, permeabilizing, and staining of nematodes was performed using previously described protocols(11, 30). Nematodes were stained using Alexa 633 phalloidin. Representative images were taken on a Zeiss LSM 510 confocal microscope with an Axioplan2 imaging system and processed using LSM image software v2.1 (Zeiss, New York, NY).

***In vivo* imaging.** Injection or infection of insects was done as described above. For nematode superinfection assays, axenic *S. feltiae* nematodes were added to LKA plates containing lawns of Xb-Sf-GFP set up as described in recovery assays. Seven days post addition of nematodes to LKA plates, the plates were water trapped, and IJs carrying GFP expressing symbiont were collected 7-14 days later. Insects pre-injected with PBS or bacterial strains or nematodes were used in a natural infection assay with the nematodes carrying GFP-expressing symbionts was done four days post injection. For all insect cadavers images were taken every 24 h for 5 d, and optimum time points (i.e. most fluorescence without oversaturation) was determined to be 4 d post-injection or infection. Analysis was done using an IVIS Imaging System 200 (Xenogen, Alameda, CA). Fluorescence was quantified by using Living Image software v2.6 (Xenogen). Five insects were imaged as technical replicates and average, and three biological replicates were performed.

Bacterial competition. Bacterial strain competition was measured four ways: bacterial cross streaking, antibiotic overlays, bacteriocin induction, and co-injection in insects. Bacterial cross streaking (33), antibiotic overlays (34), and bacteriocin induction (35) were done similarly to previously described methods. For co-injection in insects, GFP-expressing and non-expressing strains were co-injected into insects and fluorescence was monitored over time as described previously. Injections of Xb-Sf-GFP + Xb-Sa and Xb-Sf + Xb-Sa-GFP were done and compared to single injections of each GFP-expressing strain.

Statistics. Statistical analyses were performed in R (36) or Prism (GraphPad). For survival assays, log rank analyses were done. In log-rank analysis, all data points from the three blocks were combined. Each experimental block was also analyzed separately, and trends remained the same. For comparison of survival at single timepoints and population percentage difference, a t-test was done on the average of the experimental blocks to determine if the values were significantly different. Each experimental block was also analyzed separately, and trends remained the same.

REFERENCES

1. **Kondo E, Ishibashi N.** 1986. Infectivity and propagation of entomogenous nematodes, *Steinernema* spp., on the common cutworm, *Spodoptera litura* (Lepidoptera: Noctuidae). *Appl Ent Zool* **21**:95-108.
2. **Koppenhofer AM, Kaya HK.** 1996. Coexistence of two steinernematid nematode species (Rhabditida:Steinernematidae) in the presence of two host species. *Appl Soil Ecol* **4**:221-230.
3. **Půža V, Mracek Z.** 2009. Mixed infection of *Galleria mellonella* with two entomopathogenic nematode (Nematoda: Rhabditida) species: *Steinernema affine* benefits from the presence of *Steinernema kraussei*. *J Invertebr Pathol* **102**:40-43.
4. **Ehlers RU.** 2001. Mass production of entomopathogenic nematodes for plant protection. *Appl Microbiol Biotechnol* **56**:623-633.
5. **Herbert EE, Goodrich-Blair H.** 2007. Friend and foe: the two faces of *Xenorhabdus nematophila*. *Nat Rev Microbiol* **5**:634-646.
6. **Martens EC, Heungens K, Goodrich-Blair H.** 2003. Early colonization events in the mutualistic association between *Steinernema carpocapsae* nematodes and *Xenorhabdus nematophila* bacteria. *J Bacteriol* **185**:3147-3154.
7. **Poinar GOJ, Thomas GM.** 1966. Significance of *Achromobacter nematophilus* Poinar and Thomas (Achromobacteraceae: Eubacteriales) in the development of the nematode, DD-136 (*Neoplectana* sp. Steinernematidae). *Parasitology* **56**:385-390.
8. **Richards GR, Goodrich-Blair H.** 2009. Masters of conquest and pillage: *Xenorhabdus nematophila* global regulators control transitions from virulence to nutrient acquisition. *Cell Microbiol* **11**:1025-1033.
9. **Snyder H, Stock SP, Kim SK, Flores-Lara Y, Forst S.** 2007. New insights into the colonization and release processes of *Xenorhabdus nematophila* and the morphology and ultrastructure of the bacterial receptacle of its nematode host, *Steinernema carpocapsae*. *Appl Environ Microbiol* **73**:5338-5346.
10. **Richards GR, Goodrich-Blair H.** 2010. Examination of *Xenorhabdus nematophila* lipases in pathogenic and mutualistic host interactions reveals a role for *xlpA* in nematode progeny production. *Appl Environ Microbiol* **76**:221-229.
11. **Chaston JM, Murfin KE, Heath-Heckman EA, Goodrich-Blair H.** 2013. Previously unrecognized stages of species-specific colonization in the mutualism between *Xenorhabdus* bacteria and *Steinernema* nematodes. *Cell Microbiol* **15**:1545-1559.
12. **Popiel I, Grove DL, Friedman MJ.** 1989. Infective juvenile formation in the insect parasitic nematode *Steinernema feltiae*. *Parasitology* **99**:77-81.
13. **Weiss B, Aksoy S.** 2011. Microbiome influences on insect host vector competence. *Trends Parasitol* **27**:514-522.

14. **Morales-Soto N, Forst SA.** 2011. The xnp1 P2-like tail synthesis gene cluster encodes xenorhabdicolin and is required for interspecies competition. *J Bacteriol* **193**:3624-3632.
15. **Emelianoff V, Le Brun N, Pages S, Stock SP, Tailliez P, Moulia C, Sicard M.** 2008. Isolation and identification of entomopathogenic nematodes and their symbiotic bacteria from Hérault and Gard (Southern France). *J Invertebr Pathol* **98**:211-217.
16. **Tarasco E, Clausi M, Rappazzo G, Panzavolta T, Curto G, Sorino R, Oreste M, Longo A, Leone D, Tiberi R, Vinciguerra MT, Triggiani O.** 2014. Biodiversity of entomopathogenic nematodes in Italy. *J Helminthol* doi:10.1017/S0022149X14000194:1-8.
17. **Tan MW, Mahajan-Miklos S, Ausubel FM.** 1999. Killing of *Caenorhabditis elegans* by *Pseudomonas aeruginosa* used to model mammalian bacterial pathogenesis. *Proc Natl Acad Sci U S A* **96**:715-720.
18. **Moreira LA, Iturbe-Ormaetxe I, Jeffery JA, Lu G, Pyke AT, Hedges LM, Rocha BC, Hall-Mendelin S, Day A, Riegler M, Hugo LE, Johnson KN, Kay BH, McGraw EA, van den Hurk AF, Ryan PA, O'Neill SL.** 2009. A *Wolbachia* symbiont in *Aedes aegypti* limits infection with dengue, Chikungunya, and *Plasmodium*. *Cell* **139**:1268-1278.
19. **Lee MM, Stock SP.** 2010. A multigene approach for assessing evolutionary relationships of *Xenorhabdus* spp. (gamma-Proteobacteria), the bacterial symbionts of entomopathogenic *Steinernema* nematodes. *J Invertebr Pathol* **104**:67-74.
20. **Chapuis E, Emelianoff V, Paulmier V, Le Brun N, Pages S, Sicard M, Ferdy JB.** 2009. Manifold aspects of specificity in a nematode-bacterium mutualism. *J Evol Biol* **22**:2104-2117.
21. **Lancinani CA.** 1975. Parasite-induced alteracitons in host reproduction and survival. *Ecology* **56**:691.
22. **Lafferty KD, Dobson AP, Kuris AM.** 2006. Parasites dominate food web links. *Proc Natl Acad Sci U S A* **103**:11211-11216.
23. **Barber I, Dingemans NJ.** 2010. Parasitism and the evolutionary ecology of animal personality. *Philos Trans R Soc Lond B Biol Sci* **365**:4077-4088.
24. **Wilson DS, Coleman K, Clark AB, Biederman L.** 1993. Shy-bold continuum in pumpkinseed sunfish (*Lepomis gibbosus*): An ecological study of a psychological trait. *Journal of Comparative Psychology* **107**:250-260.
25. **Chaston JM, Suen G, Tucker SL, Andersen AW, Bhasin A, Bode E, Bode HB, Brachmann AO, Cowles CE, Cowles KN, Darby C, de Leon L, Drace K, Du Z, Givaudan A, Herbert Tran EE, Jewell KA, Knack JJ, Krasomil-Osterfeld KC, Kukor R, Lanois A, Latreille P, Leimgruber NK, Lipke CM, Liu R, Lu X, Martens EC, Marri PR, Medigue C, Menard ML, Miller NM, Morales-Soto N, Norton S, Ogier JC, Orchard SS, Park D, Park Y, Qurollo BA, Sugar DR, Richards GR, Rouy Z, Slominski B, Slominski K, Snyder H, Tjaden BC, van der Hoeven R, Welch RD, Wheeler C, Xiang B, Barbazuk B, et al.** 2011. The entomopathogenic bacterial

- endosymbionts *Xenorhabdus* and *Photorhabdus*: convergent lifestyles from divergent genomes. PLoS One **6**:e27909.
26. **Xu J, Hurlbert RE.** 1990. Toxicity of Irradiated Media for *Xenorhabdus* spp. Appl Environ Microbiol **56**:815-818.
 27. **Lee MM, Stock SP.** 2010. A multilocus approach to assessing co-evolutionary relationships between *Steinernema* spp. (Nematoda: Steinernematidae) and their bacterial symbionts *Xenorhabdus* spp. (gamma-Proteobacteria: Enterobacteriaceae). Syst Parasitol **77**:1-12.
 28. **Martens EC, Goodrich-Blair H.** 2005. The *Steinernema carpocapsae* intestinal vesicle contains a subcellular structure with which *Xenorhabdus nematophila* associates during colonization initiation. Cellular microbiology **7**:1723-1735.
 29. **Sicard M, Le Brun N, Pages S, Godelle B, Boemare N, Moulia C.** 2003. Effect of native *Xenorhabdus* on the fitness of their *Steinernema* hosts: contrasting types of interaction. Parasitol Res **91**:520-524.
 30. **Murfin KE, Chaston J, Goodrich-Blair H.** 2012. Visualizing bacteria in nematodes using fluorescent microscopy. J Vis Exp doi:10.3791/4298.
 31. **Teal TK, Lies DP, Wold BJ, Newman DK.** 2006. Spatiometabolic stratification of *Shewanella oneidensis* biofilms. Appl Environ Microbiol **72**:7324-7330.
 32. **Bao Y, Lies DP, Fu H, Roberts GP.** 1991. An improved Tn7-based system for the single-copy insertion of cloned genes into chromosomes of gram-negative bacteria. Gene **109**:167-168.
 33. **Anderhub B, Pitt TL, Erdman YJ, Willcox WR.** 1977. A comparison of typing methods for *Serratia marcescens*. J Hyg (Lond) **79**:89-102.
 34. **Akhurst RJ.** 1982. Antibiotic activity of *Xenorhabdus* spp., bacteria symbiotically associated with insect pathogenic nematodes of the families Heterorhabditidae and Steinernematidae. J Gen Microbiol **128**:3061-3065.
 35. **Hawlana H, Bashey F, Lively CM.** 2012. Bacteriocin-mediated interactions within and between coexisting species. Ecol Evol **2**:2521-2526.
 36. **R Core Team.** 2013. R: A language and environment for statistical computing, on R Foundation for Statistical Computing. <http://www.R-project.org/>.

SUPPLEMENTAL MATERIALS

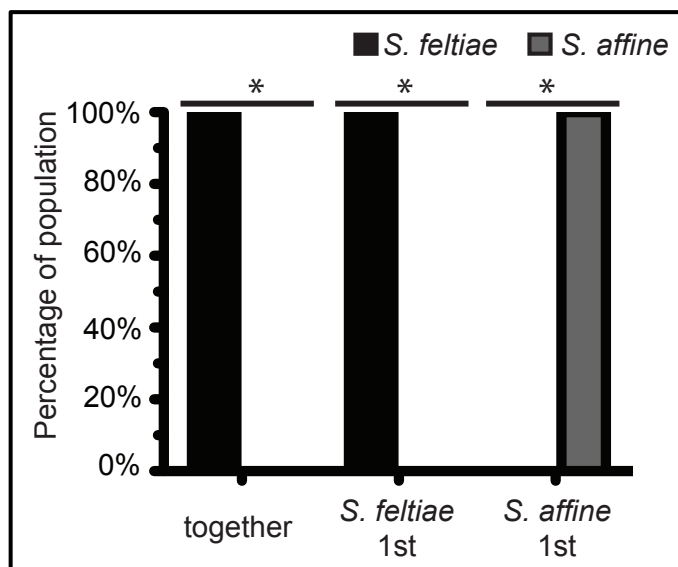


Figure 5.S1 Natural superinfections. Insect hosts were exposed to conventionally reared *S. feltiae* and conventionally reared *S. affine* either in combination (together) or sequentially (*S. feltiae* 1st or *S. affine* 1st). In sequential infections, insects were exposed to one nematode for three days followed by three days of exposure to the second nematode. The bar graph represents the percentage of the progeny population that was *S. feltiae* (black) or *S. affine* (grey). *indicate a significant difference between the progeny percentages, indicating a competitive advantage for one species ($p < 0.05$).

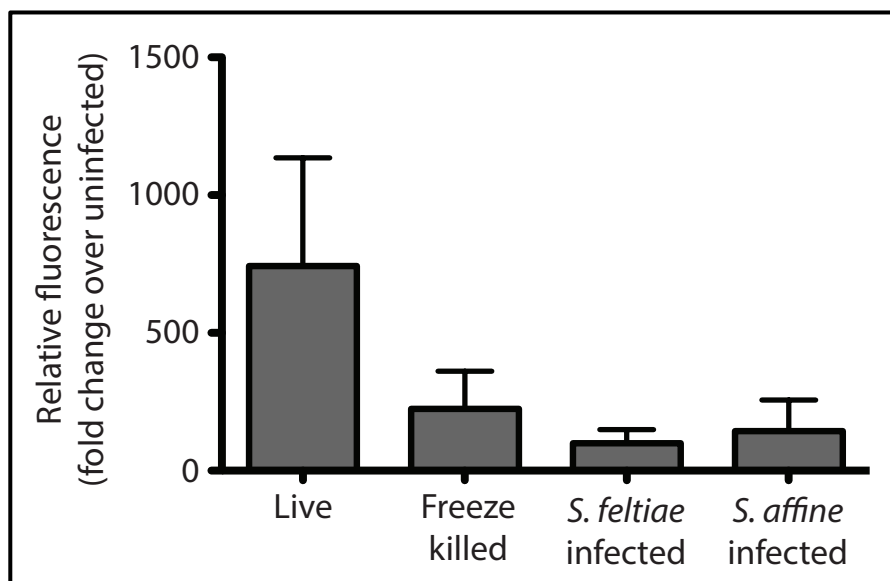


Figure 5.S2 Superinfection of cadavers by *S. feltiae* nematodes. Insects that were live, freeze killed, or previously infected by *S. feltiae* or *S. affine* nematodes were exposed to *S. feltiae* nematodes carrying GFP-expressing symbiont. The relative fluorescence per insect cadaver is shown as fold change over insects not exposed to *S. feltiae* FL nematodes. The bar graph shows the average of three biological replicates with five technical replicates per condition.

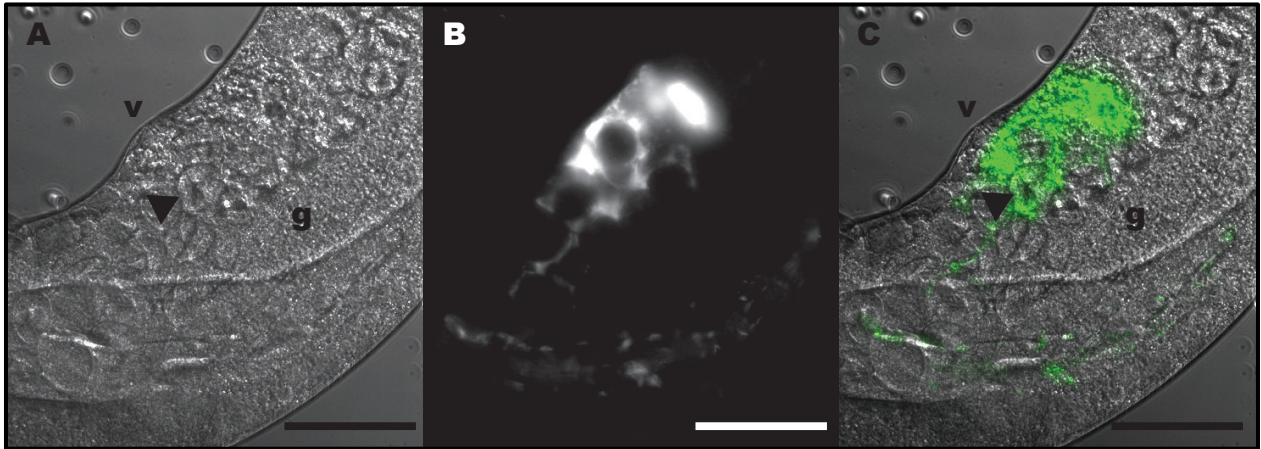


Figure 5.S3 Xb-Sa also localizes to *S. feltiae* nematode eggs. In some *S. feltiae* gravid female nematodes, bacteria were present near the eggs within the nematodes, either in the uterus or the nematode body cavity surrounding the uterus. Micrographs show the phase contrast (A), GFP (B), and overlay of phase contrast and GFP (C) of a female nematode with bacteria in this location. Abbreviations denote nematode anatomy: v (vulva) and g (gonad arm). The arrowhead points to an individual nematode egg within the uterus. Scale bars represent 50 μm .

Table S1 Testing of pre-conditioned media for adult nematode survival.

Bacterial Strain ^b	Time post-transfer ^c		
	12 h	24 h	48 h
None	Yes	Yes	Yes
Xb-Sf	Yes	Yes	Yes
Xb-Sa	Yes	Yes	Yes

^aSurvival of *S. feltiae* adult nematodes after transfer. Yes indicates all nematodes survived.

^bBacterial strain used to precondition media

^cTimes post-transfer of nematodes onto media at which survival was monitored

CHAPTER 6

Conclusion and future directions: *Xenorhabdus bovienii* bacteria – *Steinernema* species associations as a model of broad host range symbioses

INTRODUCTION

Identification of general principles within mutually beneficial symbioses (i.e. mutualisms) requires the investigation and comparison of findings within diverse mutualistic associations. One model that has been developed for this purpose is the association between *Xenorhabdus* bacterial symbionts and *Steinernema* nematode hosts. For example, the association between *X. nematophila* and *S. carpocapsae* demonstrated that a discrete set of genes can dictate symbiont specificity for transmission by hosts (1-3). This phenomenon was also identified in the squid – *Vibrio* (4, 5), plant – *Rhizobium* (6, 7), mouse – *Lactobacillus* (8), and mammalian – *Bacteriodes* (9) mutualisms. In all of these systems, there are bacterial genes necessary for colonization and/or persistence within the host, although the specific genetic determinants driving transmission differ among the associations. Indeed it has been proposed that general principles, such as this, can be identified in model systems and applied to other mutualisms (10).

Steinernema – *Xenorhabdus* associations are attractive laboratory models for the study of mutualism as they are easily maintained and genetically tractable. The ease of maintenance for this system is due to the long-term stability in storage of these nematode-bacterial pairs in the infective juvenile (IJ) state and the ease of propagation within insect hosts. Additionally, these nematodes are widely available and new isolates can be easily obtained from the environment (11, 12). The genetic tractability of this system is primarily on the bacterial side, in that many bacterial genomes are available (13-15) (Goodrich-Blair unpublished data) and many *Xenorhabdus* representatives can be genetically modified (1-3, 16, 17). However, nematode genomes are becoming available as well (Dillman *et al.* in revision at Genome Biology).

In addition to the ease of use, *Steinernema* nematode – *Xenorhabdus* bacterial associations are attractive models for host-microbe interactions because they exist as two-species pairs. *Steinernema* nematodes stably associate with a single *Xenorhabdus* species (18)

and are generally unable to associate with divergent, non-native *Xenorhabdus* species (3, 16).

Therefore, the microbiota (microbial community) of these associations is simple, which facilitates teasing apart specific mechanisms and general phenomena that are relevant to more complex multi-species microbial communities, which are relatively more difficult to study.

Within the *Xenorhabdus* genus, there are there are 22 species of bacteria (19, 20) that associate with at least one of the >70 known species of *Steinernema* nematodes from five distinct clades (21-23). Among the *Xenorhabdus* species, *X. bovienii* has the most known hosts and has been identified in combination with at least ten species of *Steinernema* nematodes from two clades (clade I and clade III) (18, 19, 23, 24), making *X. bovienii* and the associated *Steinernema* hosts an excellent model for broad host-range symbiosis. Broad-host range mutualisms between microbes and plants or animals are quite common (25-30), including between humans and their associated bacterial symbionts (31). Due to the prevalence of broad host-range associations and the significance of these symbioses, it is important that we begin to study broad host-range mutualisms and how they are impacted by microbial diversity. Specific interesting areas that may vary from binary associations include: the recognition of bacterial strains by host species, the impact of microbial symbiont diversity on host health, and the evolution and maintenance of partner pairs. Towards understanding these topics, many *Steinernema* – *Xenorhabdus* associations could be used for study.

The remainder of this chapter will detail the work that has been done to develop the *X. bovienii* – *Steinernema* spp. model, the use of this model for understanding features of broad host-range mutualism, and the future questions that this model can be used to answer.

DEVELOPMENT OF THE *X. BOVIENII* – *STEINERNEMA* SPP. SYSTEM MODEL

Work presented in this thesis and published by other groups helped define the interactions that occur between *X. bovienii* and *Steinernema* nematodes, including the

contributions of different partners to the symbiosis, physical features of bacterial colonization of nematode hosts, and quantification and characterization of bacterial symbiont strain diversity. Additionally, this work established protocols that broadened the ability to investigate diverse *Xenorhabdus* symbioses, such as genetic manipulation of the bacterium, *in vitro* and *in vivo* cultivation methods, and microscopy techniques. These advances have helped pave the way toward a comparative, genus-wide analysis of the molecular, cellular, and evolutionary aspects of the *Steinernema-Xenorhabdus* symbiosis.

Partner contributions to the symbiosis

In general, *Xenorhabdus* bacteria and *Steinernema* nematodes engage in mutualism in order to complete their dual lifecycle that includes a free-living stage within the environment and a reproductive stage within the insect host (Figure 6.1). In the environment, nematodes exist as infective juveniles (IJs) that seek and invade insect hosts. This life stage is non-feeding and is responsible for vectoring the bacterial symbiont between insect hosts (16, 32, 33). Once the nematodes are inside the insect host, the nematodes release the bacterial symbiont (34, 35), and the nematodes and bacteria then kill the insect host. Nematode reproduction and bacterial growth then occurs within the insect cadaver (36). Once all nutrients have been utilized, the nematodes and bacteria form the next generation of progeny IJs (37-39). Within this lifecycle one or both partners can contribute to insect killing, production of nutrients, tissue degradation, and defense towards competing microbes, although there is likely variation among the different members of the *Steinernema* and *Xenorhabdus* genera in their requirements for and contributions to symbiosis.

Through work reported in this thesis and elsewhere, many of the contributions of partners in *X. bovienii* – *Steinernema* nematode associations have been defined. Several bacterial strains and one nematode host, *S. feltiae*, have been shown to contribute to insect

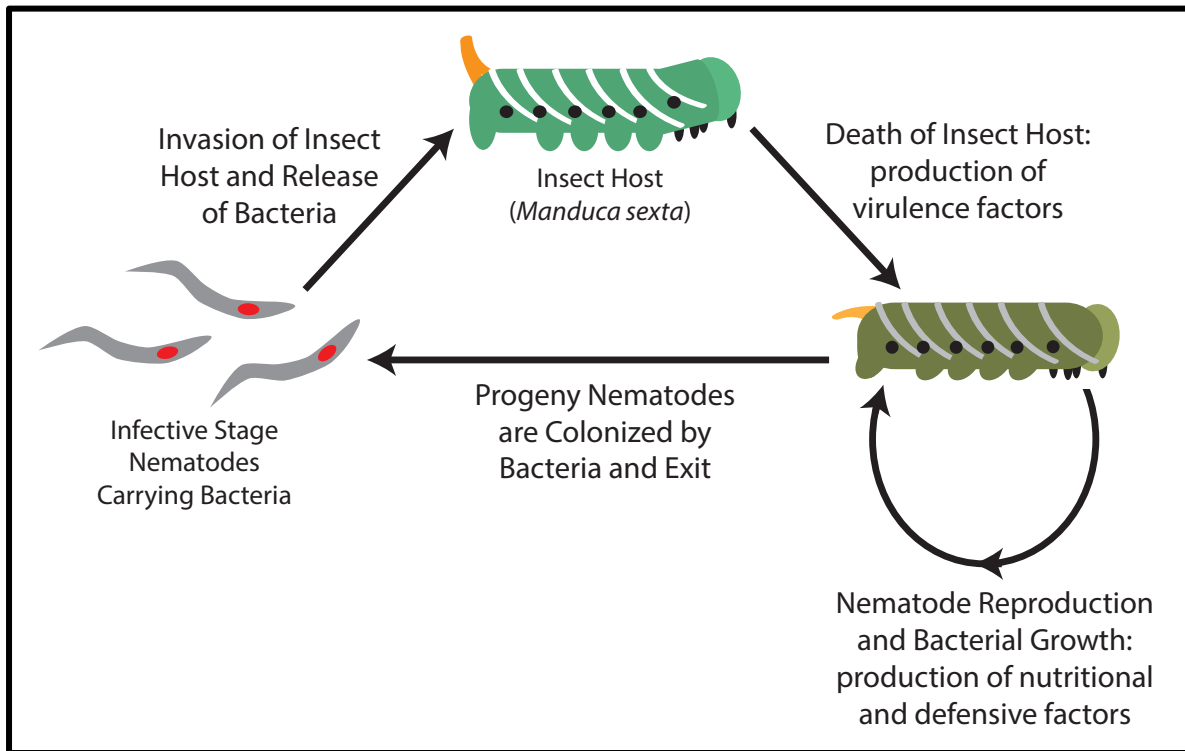


Figure 6.1 Nematode and bacterial life cycle. *Steinernema* nematodes (grey) exist in the environment in an infective stage known as the IJ, which carries the *Xenorhabdus* bacteria (red) in the intestine. IJs seek out and invade an insect host (green). The nematodes and bacteria kill the insect and reproduce in the cadaver. Once all nutrients are used, the nematodes and bacteria form the next generation of progeny IJs that exit the cadaver to seek new insects.

host killing, although the relative contributions differ among isolates (40, 41) (Chapter 2-3, Appendix 2). Insect host killing is a required step in acquiring nutrients necessary for the lifecycle. We identified many potential virulence factors in *X. bovienii* that could be contributing to insect host killing, including toxins, hemolysins, and secondary metabolites (Chapter 4). In *S. feltiae* nematodes, epicuticular lipids have been shown to be immunosuppressive (41), and potential protease virulence factors have been identified (42). Both of these likely contribute to virulence, but the identification of other factors that may contribute to the difference in virulence among isolates awaits further experimentation.

Steinernema nematodes can vary in their dependence on *Xenorhabdus* symbionts for their development and reproduction within the insect cadaver (43), ranging from entirely dependent (e.g. *S. riobrave*) to moderately dependent (e.g. *S. scapterisci*). My work indicated that *S. feltiae* nematode hosts are entirely dependent on *X. bovienii* for development within *G. mellonella* insects, as aposymbiotic nematodes did not produce progeny unless co-injected with a *X. bovienii* symbiont (Chapter 3). Another study demonstrated that an isolate of *S. feltiae* was not entirely dependent on its symbiont, although aposymbiotic reproduction of the nematodes was significantly lower than symbiotic reproduction (i.e. almost zero) (44). Differences in the studies may be due to differing nematode isolates, infection techniques, or insect sources. Growth studies also demonstrated that the *X. bovienii* physiology has a dramatic influence on development of the nematode IJ within the insect host (Chapter 2). In this novel phenotype, secondary form *X. bovienii*, although they were sufficient for nematode reproduction, were unable to support development of their *S. jolietii* hosts into the IJ life stage. These data suggest that *X. bovienii* may differentially express, depending on its phenotypic state, molecules that can promote or inhibit the development of the crucial transmission stage of its host. The identification of such molecules awaits further analysis, but could yield exciting new information about how bacteria modulate the developmental pathways of their hosts. The dependence of *S.*

jollieti IJ production on primary form *X. bovienii* is distinct from the phenotype of secondary form *X. nematophila*, which supports both reproduction and IJ development of *S. carpocapsae* nematodes in insects (45). These differences demonstrate that comparison of different *Xenorhabdus* – *Steinernema* associations will likely identify differences in symbiotic mechanisms as well as the expected similarities. Furthermore, this highlights that there is still much to learn about the exchange of molecules between hosts and symbionts with regard to types of molecules as well as expression and regulation. In addition to supporting the nutrition and development of its nematode hosts, *X. bovienii* produces a wide range of antimicrobial factors that may provide protection from competing microbes or insect scavengers that would consume the insect cadaver (46-48) (Chapter 4, Appendix 2). Together these data support the view that *X. bovienii* bacterial symbionts perform a variety of symbiotic functions for their nematode host, including nutrient provisioning, development, and protection.

Colonization of the nematode host by X. bovienii

It had been established in several *Xenorhabdus* – *Steinernema* systems that the bacterium colonizes the environmental IJ stage in order to be transmitted to subsequent generations. In the IJ, a specialized portion of the nematode intestine, known as the receptacle, houses the bacterial population. The receptacle is the intercellular space between the first few intestinal cells, anterior to the remaining collapsed intestine. Fluorescent microscopic monitoring of GFP-expressing *X. bovienii* revealed a similar colonization location in Clade III nematodes: *S. jollieti* (Chapter 1, Appendix 2), *S. puntauvense* (Appendix 1), and *S. feltiae* (Chapter 1), indicating conservation of this colonization phenotypes across all clades of nematodes so far examined. Unlike Clade II nematodes, including *S. carpocapsae* (the host of *X. nematophila*), all *X. bovienii* hosts thus far examined (from clades I and III) have an additional clear, envelope-like structure termed the vesicle within the receptacle (Appendix 2) (49). This structure may serve to

restrict bacterial growth or protect the bacteria from stress in the receptacle or during release. Further, since *X. bovienii* bacteria become free within the blood cavity of the insect host, they must have a mechanism to emerge from the vesicle, perhaps through degradation.

In addition to colonization of the IJ, my work helped establish previously unrecognized colonization events that occur within the other life stages of *S. feltiae* nematodes, including adults, juveniles, and pre-IJs (Chapter 1, Appendix 3). The bacteria were never seen in association with nematode eggs. The colonization of non-IJ life stages could function in transmission of the bacterium to progeny from adults or in transmission of the bacteria into the IJ. Alternatively, the association with non-IJ life stages may provide additional functions within the symbiosis, such as immune education (50), development (10, 51, 52), exclusion of pathogens (53), or nutrition (54, 55). Distinguishing between these possibilities will require further mechanistic studies assessing nematode immune, developmental, and nutritional pathways, as well as assessment of pathogen – nematode – symbiont interactions.

X. bovienii bacterial strain diversity

Bacteria, including those that associate with hosts, can have a tremendous amount of intra-species genetic and functional diversity (56, 57). Indeed, many pan-genomic studies of bacteria strains have determined that <50% of the genome content is shared among the bacterial strains (56-58). Similarly, as described in this thesis, *X. bovienii* bacterial symbionts that associate with various hosts also show genetic and functional diversity that impacts their ability to engage in symbiosis.

My pan-genomic analysis of nine *X. bovienii* stains revealed that 55% of the coding sequences within the genomes are shared by all strains, with 1-9% being unique to a particular strain (Chapter 3), demonstrating that *X. bovienii* strains are genetically diverse. Analyses of the unique gene sets revealed putative membrane or secreted proteins that could play role in

symbiotic functions through direct or diffusible interactions with the nematode or insect hosts. The majority of unique genes are those of unknown function, and their role in mutualism or other aspects of *X. bovienii* physiology await further experimentation. Additional genomic analyses defined a large amount of diversity in the flexible genome content (i.e. those genes found within some but not all strains) (Chapter 4). Overall, many of the mechanisms by which the bacteria likely interact with hosts (e.g. secretion systems and toxin classes) are conserved among the strains, but the regulation of proteins and the coding sequences are divergent (e.g. variation in toxin proteins and small molecule clusters). Together these data suggest that the genetic differences in *X. bovienii* strains are within the functionality and regulation of gene clusters, which may reflect a varied insect host range, different interactions with the nematode species, or differences in the encountered competitors.

In addition to genetic diversity among the bacterial strains, the ability of the bacterial strains to engage in symbiosis is also diverse. Testing of the specificity of interactions between various *X. bovienii* with *S. feltiae* showed that some strains are better able to engage in symbiotic associations with the nematode than others (44) (Chapter 3, 5). Additionally, similar trends were seen with *X. bovienii* strains interacting with different nematode host species, *S. oregonense* and *S. punctuense* (Stock personal communication). Together this supports that *X. bovienii* are genetically and functionally diverse.

PRINCIPLES OF BROAD-HOST RANGE SYMBIOSIS DETERMINED USING THE *X. BOVIENII* – *STEINERNEMA* SPP. MODEL SYSTEM

As broad host-range symbioses between animals and bacteria have yet to be extensively studied at the molecular level or with respect to evolutionary processes, there are many remaining questions about general principles, such as how the partners identify each other, if and how the symbioses are maintained over evolutionary time, how bacterial strain

variability impacts various symbiotic functions (e.g. fitness, transmission and maintenance), and how strain variability may impact host competition and health. To begin to address just a few of these questions, I utilized the *X. bovienii* – *Steinernema* system.

Differences in microbial symbionts affect host health due to coadaptation

How hosts are affected by differences in symbiont strains is beginning to be defined in a number of different symbioses. Within plant – *Rhizobium* mutualism it has been defined that host genotype x symbiont genotype differences occur in symbiotic success (59). Furthermore, numerous studies are revealing that microbial communities impact animal host health, although the contributions of individual microbial species or strains have not been established conclusively (60).

Previous work using the *X. bovienii* – *Steinernema* associations demonstrated that the bacterial strain identity can affect symbiotic success (44). Supporting this, we observed differences in several fitness parameters, including the number of progeny produced and the health of the progeny (Chapter 3). These differences also correlated with the bacterial and nematode phylogenetic framework, suggesting that fitness benefit differences may reflect coadaptation between hosts and symbionts. As symbiont-dependent differences in host health has been shown in various systems, it seems likely that fitness benefit differences based on coadaptation between hosts and symbionts occurs in a broad array of symbioses. However, the generalizability of this principle to other mutualisms awaits further analyses. This finding also raises further questions about how broad host-range symbioses are maintained over evolutionary time in order for co-adaptation to occur. There are several different mechanisms that could occur to facilitate partner maintenance, such as partner selection and partner fidelity feedback. These ideas are addressed in the next section.

Variation in bacterial symbiont strains impacts symbiotic maintenance

How broad host-range symbioses are maintained in the environment and over evolutionary time scales is a long debated question, as partner switching may occur. The potential for host switching is due to the symbiont species having the ability to associate with several different hosts. Several theories have been proposed to explain how broad host-range symbioses may occur, but there has been little experimental evidence to support any theory.

One theory for mutualism stability is partner selection (PS), where the host is able to select its particular symbiont isolate out of a pool of potential partners, including bacterial strains of the same species (61). The host would be able to select its native symbiont so that hybrid pairs (i.e. the host with a non-native symbiont) did not occur. Selection of symbionts has been shown in of some symbioses, such as the squid-*Vibrio* system, where native symbiont strains are better able to colonize the host (62, 63). However, colonization by non-native symbionts can occur, and it is unclear if there are selective pressures in place to favor the native combinations and remove such hybrid colonization.

Another theory to explain how native pairs are favored over hybrid pairs is the theory of partner fidelity feedback (PFF) (64). PFF states that the benefits of particular symbiont pairs will allow them to outcompete less ideal pairs through natural selection, therefore feeding-back to stabilize the symbiosis. This theory was originally developed to explain how cheating (i.e. one partner does not provide the symbiotic benefits but still receives them) may be removed from symbioses, but we can extend this theory to explain how native symbiont pairs may be favored over non-native pairs. When host switching occurs, the hosts that associate with the native symbiont receive more benefits and reproduce better than those hosts that associate with non-native pairs. Therefore, the native pairs are able to outcompete the non-native pairs for resources, and the non-native pairs are removed through natural selection.

Using the model association between *X. bovienii* strains and *Steinernema* nematode hosts, I obtained experimental evidence to support the theory of PFF (Chapter 3). I demonstrated that native pairs of nematode hosts and symbionts received more benefits than non-native pairs. Additionally, the relative symbiotic success of the pairs was correlated to the phylogenetic framework, suggesting that coevolution and co-adaptation between the nematodes and bacterial strains had occurred. Furthermore, all of the bacterial strains that were able to engage in symbiosis could colonize the nematode host, and in the life cycle opportunities for host switching occur. Together these data support that while host switching is possible, particular nematode – bacterial pairs are maintained over an evolutionary timescale, which may be due to the increased benefits of native pairs over non-native pairs. Further studies would be necessary to if PS and PFF mechanisms work in concert or occur only separately to maintain symbiotic pairs.

Competition between hosts can be affected by bacterial symbionts

As resources in the environment are limiting, competition is an important driver of the ecology and evolution of organisms. Bacterial symbionts likely influence competition between hosts, as host health is affected by their contributions. Additionally bacterial symbionts can affect host competition through inhibition of a competitor's bacterial symbiont (65). I identified an additional role for bacterial symbionts: conferring a competitive advantage to the host by inhibiting a competing organism through an infection-mediated process (Chapter 5).

In competition experiments, I demonstrated that the bacterial symbiont of *S. affine* is both necessary and sufficient to enable *S. affine* to outcompete *S. feltiae* (Chapter 5). I also show that this competitive advantage likely is due to the bacterial symbiont inhibiting the competing nematode host, and that the bacterium is able to kill the competitor through infection. Data from this study and others suggests that this may be a conserved mechanism for

competition between clade I and clade III *Steinernema* nematodes (24, 44, 66). However, the outcome of competition differs when different nematode isolates and species are used, suggesting potential variation in mechanism or susceptibility. Assessing the differences in general mechanism among these partner pairs (e.g. survival assays and microscopy of different combinations) would determine if mechanism and/or susceptibility differ. Such information would be useful to determine not only the general applicability of mechanisms discovered but also to assess if study of multiple isolates would uncover novel mechanisms and interactions.

While the yet-to-be-determined molecular mechanisms underlying the competition are likely specific to *Xenorhabdus* – *Steinernema* associations, my findings have revealed an unexpected way in which bacterial symbionts can contribute to competitive outcomes, and this phenomenon is likely at play in any environment where competition is occurring. This symbiont-mediated killing of competitors could occur within other symbioses where the symbiont can be externally localized with respect to its host and come into contact with potential competitors, such as in the association between *Helicobacter* spp. bacteria and the human-parasitic liver fluke *Opisthorchis viverrini* (67, 68). Alternately, symbiont-mediated killing could occur in other contexts, such as when internal bacterial symbionts of host encounter an internal parasite of their host (e.g. intestinal microbiota and intestinal parasites).

FUTURE DIRECTIONS

As summarized above, investigating the *X. bovienii* – *Steinernema* spp. symbiosis has helped answer questions surrounding broad-host range symbiotic associations. However, further studies are necessary to fully elucidate the mechanisms underlying the observed partner fidelity feedback, colonization processes, and partner contributions to symbiosis. Additionally, this system is now poised to tackle additional remaining questions pertaining to broad host-range symbiosis. These applications are detailed below.

The relative contributions of PFF and PS

In chapter 3, specificity testing suggested that PFF plays a role in stability of mutualistic associations over evolutionary time. Studies within the squid – *Vibrio* system suggest that PS between host species and bacterial strains can also facilitate symbiosis stability (62, 63). It seems likely that both mechanisms could function within the same system to contribute to stability of individual partner pairs, though the potential relative contributions of each phenomenon are unclear. The association between *X. bovienii* bacteria and *Steinernema* nematodes would be ideal to address these questions as many generations of nematodes and symbionts can be grown in competitive conditions within the laboratory environment. Such a study would first require assays to ensure that colonization differences exist with the system. Native and non-native bacterial strains could be engineered with different selectable markers for competitive colonization testing in nematode hosts. Populations of nematodes colonized by the native and non-native strains could then be grown together to assess if the nematode population was more frequently colonized by one strain. Ideally, competitive colonization differences could be assessed between strains with PS differences only, PFF differences only, and both PS and PFF differences. Comparisons between these conditions would provide information as to how these selective pressures may contribute to stability of partner pairs separately or in combination.

Use of X. bovienii strains for the discovery of novel bioactive compounds

Comparative genomic analyses of the *X. bovienii* strains in Chapter 4 demonstrated that the bacterial strains show potential for the discovery of bioactive compounds. Some of these gene classes have a clear application purpose, such as the toxins that could be used for insect pest control. However, others, such as clusters encoding small molecule biosynthetic machinery, will require further functional analysis to determine their activity and potential

application. It is likely that many of these clusters will be antibiotics, toxins or other useful compounds, such as immunosuppressants (69). Future studies could functionally characterize the variety of compounds and determine their potential applications.

Bacterial molecular mechanisms of non-native host killing

In chapter 5, survival and microscopy studies support that the *X. bovienii* bacterial symbiont of *S. affine* kills *S. feltiae* nematodes through an infection-mediated process. This killing likely involves the nematode intestine in some way. Although we know the response of the nematode to this killing process, the molecular mechanisms of pathogenesis are unknown. Elucidation of these mechanisms has potential applications in biotechnology through the development of nematicidal compounds for the control of agricultural nematode pests and human pathogenic nematodes. Further work will be necessary to determine which bacterial genes contribute to pathogenesis as well as functional studies to assess if the discovered compounds may have useful applications.

Other unanswered questions

In addition to these specific follow-up lines of inquiry, the *X. bovienii* bacterial strain – *Steinernema* spp. model has much potential for the study of other unexplored areas surrounding broad host-range symbiosis including elucidating the diversity, specificity, and evolution of colonization determinants, the coevolution of host and symbiont genomes compared with specialized symbioses, the mechanisms of co-speciation, and the frequency of host switching.

CONCLUSIONS

The association between *X. bovienii* bacteria and *Steinernema* nematodes has been well developed into a useful model system for understanding broad host-range symbioses. Already, the system has revealed new general principles, provided support to previously identified principles, and demonstrated experimental support for a suggested theory. If further developed, the model system has the potential to greatly advance our knowledge of broad host-range symbioses and their impact on the ecology and evolution of organisms.

REFERENCES

1. **Bhasin A, Chaston JM, Goodrich-Blair H.** 2012. Mutational analyses reveal overall topology and functional regions of NilB, a bacterial outer membrane protein required for host association in a model of animal-microbe mutualism. *J Bacteriol* **194**:1763-1776.
2. **Heungens K, Cowles CE, Goodrich-Blair H.** 2002. Identification of *Xenorhabdus nematophila* genes required for mutualistic colonization of *Steinernema carpocapsae* nematodes. *Mol Microbiol* **45**:1337-1353.
3. **Cowles CE, Goodrich-Blair H.** 2008. The *Xenorhabdus nematophila* nilABC genes confer the ability of *Xenorhabdus* spp. to colonize *Steinernema carpocapsae* nematodes. *J Bacteriol* **190**:4121-4128.
4. **Chavez-Dozal AA, Gorman C, Lostroh CP, Nishiguchi MK.** 2014. Gene-swapping mediates host specificity among symbiotic bacteria in a beneficial symbiosis. *PLoS One* **9**:e101691.
5. **Mandel MJ, Wollenberg MS, Stabb EV, Visick KL, Ruby EG.** 2009. A single regulatory gene is sufficient to alter bacterial host range. *Nature* **458**:215-218.
6. **Faucher C, Maillet F, Vasse J, Rosenberg C, van Brussel AA, Truchet G, Denarie J.** 1988. *Rhizobium meliloti* host range *nodH* gene determines production of an alfalfa-specific extracellular signal. *J Bacteriol* **170**:5489-5499.
7. **Kondorosi E, Banfalvi Z, Kondorosi A.** 1984. Physical and genetic analysis of a symbiotic region of *Rhizobium meliloti*: Identification of nodulation genes. *Molecular and General Genetics* **193**:445-452.
8. **Frese SA, Benson AK, Tannock GW, Loach DM, Kim J, Zhang M, Oh PL, Heng NC, Patil PB, Juge N, Mackenzie DA, Pearson BM, Lapidus A, Dalin E, Tice H, Goltsman E, Land M, Hauser L, Ivanova N, Kyrpidis NC, Walter J.** 2011. The evolution of host specialization in the vertebrate gut symbiont *Lactobacillus reuteri*. *PLoS Genet* **7**:e1001314.
9. **Lee SM, Donaldson GP, Mikulski Z, Boyajian S, Ley K, Mazmanian SK.** 2013. Bacterial colonization factors control specificity and stability of the gut microbiota. *Nature* **501**:426-429.
10. **Chaston J, Goodrich-Blair H.** 2010. Common trends in mutualism revealed by model associations between invertebrates and bacteria. *FEMS Microbiol Rev* **34**:41-58.
11. **Tarasco E, Clausi M, Rappazzo G, Panzavolta T, Curto G, Sorino R, Oreste M, Longo A, Leone D, Tiberi R, Vinciguerra MT, Triggiani O.** 2014. Biodiversity of entomopathogenic nematodes in Italy. *J Helminthol*
doi:10.1017/S0022149X14000194:1-8.
12. **Valadas V, Mracek Z, Oliveira S, Mota M.** 2011. Three species of entomopathogenic nematodes of the family Steinernematidae (Nematoda: Rhabditida) new to continental Portugal. *Nematologia Mediterranea* **39**:169-178.

13. **Chaston JM, Suen G, Tucker SL, Andersen AW, Bhasin A, Bode E, Bode HB, Brachmann AO, Cowles CE, Cowles KN, Darby C, de Leon L, Drace K, Du Z, Givaudan A, Herbert Tran EE, Jewell KA, Knack JJ, Krasomil-Osterfeld KC, Kukor R, Lanois A, Latreille P, Leimgruber NK, Lipke CM, Liu R, Lu X, Martens EC, Marri PR, Medigue C, Menard ML, Miller NM, Morales-Soto N, Norton S, Ogier JC, Orchard SS, Park D, Park Y, Qurollo BA, Sugar DR, Richards GR, Rouy Z, Slominski B, Slominski K, Snyder H, Tjaden BC, van der Hoeven R, Welch RD, Wheeler C, Xiang B, Barbazuk B, et al.** 2011. The entomopathogenic bacterial endosymbionts *Xenorhabdus* and *Photorhabdus*: convergent lifestyles from divergent genomes. *PLoS One* **6**:e27909.
14. **Latreille P, Norton S, Goldman BS, Henkhaus J, Miller N, Barbazuk B, Bode HB, Darby C, Du Z, Forst S, Gaudriault S, Goodner B, Goodrich-Blair H, Slater S.** 2007. Optical mapping as a routine tool in bacterial genome sequencing. *BMC Genomics* **8**:321.
15. **Gualtieri M, Ogier JC, Pages S, Givaudan A, Gaudriault S.** 2014. Draft genome sequence and annotation of the entomopathogenic bacterium *Xenorhabdus szentirmaii* strain DSM16338. *Genome Announc* **2**.
16. **Chaston JM, Murfin KE, Heath-Heckman EA, Goodrich-Blair H.** 2013. Previously unrecognized stages of species-specific colonization in the mutualism between *Xenorhabdus* bacteria and *Steinernema* nematodes. *Cell Microbiol* **15**:1545-1559.
17. **Veesenmeyer JL, Andersen AW, Lu X, Hussa EA, Murfin KE, Chaston JM, Dillman AR, Wassarman KM, Sternberg PW, Goodrich-Blair H.** 2014. NiID CRISPR RNA contributes to *Xenorhabdus nematophila* colonization of symbiotic host nematodes. *Mol Microbiol* **93**:1026-1042.
18. **Lee MM, Stock SP.** 2010. A multilocus approach to assessing co-evolutionary relationships between *Steinernema* spp. (Nematoda: Steinernematidae) and their bacterial symbionts *Xenorhabdus* spp. (gamma-Proteobacteria: Enterobacteriaceae). *Syst Parasitol* **77**:1-12.
19. **Tailliez P, Laroui C, Ginibre N, Paule A, Pages S, Boemare N.** 2010. Phylogeny of *Photorhabdus* and *Xenorhabdus* based on universally conserved protein-coding sequences and implications for the taxonomy of these two genera. Proposal of new taxa: *X. vietnamensis* sp. nov., *P. luminescens* subsp. caribbeanensis subsp. nov., *P. luminescens* subsp. hainanensis subsp. nov., *P. temperata* subsp. kharii subsp. nov., *P. temperata* subsp. tasmaniensis subsp. nov., and the reclassification of *P. luminescens* subsp. thracensis as *P. temperata* subsp. thracensis comb. nov. *Int J Syst Evol Microbiol* **60**:1921-1937.
20. **Tailliez P, Pages S, Edgington S, Tymo LM, Buddie AG.** 2011. Description of *Xenorhabdus magdalenensis* sp. nov., the symbiotic bacterium associated with *Steinernema australe*. *Int J Syst Evol Microbiol* doi:10.1099/ijs.0.034322-0.
21. **Nguyen KB.** 11/16/11 2010. Morphology and taxonomy of entomopathogenic nematodes. <http://entnem.ifas.ufl.edu/nguyen/morph/namespp.HTM>. Accessed

22. **Stock SP, Goodrich-Blair H.** 2012. Nematode parasites, pathogens and associates of insects and invertebrates of economic importance, p 375-425. *In* Lacey LA (ed), *Manual of Techniques in Invertebrate Pathology*, 2 ed. Elsevier Press.
23. **Stock SP, Goodrich-Blair H.** 2008. Entomopathogenic nematodes and their bacterial symbionts: the inside out of a mutualistic association. *Symbiosis* **46**:65-75.
24. **Lee MM, Stock SP.** 2010. A multigene approach for assessing evolutionary relationships of *Xenorhabdus* spp. (gamma-Proteobacteria), the bacterial symbionts of entomopathogenic *Steinernema* nematodes. *J Invertebr Pathol* **104**:67-74.
25. **Moulin L, Klonowska A, Caroline B, Booth K, Vriezen JA, Melkonian R, James EK, Young JP, Bena G, Hauser L, Land M, Kyrpides N, Bruce D, Chain P, Copeland A, Pitluck S, Woyke T, Lizotte-Waniewski M, Bristow J, Riley M.** 2014. Complete genome sequence of *Burkholderia phymatum* STM815(T), a broad host range and efficient nitrogen-fixing symbiont of *Mimosa* species. *Stand Genomic Sci* **9**:763-774.
26. **Rogel MA, Bustos P, Santamaria RI, Gonzalez V, Romero D, Cevallos MA, Lozano L, Castro-Mondragon J, Martinez-Romero J, Ormeno-Orrillo E, Martinez-Romero E.** 2014. Genomic basis of symbiovar mimosae in *Rhizobium etli*. *BMC Genomics* **15**:575.
27. **Rogel MA, Ormeno-Orrillo E, Martinez Romero E.** 2011. Symbiovars in rhizobia reflect bacterial adaptation to legumes. *Syst Appl Microbiol* **34**:96-104.
28. **Teamtisong K, Songwattana P, Noisangiam R, Piromyou P, Boonkerd N, Tittabutr P, Minamisawa K, Nantagij A, Okazaki S, Abe M, Uchiumi T, Teaumroong N.** 2014. Divergent nod-containing *Bradyrhizobium* sp. DOA9 with a megaplasmid and its host range. *Microbes Environ.*
29. **Tonk L, Sampayo EM, Weeks S, Magno-Canto M, Hoegh-Guldberg O.** 2013. Host-specific interactions with environmental factors shape the distribution of symbiodinium across the Great Barrier Reef. *PLoS One* **8**:e68533.
30. **Nishiguchi MK, Nair VS.** 2003. Evolution of symbiosis in the Vibrionaceae: a combined approach using molecules and physiology. *Int J Syst Evol Microbiol* **53**:2019-2026.
31. **D'Aimmo MR, Modesto M, Mattarelli P, Biavati B, Andlid T.** 2014. Biosynthesis and cellular content of folate in bifidobacteria across host species with different diets. *Anaerobe* **30**:169-177.
32. **Martens EC, Heungens K, Goodrich-Blair H.** 2003. Early colonization events in the mutualistic association between *Steinernema carpocapsae* nematodes and *Xenorhabdus nematophila* bacteria. *J Bacteriol* **185**:3147-3154.
33. **Sugar DR, Murfin KE, Chaston JM, Andersen AW, Richards GR, deLeon L, Baum JA, Clinton WP, Forst S, Goldman BS, Krasomil-Osterfeld KC, Slater S, Stock SP, Goodrich-Blair H.** 2012. Phenotypic variation and host interactions of *Xenorhabdus bovienii* SS-2004, the entomopathogenic symbiont of *Steinernema jolietii* nematodes. *Environ Microbiol* **14**:924-939.

34. **Poinar GOJ, Thomas GM.** 1966. Significance of *Achromobacter nematophilus* Poinar and Thomas (Achromobacteraceae: Eubacteriales) in the development of the nematode, DD-136 (*Neoaplectana* sp. Steinernematidae). *Parasitology* **56**:385-390.
35. **Snyder H, Stock SP, Kim SK, Flores-Lara Y, Forst S.** 2007. New insights into the colonization and release processes of *Xenorhabdus nematophila* and the morphology and ultrastructure of the bacterial receptacle of its nematode host, *Steinernema carpocapsae*. *Appl Environ Microbiol* **73**:5338-5346.
36. **Wang J, Bedding RA.** 1996. Population development of *Heterorhabditis bacteriophora* and *Steinernema carpocapsae* in the larvae of *Galleria mellonella*. *Fundamental and Applied Nematology* **19**:363-367.
37. **Kaplan F, Alborn HT, von Reuss SH, Ajredini R, Ali JG, Akyazi F, Stelinski LL, Edison AS, Schroeder FC, Teal PE.** 2012. Interspecific nematode signals regulate dispersal behavior. *PLoS One* **7**:e38735.
38. **San-Blas E, Gowen SR, Pembroke B.** 2008. *Steinernema feltiae*: ammonia triggers the emergence of their infective juveniles. *Exp Parasitol* **119**:180-185.
39. **San-Blas E, Pirela D, Garcia D, Portillo E.** 2014. Ammonia concentration at emergence and its effects on the recovery of different species of entomopathogenic nematodes. *Exp Parasitol* **144**:1-5.
40. **Ehlers RU, Wulff A, Peters A.** 1997. Pathogenicity of axenic *Steinernema feltiae*, *Xenorhabdus bovienii*, and the bacto-helminthic complex to larvae of *Tipula oleracea* (Diptera) and *Galleria mellonella* (Lepidoptera). *J Invertebr Pathol* **69**:212-217.
41. **Brivio MF, Moro M, Mastore M.** 2006. Down-regulation of antibacterial peptide synthesis in an insect model induced by the body-surface of an entomoparasite (*Steinernema feltiae*). *Dev Comp Immunol* **30**:627-638.
42. **Balasubramanian N, Toubarro D, Nascimento G, Ferreira R, Simoes N.** 2012. Purification, molecular characterization and gene expression analysis of an aspartic protease (Sc-ASP113) from the nematode *Steinernema carpocapsae* during the parasitic stage. *Mol Biochem Parasitol* **182**:37-44.
43. **Sicard M, Le Brun N, Pages S, Godelle B, Boemare N, Moulia C.** 2003. Effect of native *Xenorhabdus* on the fitness of their *Steinernema* hosts: contrasting types of interaction. *Parasitol Res* **91**:520-524.
44. **Chapuis E, Emelianoff V, Paulmier V, Le Brun N, Pages S, Sicard M, Ferdy JB.** 2009. Manifold aspects of specificity in a nematode-bacterium mutualism. *J Evol Biol* **22**:2104-2117.
45. **Sicard M, Tabart J, Boemare NE, Thaler O, Moulia C.** 2005. Effect of phenotypic variation in *Xenorhabdus nematophila* on its mutualistic relationship with the entomopathogenic nematode *Steinernema carpocapsae*. *Parasitology* **131**:687-694.
46. **Fang XL, Han LR, Cao XQ, Zhu MX, Zhang X, Wang YH.** 2012. Statistical optimization of process variables for antibiotic activity of *Xenorhabdus bovienii*. *PLoS One* **7**:e38421.

47. **Fang XL, Li ZZ, Wang YH, Zhang X.** 2011. In vitro and in vivo antimicrobial activity of *Xenorhabdus bovienii* YL002 against *Phytophthora capsici* and *Botrytis cinerea*. *J Appl Microbiol* **111**:145-154.
48. **Morales-Soto N, Gaudriault S, Ogier JC, Thappeta KR, Forst S.** 2012. Comparative analysis of P2-type remnant prophage loci in *Xenorhabdus bovienii* and *Xenorhabdus nematophila* required for xenorhabdicolin production. *FEMS Microbiol Lett* **333**:69-76.
49. **Kim SK, Flores-Lara Y, Patricia Stock S.** 2012. Morphology and ultrastructure of the bacterial receptacle in *Steinernema* nematodes (Nematoda: Steinernematidae). *J Invertebr Pathol* **110**:366-374.
50. **Kandasamy S, Chattha KS, Vlasova AN, Rajashekara G, Saif LJ.** 2014. Lactobacilli and Bifidobacteria enhance mucosal B cell responses and differentially modulate systemic antibody responses to an oral human rotavirus vaccine in a neonatal gnotobiotic pig disease model. *Gut Microbes* doi:10.4161/19490976.2014.969972:0.
51. **Bennuru S, Meng Z, Ribeiro JM, Semnani RT, Ghedin E, Chan K, Lucas DA, Veenstra TD, Nutman TB.** 2011. Stage-specific proteomic expression patterns of the human filarial parasite *Brugia malayi* and its endosymbiont *Wolbachia*. *Proceedings of the National Academy of Sciences of the United States of America* **108**:9649-9654.
52. **Bouskra D, Brezillon C, Berard M, Werts C, Varona R, Boneca IG, Eberl G.** 2008. Lymphoid tissue genesis induced by commensals through NOD1 regulates intestinal homeostasis. *Nature* **456**:507-510.
53. **Reid G, Bruce AW, McGroarty JA, Cheng KJ, Costerton JW.** 1990. Is there a role for lactobacilli in prevention of urogenital and intestinal infections? *Clin Microbiol Rev* **3**:335-344.
54. **Prell J, Bourdes A, Kumar S, Ludwig E, Hosie A, Kinghorn S, White J, Poole P.** 2010. Role of symbiotic auxotrophy in the *Rhizobium*-legume symbioses. *PLoS One* **5**:e13933.
55. **Salem H, Bauer E, Strauss AS, Vogel H, Marz M, Kaltenpoth M.** 2014. Vitamin supplementation by gut symbionts ensures metabolic homeostasis in an insect host. *Proc Biol Sci* **281**.
56. **Galardini M, Mengoni A, Brilli M, Pini F, Fioravanti A, Lucas S, Lapidus A, Cheng JF, Goodwin L, Pitluck S, Land M, Hauser L, Woyke T, Mikhailova N, Ivanova N, Daligault H, Bruce D, Detter C, Tapia R, Han C, Teshima H, Mocali S, Bazzicalupo M, Biondi EG.** 2011. Exploring the symbiotic pangenome of the nitrogen-fixing bacterium *Sinorhizobium meliloti*. *BMC Genomics* **12**:235.
57. **Hansen EE, Lozupone CA, Rey FE, Wu M, Guruge JL, Narra A, Goodfellow J, Zaneveld JR, McDonald DT, Goodrich JA, Heath AC, Knight R, Gordon JI.** 2011. Pan-genome of the dominant human gut-associated archaeon, *Methanobrevibacter smithii*, studied in twins. *Proc Natl Acad Sci U S A* **108 Suppl 1**:4599-4606.

58. **D'Auria G, Jimenez-Hernandez N, Peris-Bondia F, Moya A, Latorre A.** 2010. *Legionella pneumophila* pangenome reveals strain-specific virulence factors. *BMC Genomics* **11**:181.
59. **Heath KD.** 2010. Intergenomic epistasis and coevolutionary constraint in plants and rhizobia. *Evolution* **64**:1446-1458.
60. **McFall-Ngai M, Hadfield MG, Bosch TC, Carey HV, Domazet-Loso T, Douglas AE, Dubilier N, Eberl G, Fukami T, Gilbert SF, Hentschel U, King N, Kjelleberg S, Knoll AH, Kremer N, Mazmanian SK, Metcalf JL, Nealson K, Pierce NE, Rawls JF, Reid A, Ruby EG, Rumpho M, Sanders JG, Tautz D, Wernegreen JJ.** 2013. Animals in a bacterial world, a new imperative for the life sciences. *Proc Natl Acad Sci U S A* **110**:3229-3236.
61. **Douglas AE.** 2008. Conflict, cheats and the persistence of symbioses. *New Phytol* **177**:849-858.
62. **Nishiguchi MK.** 2002. Host-symbiont recognition in the environmentally transmitted sepiolid squid-*Vibrio* mutualism. *Microb Ecol* **44**:10-18.
63. **Nishiguchi MK, Ruby EG, McFall-Ngai MJ.** 1998. Competitive dominance among strains of luminous bacteria provides an unusual form of evidence for parallel evolution in Sepiolid squid-*Vibrio* symbioses. *Appl Environ Microbiol* **64**:3209-3213.
64. **Weyl EG, Frederickson ME, Yu DW, Pierce NE.** 2010. Economic contract theory tests models of mutualism. *Proc Natl Acad Sci U S A* **107**:15712-15716.
65. **Morales-Soto N, Forst SA.** 2011. The xnp1 P2-like tail synthesis gene cluster encodes xenorhabdycin and is required for interspecies competition. *J Bacteriol* **193**:3624-3632.
66. **Půža V, Mracek Z.** 2009. Mixed infection of *Galleria mellonella* with two entomopathogenic nematode (Nematoda: Rhabditida) species: *Steinernema affine* benefits from the presence of *Steinernema kraussei*. *J Invertebr Pathol* **102**:40-43.
67. **Deenonpoe R, Chomvarin C, Pairojkul C, Chamgramol Y, Loukas A, Brindley PJ, Sripa B.** 2015. The carcinogenic liver fluke *Opisthorchis viverrini* is a reservoir for species of *Helicobacter*. *Asian Pac J Cancer Prev* **16**:1751-1758.
68. **Foster JR.** 1984. Bacterial infection of the common bile duct in chronic fascioliasis in the rat. *J Comp Pathol* **94**:175-181.
69. **Schwecke T, Aparicio JF, Molnar I, Konig A, Khaw LE, Haydock SF, Oliynyk M, Caffrey P, Cortes J, Lester JB, et al.** 1995. The biosynthetic gene cluster for the polyketide immunosuppressant rapamycin. *Proc Natl Acad Sci U S A* **92**:7839-7843.

APPENDIX 1

Identification of bacterial colonization in nematodes using florescent microscopy

This appendix has been published as:

Murfin KE, Chaston J, and Goodrich-Blair, H. "Visualizing bacteria in nematodes using fluorescence microscopy." *J Vis Exp.* 2012 Oct 19;(68). doi: 10.3791/4298.

SHORT ABSTRACT

To study the mutualism between *Xenorhabdus* bacteria and *Steinernema* nematodes, methods were developed to monitor bacterial presence and location within nematodes. The experimental approach, which can be applied to other systems, entails engineering bacteria to express the green fluorescent protein and visualizing, using fluorescence microscopy bacteria within the transparent nematode.

LONG ABSTRACT

Symbioses, the living together of two or more organisms, are widespread throughout the all kingdoms of life. As two of the most ubiquitous organisms on earth, nematodes and bacteria form a wide array of symbiotic associations that range from beneficial to pathogenic or parasitic (1-3). One such association is the mutually beneficial relationship between *Xenorhabdus* bacteria and *Steinernema* nematodes, which has emerged as a model system of symbiosis (4). *Steinernema* nematodes are entomopathogenic, utilizing their bacterial symbiont to kill insects (5). For transmission between insect hosts, the bacteria colonize the intestine of the nematode's infective juvenile stage (6). Recently, several other nematode species have been shown to utilize bacteria to kill insects (7-11) and investigations have turned toward examining the interactions between the nematodes and bacteria in these systems (11).

We describe a method for visualization of a bacterial symbiont within or on a nematode host, taking advantage of the optical transparency of nematodes when viewed by microscopy. The bacteria are engineered to express a fluorescent protein, allowing their visualization by fluorescence microscopy. A variety of plasmids are available that carry genes encoding proteins that fluoresce at different wavelengths (e.g. green or red). Conjugation of such plasmids from a donor *Escherichia coli* strain into the recipient bacterial symbiont is successful for a broad range of recipient bacteria. The gene encoding the fluorescent protein can be expressed from a self-

replicating plasmid, or more stably by integration into the chromosome. The methods described were developed to investigate the association between *Steinernema carpocapsae* nematodes and *Xenorhabdus nematophila* bacteria (12). Similar methods have been used to investigate other nematode-bacterium associations (11, 13-16) and the approach therefore is generally applicable.

The method allows characterization of bacterial presence and localization within nematodes at different stages of development, providing insights into the nature of the association and the process of colonization (12, 15, 17). Microscopic analysis reveals both colonization frequency within a population (i.e. are individuals colonized or not) and distribution of colonizing bacteria to specific host tissues (12, 15, 17-19). This is an advantage over other methods of monitoring bacteria within nematode populations, such as sonication (20) or grinding (21), which can provide information about average levels of colonization, but may not, for example, discriminate populations with a high frequency of low colonization from populations with a low frequency of high colonization. Discriminating the frequency and load of colonizing bacteria can be especially important when screening or characterizing bacterial mutants for negative colonization phenotypes. Indeed, fluorescence microscopy has been used in high throughput screening of bacterial mutants for defects in colonization (13, 16), and is less laborious than previously used methods including sonication (20) and individual nematode dissection (22).

PROTOCOL TEXT**1) Construction of a fluorescent bacterial strain via conjugation**

1.1) Grow the recipient strain (symbiont to be screened) and the donor strain overnight. The donor strain, usually *Escherichia coli* should be capable of donating DNA through conjugation and should be transformed with a plasmid (Table A1.2) that carries a gene encoding a fluorescent protein. Depending on the plasmid, a helper strain may also be required. If so, this strain should also be grown overnight. The donor strain and helper strain should be grown with antibiotics to select for maintenance of the plasmid.

1.2) Subculture the donor, helper, and recipient strains into nutrient rich growth media lacking antibiotics in a 1:100 dilution.

1.3) Grow the cultures at the temperature appropriate for each strain until they reach mid-log stage growth ($OD_{600} \sim 0.6$). For *Xenorhabdus* and *E. coli* this stage of growth is reached approximately 3 to 4 hours after subculturing. This may vary on the strain, or in some cases the plasmid used

1.4) Mix the strains in a microcentrifuge tube and centrifuge for 2min at 17,900 X g (13000 rpm in most microfuges). The proportion of donor and recipient that yields best results will vary for different combinations, and may have to be empirically determined. For a *Xenorhabdus* recipient and *E. coli* donor, we use a 3:1 or 1:1 ratio. If a helper strain is needed (e.g. *E. coli*), it should be added in the same ratio as the donor.

1.5) Decant the supernatant.

- 1.6) Re-suspend the cell pellet in 30 μ l of fresh media.
- 1.7) Spot the suspension onto a nutrient rich media plate without any antibiotics, and allow the spot to dry.
- 1.8) Incubate the plate, inverted, overnight at a temperature optimal for the recipient bacterium and permissible for the donor (and helper, if applicable). The plate should be incubated at least 18 hr.
- 1.9) Scrape up the spot and streak for single colonies on a selective antibiotic plate. The antibiotics should select against the donor and for the recipient containing the plasmid. One or two additional isolation streaks may be necessary to isolate a pure culture.
- 1.10) Ensure the resulting colonies are the recipient symbiont, and not the donor strain, by screening for the presence of recipient specific phenotypes, such as colony morphology, or polymerase chain reaction detection of recipient-specific genes. Screen the colonies for presence of the plasmid by polymerase chain reaction of a known plasmid sequence and fluorescence. The colonies should fluoresce under the correct wavelength corresponding to the fluorescent protein.

2) Production of axenic nematode eggs

- 2.1) Grow 5 mL the natural bacterial symbiont overnight.

2.2) Spread 600 μ l of the bacterial culture onto 10 mm Lipid Agar plates (23). 8 to 10 plates will yield enough nematodes for most species.

2.3) Incubate in the dark without moisture at 25°C for two days.

2.4) Add 5,000 infective juvenile nematodes, or other stages depending on the nematode being used, in 500 μ l to the bacterial lawns. Incubate the plates at 25°C for 3 days.

2.5) Check your plates for the presence of adult nematodes and eggs. The adult nematodes will be large and easily visible to your eyes. Place 20 μ l of water onto a microscope slide. Using a sterile stick scrape-up a small amount of nematodes from the bacterial lawn. Place the stick into the water and allow the nematodes to swim off. Look at your slide under low magnification. For more information on appearance see the discussion and Figure A1.2.

2.6) If eggs and females are visible, continue; otherwise, continue to incubate the plates at 25°C and check for proper development every 6-12 hours. When females contain eggs, place a few ml of water on the surface of the plates. Gently swirl the plates and pour the water into a 50 ml conical tube. Nematodes should come off of the plates and no longer be visible on the plate surface. Several rinses may be necessary to harvest all the nematodes.

2.7) Allow the nematodes to settle to the bottom of the tube.

2.8) Rinse nematodes. Pipette off the excess water from the top of the tube. Refill with clean water and allow adult nematodes to settle. Pipette off the excess water.

2.9) Fill the conical tubes with egg solution. Once egg solution is added the timing of all steps with egg solution must proceed exactly as described for maximum egg yield. Incubate the tubes while gently shaking for exactly 10 minutes. Most nematodes should be dissolved by the end of the incubation.

2.10) Immediately centrifuge the conical tubes at 1250 X g for exactly 10 minutes (this includes bringing the centrifuge up to speed but not to 0 x g. Use the brake.

2.11) Immediately decant the supernatant.

2.12) Immediately re-suspend the pellet with egg solution by pipetting.

2.13) Immediately fill conical tube with egg solution and mix well by inverting 3-5 times. Then immediately spin as in 2.10.

2.14) Immediately decant the supernatant.

2.15) Re-suspend the pellet in Luria Broth (LB) by pipetting, transfer to a 15ml conical tube for improved pelleting during wash steps. Other buffers may be used depending on the nematode and bacterium. The buffer must not harm either the nematode or bacterium.

2.16) Fill the tube with LB and spin as in 2.10.

2.17) Decant the supernatant, and re-suspend in LB.

2.18) Rinse the nematodes a total of 3 times by repeating 2.14 and 2.15.

2.19) Dilute the re-suspended nematode eggs to an appropriate volume. There should be at least 10 eggs per microliter. Eggs can be stored in a 6-cm petri dish in 5 mLs LB for at least four days by adding antibiotics that inhibit colonizing bacteria and wrapping the plate in parafilm. The media will need to be washed once in 15 mL LB (as in 2.13 and 2.14). Note that eggs will hatch during this time and may not be synchronized developmentally when used in colonization assays.

3) Co-cultivation assay with fluorescent bacteria

3.1) Grow fluorescent bacteria overnight, selecting for the plasmid if necessary.

3.2) Spread 600 μ l of the bacterial culture onto 10 mm Lipid Agar plates with a sterile stick. Incubate at 25°C for two days.

3.3) Place 500-5000 axenic nematode eggs in a total of 100 to 400 μ l (optimally 2,000 nematodes in 200 μ l) onto each lipid agar plate.

3.4) Incubate in the dark without moisture at room temperature until IJs, or other stages of interest, form. IJs will be visible as a fuzzy white ring on the edge of the plate. To look at other life stages, see Protocol 4.

3.5) Place the plates in a modified White trap: Remove the lid of the lipid agar plate and place the bottom into the bottom of an empty 100 mm x 20 mm Petri dish. Fill the large Petri dish with

water, or other buffer appropriate to your nematode, to surround the small plate. The water level should be approximately half the height of the small plate.

3.6) Incubate the water trap until progeny IJs have emerged into the buffer.

3.7) Infective juvenile nematodes can be stored in water in a tissue culture flask.

4) Collection of early life stages for screening

4.1) Use steps 3.1 through 3.4 to set up the assay.

4.2) Incubate the plates until the desired life stages are present. Daily visual inspection may be necessary to determine timing. To inspect the plates, use the procedure described in Protocol 2.5. For *S. carpocapsae* eggs grown with *X. nematophila* on LA plates, gravid females will be present in 4-5 days, juveniles will be present in 7 days, and infective juveniles will start to be produced by 15-17 days.

4.3) When the desired life stages are present, collect your sample. Fill a well of a 96 well plate with 200 μ l of PBS or other appropriate buffer. Gently scrape off some of the bacterial lawn containing nematodes. A pea-sized amount (~50 μ g) will provide at least several hundred nematodes once F1 progeny are produced, but more may be necessary for earlier time points. . Place the stick into the well containing buffer.

4.4) Incubate for 30 seconds to a minute. Remove the stick and scrape off the remaining residue. Use the stick to remove any agar from the well. The nematodes should be visible within the buffer. Move the buffer mixture to a clean microfuge tube.

4.5) Treat the nematodes with levamisole or other paralyzing agent. Dissolve a few grains of levamisole into 30 μ l of water. Add 1-2 μ l of this mix for each 50 μ l of sample. After levamisole treatment the nematodes will be non-viable..

4.6) If samples will be viewed at a later date, fix as described in this step. If not, skip step 4.6. Add 200 μ l of fixative solution containing 1X buffer and 4% paraformaldehyde. Mix gently, pipetting may cause delicate life stages to lyse. Cover with foil, and incubate at room temperature on a shaker on low for at least 18 hours.

4.7) Place the tubes in a tube rack, and allow the nematodes to settle to the bottom of the tube.

4.8) Rinse nematodes to remove background. Pipette off excess liquid and add 200 – 500 μ l of buffer and gently mix. Repeat. This may be repeated a few times to remove more background if desired.

4.9) Allow the nematodes to settle to the bottom of the tube and re-suspend in the desired volume.

4.10) If the nematodes are not fixed, screen immediately. Fixed nematodes may be stored in the refrigerator for up to two weeks. Store in the dark.

5) Screening nematodes for bacterial association by microscopy

5.1) Select some nematodes to view under the microscope by removing a small sample of your mixture.

5.2) To ensure that the nematodes are still for the picture, treat with a paralytic agent as described in Protocol 4.5. If you are not taking a picture or the nematodes are already fixed, this step may be skipped.

5.3) Add 20-30 μ l of nematodes in water to your microscope slide and place a coverslip on top.

5.4) View whole nematodes using light microscopy to ensure nematodes are in the field of view.

5.5) View nematodes using the fluorescent setting on the microscope that corresponds to the fluorescence expressed by the bacteria.

5.6) To identify bacterial localization, take photos of the nematode under fluorescent setting and a light microscopy setting, and then superimpose the images. The photos need to be of the same field of view. It may be necessary to try several magnifications and views of the nematode to find the bacteria.

5.7) The distribution of nematode colonization can be quantified by counting a population of nematodes, scoring for the presence or absence of bacteria, and calculating the percent colonized. We recommend counting until at least 30 nematodes within the population are counted in each category (with or without colonization) to obtain a reliable value.

5.8) When only a few nematodes in the population are colonized, it may be necessary to count several thousand nematodes before 30 are observed. For high-throughput counting use the following steps.

5.9) Instead of counting nematodes individually, aliquot the population into multi-well plate (e.g. a 24-well plate). After the nematodes have settled to the bottom of the dish, each well can be scanned on the microscope and the number of colonized nematodes can be scored.

5.10) The total number of nematodes in a population can be identified by serial dilutions of nematodes in the well. For example, 1 mL of nematodes can be added to a well, mixed by stirring with a pipet tip, and 3 μ l can be removed and counted for quantification of the total population in the well.

5.11) The percentage of colonized nematodes can be obtained by dividing the number colonized by the total number of nematodes in the well.

REPRESENTATIVE RESULTS

Example microscope images of *Steinernema* nematodes associated with *Xenorhabdus* bacteria are shown in Figure A1.3. To create the composite image seen in Figure A1.3 A, a phase contrast image was overlaid with a fluorescent image. The arrow in Figure A1.3 A indicates the bacteria present within the infective juvenile nematode (bar = 100 μm). Figure A1.3 B was constructed in a similar manner and depicts a juvenile nematode with green fluorescent protein labeled bacter (green rods) localized throughout the nematode intestinal lumen (bar = 20 μm). A population of the nematodes from two media conditions were counted and scored for colonization by the bacterial symbiont (Table A1.1). For robust statistics, it is best to count at least 100 nematodes per sample with at least 30 falling in each category. As seen in Table A1.1, these nematodes are colonized at a level of approximately 14.6% when grown on lipid agar and 68.6% when grown on liver kidney agar. Other nematode and bacterial species have been shown to have different levels of colonization. For example, *X. nematophila* colonizes 99% of *S. carpocapsae* infective juveniles (Martens 2003), and *P. luminescens* colonizes 26% of *H. bacteriophora* infective juveniles (Ciche 2003).

FIGURES

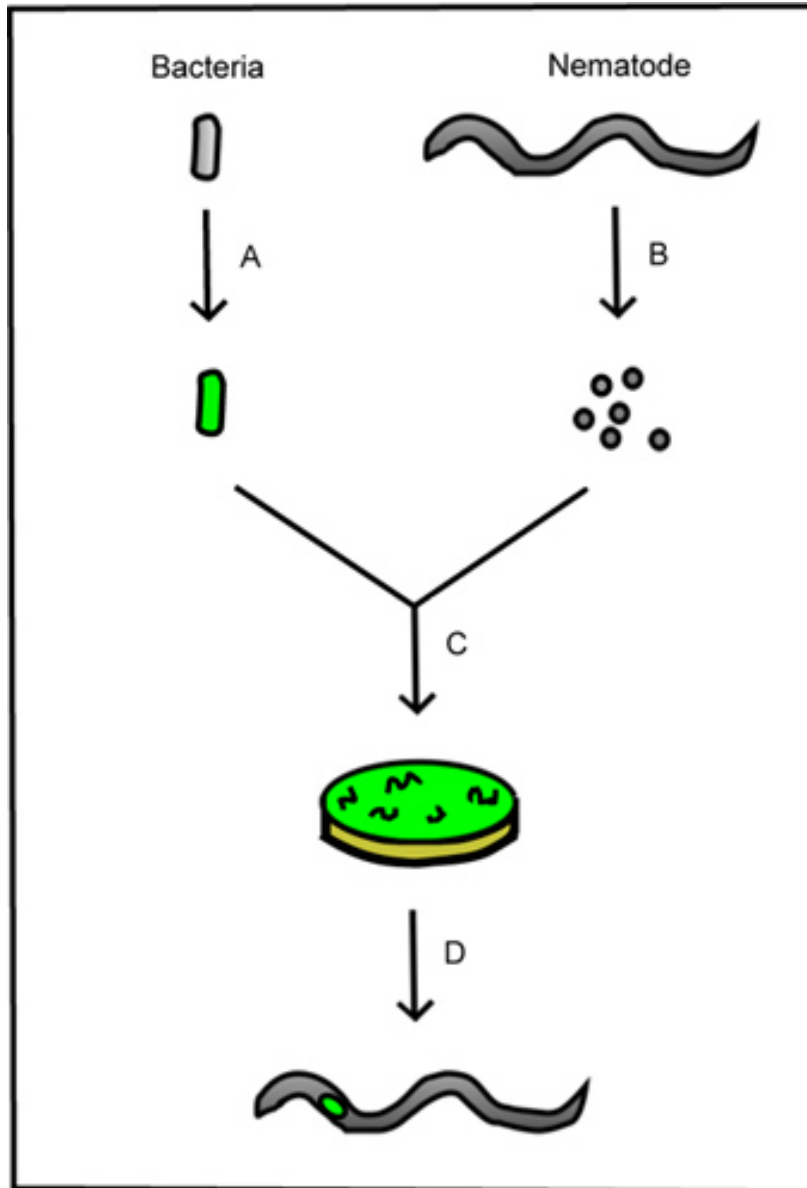


Figure A1.1 Schematic outline of the experiment. **A.** The bacterium is first labeled with the fluorescent protein. **B.** Nematode eggs are then isolated from adult nematodes to produce sterile nematodes. **C.** The sterile nematodes are combined with the fluorescent bacteria in a colonization assay. **D.** The resulting life stages are viewed under a microscope to evaluate bacterial presence within the nematode.

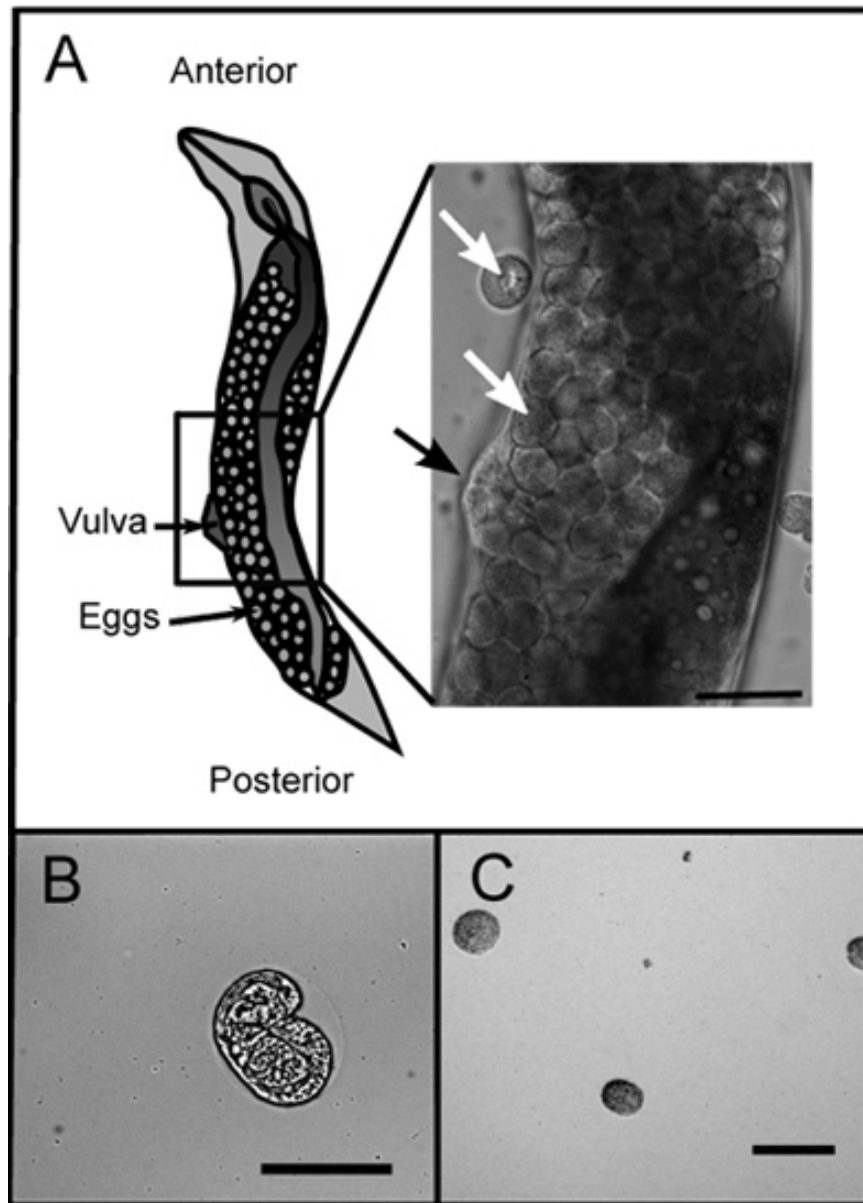


Figure A1.2 Depiction of adult females containing eggs. **A.** the schematic shown the general appearance of *Steinernema* females. Inset: DIC image of a *S. feltiae* gravid female. The back arrow indicated the vulva. White arrows show visible eggs. Image is at 20x magnification, and the scale bar represents 100 μm . **B.** DIC image of developed but unhatched *S. feltiae* nematode egg. Image is 40X magnification, and the scale bar represents 50 μm . **C.** DIC image of eggs isolated from *S. feltiae* nematodes under 10X magnification. Scale bar is 100 μm .

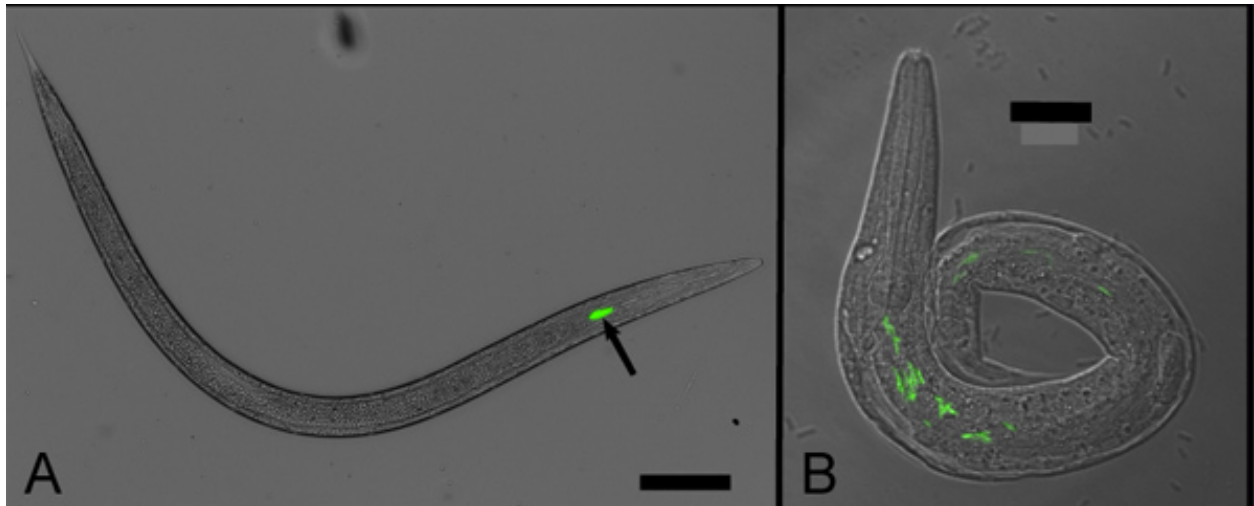


Figure A1.3 Example microscope images of nematode-bacterial association. A. *S. punctauvense* nematodes were associated with their bacterial symbiont, *X. bovienii*, expressing GFP. The image is a composite image produced by overlaying a phase contrast image with a fluorescent image from the same field of view. The arrow indicates the fluorescent bacterial symbiont within the nematode host. Scale bar represents 100 μm . **B.** This image was constructed through overlaying a fluorescent image over a DIC image. The scale bar represent 20 μm .

Strain	Number of Nematodes With Bacteria	Total Nematodes Counted	Percent of Nematodes Colonized
<i>S. punctuovense</i> Lipid Agar	30	205	14.6%
<i>S. punctuovense</i> Liver Kidney Agar	72	105	68.6%

Table A1.1 Example scoring of a nematode population for bacterial presence. In this experiment, axenic *S. punctuovense* nematodes were grown with their GFP-expressing symbiont on different growth media (lipid agar and liver kidney agar) to test for colonization defects. A total of at least one hundred nematodes per sample were counted and scored for the presence of bacteria. For statistical power, three experimental replicates should be counted with at least 30 nematodes falling in each category.

Plasmid Name	Fluorophore	Antibiotic Cassette	Insertion Site	Special Instructions	Source
mini-Tn7-KSGFP	green fluorescent protein	Kanamycin	Tn7 site, upstream of <i>glmS</i>	Requires helper plasmid	33
pECM20	green fluorescent protein	Chloramphenicol	Chromosomal insertion	Specific to <i>X. nematophila</i> (nucleotide 825459-824847)	13
pBK-miniTn7-ΩGm-DsRed	Ds red fluorescent protein	Gentamycin	Tn7 site, upstream of <i>glmS</i>	Requires helper plasmid	31
pTurboRFP-B	TurboRFP	Ampicillin	Extrachromosomal, ColE1 replicon	Origin may not replicate in all bacteria	Evrogen
pPROBE-GT	green fluorescent protein	Gentamycin	Extrachromosomal, pVS1/p15a replicons	Origin may not replicate in all bacteria	32
pPROBE-KT	green fluorescent protein	Kanamycin	Extrachromosomal, pVS1/p15a replicons	Origin may not replicate in all bacteria	32
pPROBE-NT	green fluorescent protein	Kanamycin	Extrachromosomal, pVS1/p15a replicons	Origin may not replicate in all bacteria	32
pPROBE-AT	green fluorescent protein	Ampicillin	Extrachromosomal, pVS1/p15a replicons	Origin may not replicate in all bacteria	32
pPROBE-TT	green fluorescent protein	Tetracycline	Extrachromosomal, pVS1/p15a replicons	Origin may not replicate in all bacteria	32
pPROBE-OT	green fluorescent protein	Streptomycin	Extrachromosomal, pVS1/p15a replicons	Origin may not replicate in all bacteria	32

Table A1.2 Fluorescent protein containing plasmids. A list of potential plasmids for insertion

of a fluorescent protein into the bacterial symbiont is given listed by the name of the plasmid.

Other information included are the fluorescent protein encoded, antibiotic cassette used for plasmid maintenance, other instructions for use, the source of the plasmid. The concentration noted in parentheses is the concentration of the antibiotic used for *X. nematophila*. Each of these plasmids has been used successfully in either *Xenorhabdus* or *Photorhabdus*. Additional information can be obtained from the cited citations. Depending on the bacterium being tested, some plasmids may not work based upon the fluorescent protein, antibiotic selection, insertion site, or origin of replication. The plasmids listed above contain different features that may enable use in the bacterium of interest. For example, mini-Tn7-KSGFP inserts into the attTN7 site of the chromosome, while pECM20 inserts into the *X. nematophila* chromosome by homologous recombination. Alternatively, the pPROBE plasmids are maintained extrachromosomally, and each pPROBE plasmid has the same backbone and fluorophore but have different selectable markers or origins of replication to enable their use in a variety of taxonomic or mutant backgrounds.

CONCLUSIONS

The protocol described here provides a method for the optical detection of bacteria within a nematode host (Figure A1.1). This method takes advantage of the optical transparency of nematodes and the ability to fluorescently label bacteria. By putting these together we are able to view the presence of the bacteria within the nematode host (Figure A1.3). Specifically, this approach identifies the site of bacterial localization within its host. By then counting a population of nematodes and scoring for the presence of bacteria, the distribution of the bacteria within the nematode population can be determined (Table A1.1). This method is one of the many potential techniques that can be utilized for studying the interactions between nematode hosts and bacterial symbionts. Related methods have been described previously to isolate the bacterial symbiont, grow nematodes axenically, and manipulate both partners.

This method was developed in the *Xenorhabdus nematophila*-*Steinernema carpocapsae* model system (12) and similar approaches have been used in other entomopathogenic nematode-bacterial associations (11, 13, 14, 16). Several conditions must be met in order to apply this method to other nematode-bacterial systems. First, the bacterial symbiont must be able to be isolated from the host and grown independently in culture. Second, the symbiont must be able to take up DNA through transformation or conjugation in order to introduce the fluorescent protein. Third, for the best results, the nematode must have a stage that can be made axenic and reintroduced to bacteria. However, even if the nematode cannot be isolated from the bacteria it might still be possible to visualize the association: instead of adding axenic eggs to the lawn of fluorescent bacteria, add a conventionally raised life stage and proceed with the protocol as described. Any results will suffer from the caveat that bacteria that do not express GFP will compete with GFP-expressing bacteria for localization to specific nematode tissues, and because of this, colonization should not be measured by microscopic counting. However,

unless the bacteria that do not express GFP drastically outcompete GFP-expressing bacteria, GFP-expressing bacteria should localize to nematode tissues in at least some animals in the population and suggest important tissue sites for bacterial colonization. A long-standing caveat of using fluorescent-protein expressing strains is that they may colonize a host with different efficiency than a strain that does not express fluorescent proteins (e.g. (12))

Steps described in this protocol may require optimization depending on the nematode and bacterial species that are being used. For conjugation of the bacterium some conditions that can be altered are the length and temperature of growth, the ratio of donor to recipient, and plasmid used. Examples of relevant plasmids are listed in Table A1.2. All of these plasmids have been successfully used in either *Xenorhabdus* or *Photorhabdus* bacteria in association with their nematode host(24-26). To ensure stable maintenance of the fluorescent protein during nematode colonization it is best to use a plasmid that will insert into the chromosome of the target bacterium. Further, some bacteria may not take up these plasmids. For example, pECM20 has only been used in *X. nematophila* and very closely related bacterial strains 14 because this plasmid inserts into the chromosome using a homologous region between the plasmid and chromosome; the plasmid will not insert if the target bacterium lacks this region. To use this plasmid for other bacteria, the *X. nematophila*-specific region must be substituted with a genomic region from the target bacterium. Some plasmid-transformation schemes will also require certain alterations from Protocol 1. For example, mini-Tn7-KSGFP and pBK-miniTn7-ΩGm-DsRed require a helper plasmid containing transposition genes (tsnABCDE)(24-26) to insert into the bacterial chromosome. Conjugation is most efficient with these Tn7-based plasmids, when 2-hour cultures (~OD6000.3-0.4) are mixed in equal ratios. After successful conjugation it is important to utilize correct selective plates corresponding to the plasmid used. The selective plates should contain the antibiotic encoded on the plasmid to

select for the presence of the plasmid in the recipient and a counter-selection against the donor and helper strains. For example, when conjugating pECM20 in *X. nematophila* the counter-selection used is ampicillin because *X. nematophila* is ampicillin resistant and the donor strain is ampicillin sensitive. If antibiotic counter-selection is unavailable in your system, a diaminopimelic acid(DAP) requiring donor may be used. To grow DAP-requiring strains, DAP is added to solid and liquid growth media during pre-conjugation and conjugation steps, and omitted during counter-selection stages. When DAP is absent the donor strain will not grow and is effectively counterselected. To ensure successful egg isolation it is essential to accurately check for egg production (Figure A1.2). At the time of isolation, female nematodes should be full of eggs and some eggs should be visible in the media (Figure A1.2 A). If female nematodes are producing fertilized eggs at least some supernatant eggs will have visibly developed as unhatched nematodes (Figure A1.2 B). For *S. carpocapsae*, the eggs will change from spherical to slightly oblong prior to developing nematodes and hatching. The timing or conditions of nematode growth may also need to be altered to maximize fertilized egg yield, including shortening or lengthening the period of time before egg harvesting, or using alternate media appropriate to the specific nematode species. At the end of the isolation, eggs should be easily visible within the buffer (Figure A1.2 C). Parameters in the egg isolation protocol that may require optimization include bleach and KOH concentrations in the egg solution, incubation time in egg solution, or centrifugation speed. If the egg isolation produces eggs but no nematodes develop during the co-cultivation, it is possible that the isolated eggs are non-viable. To check for viability, leave the isolated eggs in buffer and wait for nematodes to hatch. The eggs should hatch within one or two days of isolation and then the juvenile nematodes can be used in the co-cultivation assay. If the eggs hatch but do not develop during the co-cultivation assay, it may be necessary to change the growth conditions or medium used for co-cultivation. We note that previous studies have isolated bacteria-free nematodes by soaking the nematodes in an

antibiotic cocktail (e.g. ^{3,37}). The approach we describe here is free of some of the caveats of antibiotic soaking, including complications with using bacteriostatic antibiotics, antibiotic-resistant contaminating bacteria, and antibiotic effects on the nematodes. Certain stages of nematodes may also be resistant to antibiotics and retain their bacterial symbionts³. Finally, we note that for microscopy, the concentration of levamisole necessary for nematode immobilization may vary with different nematode clades.

Once this method has been established in the system of interest, it is possible to alter the technique to derive more information. By looking at earlier time points in the nematode life cycle (Protocol 4), one may be able to identify how the bacterium and nematode initiate their association. In addition, this approach can be used to conduct a high throughput mutant screens to identify bacterial factors involved in the symbiosis, using fluorescence to detect colonization. Other methods such as signature tagged mutagenesis require the use of radioactively labeled probes and are more time consuming. Therefore, the use of fluorescence microscopy for bacterial symbiont visualization in nematodes is an effective and efficient screening tool for investigating bacterial interactions with a nematode host.

ACKNOWLEDGMENTS

The authors wish to thank Eugenio Vivas, Kurt Heungens, Eric Martens, Charles Cowles, Darby Sugar, Eric Stabb, and Todd Ciche for their contributions to the development of this protocol. KEM was supported by National Institutes of Health (NIH) National Research Service Award T32 AI55397. This work was supported by grants from the National Science Foundation (IOS-0920631 and IOS-0950873).

REFERENCES

1. **Lamshead PJD, Boucher G.** 2003. Marine nematode deep-sea biodiversity - hyperdiverse or hype? *Journal of Biogeography* **30**:475-485.
2. **Holterman M, van der Wurff A, van den Elsen S, van Megen H, Bongers T, Holovachov O, Bakker J, Helder J.** 2006. Phylum-wide analysis of SSU rDNA reveals deep phylogenetic relationships among nematodes and accelerated evolution toward crown Clades. *Mol Biol Evol* **23**:1792-1800.
3. **Poinar GO, Jr., Hansen EL.** 1986. Associations between nematodes and bacteria. *Helminthological Abstracts, Series B* **55**:61-79.
4. **Herbert EE, Goodrich-Blair H.** 2007. Friend and foe: the two faces of *Xenorhabdus nematophila*. *Nat Rev Microbiol* **5**:634-646.
5. **Kaya HK, Gaugler R.** 1993. Entomopathogenic nematodes. *Annu Rev Entomol* **38**:181-206.
6. **Goodrich-Blair H.** 2007. They've got a ticket to ride: *Xenorhabdus nematophila*-*Steinernema carpocapsae* symbiosis. *Curr Op Microbiol* **10**:225-230.
7. **Zhang C, Liu J, Xu M, Sun J, Yang S, An X, Gao G, Lin M, Lai R, He Z, Wu Y, Zhang K.** 2008. *Heterorhabditoides chongmingensis* gen. nov., sp. nov. (Rhabditida: Rhabditidae), a novel member of the entomopathogenic nematodes. *J Invertebr Pathol* **98**:153-168.
8. **Ye WM, Torres-Barragan A, Cardoza Y.** 2010. *Oscheius carolinensis* n. sp (Nematoda: Rhabditidae), a potential entomopathogenic nematode from vermicompost. *Nematology* **12**:121-135.
9. **Abebe E, Jumba M, Bonner K, Gray V, Morris K, Thomas WK.** 2010. An entomopathogenic *Caenorhabditis briggsae*. *The Journal of experimental biology* **213**:3223-3229.
10. **Torres-Barragan A, Suazo A, Buhler WG, Cardoza YJ.** 2011. Studies on the entomopathogenicity and bacterial associates of the nematode *Oscheius carolinensis*. *Biol Control* **59**:123-129.
11. **Abebe E, Abebe-Akele F, Morrison J, Cooper V, Thomas WK.** 2011. An insect pathogenic symbiosis between a *Caenorhabditis* and *Serratia*. *Virulence* **2**:158-161.
12. **Martens EC, Heungens K, Goodrich-Blair H.** 2003. Early colonization events in the mutualistic association between *Steinernema carpocapsae* nematodes and *Xenorhabdus nematophila* bacteria. *J Bacteriol* **185**:3147-3154.
13. **Easom CA, Joyce SA, Clarke DJ.** 2010. Identification of genes involved in the mutualistic colonization of the nematode *Heterorhabditis bacteriophora* by the bacterium *Photorhabdus luminescens*. *BMC Microbiol* **10**:45.
14. **Ciche TA, Ensign JC.** 2003. For the insect pathogen, *Photorhabdus luminescens*, which end of a nematode is out? *Appl Environ Microbiol* **69**:1890-1897.

15. **Ciche TA, Kim KS, Kaufmann-Daszczuk B, Nguyen KCQ, Hall DH.** 2008. Cell invasion and matricide during *Photorhabdus luminescens* transmission by *Heterorhabditis bacteriophora* nematodes. *Appl Environ Microbiol* **74**:2275-2287.
16. **Somvanshi VS, Kaufmann-Daszczuk B, Kim KS, Mallon S, Ciche TA.** 2010. *Photorhabdus* phase variants express a novel fimbrial locus, *mad*, essential for symbiosis. *Mol Microbiol* **77**:1021–1038.
17. **Martens EC, Russell FM, Goodrich-Blair H.** 2005. Analysis of *Xenorhabdus nematophila* metabolic mutants yields insight into stages of *Steinernema carpocapsae* nematode intestinal colonization. *Mol Microbiol* **51**:28-45.
18. **Sugar DR, Murfin KE, Chaston JM, Andersen AW, Richards GR, Deleon L, Baum JA, Clinton WP, Forst S, Goldman BS, Krasomil-Osterfeld KC, Slater S, Stock SP, Goodrich-Blair H.** 2011. Phenotypic variation and host interactions of *Xenorhabdus bovienii* SS-2004, the entomopathogenic symbiont of *Steinernema jolietii* nematodes. *Env Microbiol* doi:10.1111/j.1462-2920.2011.02663.x.
19. **Cowles CE, Goodrich-Blair H.** 2008. The *Xenorhabdus nematophila* *nilABC* genes confer the ability of *Xenorhabdus* spp. to colonize *Steinernema carpocapsae* nematodes. *J Bacteriol* **190**:4121-4128.
20. **Heungens K, Cowles CE, Goodrich-Blair H.** 2002. Identification of *Xenorhabdus nematophila* genes required for mutualistic colonization of *Steinernema carpocapsae* nematodes. *Mol Microbiol* **45**:1337-1353.
21. **Goetsch M, Owen H, Goldman B, Forst S.** 2006. Analysis of the PixA inclusion body protein of *Xenorhabdus nematophila*. *J Bacteriol* **188**:2706-2710.
22. **Martens EC, Gawronski-Salerno J, Vokal DL, Pellitteri MC, Menard ML, Goodrich-Blair H.** 2003. *Xenorhabdus nematophila* requires an intact *iscRSUA-hscBA-fdx* locus to colonize *Steinernema carpocapsae* nematodes. *J Bacteriol* **185**:3678-3682.
23. **Vivas EI, Goodrich-Blair H.** 2001. *Xenorhabdus nematophilus* as a model for host-bacterium interactions: *rpoS* is necessary for mutualism with nematodes. *J Bacteriol* **183**:4687-4693.
24. **Lambertsen L, Sternberg C, Molin S.** 2004. Mini-Tn7 transposons for site-specific tagging of bacteria with fluorescent proteins. *Environ Microbiol* **6**:726-732.
25. **Miller WG, Leveau JH, Lindow SE.** 2000. Improved *gfp* and *inaZ* broad-host-range promoter-probe vectors. *Mol Plant Microbe Interact* **13**:1243-1250.
26. **Teal TK, Lies DP, Wold BJ, Newman DK.** 2006. Spatiometabolic stratification of *Shewanella oneidensis* biofilms. *Appl Environ Microbiol* **72**:7324-7330.

APPENDIX 2

Phenotypic variation and host interactions of *Xenorhabdus bovienii* SS-2004, the entomopathogenic symbiont of *Steinernema jolietii* nematodes

This work has been published as:

Sugar DR, **Murfin KE**, Chaston JM, Andersen AW, Richards GR, Deléon L, Baum JA, Clinton WP, Forst S, Goldman BS, Krasomil-Osterfeld KC, Slater S, Stock SP, and Goodrich-Blair H. 2011. "Phenotypic variation and host interactions of *Xenorhabdus bovienii* SS-2004, the entomopathogenic symbiont of *Steinernema jolietii* nematodes." *Environ Microbiol.* 2012 Apr;14(4):924-39. doi: 10.1111/j.1462-2920.2011.02663.x

ABSTRACT

Xenorhabdus bovienii (SS-2004) bacteria reside in the intestine of the infective-juvenile (IJ) stage of the entomopathogenic nematode, *Steinernema jolietii*. The recent sequencing of the *X. bovienii* genome facilitates its use as a model to understand host-symbiont interactions. To provide a biological foundation for such studies, we characterized *X. bovienii* in vitro and host-interaction phenotypes. Within the nematode host *X. bovienii* was contained within a membrane bound envelope that also enclosed the nematode-derived intravesicular structure. *S. jolietii* nematodes cultivated on mixed lawns of *X. bovienii* expressing green or DsRed fluorescent proteins were predominantly colonized by one or the other strain, suggesting the colonizing population is founded by a few cells. *X. bovienii* exhibits phenotypic variation between orange-pigmented primary form and cream-pigmented secondary form. Each form can colonize IJ nematodes when cultured *in vitro* on agar. However, IJs did not develop or emerge from *Galleria mellonella* insects infected with secondary form. Unlike primary-form infected insects that were soft and flexible, secondary-form infected insects retained a rigid exoskeleton structure. *X. bovienii* primary and secondary form isolates are virulent toward *Manduca sexta* and several other insects. However, primary form stocks present attenuated virulence, suggesting that *X. bovienii*, like *X. nematophila* may undergo virulence modulation.

INTRODUCTION

Entomopathogenic nematodes in the genus *Steinernema* are mutualistically associated with Gamma-proteobacteria in the genus *Xenorhabdus*. Together, *Steinernema-Xenorhabdus* complexes infect, kill, and reproduce in the larval stage of a wide range of insect hosts, including those in the orders Lepidoptera, Diptera, and Coleoptera (1). The *Steinernema* nematode harbors *Xenorhabdus* bacteria in a modified portion of the intestine, and the bacteria are released by defecation when the nematode infects an insect and reaches the insect's body cavity (hemocoel) (2-4). After reproduction, nematode progeny become colonized by *Xenorhabdus* bacteria and emerge from the cadaver to seek a new host.

Since *Xenorhabdus* spp. are mutualists (of nematodes) and pathogens (of insects) they have become a model for studying both types of associations (5, 6) from cellular, molecular and evolutionary perspectives. Furthermore, unlike many current model systems to study host-microbe interactions, the mutualistic and pathogenic traits of *Xenorhabdus* bacteria are conserved among all members of the genus, facilitating comparative insights into the biology and evolution of these processes.

Twenty species of *Xenorhabdus* are currently recognized (7, 8) and the genomes of two, *X. nematophila* (ATCC 19061: genome accession #NC_014228, plasmid accession #NC_014170) and *X. bovienii* (SS-2004: accession #NC_013892), have been sequenced by our group. *X. nematophila* is known to colonize three nematode species from two clades, while *X. bovienii* strains appear to be more widely distributed, colonizing at least eight *Steinernema* spp. from three clades (9-16). However, *X. bovienii* comprises multiple phylotypes (7, 10) each of which may have a distinct host range. Indeed, variations have been observed in the ability of *X. bovienii* strains to colonize the nematode *S. feltiae* (16). The *Steinernema-Xenorhabdus* mutualistic association that has been most extensively studied at the molecular and cellular

level is that between *X. nematophila* and *S. carpocapsae* (17). This study is focused on the relationship between *X. bovienii* and the nematode *Steinernema jolietii*.

Generally, both *Steinernema* nematodes and *Xenorhabdus* bacteria contribute to pathogenesis. The nematode produces a factor that can degrade inducible immune proteins (18) but most *Xenorhabdus* bacteria are pathogenic if injected alone (without the nematode host) directly into the hemocoel of a susceptible host (19). *Xenorhabdus spp.* are able to suppress immunity and produce virulence factors, including toxins that contribute to rapid killing of the insect host (reviewed in (5)).

Nematode reproduction is promoted in the insect by the presence of the bacterial symbiont (20-23), with *X. nematophila* producing lipase and hemolysin activities necessary for nematode reproduction (21) and virulence in the insect (24, 25), respectively. In addition, *Xenorhabdus* promotes nematode development by protecting the insect cadaver from scavengers and other microbes (26, 27) through the production of a wide array of antimicrobials (28-31) including bacteriocins that inhibit invasion of the cadaver by non-specific symbionts (27, 32).

Steinernema and *Xenorhabdus* reproduce within the insect cadaver until nutrient depletion and high nematode population density triggers development of the nematode into a non-feeding stage known as the Infective Juvenile (IJ) (33). The IJs become colonized by the bacterial symbionts in the anterior intestinal lumen, a region known as the receptacle (4, 34). In *S. carpocapsae*, the receptacle comprises the lumen between the two most anterior intestinal cells, which are morphologically distinct from other intestinal cells (4, 35, 36). The *X. nematophila* population in the *S. carpocapsae* receptacle is founded by 1-2 individual cells that grow to fill the space (37), where they adhere to a cluster of spheres termed the intravesicular structure (IVS) that is associated with a glycan-containing mucous material (35). Once formed, IJ progeny emerge from the spent insect cadaver to search for new hosts to infect (38).

All *Xenorhabdus* species reported to date undergo phenotypic variation characterized by the switching between two cell types known as primary and secondary forms. Although the phenotypic differences between primary and secondary forms can vary depending on strain and species (19), typically the primary, but not secondary form cells are motile, pigmented, agglutinate red blood cells and produce fimbriae, hemolysins, proteases, antimicrobials, and crystalline inclusion bodies (39-42). *Xenorhabdus* bacteria isolated from nematode hosts typically are in the primary form, but in laboratory culture conditions some cells convert to the secondary form. Although again it varies depending on strain and species, some secondary form isolates can revert to the primary form, while others appear to be stable (43). Studies to date indicate the mechanism underlying phenotypic variation does not involve DNA rearrangements (44) changes in plasmid content (45), or recombination-dependent mechanisms (46). In *X. nematophila* the transcription factor Lrp is a positive regulator of primary form traits; *lrp* mutants are phenotypically secondary form (47), suggesting phenotypic variation may be an epigenetic phenomenon.

The sequenced strain of *X. bovienii* (SS-2004) (Chaston, Suen *et al.*, in press) was isolated from the nematode *S. jolietii* (48), but to date there is no published literature describing this strain. A primary goal of our research is to identify molecular mechanisms underlying the *X. bovienii*-*S. jolietii* association using the genome sequence as a resource. We anticipate that comparing this system to the more extensively studied *X. nematophila*-*S. carpocapsae* association and to other *X. bovienii* host associations will provide insights into the common and diverse features of *Steinernema*-*Xenorhabdus* interactions with each other and with insect hosts. Toward these goals, in this study we investigated general characteristics of *X. bovienii* SS-2004 as well as its interactions with its *S. jolietii* nematode and insect hosts.

Table A2.1 Strains and plasmids used in this study

Lab Strain Number	Description/Use	Reference/Source
<i>Xenorhabdus</i> strains		
HGB800	<i>X. nematophila</i> ATCC 19061, wild-type	American Type Culture Collection (ATCC)
HGB1053	<i>X. bovienii</i> SS-2004 Jollieti 2000 stock	B. Goldman (Monsanto)
HGB1054	<i>X. bovienii</i> SS-2004 Jollieti 2000-2°	This study
HGB1055	<i>X. bovienii</i> SS-2004 Jollieti 2000-1°	This study
HGB1269	<i>X. bovienii</i> Jollieti 2007 stock	This study
HGB1267	<i>X. bovienii</i> Jollieti 2007-2°	This study
HGB1268	<i>X. bovienii</i> Jollieti 2007-1°	This study
HGB1245	HGB1054-GFP (2000-2°;GFP)	This study
HGB1263	HGB1055-GFP (2000-1°;GFP)	This study
HGB1281	HGB1054-DsRed (2000-2°;DsRed)	This study
HGB1285	HGB1055-DsRed (2000-1°;DsRed)	This study
HGB1282	HGB1267-GFP (2007-2°;GFP)	This study
HGB1283	HGB1268-GFP (2007-1°;GFP)	This study
HGB1286	HGB1267-DsRed (2007-2°;DsRed)	This study
HGB1287	HGB1268-DsRed (2007-1°;DsRed)	This study
Other bacterial strains		
HGB1006	<i>E. coli</i> K12 test strain for antibiotic	J. Imlay
HGB005	<i>E. coli</i> DH5 α test strain for antibiotic	Bethesda Research Laboratory
HGB006	<i>E. coli</i> S17-1 λ <i>pir</i> test strain for antibiotic	(86)
BW29427	<i>E. coli</i> (<i>thrB1004 pro thi rpsL hsdS lacZ</i> Δ <i>M15 RP4-1360</i> Δ (<i>araBAD</i>)567 Δ <i>dapA1341::[erm pir (wt)]</i>); Donor for conjugations: Strep ^R	K.A. Datsenko and B.L. Wanner
HGB1262	BW29427+pURR25; Strep ^R , Kan ^R	D. Lies and D. Newman
HGB1266	BW29427+pBK-mini-Tn7(Gm) <i>PA1/04/03</i> -DsRed; Strep ^R , Gm ^R	This study
HGB1284	BW29427+ pUX-BF13; Strep ^R , Amp ^R	D. Lies and D. Newman
<i>B. subtilis</i> 168 test strain for antibiotic		
Plasmids		
pURR25	MTn7 <i>PA1/03/04</i> gfpmut3*Mini-Tn7-KSGFP	D. Lies and D. Newman
pUX-BF13	Tn7 transposase, Amp ^R	(78)
pBK-mini-Tn7(Gm) <i>PA1/04/03</i> -DsRed	Mini-Tn7-DsRed	L. Lambertsen

RESULTS AND DISCUSSION

To characterize *X. bovienii* (SS-2004) host-interaction phenotypes, in 2007 we isolated individual bacterial colonies from the same *S. jolietii* nematode host lineage, and compared them to *X. bovienii* stocks isolated from *S. jolietii* in 2000, at the time of sequencing. Both stocks contained two colony morphologies, cream and orange, on LB agar (Figure A2.1). 16S rRNA sequencing confirmed that all isolates were *X. bovienii* (data not shown). When isolated cream and orange colonies were re-streaked, each gave rise to a mixed population of orange and cream colonies. For both orange and cream colonies, the stability of the colony type increased with increasing number of re-streaks. From each *X. bovienii* SS-2004 stock individual stable orange and cream colonies were isolated and a variety of phenotypes were analyzed (Table A2.2). Small colony variants were observed in the 2007, but not the 2001 orange isolate after growth on LB medium (Figure A2.1). Both cell types had similar growth rates in LB broth, defined medium, and hemolymph, and exhibited motility, antibiotic activity against *Bacillus subtilis*, and hemolysis toward rabbit and horse red blood cells. Orange but not cream colony isolates bound bromothymol blue dye, lysed sheep red blood cells, agglutinated horse red blood cells, and produced antibiotic activities against *Escherichia coli*. Conversely, cream colony isolates but not orange demonstrated lipase activity against Tween 20 substrate. Based on these tests we concluded that orange colony isolates are the primary form while cream color isolates are the secondary form (39, 49). Hereafter, isolates will be referred to by the stock from which they were isolated (2000 or 2007) and their phenotypic form (orange, primary [1°]; cream, secondary [2°]). The majority of stationary phase LB-grown primary and secondary cells were rod shaped, but 1° form cultures contained a higher frequency than secondary of long rods (Figure A2.1).

Table A2.2 Phenotypes of *X. bovienii* SS-2004

Strain	Colony Color ^a	Dye binding (NBTA)	Growth Rate (h/generation) ^b			Motility ^c	Lipase ^d	Lecthinase ^e	Protease ^f	Hemolysin ^g		Hem-agglutination ^h	Antibiotic Production ⁱ
			Luria Broth	Minimal	Hemolymph					Sheep/Rabbit/ Horse	Sheep/Rabbit/ Horse		
2000-1 ^o	Orange	+	1.27 +/- 0.09	5.7 +/- 1.8	4.9 +/- 0.6	+	-	-	+	+/+/+	+/+	+	+
2000-2 ^o	Cream	-	1.27 +/- 0.07	5.2 +/- 1.1	4.4 +/- 1.2	+	+	+	+/+	-/+/+	-/+	-	+
2007-1 ^o	Orange	+	1.16 +/- 0.10	6.4 +/- 2.5	4.1 +/- 1.1	+	-	-	+	NT	NT	+	+
2007-2 ^o	Cream	-	1.24 +/- 0.10	5.9 +/- 0.3	4.2 +/- 1.1	+	+	+	+/+	NT	NT	-	+

^aColony color was observed on LB plates after 24 h incubation at 30 °C.

^bGrowth rate in LB, minimal medium, and hemolymph presented as the slope of log10-transformed OD values from exponential part of growth curve.

^cSize of colony (mm), 24 h after inoculation on swim plates (0.25% agar).

^dPresence (+) or absence (-) of halo surrounding the bacterial colony, 3 days after inoculation on Tween 20-containing plates

^ePresence (+) or absence (-) of halo surrounding the bacterial colony, 4 days after inoculation on egg yolk-containing plates

^fSubjective evaluation of halo surrounding the bacterial colony, 3 days after inoculation on milk (protease) or blood (hemolysin) containing plates. NT; Not tested

^gAbility to keep red blood cells in suspension (+) or not (-). NT; Not tested

^hPresence (+) or absence (-) of halo surrounding the bacterial colony, 3 days after inoculation of the indicated tester bacterium.

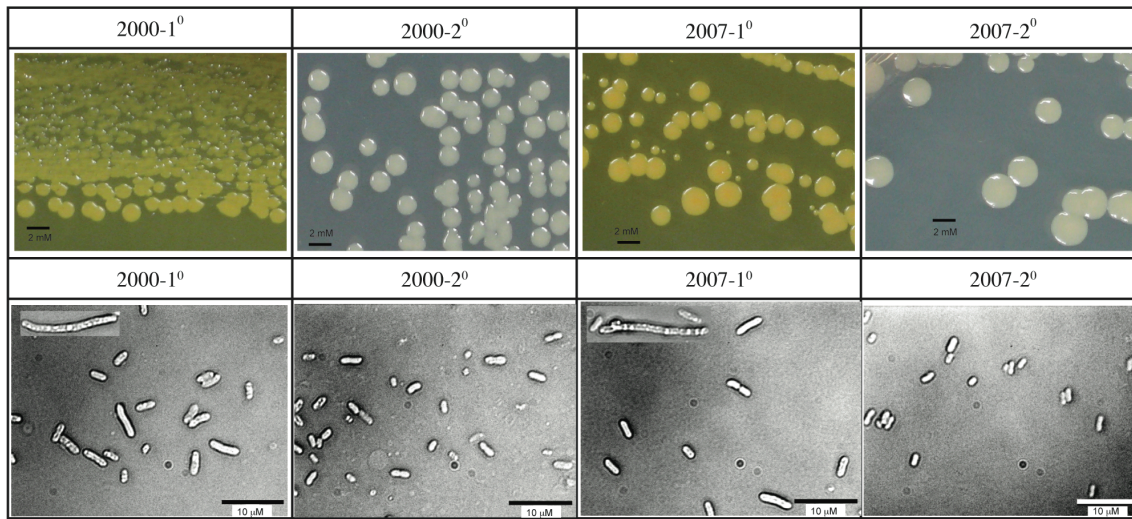


Figure A2.1 Colony and cell morphology of *X. bovienii* primary and secondary variants.

When streaked on LB agar, *X. bovienii* primary form colonies produce an orange pigment, causing both colonies and the surrounding agar to appear orange, while secondary form colonies are cream colored (size bars: 2 mm). Cultures were grown overnight in LB broth, and DIC microscopy revealed rod shaped cells, with primary form variant cultures containing a higher frequency of elongated cells (insets) (size bars: 10 μM).

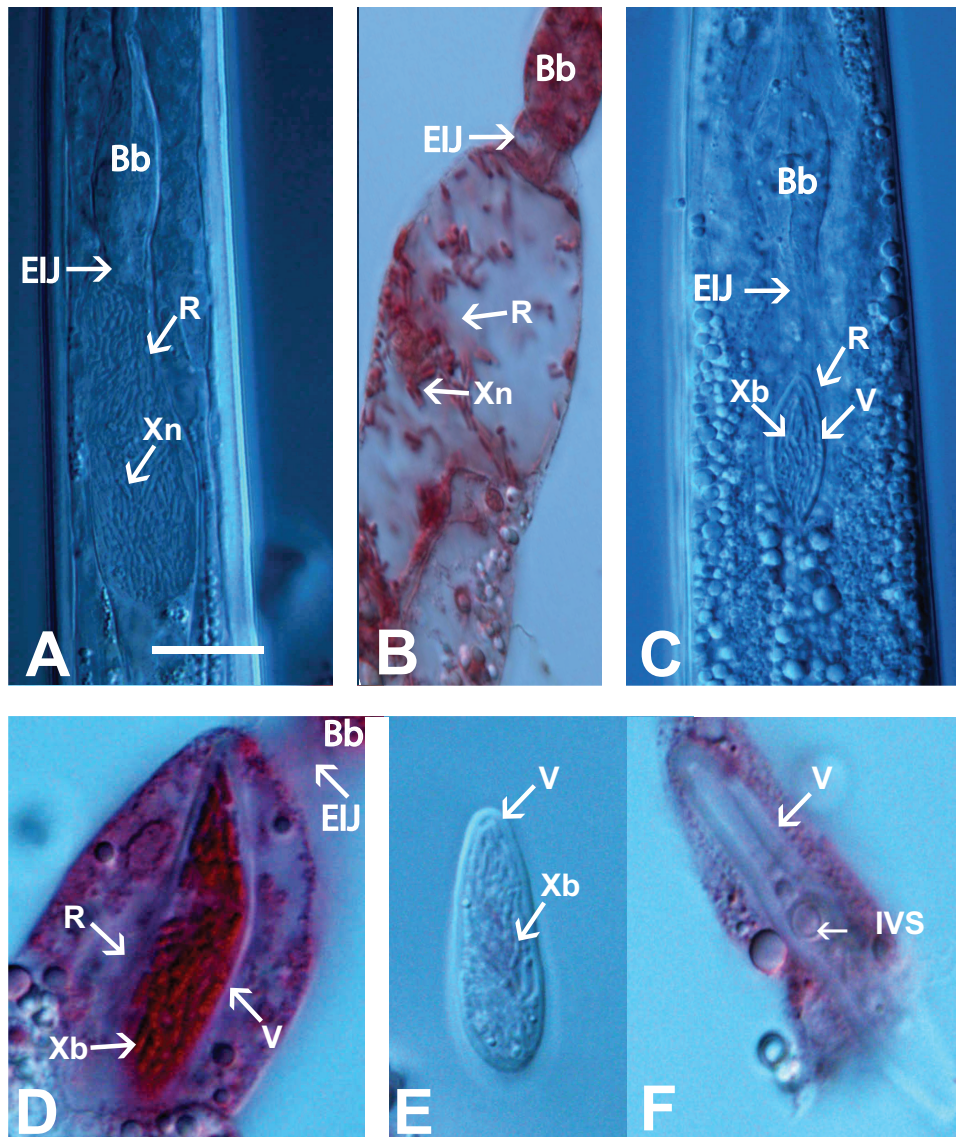


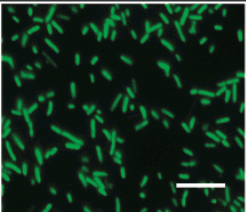
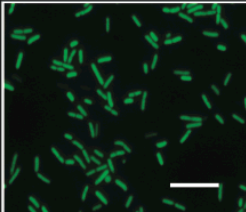
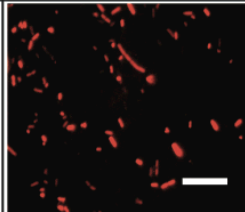
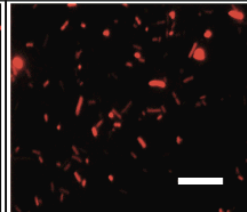
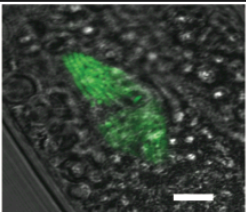
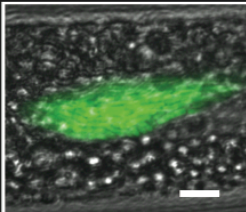
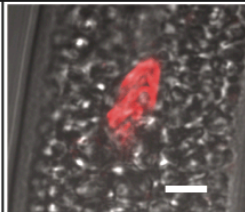
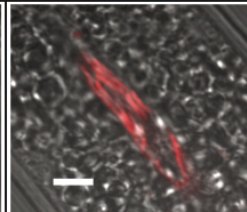
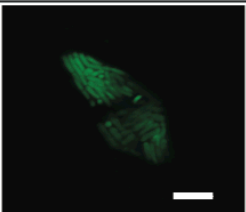
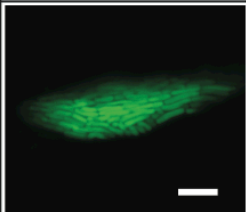
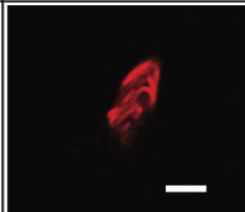
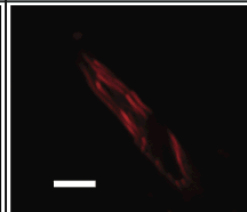
Figure A2.2 A. *S. carpocapsae* (A-B) and *S. jolietii* (C-F) intestinal receptacle. A *in situ* colonized *S. carpocapsae* receptacle; B. Extruded colonized *S. carpocapsae* receptacle; C. *in situ* colonized *S. jolietii* receptacle; D. Extruded receptacle of *S. jolietii* showing colonized vesicle with thick membrane; E. Extruded colonized vesicle of *S. jolietii*; F. Uncolonized vesicle with thick membrane and IVS, extruded from an *S. jolietii* IJ cultured on liver-kidney agar in the absence of bacteria. .References: Bb; basal bulb, EIJ: esophago-intestinal junction, R: receptacle, V: vesicle, Xn: *X. nematophila* bacteria, Xb: *X. bovienii* bacteria, IVS: intra vesicular structure. Scale bar for all images as in A: A-C= 20 μ m; D-E= 7 μ m; F= 15 μ m.

***X. bovienii* (SS-2004) colonization of *S. jollieti* nematodes.** *X. bovienii* (2000-1°) was visualized within the *S. jollieti* colonization site in both in situ and extruded receptacles (Figure A2.2). The *S. jollieti* colonization site shares several features in common with that of *S. carpocapsae*. In both nematodes, the bacteria colonize the nematode's intestinal receptacle (Figure A2.2A-D). The receptacle of these two nematode species also possesses a cluster of nematode-derived spheres, termed the intravesicular structure (IVS) (Fig 2F and data not shown). However, the *S. jollieti* receptacle has a non-cellular, cellophane-like envelope or membrane that is not apparent in *S. carpocapsae*. We refer to this novel structure as the 'vesicle', by definition "a small sac." This vesicle is resistant to mechanical disruption and contains *X. bovienii* bacterial cells as well as the IVS (Figure A2.2 D-F). Vesicle formation does not depend on the presence of bacteria, since it is present in axenically cultured *S. jollieti* nematodes (Figure A2.2F) as well as in *S. feltiae* nematodes that are phylogenetically closely related to *S. jollieti* (13). However, both the receptacle and the vesicle can stretch to accommodate the bacterial load (data not shown). At present there is no information about the chemical composition, physical nature, or function of this vesicle. We speculate it may serve to restrict bacterial growth, to facilitate timed release of bacteria into insect prey, or to protect symbiont bacteria from stress within the receptacle or insect hemolymph.

X. bovienii SS-2004 primary and secondary form colonization of *S. jollieti* nematodes was monitored in IJ progeny from nematodes cultivated on bacterial lawns (*in vitro* co-cultivation). To assess colonization levels, we initially used a method developed for *X. nematophila*, in which the average number of bacteria per IJ is calculated by sonicating and dilution plating approximately $\sim 10^4$ surface sterilized IJs. However, we found that this method yielded a very low ($\sim 4-7$) average CFU/IJ of *X. bovienii* from *S. jollieti* nematodes. Since numerous bacteria within individual *S. jollieti* IJs were visible by microscopy (Figure A2.2) we considered the possibility that the larger size of *S. jollieti* IJs relative to *S. carpocapsae* (36, 48),

or the presence of the thick-walled vesicle, might reduce the efficiency of bacterial release during sonication. Efficiency was improved by limiting the number of sonicated nematodes to 100. Using this revised method, we determined that primary and secondary *X. bovienii* SS-2004 isolates each colonized *S. jolietii* nematodes at similar levels to each other (2000-1°, 59.7 ± 28.2 ; 2000-2°, 55.3 ± 22.4 average CFU/IJ \pm SEM, $P > 0.05$, $n=3$), similar to the average *X. nematophila* CFU/ *S. carpocapsae* nematode IJ obtained using the sonication method (37). It has been reported that *X. bovienii* strains do not colonize its nematode hosts at as high a level as *X. nematophila*, as determined by crushing nematodes and plating the resulting suspension (15, 16). Our data suggest that *X. bovienii* loads may be higher than estimated by this method.

To calculate the distribution of *X. bovienii* SS-2004 within *S. jolietii* populations (colonization efficiency), *X. bovienii* SS-2004 form variants were engineered to express the green fluorescent protein (GFP) (see Materials and Methods) (Figure A2.3). The average CFU/IJ (determined by sonication and plating) achieved by the fluorescent strains (Figure A2.3) was not significantly different from their parental strains ($P > 0.05$). For each variant, approximately 200 (2 sets of 100) nematodes per experiment were randomly selected and the frequency of colonization (indicated by fluorescence within the colonization site) was determined. Primary and secondary form cells were not significantly different ($P=0.18$, Student's t-test) in their frequency of occurrence within nematodes: *X. bovienii* 2000-1°/GFP colonized $97.3 \pm 1.2\%$ of nematodes and 2000-2°/GFP cells were visible in $71.5 \pm 41.3\%$ of nematodes (Figure A2.3) and did not switch forms within the IJ (data not shown). Within the vesicle, the bacteria are tightly packed together longitudinally (Figure A2.3). In contrast, in *S. carpocapsae* nematodes, *X. nematophila* cells are more loosely packed within the receptacle and are not bound by a vesicle (4).

	2000-1 ⁰ / GFP	2000-2 ⁰ / GFP	2000-1 ⁰ / DsRed	2000-2 ⁰ / DsRed
A. Cellular Morphology				
B. Nematode Colonization Overlay				
C. Nematode Colonization Fluores- cence				
D. CFU/IJ	63.3 +/- 34.8 (28-133)	32.3 +/- 6.9 (20-44)	58.7 +/- 20.7 (37-100)	26.3 +/- 4.7 (19-35)
E. Colonized Nematodes	97.3 +/- 1.2 (95-99)	71.5 +/- 41.3 (48-91)	8.1 +/- 2.8 (3-13)	1.5 +/- 0.9 (1-2)

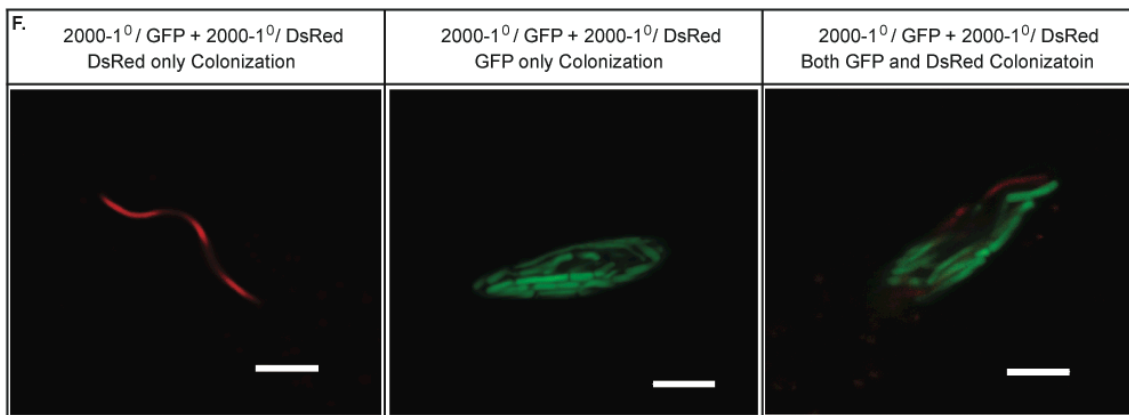


Figure A2.3 *X. bovienii* colonization frequency. *X. bovienii* primary (1°) or secondary (2°) cells expressing green fluorescent protein (GFP) or DsRed protein (DsRed) were visualized after (A) growth in liquid culture or (B and C) within nematode intestines using an epifluorescence or confocal microscope respectively. In (B) confocal images overlay DIC images. Size bars for A, B, and C represent 5 microns. (D) Nematodes were cultivated on lawns of each bacterial strain, and the average CFU per infective juvenile (CFU/IJ) was calculated by sonication and plating and (E) the percentage of colonized nematodes (% colonized nematodes) were determined by microscopy. The experiment was conducted three independent times. Standard error of the mean and range (in parentheses) are provided. (F) Mixed lawns of *X. bovienii* expressing GFP or DsRed were cultivated with nematodes. Nematodes colonized by GFP-expressing cells, DsRed-expressing cells, or both were apparent within the population. Shown are confocal images of each type, with the size bar representing 5 microns.

Since the IJ is a non-feeding stage, the events necessary for intestinal colonization initiation must precede its development. Experimental evidence suggests that 1-2 *X. nematophila* bacterial cells initiate colonization in *S. carpocapsae* then grow within the receptacle after IJ formation (37, 50). To begin to assess the colonization process in the *S. jollieti*-*X. bovienii* mutualism we determined the monoclonal and bi-clonal colonization frequency of IJs cultured on mixed lawns of 2000-1° *X. bovienii* expressing either GFP or DsRed fluorescent protein. As in *X. nematophila* (37), expression of DsRed significantly lowered the frequency of colonization ($P < 0.05$, Student's t-test), with only $8 \pm 2.6\%$ and $1.5 \pm 0.9\%$ of nematodes being colonized by DsRed-expressing primary and secondary form cells (Figure A2.3). Furthermore, DsRed expressing cells did not pack the receptacle as tightly as GFP-expressing cells, and appeared filamentous (Figure A2.3). Despite the dramatically low frequency of colonization, the average DsRed expressing *X. bovienii* SS-2004 CFU/IJ was not significantly different from either *X. bovienii* SS-2004 without fluorescent protein, or expressing GFP. One possible explanation for this result is that in some nematodes the bacteria are no longer expressing DsRed and are not readily apparent by microscopy. In addition, the maximum CFU/IJ we obtain with our modified sonication method may be a gross under-estimate of the actual number of bacteria in nematodes colonized by wild type cells (see above), and is insufficient to detect differences in colonization level for *X. bovienii* SS-2004.

Although the DsRed-expressing strains are at a colonization disadvantage relative to GFP-expressing strains, we visually determined the frequency of nematodes colonized by GFP, DsRed, or both, after cultivation on a mixed (50:50) lawn of green and red primary form cells (Figure A2.3 F). Of the colonized nematodes derived from such lawns, $90.4 \pm 8.2\%$ fluoresced either all green (72.4%) or all red (18.0%), while nematodes visibly colonized by both types of bacteria represented only 9.6% of the population. Based on this frequency we calculated that,

like *X. nematophila* (37), the final population of *X. bovienii* SS-2004 within an individual infective juvenile nematode is derived from 1-2 individual cells (see experimental procedures).

The colonization assays described above were conducted *in vitro* (*i.e.* on agar plates rather than within insects). Although colonization trends of *S. carpocapsae* IJs cultured *in vitro* on lawns of *X. nematophila* bacteria generally mirror those from *in insecta* cultivations (51), *S. carpocapsae* IJs that develop within insects have higher bacterial loads than those that develop on bacterial agar lawns (36, 52). To determine if *in vivo* cultivation within a host influences *X. bovienii* SS-2004 colonization of *S. jolietii* nematodes, we injected *Galleria mellonella* insects with *X. bovienii* SS-2004 bacteria and *S. jolietii* nematodes, and calculated average CFU/IJ for emerging progeny nematodes. *X. bovienii* 2000-primary colonized nematodes cultured in *G. mellonella* at 19.7 ± 10.9 CFU/IJ \pm S.D. (n=2). Nematode IJs did not emerge from insects infected with secondary-phase cells, even after 4 weeks of incubation (data not shown). Dissection of insects at various time points after injection revealed that nematodes developed in both primary- and secondary-injected cadavers (Figure A2.4 A), but that IJ formation occurred only in the former (Figure A2.4 C and E), not in the latter (Figure A2.4 B and D) indicating that specifically in insects (not *in vitro* on lipid agar plates), secondary form cells lack an activity necessary for, or produce an activity inhibitory to development of infective juveniles.

In four independent experiments, primary cell-infected insects reproducibly had a soft and spongy texture 3-5 days post-infection, while the secondary-form infected insects maintained a rigid exoskeleton (Figure A2.4 F), even at 14 d post-infection, relative to a time of emergence of 8-10 days from insects infected with primary form cells. One possible explanation for this finding is that secondary form *X. bovienii* SS-2004 may lack one or more activities (e.g. secreted enzymes) necessary for degradation of the insect cadaver exoskeleton. If so, this activity appears to be expressed specifically in the presence of the nematode and only by primary form cells, since insect cadavers injected with primary or secondary bacteria alone (in

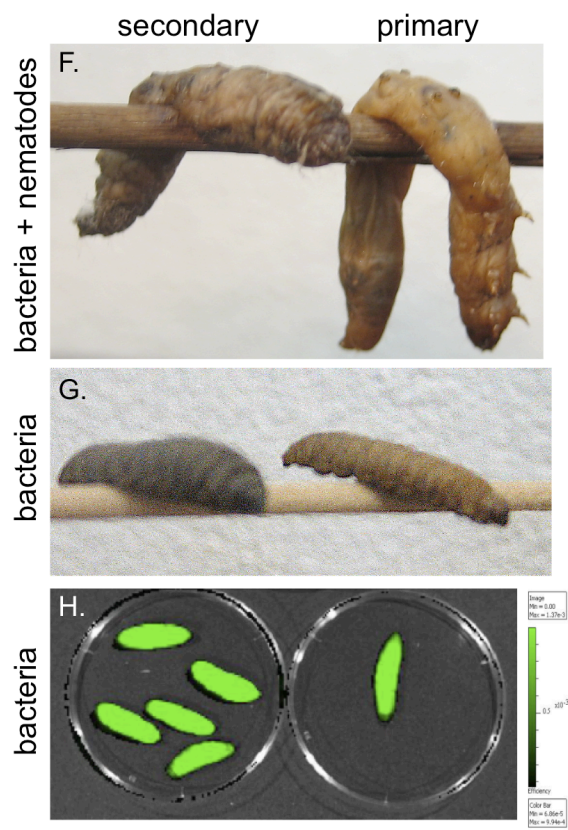
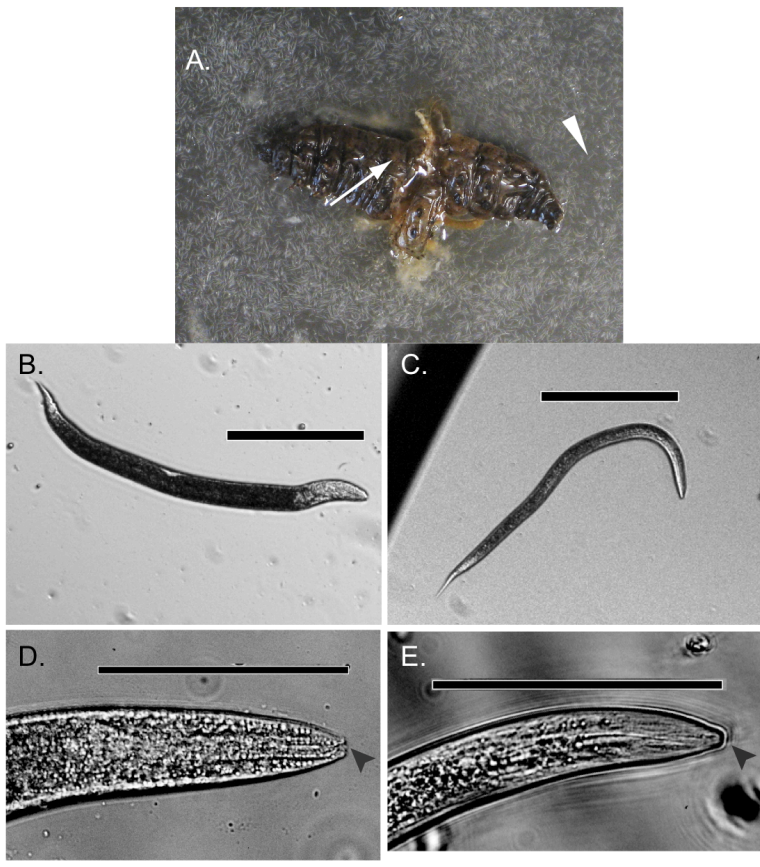


Figure A2.4 Nematode-infected *G. mellonella* with primary form, but not secondary form *X. bovienii* produce infective juveniles and are flaccid and liquefied. At 7 d post-infection with nematodes and secondary form *X. bovienii* (HGB1054) *G. mellonella* insect cadavers (white arrow) are filled with non-emergent juvenile nematodes that can be seen in the water surrounding the cadaver upon dissection (an individual nematode among many is indicated by a white arrowhead) (A). However, phase contrast microscopy revealed that none of these is in the IJ stage (B and D) as indicated by body morphology and the presence of an open mouth (arrow). In contrast, juveniles from primary-form infected cadavers (C and E) are infective juveniles with closed mouths (arrow). Scale bars in B and C are 200 microns, and in D and E, 100 microns. *G. mellonella* insects 3 d post-infection with nematodes and bacteria (F) are flaccid if the injected bacteria are primary, but rigid if the injected bacteria are secondary. The flaccid insect cadaver phenotype associated with primary-form infection requires the presence of nematodes, since *G. mellonella* insects injected with either primary or secondary form bacteria, but without nematodes, are rigid (G). Both primary and secondary form bacteria are able to reproduce within the cadaver, as indicated by in vivo imaging system visualization of fluorescence in cadavers 7 days post-injection with secondary (HGB1245) or primary (HGB1263) *X. nematophila* strains expressing the green fluorescent protein (H). Images were taken using GFP-appropriate excitation and emission filters. Color corresponds to varying levels of emitted fluorescence, with a color spectrum of corresponding fluorescence levels shown on the right. Control insects without bacteria expressing green fluorescent protein showed no detectable fluorescence at these settings (not shown).

the absence of nematodes) were rigid (Figure A2.4 G), even at high bacterial loads (Figure A2.4 H).

Candidates for a bacterial factor contributing to the flaccid cadaver phenotype are the "Makes caterpillars floppy" (Mcf) toxins, Mcf1 (PLU4142, NP_931332) and Mcf2 (PLU3128, AAR21118), discovered in the entomopathogenic nematode symbiont *Photorhabdus luminescens*. *E. coli* expressing *mcf1* is toxic when injected into *M. sexta* larvae, and the larval cadavers lose body turgor and become "floppy" (53). Mcf2 has an N-terminal truncation relative to Mcf1, but is similar in its toxicity (54). *Pseudomonas fluorescens* encodes an *mcf1* homolog (*fitD*), deletion of which decreases toxicity, melanization, and "floppiness" in *Manduca sexta* and *G. mellonella* insects (55). The *X. bovienii* SS-2004 genome encodes one *mcf* homolog (XBJ1_2410, YP_003468304, 2533 aa) in contrast to *X. nematophila* which encodes two: *mcf1* (XNC1_2028, YP_003712268) and *mcf2* (XNC1_2265, YP_003712501). XBJ1_2410 and *P. luminescens* Mcf2 share 76% and 31% identity in the N- and C-terminal thirds of the proteins, respectively. However, the middle third of XBJ1_2410 is distinct from *P. luminescens* Mcf2 and contains a cysteine peptidase domain (aa945-1100) (pfam11713, E-value: 8.5e-34) (56-58). This domain is also present in *X. nematophila mcf2*. It will be of interest to determine if XBJ1_2410 expression phenotypically varies and if its expression or product activity is influenced by the presence of the nematode, as would be expected if Mcf2 is responsible for the flaccid phenotype observed in insects injected with primary-form *X. bovienii* and *S. jollieti* nematodes.

Our data are also consistent with the possibility that the nematode produces one or more activities necessary for insect bioconversion, but only in the presence of primary form bacteria. Indeed, *S. carpocapsae* expresses proteases specifically in the infective juvenile stage that have activity against insect tissues (59, 60). Expression of these proteases may be triggered by primary form bacteria.

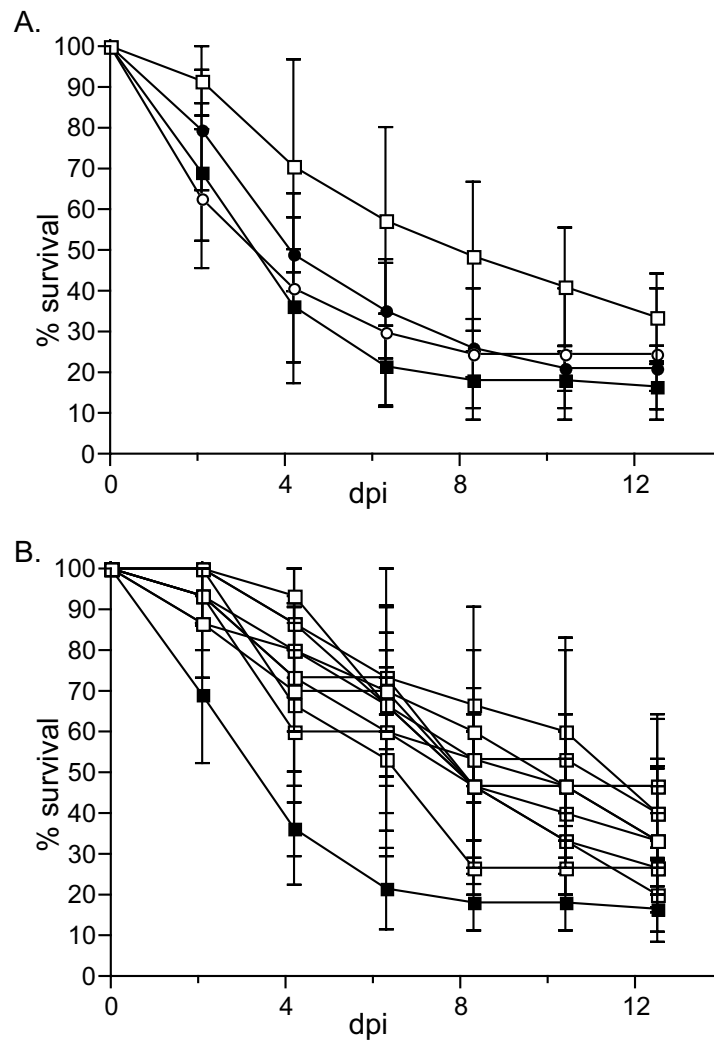


Figure A2.5 *X. bovienii* virulence in *M. sexta* larvae. Approximately 100 CFU of bacteria in late logarithmic phase growth ($OD_{600} \sim 0.8$) were injected into each 4th instar *Manduca sexta* larvae (10 insects per treatment) and the percent of insects surviving each treatment (% survival) was monitored for approximately 13 days post-injection (dpi). A) Insects were injected with primary (squares) or secondary (circles) *X. bovienii* isolates from 2000 (open symbols) or 2007 (closed symbols). B) Individual primary form colonies were isolated from the parent stock and each was injected into insects as above (open squares). Closed squares show the survival curve of insects injected with *X. bovienii* 2007-1° (same as in A). Each experiment was conducted at least 3 independent times.

***X. bovienii* (SS-2004) virulence in *M. sexta* and other agricultural insect pests.**

Virulence of *X. bovienii* (SS-2004) variants was measured as the percent survival of 4th instar *M. sexta* larvae after injection with approximately 100 cfu of bacteria (Figure A2.5 A). *X. bovienii* 2000-2°, 2007-1°, and 2007-2° each killed ~59% of insects by 96 h post-injection. However, 2000-1° cells killed only 20% of insects by that time, and both the percent mortality and time to death of insects injected with this strain were significantly different from that caused by the other three strains ($p < 0.0001$). We considered the possibility that we had inadvertently chosen an attenuated variant from the 2000 stock and therefore examined the virulence of ten additional 2000-1° colonies. None were able to kill insects to the same levels as 2000-2°, 2007-1°, and 2007-2° (Figure A2.5 B). These data indicate that *X. bovienii* primary form cells can become attenuated for virulence, and that the majority of, if not all the primary form cells in the *X. bovienii* 2000 stock, but not the 2007 stock, have done so. Recently, it was reported that variants of *X. nematophila* arise within a population that are heritably and reversibly attenuated for virulence and immune suppression (61). These virulence modulated (vmo) strains arise in laboratory stocks of *X. nematophila* but the mechanism underlying the modulation and the conditions that trigger modulation are unknown (61). It is possible that the 2000 stock of *X. bovienii* was exposed to conditions (e.g. prolonged freezer storage) that promoted virulence modulation. Alternatively, some other phenomenon, such as a genetic mutation that altered virulence, may have occurred. The latter possibility is less likely since the genetic mutation would have had to selectively impact only the primary form cells in the population (secondary form colonies are virulent). We therefore favor the idea that laboratory-derived conditions promoted virulence modulation of the *X. bovienii* 2000 stock, and the intriguing corollary that primary form cells are more susceptible than secondary form cells to this modulation.

We also tested the oral toxicity of primary forms of both *X. bovienii* and *X. nematophila* against a number of known insect pathogens of plants (Table A2.3). *X. bovienii* exhibited a

Table A2.3 Toxicity of *X. bovienii* concentrated protein samples against selected insect pests of plants.

Insect	Percent Mortality ^a	
	<i>X. bovienii</i>	<i>X. nematophila</i>
Black Cutworm	0	0
Corn Earworm	87 ± 12	11 ± 9.6
Southern Corn Rootworm	0	0
Western Corn Rootworm	45.8 ± 12.3	0
Western Tarnished Plant Bug	100	0

^aPercent mortality ± standard deviation across three microtiter dish columns of each treatment

broader host range of secreted toxicity, with concentrated supernatants (>10 kDa) causing mortality in the Western Tarnished Plant Bug, Corn Ear Worm, and Western Corn Rootworm. In contrast, *X. nematophila* supernatants caused mortality only in Corn Ear Worm, and at lower levels (11% mortality) than that caused by *X. bovienii* (87%). In light of these results it is curious that the *X. bovienii* genome encodes a narrower repertoire of insecticidal Tc toxins than does the *X. nematophila* genome. Tc toxins are large molecular weight complexes of A, B, and C subunits (62). *X. bovienii* encodes 3 A subunits, 2 B subunits, and 2 C subunits, while *X. nematophila* encodes 7, 3, and 3 of each type respectively (see supplemental Text S5 in (63). The apparently broader host range of *X. bovienii* may be due to broader target specificity of its TC toxins (64). Alternatively, *X. bovienii* may encode one or more additional toxins that expand its target host range.

CONCLUSIONS

Although *X. bovienii* (SS-2004) and *X. nematophila* (ATCC 19061) colonize nematodes from different clades, we found many aspects of their physiology and host interactions to be similar. Both form mono- or bi-clonal populations within the nematode, undergo phenotypic variation of multiple activities, and exhibit heritable virulence variability. Also, the secondary forms of both strains express more lipase and lecithinase activities than their primary counterparts, are virulent in insects and colonize nematodes. Characteristics that distinguish *X. bovienii* from *X. nematophila* include that *X. bovienii* primary form colonies and cultures are pigmented orange, while those of *X. nematophila* are cream. Also, *X. bovienii* exhibits antimicrobial activities against *E. coli* and *B. subtilis*, and only the former is subject to phenotypic variation. In contrast only *X. nematophila* activity against *B. subtilis* is subject to phenotypic variation. The *X. nematophila* *xcn* locus is necessary for the production of the antibiotic xenocoumacin, which has activity against *Micrococcus luteus* (31). The genome of *X.*

bovieni lacks *xcn* gene homologs, indicating *X. bovieni* produces antibiotics that are distinct from those of *X. nematophila*. A further distinction between *X. bovieni* and *X. nematophila* is that the secondary form of the former, but not the latter, has a defect in supporting infective juvenile development within insect cadavers, and also fails to cause cadaver flaccidity. It remains to be determined whether or not these two defects are related, and what the molecular bases are for these phenotypes. Finally, a striking difference exists in the colonization site occupied by these two species of bacteria: when colonizing the nematode *X. bovieni* cells are bound within an envelope structure (vesicle) while *X. nematophila* are freely distributed in the receptacle. The fact that the host nematode tissues with which *X. bovieni* and *X. nematophila* cells interact suggests that the molecular requirements necessary to persist in this environment may differ between the two symbionts.

ACKNOWLEDGEMENTS

We wish to thank Dr. Sergei Spiridonov, Dr. Maurice Moens, and Dr. Kurt Heungens for helping us obtain *Steinernema jolietii* nematodes and Ting-Li Lin from the UW-Madison CALS Statistics Consulting Center for analyzing the virulence data. We would also like to thank Dr. Elizabeth A. Husa for her assistance in using the in vivo imaging system, and Sam-Kyu Kim for technical help. This work was supported by collaborative grants from the National Science Foundation awarded to H.G.-B. (NSF IBN-0416783; IOS-0920631), S.F. (NSF IOB-0416747; IOS-0919912), and S.P.S. (NSF IOB-0146644; IOS- 0919565), an Investigators in Pathogenesis of Infectious Disease Award from the Burroughs Wellcome Fund (H.G.B.), and the National Institutes of Health Grant GM59776 (H.G.B.). J.M.C. and K.E.M. were supported by National Institutes of Health (NIH) National Research Service Award T32 AI55397 and J.M.C was also supported by a National Science Foundation (NSF) Graduate Research Fellowship. G.R.R. was supported by a National Institutes of Health National Research Service Award T32 G07215. L.dL. was funded by the NSF Research Experience for Microbiology Project 0552809.

MATERIALS AND METHODS

Organisms and growth conditions. Strains used are listed in Table A2.1. The *X. bovienii* strain used in this study was deposited on Jun. 28, 2000 with the Agriculture Research Culture Collection (NRRL) International Depository Authority at 1815 North University Street, in Peoria, Ill. 61604 U.S.A., according to the Budapest Treaty on the International Recognition of the Deposit of Microorganisms for the Purpose of Patent Procedures and was designated as NRRL-30311. Permanent stocks of all cultures were stored in Luria-Bertani (LB) broth (65) supplemented with 20% glycerol at -80°C. Unless otherwise stated, cultures were grown at 30°C, in LB broth that had not been exposed to light or on LB agar that was supplemented with 0.1% pyruvate (66). When appropriate, media were supplemented with antibiotics, including ampicillin (150 µg/ml), kanamycin (50 µg/ml), chloramphenicol (30 µg/ml), erythromycin (200 µg/ml), or tetracycline (15 µg/ml) were added as indicated. *X. bovienii* (SS-2004), like other *Xenorhabdus* spp. is catalase negative and is resistant to ampicillin, but is sensitive to the other antibiotics listed above. However, the genome of *X. bovienii* does encode a homolog of chloramphenicol transacetylase that confers resistance to 30 µg/ml chloramphenicol when present in high copy (data not shown). Lipid agar (LA), used to co-culture all strains of nematodes on respective bacterial lawns was prepared as previously described (67). All nematode strains were propagated as previously described (37) through last instar *Galleria mellonella* larvae. *In vitro*, aposymbiotic cultivation of nematodes to produce uncolonized IJs of both *S. jolietii* and *S. carpocapsae*, was performed using liver-kidney agar as previously described (23, 35). *X. bovienii* growth rates in insect hemolymph were performed by harvesting *Manduca sexta* hemolymph as previously described (68), performing a 1:100 subculture of rinsed *X. bovienii* cells into insect hemolymph and growing the cells at 30°C with shaking. The optical density (OD₆₀₀) of the hemolymph culture was recorded every hour for 24 hours using a Beckman Coulter DTX880 Multimode Detector. Similarly, *X. bovienii* growth rates in defined

medium broth were performed by subculturing 1:100 rinsed *X. bovienii* cells into minimal media broth (68) and growing the cells at 30°C with shaking. The optical density (OD₆₀₀) of the minimal media broth culture was recorded every hour for 24 hours.

Phenotypic assays. *X. bovienii* colony color and morphology were observed after growth for 24-36 h at 30°C in or on LB medium. Haemolysin activity (69) against mammalian erythrocytes (Colorado Serum Company, Denver, CO), Tween 20 lipolytic activity (70), lecithinase activity (71, 72), proteolytic activity (73), haemagglutination (74), motility (67), antibiotic activity (28, 75) and dye binding assays (39) were conducted as described in the literature.

Determination of 16S rDNA sequences. Crude DNA extracts from fresh overnight bacterial cultures were used as templates in ExTaq (Takara, Otsu, Shiga, Japan) polymerase chain reactions (PCR) with the universal primers 27F: 5'-AGAGTTTGATCATGGCTCAG-3', and 1492R: 5'-TACGGTTACCTTGTTACGACTT-3' (76). Amplified products were then sequenced at UW-Madison Biotechnology Center using Big Dye version 3.1 (Applied Biosystems, Foster City, CA) with the primers above in addition to Xn850R: 5'-CATTGAGTTTTAACCTTGCG-3'. Sequence similarity to 16S rRNA sequences in the national database were determined using BLAST (77).

Construction and visualization of fluorescent-protein expressing *X. bovienii* strains. To generate *X. bovienii* strains expressing GFP or DsRed, pURR25 (mini-Tn7-KSGFP) or pBK-mini-Tn7(Gm)PA1/04/03-DsRed respectively were conjugated from BW29427, with the helper strain BW29427 (pUX-BF13) (78) according to previously described methods (67), except the donor and helper strains were eliminated by selection of colonies on media without diaminopimelic acid (80 µg/ml) and *X. bovienii* exconjugants were selected on pyruvate (0.1%),

ampicillin (150 $\mu\text{g/ml}$), and kanamycin (50 $\mu\text{g/ml}$). The resulting colonies were confirmed to be *X. bovienii* based on 16S rRNA sequencing.

Microscopy. Phase-contrast, differential interference contrast, and fluorescence microscopy were performed using a Nikon Eclipse TE300 inverted microscope. Fluorescence microscopy was performed using fluorescein isothiocyanate, tetramethyl rhodamine isocyanate (FITC), tetramethyl rhodamine isothiocyanate (TRITC) and triple-band DAPI (4,6-diamidino-2-phenylindole)-FITC-TRITC filter sets (Chroma, Brattleboro, Vt.; items 31001, 31002, and 82000, respectively). Images were recorded using an ORCA digital camera (model C4742-95-10R; Hamamatsu, Hamamatsu City, Japan) and Metamorph version 4.5r6 software (Universal Imaging Corporation, West Chester, PA). Additional images were obtained using a Zeiss LSM 510 Axioplan II confocal microscope (Zeiss, New York, NY). For cell morphology analysis, bacterial cells were immobilized on 3% agarose pads and viewed using DIC microscopy at 100X magnification. When visualizing *X. bovienii* (SS-2004) within whole nematodes, nematodes were paralyzed and immobilized with 1% levamisole in agarose as previously described (37) using confocal microscopy between 400X and 1000X. For microscopy of progeny nematodes, nematodes were immobilized as mentioned above and viewed using phase contrast microscopy under 40X and 400X magnification. To visualize the receptacle and vesicle (Figure A2.2), nematode intestines were extruded by cutting the nematode head with a razor blade, then were maintained in M9 buffer and stained with 0.001% Neutral Red in M9 buffer. The photograph shown in Figure A2.2 was taken with Olympus BX51 equipped with digital camera. Extended focal length images were taken and stacked by using Microsuite image analyzing software.

Photography and *in vivo* imaging. Additional photography for colony morphology and insect

cadavers was done using a Canon Powershot camera. Scale bars were inserted using Metamorph version 4.5r6 software (Universal Imaging Corporation, West Chester, PA). Seven days after injection, 1 to 10 insects per experiment were visualized by using an IVIS Imaging System 200 (Xenogen Corp., Alameda, CA). Fluorescence was quantified by using Living Image software v2.6 (Xenogen).

Host interaction assays. Axenic *S. jolietii* eggs were isolated from adult female nematodes as previously described for *S. carpocapsae* (79) and were stored in 5 ml LB broth supplemented with ampicillin, kanamycin, and chloramphenicol. Axenic eggs were collected and rinsed with sterile LB broth prior to inoculation onto LA plates (in vitro cultivation) or injection into *G. mellonella* (in vivo cultivation). *X. bovienii* co-cultivation with *S. jolietii* nematodes on lipid agar plates was as described for *X. nematophila* and *S. carpocapsae* co-cultivations (50). For in vivo colonization assays ~700 μ l of fresh overnight bacterial cultures was mixed with ~500-1500 axenic nematode eggs and/or J1 juveniles and 12.5 μ l of the mixture was injected into the haemocoel of *Galleria mellonella* larvae (Vanderhorst Wholesale, NJ) with a 30-gauge syringe (Hamilton, Reno, NV). Approximately 15 *G. mellonella* larvae were injected per bacterial treatment and once injected, the insects were placed in modified White traps as previously described (80).

Collected nematodes were assessed by sonication for *X. bovienii* colonization as previously described for *X. nematophila* (81) except that *S. jolietii* were surface sterilized for 3 min. with 0.5% NaOCl. Approximately 10^2 surface sterilized nematodes were sonicated (Branson Ultrasonics, Danbury, CT) for 60-90 seconds each and the sonicate solution was diluted and plated to enumerate colonies. The number of individual cells that are the founders of the final population of *X. bovienii* bacteria within a single *S. jolietii* IJ was calculated from the percentage of nematodes carrying either green or red fluorescence (90.4%) using the

mathematical model described by Wollenberg and Ruby (82): $p(\text{red})^x + p(\text{green})^x = p(\text{single})$. In this formula, x is the initiating cell number, $p(\text{single})$ is the probability of observing a nematode with only red or green fluorescence, and $p(\text{red})$ and $p(\text{green})$ are the initial proportions of each bacterium in the input lawn (0.5 each). Based on our observations that 90.4% of *S. jolietii* nematodes were colonized by either red or green fluorescent bacteria (but not both): $0.5^x + 0.5^x = 0.94^x$ and $x = 1.1$.

X. bovienii injection virulence assays in *Manduca sexta* insect larvae were performed as previously described (75). For feeding toxicity screens against multiple insects, *X. bovienii* and *X. nematophila* (ATCC19061) were streaked onto LB agar plates from frozen glycerol stocks and incubated for 16 h at 25°C. Individual colonies were used to inoculate 4 x 2 ml TB media each and were grown on a roller drum incubator for 45 h at 25°C. After pelleting the bacteria, supernatants from each strain were combined (8 ml total) and concentrated in an Amicon 10 MWCO to 1.2 ml (6x, protein fraction). The flow-through was also collected. Both fractions were tested in a feeding assay for toxicity against 20-24 insects. The flow-through did not cause mortality in any insect. Artificial diet feeding assays were conducted as described by (83) except that assays were run for 5 days. Feeding assays were conducted with neonate larvae (<24 hr post hatch) of the coleopteran species *Diabrotica virgifera virgifera* (Western corn rootworm, WCR) and *Diabrotica undecimpunctata howardii* (Southern corn rootworm, SCR) (both obtained from Crop Characteristics, Inc.; Farmington, MN) using corn rootworm artificial diet and the lepidopteran species: *Agrotis ipsilon* [Hufnagel] (black cutworm, BCW) and *Helicoverpa zea* [Boddie] (corn earworm, CEW) (both obtained from Benzon, Inc.; Carlisle, PA) using Multiple Species diet (Southland, Lake Village, AK). Feeding assays with the hemipteran species *Lygus hesperus* were based on a 96 well micro-titer plate format using a sachet system as previously described (84). The *Lygus hesperus* (Western tarnished plant bug, WT) artificial diet was obtained from Bio-Serv[®] (Bio-Serv[®] Diet F9644B, Frenchtown, NJ) and prepared as previously

described (85). Samples were prepared by mixing one hundred microliters of the test sample with one hundred microliters of blended diet (1:1). A sheet of Parafilm[®] (Pechiney Plastic Packing, Chicago, IL) was placed over a vacuum manifold designed for 96-well format (Analytical Research Systems, Gainesville, FL) and a vacuum of approximately -20 millimeters mercury was applied, sufficient to cause extrusion of the Parafilm[®] into the wells. Twenty or forty microliters of test sample were added to the Parafilm[®] wells. A sheet of Mylar film (Clear Lam Packaging, Inc., Elk Grove Village, IL) was placed over the Parafilm[®] and sealed gently with a tacking iron (Bienfang Sealector II, Hunt Corporation, Philadelphia, PA). The Parafilm[®] sachets were placed over a flat-bottom 96-well plate containing *Lygus* eggs suspended in a 0.19% agar solution. Upon hatching, *Lygus* nymphs were allowed to feed on the sachet diet for 5 days. Stunting and mortality scores were determined on day 5 and compared to the untreated control. Data were analyzed using JMP4 statistical software.

Statistical analysis. Colonization assays were analyzed using a paired, two-tailed Student's t-test assuming unequal variance. Survival curves of *M. sexta* injected with different treatments were analyzed using a proportional hazards model and the final survival values were analyzed with a logistic regression model.

REFERENCES

1. **Ehlers R-U.** 2001. Mass production of entomopathogenic nematodes for plant protection. *Appl Microbiol Biotechnol* **56**:623-633.
2. **Martens EC, Vivas EI, Heungens K, Cowles CE, Goodrich-Blair H.** 2004. Investigating mutualism between entomopathogenic bacteria and nematodes. *Nematol Monographs Persp* **2**:447-462.
3. **Poinar GO.** 1966. The presence of *Achromobacter nematophilus* in the infective stage of a *Neoaplectana* sp. (Steinernematidae: Nematoda). *Nematologica* **12**:105-108.
4. **Snyder HA, Stock SP, Kim SK, Flores-Lara Y, Forst S.** 2007. New insights into the colonization and release process of *Xenorhabdus nematophila* and the morphology and ultrastructure of the bacterial receptacle of its nematode host, *Steinernema carpocapsae*. *Appl Environ Microbiol* **73**:5338-5346.
5. **Herbert EE, Goodrich-Blair H.** 2007. Friend and foe: the two faces of *Xenorhabdus nematophila*. *Nat Rev Microbiol* **5**:634-646.
6. **Richards GR, Goodrich-Blair H.** 2009. Masters of conquest and pillage: *Xenorhabdus nematophila* global regulators control transitions from virulence to nutrient acquisition. *Cell Microbiol* **11**:1025-1033.
7. **Lee MM, Stock SP.** 2010. A multigene approach for assessing evolutionary relationships of *Xenorhabdus* spp. (gamma-Proteobacteria), the bacterial symbionts of entomopathogenic *Steinernema* nematodes. *J Invertebr Pathol* **104**:67-74.
8. **Tailliez P, Laroui C, Ginibre N, Paule A, Pages S, Boemare N.** 2010. Phylogeny of *Photorhabdus* and *Xenorhabdus* based on universally conserved protein-coding sequences and implications for the taxonomy of these two genera. Proposal of new taxa: *X. vietnamensis* sp. nov., *P. luminescens* subsp. caribbeanensis subsp. nov., *P. luminescens* subsp. hainanensis subsp. nov., *P. temperata* subsp. khanii subsp. nov., *P. temperata* subsp. tasmaniensis subsp. nov., and the reclassification of *P. luminescens* subsp. thracensis as *P. temperata* subsp. thracensis comb. nov. *Int J Syst Evol Microbiol* **60**:1921-1937.
9. **Fischer-Le Saux M, Arteaga-Hernández E, Mráček Z, Boemare N.** 1999. The bacterial symbiont *Xenorhabdus poinarii* (Enterobacteriaceae) is harbored by two phylogenetic related host nematodes: the entomopathogenic species *Steinernema cubanum* and *Steinernema glaseri* (Nematoda: Steinernematidae). *FEMS Microbiol Ecol* **29**:149-157.
10. **Fischer-Le Saux M, Mauleon H, Constant P, Brunel B, Boemare N.** 1998. PCR-ribotyping of *Xenorhabdus* and *Photorhabdus* isolates from the Caribbean region in relation to the taxonomy and geographic distribution of their nematode hosts. *Appl Environ Microbiol* **64**:4246-4254.
11. **Mráček Z, Nguyen KB, Tailliez P, Boemare N, Chen S.** 2006. *Steinernema sichuanense* n. sp. (Rhabditida, Steinernematidae), a new species of entomopathogenic

- nematode from the province of Sichuan, east Tibetan Mts., China. *J Invertebr Pathol* **93**:157-169.
12. **Spiridonov SE, Krasomil-Osterfeld K, Moens M.** 2004. *Steinernema jolietii* sp. n. (Rhabditida: Steinernematidae), a new entomopathogenic nematode from the American Midwest. *Russ J Nematol* **12**:85-95.
 13. **Lee MM, Stock SP.** 2010. A multilocus approach to assessing co-evolutionary relationships between *Steinernema* spp. (Nematoda: Steinernematidae) and their bacterial symbionts *Xenorhabdus* spp. (gamma-Proteobacteria: Enterobacteriaceae). *Syst Parasitol* **77**:1-12.
 14. **Akhurst RJ, Boemare NE.** 1988. A numerical taxonomic study of the genus *Xenorhabdus* (Enterobacteriaceae) and proposed elevation of the subspecies of *Xenorhabdus nematophilus* to species. *J Gen Microbiol* **134**:1835-1846.
 15. **Emelianoff V, Le Brun N, Pagés S, Stock SP, Tailliez P, Moulia C, Sicard M.** 2008. Isolation and identification of entomopathogenic nematodes and their symbiotic bacteria from Hérault and Gard (Southern France). *J Invertebr Pathol* **99**:20-27.
 16. **Chapuis E, Emelianoff V, Paulmier V, Le Brun N, Pages S, Sicard M, Ferdy JB.** 2009. Manifold aspects of specificity in a nematode-bacterium mutualism. *J Evol Biol* **22**:2104-2117.
 17. **Goodrich-Blair H.** 2007. They've got a ticket to ride: *Xenorhabdus nematophila*-*Steinernema carpocapsae* symbiosis. *Curr Op Microbiol* **10**:225-230.
 18. **Götz P, Bowman A, Bowman HG.** 1981. Interactions between insect immunity and an insect-pathogenic nematode with symbiotic bacteria. *Proc Royal Soc London B* **212**:333-350.
 19. **Akhurst RJ, Boemare N.** 1990. Biology and Taxonomy of *Xenorhabdus*, p 75-87. In Gaugler R, Kaya HK (ed), *Entomopathogenic Nematodes in Biological Control*. CRC Press, Inc., Boca Raton.
 20. **Poinar GOJ, Thomas GM.** 1966. Significance of *Achromobacter nematophilus* Poinar and Thomas (Achromobacteraceae: Eubacteriales) in the development of the nematode, DD-136 (*Neoaplectana* sp. Steinernematidae). *Parasitol* **56**:385-390.
 21. **Richards GR, Goodrich-Blair H.** 2010. Examination of *Xenorhabdus nematophila* lipases in pathogenic and mutualistic host interactions reveals a role for *xlpA* in nematode progeny production. *Appl Environ Microbiol* **76**:221-229.
 22. **Mitani DK, Kaya HK, Goodrich-Blair H.** 2004. Comparative study of the entomopathogenic nematode, *Steinernema carpocapsae*, reared on mutant and wild-type *Xenorhabdus nematophila*. *Biol Control* **29**:382-391.
 23. **Sicard M, Le Brun N, Pages S, Godelle B, Boemare N, Moulia C.** 2003. Effect of native *Xenorhabdus* on the fitness of their *Steinernema* hosts: contrasting types of interactions. *Parasitol Res* **91**:520-524.

24. **Cowles KN, Goodrich-Blair H.** 2005. Expression and activity of a *Xenorhabdus nematophila* haemolysin required for full virulence towards *Manduca sexta* insects. *Cell Microbiol* **2**:209-219.
25. **Vigneux F, Zumbihl R, Jubelin G, Ribeiro C, Poncet J, Baghdiguian S, Givaudan A, Brehelin M.** 2007. The *xaxAB* genes encoding a new apoptotic toxin from the insect pathogen *Xenorhabdus nematophila* are present in plant and human pathogens. *J Biol Chem* **282**:9571-9580.
26. **Zhou X, Kaya HK, Heungens K, Goodrich-Blair H.** 2002. Response of ants to a deterrent factor(s) produced by the symbiotic bacteria of entomopathogenic nematodes. *Appl Environ Microbiol* **68**:6202-6209.
27. **Morales-Soto N, Forst SA.** 2011. The *xnp1* P2-like tail synthesis gene cluster encodes xenorhabdycin and is required for interspecies competition. *J Bacteriol* **193**:3624-3632.
28. **Akhurst RJ.** 1982. Antibiotic activity of *Xenorhabdus spp.* bacteria symbiotically associated with insect pathogenic nematodes of the families *Heterorhabditidae* and *Steinernematidae*. *J Gen Microbiol* **128**:3061-3065.
29. **Fang XL, Li ZZ, Wang YH, Zhang X.** 2011. In vitro and in vivo antimicrobial activity of *Xenorhabdus bovienii* YL002 against *Phytophthora capsici* and *Botrytis cinerea*. *J Appl Microbiol* **111**:145-154.
30. **Fuchs SW, Proschak A, Jaskolla TW, Karas M, Bode HB.** 2011. Structure elucidation and biosynthesis of lysine-rich cyclic peptides in *Xenorhabdus nematophila*. *Organic & biomolecular chemistry* **9**:3130-3132.
31. **Park D, Ciezki K, van der Hoeven R, Singh S, Reimer D, Bode HB, Forst S.** 2009. Genetic analysis of xenocoumacin antibiotic production in the mutualistic bacterium *Xenorhabdus nematophila*. *Mol Microbiol* **73**:938-949.
32. **Hawlana H, Bashey F, Lively CM.** 2010. The evolution of spite: population structure and bacteriocin-mediated antagonism in two natural populations of *Xenorhabdus* bacteria. *Evolution; international journal of organic evolution* **64**:3198-3204.
33. **Popiel I, Grove DL, Friedman MJ.** 1989. Infective juvenile formation in the insect parasitic nematode *Steinernema feltiae*. *Parasitol* **99**:77-81.
34. **Bird AF, Akhurst RJ.** 1983. The nature of the intestinal vesicle in nematodes of the family Steinernematidae. *Int J Parasitol* **13**:599-606.
35. **Martens EC, Goodrich-Blair H.** 2005. The *Steinernema carpocapsae* intestinal vesicle contains a subcellular structure with which *Xenorhabdus nematophila* associates during colonization initiation. *Cell Microbiol* **7**:1723-1735.
36. **Flores-Lara Y, Renneckar D, Forst S, Goodrich-Blair H, Stock P.** 2007. Influence of nematode age and culture conditions on morphological and physiological parameters in the bacterial vesicle of *Steinernema carpocapsae* (Nematoda: Steinernematidae). *J Invertebr Pathol* **95**:110-118.

37. **Martens EC, Heungens K, Goodrich-Blair H.** 2003. Early colonization events in the mutualistic association between *Steinernema carpocapsae* nematodes and *Xenorhabdus nematophila* bacteria. *J Bacteriol* **185**:3147-3154.
38. **San-Blas E, Gowen SR, Pembroke B.** 2008. *Steinernema feltiae*: ammonia triggers the emergence of their infective juveniles. *Exp Parasitol* **119**:180-185.
39. **Boemare NE, Akhurst RJ.** 1988. Biochemical and physiological characterization of colony form variants in *Xenorhabdus* spp. (Enterobacteriaceae). *J Gen Microbiol* **134**:751-761.
40. **Forst S, Clarke D.** 2002. Bacteria-nematode symbioses, p 57-77. *In* Gaugler R (ed), *Entomopathogenic Nematology*. CABI Publishing, Wallingford, UK.
41. **Smits WK, Kuipers OP, Veening JW.** 2006. Phenotypic variation in bacteria: the role of feedback regulation. *Nat Rev Microbiol* **4**:259-271.
42. **Volgyi A, Fodor A, Szentirmai A, Forst S.** 1998. Phase variation in *Xenorhabdus nematophilus*. *Appl Environ Microbiol* **64**:1188-1193.
43. **Campos-Herrera R, Tailliez P, Pages S, Ginibre N, Gutierrez C, Boemare NE.** 2009. Characterization of *Xenorhabdus* isolates from La Rioja (Northern Spain) and virulence with and without their symbiotic entomopathogenic nematodes (Nematoda: Steinernematidae). *J Invertebr Pathol* **102**:173-181.
44. **Akhurst RJ, Smigielski AJ, Mari J, Boemare N, Mourant RG.** 1992. Restriction analysis of phase variation in *Xenorhabdus* spp. (Enterobacteriaceae), entomopathogenic bacteria associated with nematodes. *Syst Appl Microbiol* **15**:469-473.
45. **Leclerc MC, Boemare NE.** 1991. Plasmids and phase variation in *Xenorhabdus* spp. *Appl Environ Microbiol* **57**:2597-2601.
46. **Pinyon RA, Hew FH, Thomas CJ.** 2000. *Xenorhabdus bovienii* T228 phase variation and virulence are independent of RecA function. *Microbiol* **146 (Pt 11)**:2815-2824.
47. **Cowles KN, Cowles CE, Richards GR, Martens EC, Goodrich-Blair H.** 2007. The global regulator Lrp contributes to mutualism, pathogenesis and phenotypic variation in the bacterium *Xenorhabdus nematophila*. *Cell Microbiol* **9**:1311-1323.
48. **Spiridonov SE, Akhmedov EN, Belostotskaya FN.** 1991. Proliferation of symbiotic bacteria in the intestinal vesicles of invasive larvae of *Neoaplectana* spp. (Nematoda, Steinernematidae). *Helminthologia* **28**:141-142.
49. **Akhurst RJ.** 1980. Morphological and functional dimorphism in *Xenorhabdus* spp., bacteria symbiotically associated with the insect pathogenic nematodes *Neoaplectana* and *Heterorhabditis*. *J Gen Microbiol* **121**:303-310.
50. **Martens EC, Russell FM, Goodrich-Blair H.** 2005. Analysis of *Xenorhabdus nematophila* metabolic mutants yields insight into stages of *Steinernema carpocapsae* nematode intestinal colonization. *Mol Microbiol* **51**:28-45.

51. **Cowles CE, Goodrich-Blair H.** 2008. The *Xenorhabdus nematophila* *niABC* genes confer the ability of *Xenorhabdus* spp. to colonize *Steinernema carpocapsae* nematodes. *J Bacteriol* **190**:4121-4128.
52. **Goetsch M, Owen H, Goldman B, Forst S.** 2006. Analysis of the PixA inclusion body protein of *Xenorhabdus nematophila*. *J Bacteriol* **188**:2706-2710.
53. **Daborn PJ, Waterfield N, Silva CP, Au CP, Sharma S, ffrench-Constant RH.** 2002. A single *Photorhabdus* gene, makes caterpillars floppy (*mcf*), allows *Escherichia coli* to persist within and kill insects. *Proc Natl Acad Sci USA* **99**:10742-10747.
54. **Waterfield N, Daborn PJ, Dowling AJ, Yang G, Hares M, ffrench-Constant RH.** 2003. The insecticidal toxin makes caterpillars floppy 2 (*Mcf2*) shows similarity to *HrmA*, an avirulence protein from a plant pathogen. *FEMS Microbiol Lett* **229**:265-270.
55. **Pechy-Tarr M, Bruck DJ, Maurhofer M, Fischer E, Vogne C, Henkels MD, Donahue KM, Grunder J, Loper JE, Keel C.** 2008. Molecular analysis of a novel gene cluster encoding an insect toxin in plant-associated strains of *Pseudomonas fluorescens*. *Environ Microbiol* **10**:2368-2386.
56. **Marchler-Bauer A, Anderson JB, Chitsaz F, Derbyshire MK, DeWeese-Scott C, Fong JH, Geer LY, Geer RC, Gonzales NR, Gwadz M, He S, Hurwitz DI, Jackson JD, Ke Z, Lanczycki CJ, Liebert CA, Liu C, Lu F, Lu S, Marchler GH, Mullokandov M, Song JS, Tasneem A, Thanki N, Yamashita RA, Zhang D, Zhang N, Bryant SH.** 2009. CDD: specific functional annotation with the Conserved Domain Database. *Nucleic Acids Res* **37**:D205-210.
57. **Marchler-Bauer A, Bryant SH.** 2004. CD-Search: protein domain annotations on the fly. *Nucleic Acids Res* **32**:W327-331.
58. **Marchler-Bauer A, Lu S, Anderson JB, Chitsaz F, Derbyshire MK, DeWeese-Scott C, Fong JH, Geer LY, Geer RC, Gonzales NR, Gwadz M, Hurwitz DI, Jackson JD, Ke Z, Lanczycki CJ, Lu F, Marchler GH, Mullokandov M, Omelchenko MV, Robertson CL, Song JS, Thanki N, Yamashita RA, Zhang D, Zhang N, Zheng C, Bryant SH.** 2011. CDD: a Conserved Domain Database for the functional annotation of proteins. *Nucleic Acids Res* **39**:D225-229.
59. **Jing Y, Toubarro D, Hao Y, Simoes N.** 2010. Cloning, characterisation and heterologous expression of an astacin metalloprotease, Sc-AST, from the entomoparasitic nematode *Steinernema carpocapsae*. *Mol Biochem Parasitol* **174**:101-108.
60. **Toubarro D, Lucena-Robles M, Nascimento G, Santos R, Montiel R, Verissimo P, Pires E, Faro C, Coelho AV, Simoes N.** 2010. Serine protease-mediated host invasion by the parasitic nematode *Steinernema carpocapsae*. *J Biol Chem* **285**:30666-30675.
61. **Park Y, Herbert EE, Cowles CE, Cowles KN, Menard ML, Orchard SS, Goodrich-Blair H.** 2007. Clonal variation in *Xenorhabdus nematophila* virulence and suppression of *Manduca sexta* immunity. *Cell Microbiol* **9**:645-656.

62. **ffrench-Constant R, Waterfield N.** 2006. An ABC guide to the bacterial toxin complexes. *Adv Appl Microbiol* **58**:169-183.
63. **Chaston JM, Suen G, Tucker SL, Andersen AW, Bhasin A, Bode E, Bode HB, Brachmann AO, Cowles CE, Cowles KN, Darby C, de Léon L, Drace K, Du Z, Givaudan A, Herbert Tran EE, Jewell KA, Knack JJ, Krasomil-Osterfeld KC, Kukor R, Lanois A, Latreille P, Leimgruber NK, Lipke CM, Liu R, Lu X, Martens EC, Marri PR, Médigue C, Menard ML, Miller NM, Morales-Soto N, Norton S, Ogier J-C, Orchard SS, Park D, Park Y, Qurollo BA, Sugar DR, Richards GR, Rouy Z, Slominski B, Slominski K, Snyder H, Tjaden BC, van der Hoeven R, Welch RD, Wheeler C, Xiang B, Barbazuk B, et al.** The entomopathogenic bacterial endosymbionts *Xenorhabdus* and *Photorhabdus*: Convergent lifestyles from divergent genomes. Submitted.
64. **Sergeant M, Jarrett P, Ousley M, Morgan JA.** 2003. Interactions of insecticidal toxin gene products from *Xenorhabdus nematophilus* PMFI296. *Appl Environ Microbiol* **69**:3344-3349.
65. **Miller JH.** 1972. *Experiments in Molecular Genetics*. Cold Spring Harbor Laboratory Press, Cold Spring Harbor, N. Y.
66. **Xu J, Hurlbert RE.** 1990. Toxicity of irradiated media for *Xenorhabdus* spp. *Appl Environ Microbiol* **56**:815-818.
67. **Vivas EI, Goodrich-Blair H.** 2001. *Xenorhabdus nematophilus* as a model for host-bacterium interactions: *rpoS* is necessary for mutualism with nematodes. *J Bacteriol* **183**:4687-4693.
68. **Orchard SS, Goodrich-Blair H.** 2004. Identification and functional characterization of a *Xenorhabdus nematophila* oligopeptide permease. *Appl Environ Microbiol* **70**:5621-5627.
69. **Rowe GE, Welch RA.** 1994. Assays of hemolytic toxins. *Methods Enzymol* **235**:657-667.
70. **Sierra G.** 1957. A simple method for the detection of lipolytic activity of micro-organisms and some observations on the influence of the contact between cells and fatty substrates. *Antonie van Leeuwenhoek* **23**:15-22.
71. **Boemare N, Thaler, J.O., Lanois, A.** 1997. Simple bacteriological tests for phenotypic characterization of *Xenorhabdus* and *Photorhabdus* phase variants. *Symbiosis* **22**:167-175.
72. **Thaler JO, Duvic B, Givaudan A, Boemare N.** 1998. Isolation and entomotoxic properties of the *Xenorhabdus namatophilus* F1 Lecithinase. *Appl Environ Microbiol* **64**:2367-2373.
73. **Boemare N, Thaler JO, Lanois A.** 1997. Simple bacteriological tests for phenotypic characterization of *Xenorhabdus* and *Photorhabdus* phase variants. *Symbiosis* **22**:167-175.

74. **Moureaux N, Karjalainen T, Givaudan A, Bourlioux P, Boemare N.** 1995. Biochemical characterization and agglutinating properties of *Xenorhabdus nematophilus* F1 fimbriae. *Appl Environ Microbiol* **61**:2707-2712.
75. **Herbert EE, Cowles KN, Goodrich-Blair H.** 2007. CpxRA regulates mutualism and pathogenesis in *Xenorhabdus nematophila*. *Appl Environ Microbiol* **73**:7826-7836.
76. **Lane DJ.** 1991. 16S/23S rRNA sequencing, p 115-175. *In* Stackebrandt E, Goodfellow M (ed), *Nucleic Acid Techniques in Bacterial Systematics*. Blackwell, Oxford.
77. **Altschul SF, Madden TL, Schaffer AA, Zhang J, Zhang Z, Miller W, Lipman DJ.** 1997. Gapped BLAST and PSI-BLAST: a new generation of protein database search programs. *Nucleic Acids Res* **25**:3389-3402.
78. **Bao Y, Lies DP, Fu H, Roberts GP.** 1991. An improved Tn7-based system for the single-copy insertion of cloned genes into chromosomes of Gram-negative bacteria. *Gene* **109**:167-168.
79. **Cowles CE, Goodrich-Blair H.** 2004. Characterization of a lipoprotein, NilC, required by *Xenorhabdus nematophila* for mutualism with its nematode host. *Mol Microbiol* **54**:464-477.
80. **Kaya HK, Stock SP.** 1997. Techniques in insect nematology, p 281-324. *In* Lacey LA (ed), *Manual of Techniques in Insect Pathology*. Academic Press, London.
81. **Heungens K, Cowles CE, Goodrich-Blair H.** 2002. Identification of *Xenorhabdus nematophila* genes required for mutualistic colonization of *Steinernema carpocapsae* nematodes. *Mol Microbiol* **45**:1337-1353.
82. **Wollenberg MS, Ruby EG.** 2009. Population structure of *Vibrio fischeri* within the light organs of *Euprymna scolopes* squid from two Oahu (Hawaii) populations. *Appl Environ Microbiol* **75**:193-202.
83. **Baum JA, Bogaert T, Clinton W, Heck GR, Feldmann P, Ilagan O, Johnson S, Plaetinck G, Munyikwa T, Pleau M, Vaughn T, Roberts J.** 2007. Control of coleopteran insect pests through RNA interference. *Nat Biotechnol* **25**:1322-1326.
84. **Habibi J, Brandt SL, Coudron TA, Wagner RM, Wright MK, Backus EA, Huesing JE.** 2002. Uptake, flow, and digestion of casein and green fluorescent protein in the digestive system of *Lygus hesperus* Knight. *Arch Insect Biochem Physiol* **50**:62-74.
85. **Habibi J, Backus EA, Coudron TA, Brandt SL.** 2001. Effect of different host substrates on hemipteran salivary protein profiles. *Entomol Exp Appl* **98**:369-375.
86. **Simon R, Prierer U, Pühler A.** 1983. A broad host range mobilization system for *in vivo* genetic engineering: transposon mutagenesis in gram negative bacteria. *Biotechnol* **1**:784-791.

APPENDIX 3

Previously unrecognized stages of species-specific colonization in the mutualism
between *Xenorhabdus* bacteria and *Steinernema* nematodes

This appendix has been published as:

Chaston J, **Murfin KE**, Heath-Heckman, EA, and Goodrich-Blair, H. "Previously unrecognized stages of species-specific colonization in the *Xenorhabdus-Steinernema* mutualism" *Cell Microbiol.* 2013 Sep;15(9):1545-59. doi: 10.1111/cmi.12134

ABSTRACT

The specificity of a horizontally transmitted microbial symbiosis is often defined by molecular communication between host and microbe during initial engagement, which can occur in discrete stages. In the symbiosis between *Steinernema* nematodes and *Xenorhabdus* bacteria, previous investigations focused on bacterial colonization of the intestinal lumen (receptacle) of the nematode infective juvenile (IJ), as this was the only known persistent, intimate, and species-specific contact between the two. Here we show that bacteria colonize the anterior intestinal cells of other nematode developmental stages in a species-specific manner. Also, we describe three processes that only occur in juveniles that are destined to become IJs. First, a few bacterial cells colonize the nematode pharyngeal-intestinal valve (PIV) anterior to the intestinal epithelium. Second, the nematode intestine constricts while bacteria initially remain in the PIV. Third, anterior intestinal constriction relaxes and colonizing bacteria occupy the receptacle. At each stage, colonization requires *X. nematophila* symbiosis region 1 (SR1) genes and is species-specific: *X. szentirmai*, which naturally lacks SR1, does not colonize unless SR1 is ectopically expressed. These findings reveal new aspects of *Xenorhabdus* bacteria interactions with and transmission by their *Steinernema* nematode hosts, and demonstrate that bacterial SR1 genes aid in colonizing nematode epithelial surfaces.

INTRODUCTION

Most plants and animals are in contact with diverse bacterial species within their native environments (e.g. (1)). From these varied microbial assemblages, host plants and animals engage in intimate associations with specific microbes by concomitantly recruiting certain partners while excluding non-partners. Such associations can be maintained between generations by vertical or horizontal transmission of the specific microbial partner(s) (symbiont) to progeny: Vertically transmitted symbionts are supplied directly from parent to offspring, typically through the germline, while horizontal acquisition occurs from the environment (reviewed in (2)). In the latter case, within the environment, host offspring may be exposed to many different types of bacteria, forcing the need for selection of specific partners from diverse non-partner species. The molecular and cellular events that allow recognition and acquisition of specific partners from a background of non-partners are beginning to be revealed through the study of several experimentally tractable, naturally occurring, mutually beneficial associations between plants or animals and bacteria (3-5), such as that between entomopathogenic *Steinernema* nematodes and their *Xenorhabdus* bacterial symbionts.

Steinernema nematodes horizontally acquire their beneficial *Xenorhabdus* bacterial partners. The nematode infective juvenile (IJ), a modified J3 or dauer stage of the nematode, carries colonizing bacteria in the receptacle, a structure at the anterior of the nematode intestine ((6-9) see also Figure A3.1). P (parental) generation IJs infect insects, penetrating through natural openings and releasing colonizing bacteria into the insect hemocoel (10). Together the nematode and the bacteria kill the insect and the bacteria divide and provide nutrition, directly or indirectly, to infecting nematodes, which moult from a modified J3 stage into adults that reproduce. F1-generation eggs hatch and moult through juvenile to adult stages. Reproduction continues through two or three generations (11) until conditions inside the cadaver, including low nutrient availability and high nematode density (12), cue IJ development. The IJ receptacle

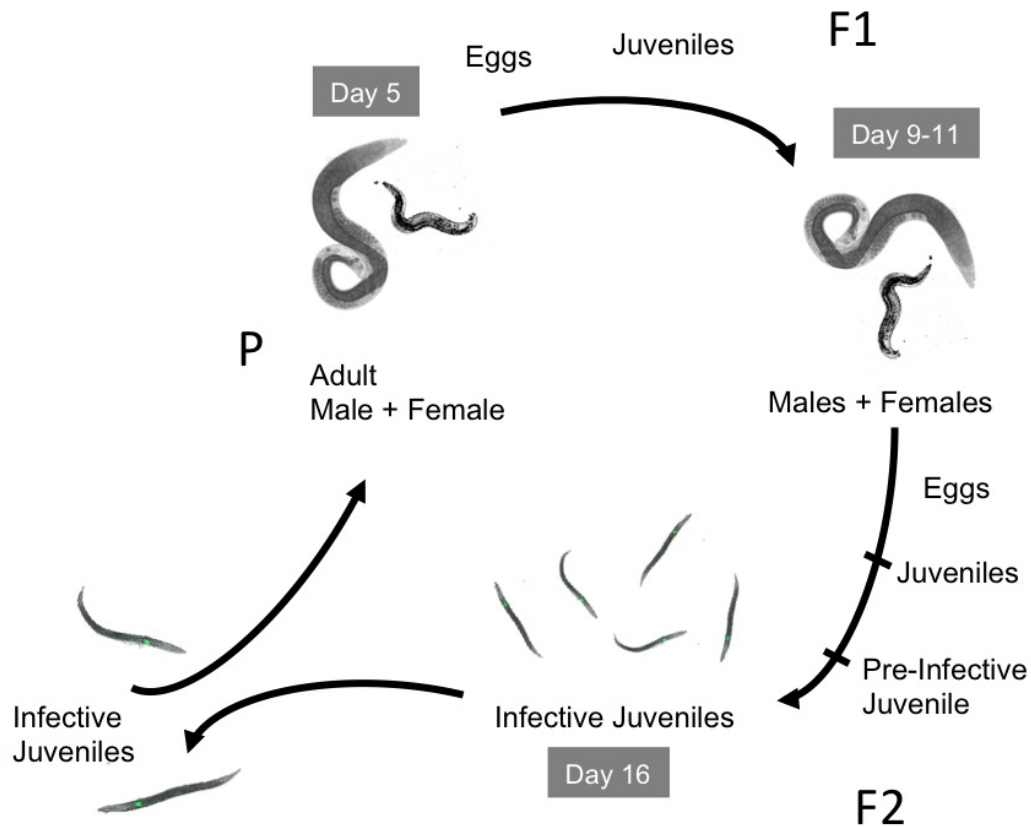


Figure A3.1 Model for nematode reproduction. In the wild, nematode IJs penetrate an insect host, release their bacteria, and develop into reproductive adults that give rise to F1 progeny that also develop into adults and reproduce. The resulting F2 progeny develop into pre-IJs that reacquire their symbiotic bacteria, develop into IJs, and leave the insect host in search of new prey. In this study, nematodes were grown on lipid agar medium in the laboratory, and the life cycle followed the same scheme. Nematode development was not synchronized within the population, but days indicated give approximate timing of generations during growth on laboratory medium. The figure is adapted from (11).

is formed as the lumen between two nucleated intestinal cells, and becomes recolonized with bacteria (8, 13). The IJ migrates away from the insect cadaver seeking a new living host insect to infect. This growth cycle can be recapitulated in the laboratory on artificial media (14-17).

Previous studies revealed early events in and features of *X. nematophila* colonization of the receptacle in *S. carpocapsae* IJs. The population of bacteria within a *S. carpocapsae* IJ receptacle is founded by one or a few colonizing *X. nematophila* cells: most individual IJs that form in the presence of multiple clonal variants of wild type *X. nematophila* are colonized by only one clone (Martens *et al.*, 2003). In newly formed (immature) IJs, an oligo-colonized state has been observed, in which fewer than 10 individual bacterial cells can be seen within the receptacle (18), often adhering to a nematode-derived anucleate cluster of spherical bodies collectively called the intravesicular structure (IVS) (13, 19). A mucus-like substance surrounding the IVS stains positively with wheat-germ agglutinin, suggesting the presence of *N*-acetyl glucosamine or *N*-acetyl neuraminic acid (13). As the IJ matures over the course of approximately one week, the few colonizing bacteria within the receptacle grow to a final population of ~ 50-200 bacterial cells (18). *X. nematophila* mutants defective in the synthesis of certain vitamins or amino acids fail to grow within the receptacle, and ultimately are cleared from this site (13), suggesting the host is capable of eliminating non-cooperative, non-functional symbionts.

Entry into the *Steinernema* nematode receptacle is limited to specific partner *Xenorhabdus* bacteria. For example, *S. feltiae* IJs show preference for colonization by *X. bovienii* strains while *S. carpocapsae* is highly specific for colonization by *X. nematophila* (20-23). In the latter association, molecular determinants, nematode intestine localization (*nil*) factors A, B, and C, have been identified that contribute to specificity. These three genes are encoded on a 3.5-kB genetic locus called symbiosis region 1 (SR1) that is not found in other

Xenorhabdus species, and each is independently necessary for nematode receptacle localization (24). Additionally, SR1 is sufficient to confer entry into the nematode receptacle on otherwise non-colonizing *Xenorhabdus* species (22), albeit with lower levels of colonization than *X. nematophila*. An *X. nematophila* mutant lacking SR1 is not able to colonize the nematode receptacle, but certain mutations in *nilA* or *nilB* lead to a partial colonization defect (22, 24, 25). Analysis of these mutants indicated that the *nil* genes function during entry into and growth within the nematode receptacle. Characterization of the Nil factors has demonstrated that NilB is an outer membrane beta barrel protein (25) and NilC is an outer-membrane-tethered periplasmic lipoprotein (26), suggesting that they may interact directly with host surfaces to mediate host colonization.

Experiments that described *S. carpocapsae* IJ colonization events did not reveal if individual clones of colonizing *X. nematophila* are selected during initiation or outgrowth. Furthermore, the events leading up to the oligo-colonized state of the immature IJ, including the process by which non-partner bacteria are excluded, have not been elucidated. To lend insights into these questions, we characterized *X. nematophila* colonization of *S. carpocapsae* adult and juvenile stages that precede IJ formation. We further interrogated the specificity of these events in *S. carpocapsae* using a *X. nematophila* non-colonizing Δ SR1 mutant and a non-colonizing, non-native *Xenorhabdus* species, *X. szentirmaii*. Finally, we demonstrate the conservation of the colonization process among members of the *Steinernema* genus by investigating early host-association events of *S. feltiae* and its symbiont, *X. bovienii*.

RESULTS

***X. nematophila* bacteria colonize the anterior intestinal epithelia of adult and juvenile**

stage *S. carpocapsae* nematodes. To observe colonization events between *X. nematophila* and *S. carpocapsae* nematodes we engineered *X. nematophila* to express the green fluorescent protein (GFP), allowing visualization of single bacterial cells inside nematodes (Martens *et al.*, 2003, Martens *et al.*, 2005, Sugar *et al.*, 2012, Murfin *et al.*, 2012) and categorization of nematodes as colonized or un-colonized as they developed on lipid agar plates. Lack of synchrony in nematode development precluded definitive temporal assignment of events, and the exact timing of nematode development varied within and across generations in multiple experiments. Nonetheless, bacterial localization patterns in the animal host over time (days and nematode generations) were reproducible across multiple experiments relative to nematode developmental changes. Unexpectedly, we observed that adult and juvenile nematodes developing on lipid agar plates were colonized by *X. nematophila* bacteria. Adults in all generations had bacterial cells clustered on the epithelial cell surface within the anterior intestinal lumen (Figure A3.2 C-D). As in many nematode taxa, this intestinal region formed a caecum surrounding the basal bulb, a posterior portion of the pharynx that pumps and grinds food (27), and the pharyngeal-intestinal valve (PIV), a compact set of cells that form a channel linking the pharyngeal and intestinal lumina (Figure A3.2 A) (28, 29). The bacteria colonizing this region in adults were not likely to be transmitted directly to progeny, since eggs laid in the surrounding media were not visibly associated with bacteria (data not shown). In addition, recently hatched juvenile nematodes lacked anterior intestine localization of bacteria (Figure A3.2 B). This un-colonized state was transient and soon after hatching juvenile nematodes were apparent with bacteria that localized to the anterior intestinal caecum (AIC) (Figure A3.2 E-F). Thus, bacterial localization at the AIC occurred in both juvenile and adult stages of nematodes. GFP-expressing bacteria were often visible indiscriminately throughout the

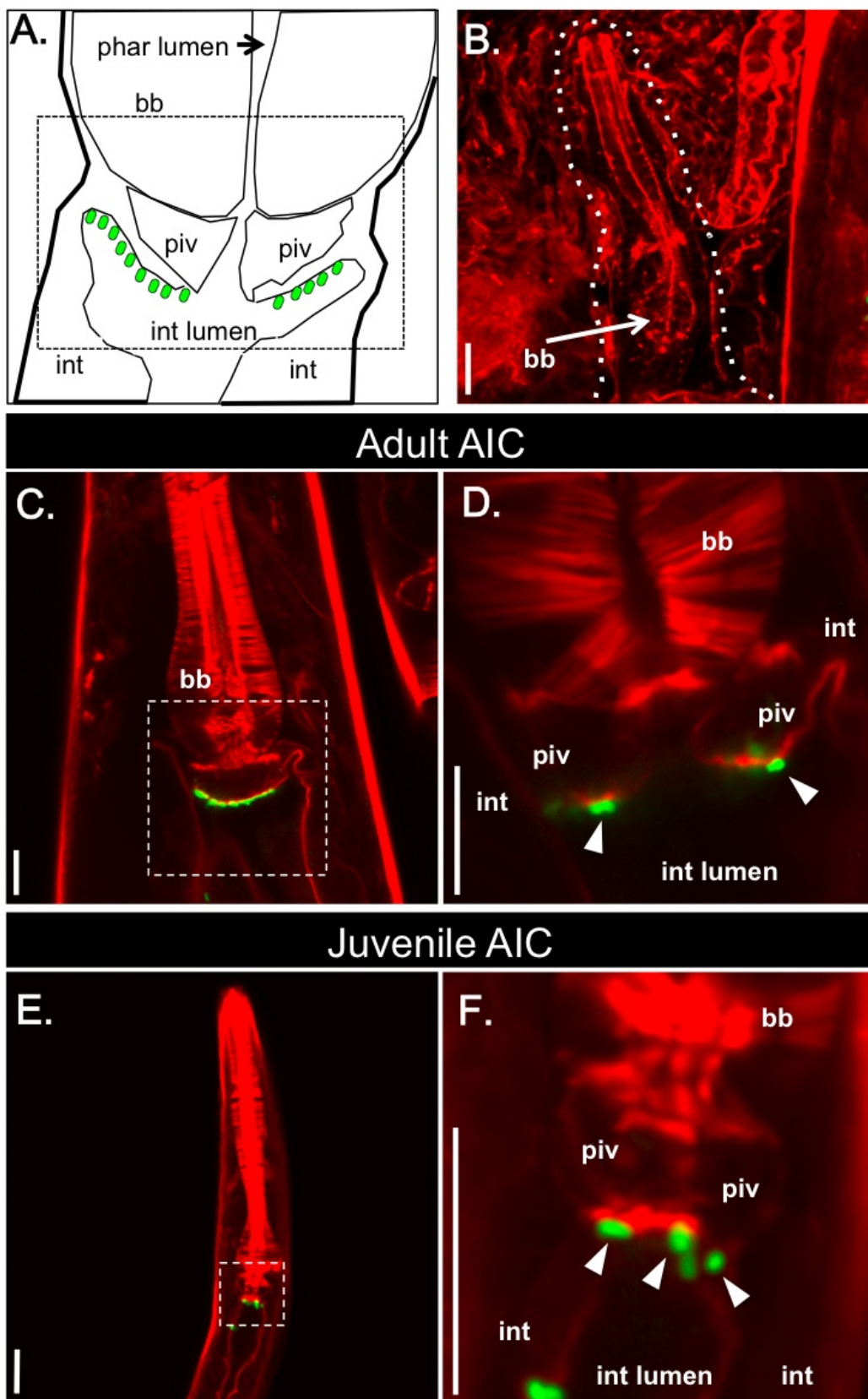


Figure A3.2 *X. nematophila* bacteria localize specifically to the anterior intestinal caecum (AIC) in adult and juvenile *S. carpocapsae* nematodes. *S. carpocapsae* nematode tissue is stained with rhodamine phalloidin (f-actin; red) and *X. nematophila* bacteria express green-fluorescent protein (green). A) Schematic diagram representing the pharyngeal region, based on a transmission electron micrograph of a *Caenorhabditis elegans* hermaphrodite nematode (<http://www.wormatlas.org/hermaphrodite/pharynx/Images/phafig11leg.htm>). AIC-localized *X. nematophila* cells are represented by green ovals. B) A recently hatched juvenile nematode lacks AIC-localized *X. nematophila*. A white dashed line outlines the juvenile, next to an adult nematode (at right). C) An adult *S. carpocapsae* female with AIC-localized *X. nematophila*. D) Enlarged image of the boxed region in (C) at a different tissue depth, in which individual bacterial cells expressing GFP are visible (arrowheads); the focal plane of the image in (C) reveals the lumen of the pharyngeal intestinal valve (piv), and the presence of bacteria on the intestinal tissue surface. E) *S. carpocapsae* juvenile nematode with *X. nematophila* bacteria localized at the AIC. F) Enlarged image of the nematode shown in E (boxed region) at a different tissue depth with visible GFP-expressing *X. nematophila* cells (arrowheads) colonizing the AIC. Pharyngeal lumen (phar lumen); basal bulb (bb), pharyngeal-intestinal valve (piv); intestinal cells (int), intestinal lumen (int lumen). Scale bars = 10 μm .

intestine of developing nematodes at all stages (data not shown), consistent with the fact that *S. carpocapsae* is bacteriovorous and may be digesting some *X. nematophila* cells (30).

***X. nematophila* colonize the *S. carpocapsae* pharyngeal-intestinal valve region of pre-IJs.**

In the F2 generation, *S. carpocapsae* juveniles undergo an alternate developmental pathway leading from J2 juveniles to the IJ (Figure A3.1). During this generation, prior to IJ development, J2 juveniles (scored based on their size) lacked AIC-localized bacteria and instead had one or a few individual cells associated with the PIV (Figure A3.3 A,B). At this stage, in nematodes with PIV-localized bacteria, the intestinal space was open (Figure A3.3 A).

Using confocal microscopy we sought to determine if PIV-localized bacteria are intracellular within PIV cells or extracellular within a luminal PIV space. A 3-D model of a PIV, constructed from a series of sequential confocal micrographs showed regions devoid of f-actin staining that linked the PIV with the intestinal lumen (Supp. movie 1; the series of images prior to 3-D reconstruction is shown in Supp. movie 2). Bacteria within the PIV had relatively large unstained regions around them, possibly suggesting an extracellular luminal space or pouch within which the bacteria reside. Further, multiple bacterial cells appeared to be in the process of entering or exiting the PIV without being entirely surrounded by stained actin, suggesting the possibility that the bacteria enter the PIV without being intracellular. Although not conclusive, these data are most consistent with a model that *X. nematophila* gain entry to the PIV through extracellular channels and colonize an extracellular pouch within the PIV.

Following the appearance of PIV localization, nematodes with constricted intestines were observed (Figure A3.3 C-D). When nematodes with constricted intestines first appeared, colonizing bacteria remained localized in the PIV: close inspection by rhodamine phalloidin staining of a subset of nematodes with constricted intestines revealed PIV-associated bacteria (Figure A3.3 D). As nematode development progressed toward the IJ stage the formation of the

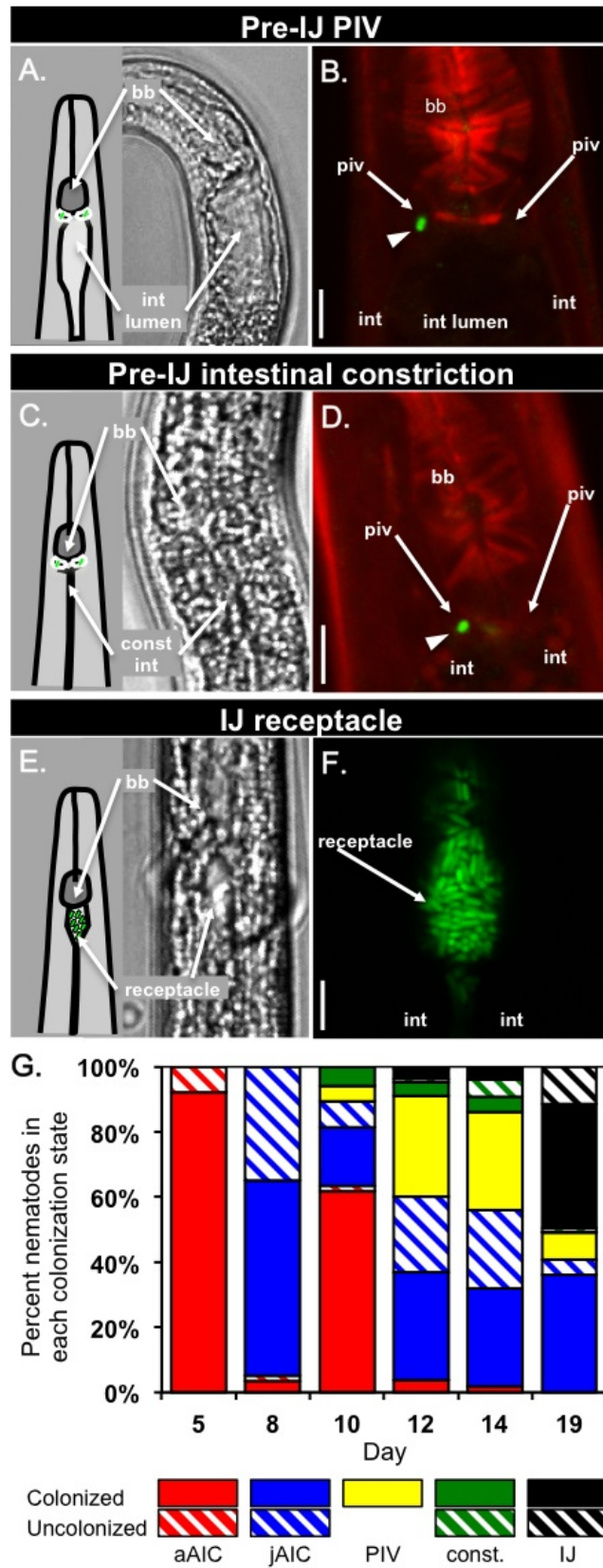


Figure A3.3 Bacterial colonization and intestinal constriction of nematode pre-IJ

stages. DIC images (A, C, E) were taken on a Nikon Eclipse TE300 inverted microscope.

Confocal images (B, D, F) of different nematodes at similar stages as in A, C, and E were taken on a Zeiss LSM 510 confocal microscope. A-B) In pre-IJ nematodes with one or a few bacterial

cells visible within the PIV region (one bacterial cell is visible in the focal plane in panel B

(arrowhead)) the intestinal lumen is open (arrow in A; black space in B). C-D) Pre-IJs in the

population exhibit a constricted intestine (IC; compare panels C and A) and bacterial cells are

visible in or near the PIV. Note that spheres in panel D are within nematode tissue and not the

intestinal lumen. E-F) Subsequently, nematodes display de-constriction of the anterior intestine

and *X. nematophila* bacteria are apparent within the resulting receptacle space. In B and D

nematode tissue is stained with rhodamine phalloidin (f-actin; red). In B, D, and F, *X.*

nematophila express green-fluorescent protein (green). G) The average frequency of adults and

juveniles with bacteria localized at different tissues over time in a representative experiment

(see legend). Abbreviations: basal bulb (bb); pharyngeal-intestinal valve (piv); intestinal lumen

(int lumen); intestinal epithelium cells (int); constricted intestine (const int). Legend

abbreviations: adult AIC (aAIC), juvenile AIC (jAIC), intestinal constriction (const.). Scale bars =

5 μ m.

nematode outer cuticle, which limits penetration by stains and dyes, confounded subsequent observation of stained PIV tissues by confocal microscopy. Therefore, at later time points, we were unable to determine if bacteria within nematodes with constricted intestines occupied the PIV or the constricted intestinal lumen. As the constricted intestine phenotype became less frequent, most nematodes in the population were IJs with colonized receptacles (Fig 3E-F).

The events occurring during IJ development can be categorized into at least three sequential and distinct steps: 1) colonization of the PIV by a few bacterial cells (Figure A3.3 A-B); 2) constriction of the nematode intestine, with bacteria colonizing the PIV at least through early stages of this process (Figure A3.3 C-D); 3) expansion of the anterior intestine to form a receptacle with colonizing bacteria (Figure A3.3 E-F). These events were unique to F2 generation juveniles that would become IJs and were not observed in F1 generation juveniles that moulted from J1 directly through J4 stages into adults. Therefore, they are part of a developmental process specific to IJ development and hereafter we refer to any nematodes that undergo these processes as pre-IJs.

Taken together, these findings demonstrate that *X. nematophila* bacteria associate with previously unrecognized *S. carpocapsae* nematodes tissues and life stages. The frequency of each type of colonization changed over time, with AIC localization, PIV localization, PIV colonization during intestinal constriction, and receptacle colonization occurring sequentially (Figure A3.3 G; a representative experiment). Also, these events occurred in most of the nematodes (Table A3.1). To assess if these events occur in nematodes that develop inside insects, we co-injected axenic nematodes and GFP-expressing *X. nematophila* bacteria into *Galleria mellonella* waxworm larvae and observed the colonization status of nematodes every 2 days from the appearance of F1 nematodes to IJ development. More than 85% of nematodes carried colonizing bacteria at each time point, and each colonization state (adult AIC, juvenile

Table A3.1. Composite *S. carpocapsae* colonization data^a

	<i>X. nematophila</i>		<i>X. szentirmaii</i>	
	SR1+ (wild-type)	ΔSR1	SR1- (wild-type)	SR1+
Adult AIC	95.4% (350) ^A	16.7% (323) ^B	14.1% (814) ^B	83.4% (825) ^C
Juvenile AIC	81.4% (1834) ^A	10.3% (2374) ^B	6.2% (2894) ^C	64.8% (2899) ^D
Pre-IJ PIV	60.4% (546) ^A	0.1% (1569) ^B	0.1% (2485) ^B	15.4% (1069) ^C
Pre-IJ constricted intestine	66.4% (235) ^A	0% (285) ^B	0.3% (367) ^B	29.1% (492) ^C
IJ receptacle colonization	79.3% (767) ^A	0.5% (765) ^B	0.8% (1322) ^B	31.7% (1299) ^C

^aData represent combined total frequency of localization in different nematode stages and tissues from three (*X. nematophila*) or four (*X. szentirmaii*) independent experiments. The total number of nematodes counted in each category is indicated in parentheses. Within each nematode life stage, values with the same letter were not significantly different from each other (Fisher's exact test; $P < 0.001$).

AIC, PIV colonization, intestinal constriction, and IJ receptacle colonization) was observed in at least one time point for each experiment (data not shown). These findings demonstrate that these events occur in nematodes developing within a host and are not an artefact of laboratory culture.

***X. nematophila* colonization of the AIC and PIV requires SR1 genes.** *X. nematophila nilA*, *nilB*, and *nilC*, encoded on SR1, are necessary for *X. nematophila* and sufficient for other *Xenorhabdus* species to colonize the IJ receptacle of *S. carpocapsae* (22, 24). To assess if SR1 contributes to the colonization events described above, we monitored the localization of a GFP-expressing *X. nematophila* Δ SR1 deletion mutant in adult, juvenile, and pre-IJ nematodes relative to age-matched nematodes colonized with GFP-expressing *X. nematophila*. Combined across all experiments and time points, the frequency of *S. carpocapsae* AIC colonization by the *X. nematophila* Δ SR1 deletion mutant was significantly lower than the frequency of AIC colonization by wild type *X. nematophila* ($p < 0.05$; Figure A3.4 A-C). When considering individual time points most displayed significant differences between AIC-colonization frequencies of Δ SR1 deletion mutant and wild-type-*X. nematophila* in age-matched nematodes ($p < 0.05$; data not shown). These data demonstrate that SR1 contributes to colonization of the nematode AIC, though the effect is only experimentally significant after the initial P-generation.

Juveniles and pre-IJs are not morphologically distinguishable by our methods, so we defined pre-IJs by their occurrence in the F2 generation on wild type *X. nematophila* lawns concomitant with PIV-colonization and intestinal constriction. We therefore predicted the timing of nematode pre-IJ formation on Δ SR1 mutant lawns based on comparison to wild type controls within each experiment. When pre-IJs were developing on wild-type lawns, nearly all of the juvenile nematodes developing on the Δ SR1 mutant lacked PIV-colonizing bacteria (Figure A3.4A,D). This low frequency of PIV colonization demonstrates the Δ SR1 mutant has a

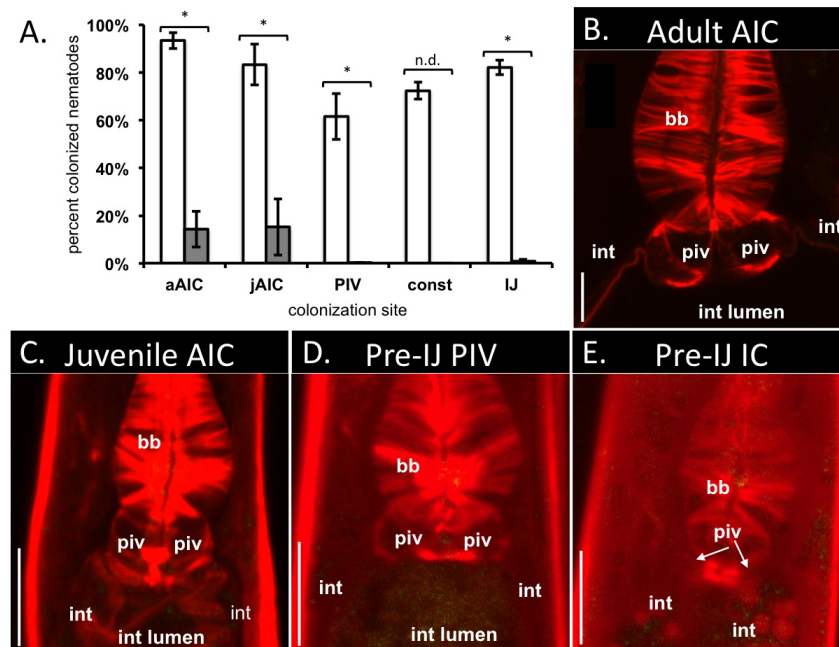


Figure A3.4 *X. nematophila* requires SR1 for localization to the AIC and PIV. Nematodes were grown on a GFP-expressing *X. nematophila* Δ SR1 mutant (green; no bacteria visible) or wild type and actin was visualized with rhodamine phalloidin (actin; red). A) Average (\pm S.E.M.) frequency of nematode colonization for adults, juveniles, pre-IJs, and IJs by *X. nematophila* wild type (Tn7-SR1) (white bars) or a Δ SR1 mutant (gray bars). Significantly fewer nematodes carried colonizing Δ SR1 mutant bacteria than wild type bacteria in each tested colonization state.. Statistical significance was determined using a generalized linear mixed effects model ($p < 0.05$). B, C) Unlike wild type *X. nematophila*, the Δ SR1 mutant did not localize to the AIC of most adult (B) or juvenile (C) nematodes. D, E) F2 juvenile nematodes that were developmentally similar to pre-IJs did not display PIV colonization (pre-IJ PIV) either prior to (D) or during pre-IJ intestinal constriction (IC) (E). Abbreviations: basal bulb (bb); pharyngeal-intestinal valve (piv); intestinal lumen (int lumen); intestinal epithelium cells (int), adult AIC (aAIC), juvenile AIC (jAIC), intestinal constriction (const), statistics not determined (n.d.). Nematode actin was stained with rhodamine-phalloidin (red) and bacteria expressed green fluorescent protein (green). Size bars: 10 μ m.

severe and significant defect in colonizing the nematode PIV (Figure A3.4 A). Similarly, no nematodes with visibly constricted intestines had colonizing bacteria (e.g. Figure A3.4 E; see methods for why statistics were not performed), and only 4 of 765 IJs carried colonizing bacteria. This frequency of IJ receptacle colonization is much higher than those reported for this Δ SR1 mutant within mature IJs (~0.05%) (25). However, there is precedence for *X. nematophila* mutants initially colonizing immature IJs then disappearing from the IJ population over time after failing to grow within the receptacle (31). At least one of the SR1 genes has been implicated not only in initiation of colonization but also in growth within the receptacle (22). Therefore, the relatively high frequency of colonization observed in this study may reflect that the immature IJs we examined have not yet cleared the Δ SR1 mutant from their receptacles. Regardless, the Δ SR1 mutant colonized significantly fewer IJs than wild type *X. nematophila* (Figure A3.4 A). These findings indicate that the Δ SR1 mutant is defective in the early stages of nematode colonization during AIC and/or PIV colonization.

We tested if the AIC and PIV colonization defects of the Δ SR1 mutant also occur during nematode development in *G. mellonella* insect hosts. When we injected *G. mellonella* with axenic IJs and the GFP-expressing Δ SR1 mutant, we observed similar trends as when nematodes were raised on laboratory media. At the AIC colonization stage, the frequency of nematodes with colonizing Δ SR1 bacteria was higher in insects (up to 50% colonized nematodes) than *in vitro* conditions, but was still less than the frequency of colonization with wild type (~85%). As pre-IJs and IJs dominated the population in later time points, fewer than 5% of nematodes were colonized (data not shown).

X. nematophila* SR1 is sufficient for *X. szentirmaii* AIC and PIV colonization of *S.

***carpocapsae* nematodes.** We have shown that SR1 is necessary for normal *X. nematophila* localization to *S. carpocapsae* AIC and PIV tissues. Since, other than *X. nematophila*, SR1 is

absent from all *Xenorhabdus* species tested to date (22, 24), we reasoned that non-native *Xenorhabdus* species should not colonize *S. carpocapsae* AIC and PIV tissues. To test this we cultivated *S. carpocapsae* on GFP-expressing *X. szentirmaii* (Figure A3.5 A). *S. carpocapsae* developed on *X. szentirmaii* lawns, in contrast to previous unsuccessful attempts (22), possibly due to some unknown aspect of technical variability (e.g. agar thickness, absolute temperature). Over 4 experiments, most adult and juvenile nematodes lacked AIC-localized *X. szentirmaii* bacteria (Figure A3.5 A-C), and nearly all late-stage nematodes lacked tissue localized bacteria. Out of 3356 juveniles and pre-IJs observed, 3 nematodes carried PIV-localized bacteria and 1 nematode carried bacteria during intestinal constriction. Of the 1322 progeny IJs observed, 10 carried receptacle-colonizing bacteria.

In contrast, when we provided SR1 to GFP-expressing *X. szentirmaii*, the bacteria localized to specific nematode tissues at significantly higher frequencies during all stages ($p < 0.05$, Figure A3.5 A) except intestinal constriction ($p = 0.14$). Across 4 experiments, 77% of adult nematodes and 57% of juveniles had AIC-colonizing *X. szentirmaii* carrying SR1. *S. carpocapsae* AIC colonization by *X. szentirmaii*-SR1 was not visibly distinguishable from AIC-colonization by *X. nematophila* bacteria (Figure A3.5 D-E). Further, as pre-IJs developed, bacteria were localized within the PIV of 26% of juvenile nematodes (Figure A3.5 F), and colonized 21% of nematodes with constricted intestines and 35% of IJ receptacles. Variation across experiments likely contributed to the fact that differences due to SR1 in *X. szentirmaii* colonization of nematodes with constricted intestines were not significant. Regardless, our data show that *X. szentirmaii* carrying SR1 are able to colonize the AIC, PIV, and receptacle of *S. carpocapsae* nematodes.

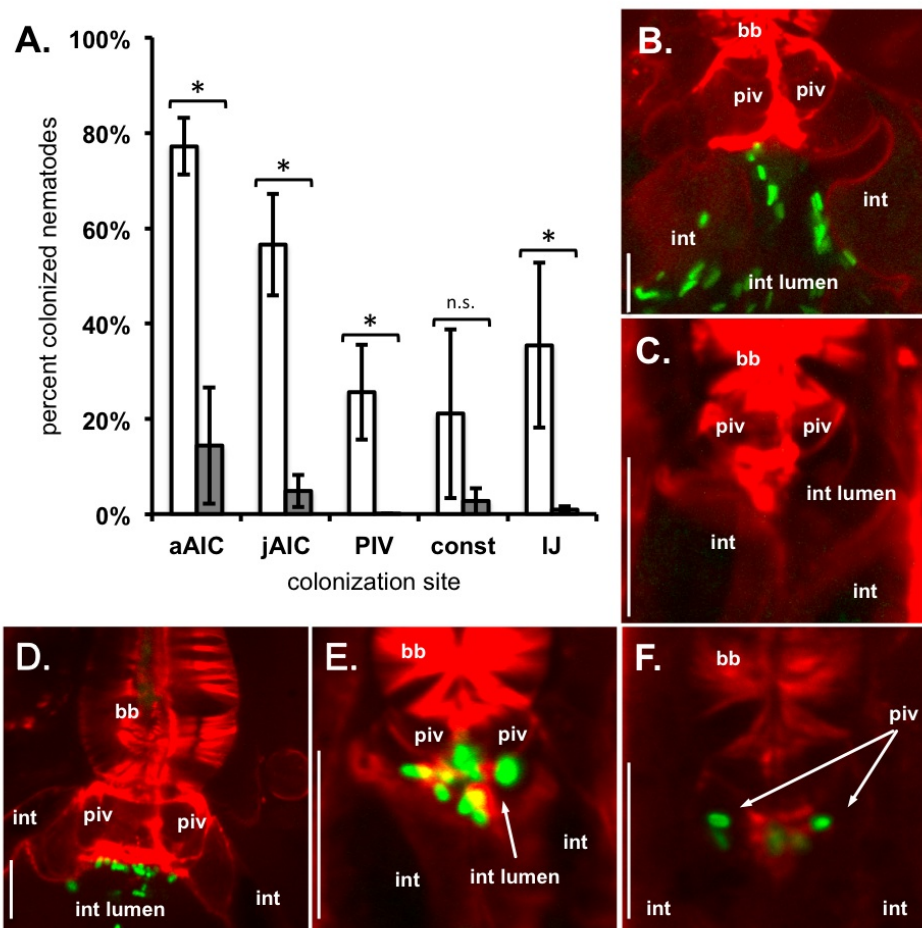


Figure A3.5 *X. nematophila* SR1 confers upon *X. szentirmaii* the ability to colonize the

AIC and PIV of *S. carpocapsae* nematodes. *S. carpocapsae* nematodes were grown on GFP-expressing *X. szentirmaii* strains carrying either Tn7/SR1 or empty Tn7. Developing nematodes were visualized by confocal microscopy. *S. carpocapsae* nematode actin was stained with rhodamine-phalloidin (red) and *X. nematophila* bacteria expressed green-fluorescent protein (green). A) Average (\pm S.E.M.) frequency of nematode colonization for adults, juveniles, pre-IJs, and IJs by *X. szentirmaii* Tn7/SR1 (white bars) or *X. szentirmaii* empty Tn7 (wild type) (grey bars). When *X. szentirmaii* did not contain SR1, significantly fewer nematodes carried colonizing bacteria in each colonization state except pre-IJs during intestinal constriction ($p = 0.14$). Statistical significance was determined using a generalized linear mixed effects model ($p < 0.05$). B, C) *X. szentirmaii* eTn7 (lacking SR1) does not localize to *S. carpocapsae* adult (B) or juvenile (C) AIC. D, E) *X. szentirmaii* Tn7/SR1 (carrying SR1) localizes to the AIC of adult (D) and juvenile (E) nematodes. F) *X. nematophila* bacteria localize to the pre-IJ PIV. Abbreviations: basal bulb (bb); pharyngeal-intestinal valve (piv); intestinal lumen (int lumen); intestinal epithelium cells (int); adult AIC (aAIC); juvenile AIC (jAIC); intestinal constriction (const); no statistical difference (n.s.). Size bars: 10 μm .

AIC and PIV colonization are not unique to the *S. carpocapsae* - *X. nematophila*

mutualism. Since SR1 is necessary for AIC and PIV colonization, is sufficient to confer at least the AIC phenotype, and is specific to *X. nematophila*, it is possible that the events we have described here are unique to the *S. carpocapsae* – *X. nematophila* mutualism. To address this possibility, we examined early colonization events in another *Steinernema* species, *S. feltiae*, by its *Xenorhabdus* symbiont, *X. bovienii*. *X. bovienii* strains do not appear to encode SR1 (unpubl. data), its hosts (including *S. feltiae*) are in different phylogenetic sub-clades than *S. carpocapsae* (32), and the receptacle structures of its hosts are distinct from those of *S. carpocapsae*: *X. bovienii* host receptacles have a non-cellular envelope (vesicle) that encloses *X. bovienii* symbionts (19). These differences lend strength to the hypothesis that if *X. bovienii* engages in AIC and PIV colonization during intestinal constriction with its animal host, these events may be conserved among *Xenorhabdus/Steinernema* associations. Using liver-kidney agar cultivation (a medium that supports higher colonization frequency for *S. feltiae* nematodes than does lipid agar medium), GFP-expressing *X. bovienii* bacteria were observed localized at the AIC of both adult and juvenile *S. feltiae* nematodes (Figure A3.6 B-C). Further, in the F2 generation when pre-IJs are expected to form, we observed individual PIV-localized *X. bovienii* (Figure A3.6 D). PIV colonization was also observed in *S. feltiae* nematodes with constricted intestines, and in those in which the cuticle and sealed mouth deterred staining (Figure A3.6 E). In subsequent time points, *S. feltiae* nematodes were present in which *X. bovienii* had fully colonized the vesicle within the receptacle (Figure A3.6 F). Most nematodes carried bacteria localized to these specific tissues (Figure A3.6 A, Table A3.2). Overall, our data indicate that different *Steinernema* nematodes undergo similar events during colonization by their respective *Xenorhabdus* bacterial symbionts. We note that receptacle-localized *X. bovienii* were long rods, similar to a previous report of another *X. bovienii* strain (SS-2004) colonizing *Steinernema jolietti* nematodes (33), but *X. bovienii* cells were short rods during AIC and early PIV colonization,

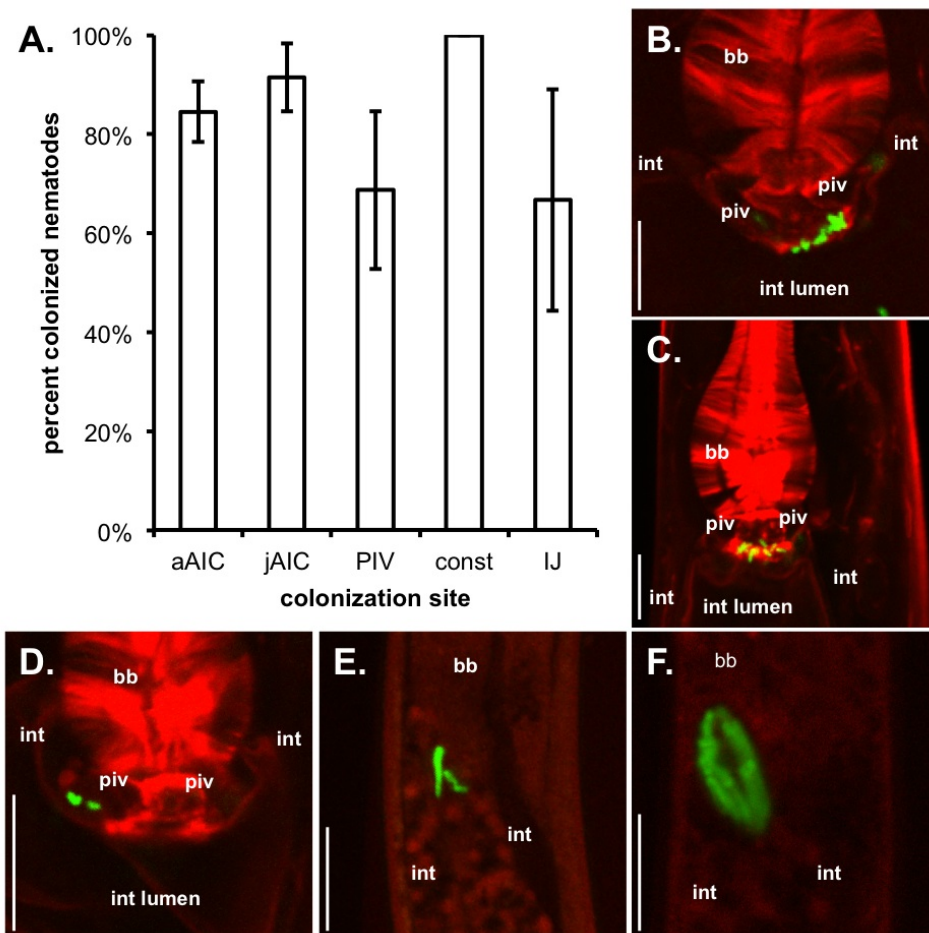


Figure A3.6 Spatial and temporal events in the *X. nematophila* / *S. carpocapsae* association are observed in the association between *X. bovienii* and *S. feltiae*. Nematodes were grown on a GFP-expressing *X. bovienii* and bacterial localization to nematode specific tissues was observed over an 11-day period until infective juveniles made up > 50% of the nematode population. A) Average adult, juvenile, pre-IJ, and IJ colonization (+/- S.E.M.). B) Localization of *X. bovienii* bacteria to the anterior intestinal caecum (AIC) of adult *S. feltiae* nematodes. C) AIC localization of *X. bovienii* bacteria in juvenile *S. feltiae* nematodes. D) Pharyngeal intestinal valve (PIV) colonization by *X. bovienii* bacteria in pre-infective juvenile (pre-IJ) nematodes. E) *X. bovienii* localization at the anterior of the constricted pre-IJ intestine (IJ). F) Colonization of the *S. feltiae* receptacle by *X. bovienii* bacteria. Abbreviations: basal bulb (bb); pharyngeal-intestinal valve (piv); intestinal lumen (int lumen); intestinal epithelium cells (int). Legend abbreviations: adult AIC (aAIC); juvenile AIC (jAIC); intestinal constriction (const). Nematode actin was stained with rhodamine-phalloidin (red) and bacteria expressed green fluorescent protein (green). Size bars: 10 μ m.

Table A3.2 Composite frequency of *X. bovienii* tissue localization in *S. feltiae*^a

Stage and Tissue	Frequency of localization
Adult AIC	100.0% (250)
Juvenile AIC	95.7% (3095)
Pre-IJ PIV	71.5% (467)
Pre-IJ constricted intestine	100.0% (222)
IJ receptacle colonization	73.9% (1481)

^aData represent combined totals from two independent experiments, each with three replicates. The total number of counted nematodes is indicated in parentheses.

suggesting physiological differences of the cells at these stages relative to those in the receptacle.

CONCLUSIONS

In this study we report heretofore-unrecognized stages of intimate association between *Xenorhabdus* bacteria and *Steinernema* nematodes. It has long been held that the *Steinernema* IJ is the only life stage of the nematode that is specifically colonized by bacteria, and that interactions between other *S. carpocapsae* life stages are transient and non-specific. Reasons for this supposition include that the IJ carries the bacteria in an easily observed discrete location (the receptacle) while other stages lack obvious specialized structures for harboring bacteria (6, 34). Also, intimate bacterial colonization of the IJ, in contrast to other life stages, serves a clear and essential function in the symbiosis: transmission of the symbiont between insect hosts. Finally, a practical reason is that IJs, relative to the other stages, can be easily isolated and assessed for internal bacterial content (18). In this work we were able to move beyond this technical hurdle by using GFP-expressing bacteria and fluorescence microscopy to monitor bacterial colonization (33, 35) throughout the life cycles of two *Steinernema* species from different phylogenetic sub-clades (32). Our findings challenge previously held notions by revealing that throughout the reproductive life cycle of both *Steinernema* species bacteria colonize nematode tissues in the region around the pharyngeal-intestinal junction. Bacterial cells colonized the anterior, but not other areas, of the intestines of adults and juveniles from F1 and F2 generations (Figs. 2 and 6). Then, as IJs formed, three novel events were observed: 1) individual bacterial cell colonization of the PIV of pre-IJs; 2) constriction of the nematode intestine; and 3) de-constriction of only the anterior-most regions of the intestine to form the receptacle, which was colonized by bacteria concomitant with formation of the IJ cuticle.

Taken together with previous findings, our work suggests a temporal model of colonization events occurring during the *Steinernema* life cycle, summarized in Figure A3.7.

First, through post-hatching feeding by the nematode (e.g. Figure A3.7 D), the bacteria must gain access to and survive within the nematode intestine. Next, the bacteria localize to the AIC (Figure A3.7 C,E). In the F2 generation of juveniles, comprised of pre-IJs that will become IJs, AIC colonization decreases in frequency, while PIV colonization frequency increases, followed by constriction of almost all of the nematode intestine (Figure A3.7 G, H). At some stage following PIV colonization and intestinal constriction, the anterior of the intestine de-constricts and bacteria are observed attached to the IVS in the receptacle (e.g. (13)). We were unable to document the transition from PIV to receptacle colonization because of poor penetration of rhodamine phalloidin through the IJ cuticle. However, it is likely that receptacle bacteria are derived from PIV colonizers, since at this stage of the process the nematode is non-feeding and does not have access to external populations of *Xenorhabdus* bacteria (6, 34). The transition from PIV to receptacle colonization may occur by bacterial migration, or by a developmental process in which the colonized region of the PIV becomes the nematode receptacle. Following association with the IVS, the bacteria divide and fill the receptacle (Figure A3.7 I; (18)).

The same general events shown in Figure A3.7 occur in both *S. carpocapsae* and *S. feltiae*, nematodes that are in distinct phylogenetic sub-clades, indicating that the overall processes are likely conserved among *Steinernema-Xenorhabdus* symbioses. However, since *S. carpocapsae* and *S. feltiae* IJ receptacles are colonized preferentially by their native symbionts (20-23) some aspect(s) of the interactions between the nematode and bacteria, likely at the molecular level, must allow for recognition and selection of the native symbiont and exclusion of non-native *Xenorhabdus*. In *S. carpocapsae*, specificity occurs during AIC-localization and involves SR1: an *X. nematophila* Δ SR1 mutant localizes to the AIC in fewer *S. carpocapsae* nematodes than does wild type (Figure A3.3 A) and *X. szentirmaii* colonization of these tissues is allowed by the presence of *X. nematophila* SR1 (Figure A3.5). The ability of the

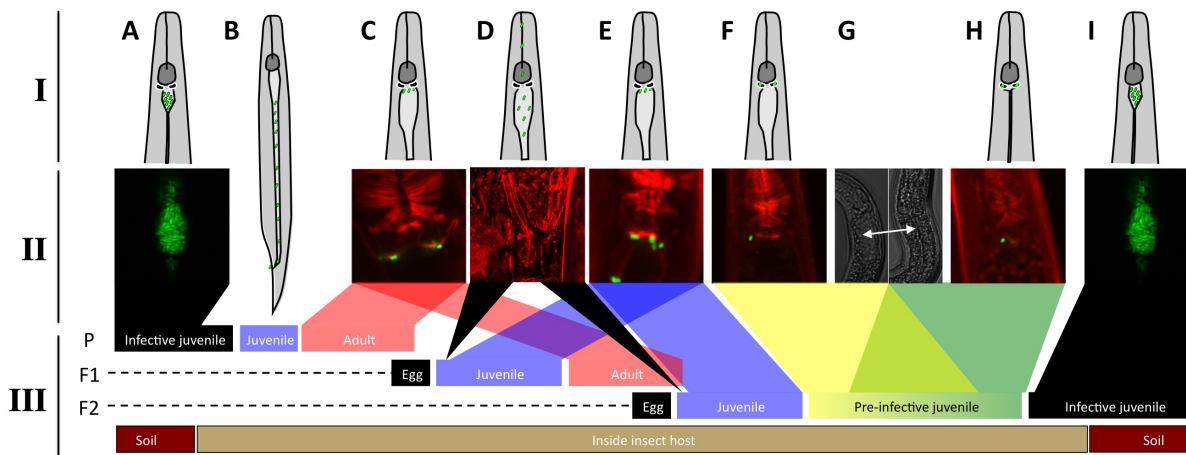


Figure A3.7 Spatial and temporal bacterial colonization events during *Steinerinema* development using schematics (I), representative micrographs (II), and a timeline (III) A) A colonized infective juvenile (IJ) (B) releases its bacteria by defecation after insect penetration (see (49)) and moults into adult stages. C) Adults that develop from IJs carry bacteria localized at the anterior intestinal caecum. D) Newly hatched juvenile nematodes lack bacteria that specifically localize to the anterior intestinal caecum. E) After hatching, juvenile (and later, adult) nematodes have bacteria localized to the anterior intestinal caecum. F2 juveniles carry bacteria at the anterior intestinal caecum, and this generation develops into infective juveniles through a pre-IJ stage. The beginning of pre-IJ development is distinguished by F) bacterial colonization of the PIV, and subsequently, intestinal constriction (G and H). I) After relaxation of the anterior intestinal constriction, bacteria are observed localized to the receptacle and over time bacteria grow to completely fill the receptacle (18). Through these events IJs acquire a complement of symbionts that they carry as they leave the nutrient depleted insect cadaver in search of a new insect host. Abbreviations: parental generation (P), first generation offspring (F1), second-generation offspring (F2)

X. nematophila Δ SR1 mutant to initially localize to the AIC of a small number of adult and juvenile nematodes may indicate that SR1-encoded proteins increase the efficiency of binding to these tissues, or that they are necessary for persistence at this location. Characterizing the roles of other bacterial gene products in each of the stages shown in Figure A3.7 will help demonstrate what other molecular dialogues are at work as *Xenorhabdus* symbionts colonize their nematode hosts.

X. nematophila colonization of the PIV is similar to a process that occurs during *Photorhabdus luminescens* bacterial colonization of the IJ stage of its specific nematode host, *Heterorhabditis bacteriophora* (36). In both systems, bacteria localize to the PIV, indicating this may be a conserved process in Heterorhabditid and Steinernematid nematodes, despite their relatively distant phylogenetic relationship (37). However, subsequent events are likely distinct between genera, since the IJ stage of *H. bacteriophora* lacks a receptacle (instead, bacteria are more widely distributed within a non-constricted intestinal lumen) (38). Also, events preceding PIV colonization differ between these two symbioses. *P. luminescens* bacteria adhere to posterior intestinal cells of adult females prior to invading and replicating within intracellular vacuoles which lyse to inoculate juvenile nematodes inside the maternal body cavity with *P. luminescens*. In neither *S. carpocapsae* nor *S. feltiae* did we observe bacterial binding to or invasion of posterior adult intestinal cells (data not shown).

It was previously demonstrated that *Xenorhabdus* populations face a bottleneck that leads to the clonality of bacteria within the IJ receptacle (18). Clonal symbiont populations have been experimentally demonstrated in multiple mono-specific host-microbe symbioses (18, 33, 39, 40) and suggested qualitatively in others (36, 41, 42). This strain bottlenecking may reduce the prevalence of symbionts that reap host rewards without paying the "goods and services" provided to the host (cheaters; (43)). Bottlenecking may result from non-specific (e.g. spatial restriction) and specific (e.g. molecular recognition) processes that restrict symbiont number

and type during transmission. Since only few individual cells of *X. nematophila* and *X. bovienii* localize to the pre-IJ PIV of their respective nematode hosts, we suggest that PIV colonization is the selective event in nematodes that results in clonal bottlenecking of the symbiont. Based on 3-dimensional reconstructed images of *S. carpocapsae* colonized PIV we propose a model that bacteria occupy an extracellular pouch within the PIV that is connected to the intestinal lumen by channels (supplemental videos S1 and S2). The channels may restrict entry into the PIV to only one individual bacterial cell on either side (e.g. Figure A3.3 B) that each then continue dividing within the PIV pouch (e.g. Figure A3.6 C).

Our findings reveal new insights into the *Xenorhabdus-Steinernema* association and challenge the long-held assumption that only the IJ stage of the nematode is intimately associated with colonizing bacteria. Previous models also presumed that the key events of colonization initiation occurred within the receptacle. We have shown that *X. nematophila* occupies at least four distinct *S. carpocapsae* nematode host niches (intestine, AIC, PIV, receptacle) during inter-generational transmission, each of which may play a role in symbiotic partner selection. Now that these colonization states have been described, further investigation will be necessary to elucidate the temporal and molecular processes and functions of each. For example, is AIC colonization initiated once in the juvenile stage or is it a continuous and dynamic process throughout nematode development? Are the bacteria that colonize the PIV derived from the AIC-localized bacterial population or do they result from a distinct initiation event? Finally, the finding that *Xenorhabdus* bacteria colonize non-transmission stage juvenile and reproductive adult *Steinernema* nematodes raises the intriguing possibility that these interactions facilitate bacterial contributions to host nutrition and reproduction. For example, the intimate association between the AIC intestinal epithelia and bacteria may allow nutrient exchange between these cells. The adult and juvenile colonization stages described here also may be essential for reliable transmission of only the proper, cognate symbiont in the nematode

IJ. In support of this idea, localization to the AIC and within the PIV of *S. carpocapsae* nematodes is specific to *X. nematophila*, suggesting that these are symbiont selective stages at which *S. carpocapsae* engages in partner choice. Further, since only a few bacterial cells were observed within the PIV, symbiont bottlenecks may occur at this stage. Future studies in this and other model animal-microbe mutualisms will reveal the nature and frequency of selective events encountered by symbionts during transmission.

ACKNOWLEDGEMENTS

This work was supported by grants awarded to H.G-B. from the National Science Foundation (IOS-0950873 and IOS-0920631). K.E.M. and J.M.C. were supported by a National Institutes of Health (NIH) National Research Service Award T32 (AI55397 "Microbes in Health and Disease"). J.M.C. was also supported by a National Science Foundation (NSF) Graduate Research Fellowship. E. A. H-H. was supported by grants awarded to Margaret McFall-Ngai (NIH AI50661) and Edward G. Ruby and M. M-N. (NIH RR12294). We are indebted to M. Altura, J. Troll, and M. McFall-Ngai for assistance with confocal microscopy and nematode tissue staining. The authors have no conflicts of interest to declare.

MATERIALS AND METHODS

Strains, media, and growth conditions. *Xenorhabdus* bacteria used in this study were grown on a roller at 30°C in lysogeny broth (LB) stored in the dark (44) and supplemented with ampicillin (150 µg/ml) (Table A3.3). *Escherichia coli* were grown in LB on a roller at 30°C or 37°C. A GFP-expressing *X. nematophila* ΔSR1 mutant, HGB1430, was created previously (25). To create GFP-expressing ΔSR1 Tn7-SR1, a previously created Tn7-SR1 construct (22), which inserts into a region (*attTn7*) that does not impair nematode colonization in *X. nematophila*, was transferred to HGB1430 by triparental conjugation (26). We also transferred the empty Tn7 plasmid (pEVS107) to HGB1430 to create ΔSR1 empty Tn7 (eTn7). To express SR1 in *X. szentirmaii*, Tn7-SR1 was transferred to *X. szentirmaii* (HGB836, a gift from A. Fodor) by triparental conjugation to create HGB1323: *X. szentirmaii* Tn7-SR1. As a negative control, the empty vector was transferred into *X. szentirmaii* (HGB836) to create HGB1322: *X. szentirmaii* eTn7. To create GFP-expressing *X. szentirmaii* strains, pJMC001, which integrates into the *X. nematophila* chromosome at a site that does not impair nematode colonization (18, 25), was conjugated into each of the *X. szentirmaii* Tn7 strains, and for each a visually green colony was stocked as a GFP-expressing strain. *X. bovienii*-GFP was created by introduction of GFP in the *attTn7* site using mini-Tn7-KSGFP (a gift from T. Ciche; (45)). Strains were verified for GFP expression and *X. bovienii* characteristics (i.e. ampicillin resistance, pigmentation, negative catalase).

Nematode cultivations. Nematode cultivations were performed by inoculating surface-sterilized axenic infective juveniles prepared as described previously (25) to overnight lawns of *Xenorhabdus* bacteria on lipid agar plates (16). For *Steinernema feltiae*, nematodes were grown on liver-kidney agar (46) instead of lipid agar because nematode colonization frequency is higher on the former. For each bacterial phenotype measured (adult and juvenile AIC-localization, PIV-localization, intestinal localization during intestinal constriction, and receptacle

Table A3.3 Bacterial strains and plasmids used in this study.

Strain	Plasmid	Species	Comments	Reference/Source
HGB283	pUX-BF13	<i>E. coli</i>	Triparental mating helper	(47)
HGB1783	pJMC001	<i>E. coli</i>	GFP donor plasmid	(25)
HGB783	pEVS107/SR1	<i>E. coli</i>	Tn7/SR1 donor plasmid	(26)
HGB281	pEVS107	<i>E. coli</i>	eTn7 donor plasmid	(48)
HGB1262	pURR25 mini Tn7KS-GFP	<i>E. coli</i>	Tn7/GFP donor plasmid	D. Lies and D. Newman (45)
HGB1430		<i>X. nematophila</i>	GFP expressing, Δ SR1 mutant	(25)
HGB1508		<i>X. nematophila</i>	HGB1430 eTn7	This study
HGB1509		<i>X. nematophila</i>	HGB1430 Tn7/SR1	This study
HGB836		<i>X. szentirmaii</i>	Wild type	A. Fodor
HGB1322		<i>X. szentirmaii</i>	HGB836 eTn7	This study
HGB1323		<i>X. szentirmaii</i>	HGB836 Tn7/SR1	This study
HGB1786		<i>X. szentirmaii</i>	HGB1322 GFP expressing, eTn7	This study
HGB1787		<i>X. szentirmaii</i>	HGB1323 GFP expressing, Tn7/SR1	This study
HGB1699		<i>X. bovienii</i>	wild type; symbiont of <i>S. feltiae</i>	This study
HGB1865		<i>X. bovienii</i>	HGB1699 attTn7::Tn7/GFP	This study

localization), we performed at least two experiments, each with three biological replicates per experiment. We counted a biological replicate as a different lipid agar plate preparation of bacteria and nematodes, and we used the same plate for counts on different days throughout the experiment. We counted approximately 100 nematodes per replicate, and assessed multiple time points per experiment. We display a representative temporal progression for nematodes colonized with each *X. nematophila* and *X. szentirmaii* strain in Figure S1. For *X. nematophila* WT and Δ SR1, we performed three experiments each with three biological replicates per time point except where noted in brackets: Expt. 1 (d 4 [2 replicates for WT] and 7 [2 replicates for WT]), Expt. 2 (d 5, 8, 10, 12 [2 replicates for WT], 14 [2 replicates for Δ SR1], and 19), and Expt. 3 (d 7-12). For *X. szentirmaii* WT and Tn7-SR1 we performed four experiments, each with three biological replicates per time point except where noted in brackets: Expt. 1 (d 4 [2 replicates for Tn7; 1 replicate for Tn7-SR1] and 7 [2 replicates for Tn7; 1 replicate for Tn7-SR1]), Expt. 2 (d 5, 8, 10, 12, 14, 17, 19, 21, and 24), Expt. 3 (d 10, 12, 14, 15, and 16 [2 replicates for WT]), and Expt. 4 (d 9-15). *S. feltiae* nematodes grown on *X. bovienii* were examined in two experiments with three biological replicates per experiment: Expt. 1 (d 8, 10-18) and Expt. 2 (d 8-12). For *in vivo* co-cultivations, approximately 50 surface-sterilized axenic IJs were co-injected with 200 CFU of log-phase cultures of bacteria (either *X. nematophila* WT or the Δ SR1 mutant) into *Galleria mellonella* insects. Two insect cadavers were dissected as biological replicates every other day from 5 to 11 days post injection to collect nematodes for microscopy as described above. Insects were individually dissected in 2mL of PBS, and emergent nematodes were rinsed three times in fresh PBS to remove background bacteria and insect tissues. The entire experiment was performed twice.

Specimen preparation, microscopy, and statistical analysis. To visualize bacterial localization within a nematode host, nematodes were removed from the agar surface,

suspended in phosphate buffered saline supplemented with 2 nM levamisole (a paralyzing agent), transferred to a glass slide and viewed by microscopy. Nematodes were viewed on a Nikon Eclipse TE300 inverted microscope (Nikon, Melville, NY, USA) as described previously (18) or a Zeiss LSM 510 confocal microscope (Zeiss, Thornwood, NY, USA) as described previously (33). DIC images were collected using MetaMorph software and lightened in Powerpoint 2011 (Microsoft). Confocal images and videos were analyzed using the LSM image browser (Zeiss). Nematodes were individually examined and assessed for relevant phenotypes (e.g. AIC- colonization). PIV-localization was scored positive if a J2 juvenile had one or a few colonizing bacteria bilaterally distributed at the anterior nematode intestine. Bacterial intestinal localization during intestinal constriction was scored as positive if any colonizing bacteria were observed at the anterior nematode intestine when the intestine was tightly constricted during pre-IJ development. While the nematode population was relatively synchronized, our counts represent the percentage of juveniles visible and do not strictly correlate with a single generation (e.g. early F2 juveniles may have been counted along with late F1 juveniles on day 8 or 10).

To observe bacterial colonization with stained nematode tissue, specimens were stained with 6.6 μ M rhodamine phalloidin (Sigma) or 0.125 mg/ml Alexa Fluor 633 concanavalin A (Invitrogen; dissolved in 0.1M sodium bicarbonate) (gifts from M. McFall-Ngai). To prevent photobleaching of fluorophores, samples were prepared in the dark. Nematode cultures were resuspended in PBS + 4% final concentration paraformaldehyde and fixed for at least 18 hours. Samples were washed at least three times in PBS, permeabilized in PBS-T (1% final volume Triton X-100) for at least 18 hours, and infiltrated with stains + 1% Triton X-100 for at least 18 hours prior to visualization.

Two different statistical tests were applied to the data. In each case we tested adult AIC, juvenile AIC, pre-IJ PIV, pre-IJ intestinal constriction, and IJ receptacle colonization separately.

First, we applied a 2-tailed Fisher's exact test (<http://www.langsrud.com/fisher.htm>) to the difference in colonization frequency of wild type- and mutant-colonized nematodes each day that colonization frequencies were assessed (data not shown). We also applied this test to the sum of the frequencies of colonization across all experiments (presented in Table A3.1). To assess the reproducibility of the statistical differences across experiments, we used a generalized linear mixed effects model (Bates *et al.*, 2012) in R (R, 2012) with a binomial family, with the mutant as a fixed effect, and experiment, day, and replicate as random effects, and day and replicate nested within experiment (presented in Figs. 4A and 5A). We did not perform tests for intestinal constriction in *X. nematophila* because the Δ SR1 mutant did not colonize any nematodes, and the package does not accurately reflect differences when all of one sample is 0. To calculate the values presented in Figs. 4A, 5A, and 6A (there was no statistical comparison for 6A), the average colonization frequency across all time points was first calculated for each replicate, then replicates were averaged to yield the average colonization frequency for each experiment. Finally, the average colonization frequencies of all experiments were averaged (and the S.E.M. calculated) and presented as percent colonized nematodes in Figs. 4A, 5A, and 6A. Statistical cutoffs were performed at $p < 0.05$ for all tests.

Because we were unable to distinguish uncolonized (AIC) juvenile nematodes from uncolonized (PIV) pre-IJ nematodes, we assessed the frequency of nematode colonization for each colonization phenotype relative to the same pool of uncolonized juvenile nematodes. For example, at day 10 we observed wild type *X. nematophila* AIC localization in 23, 7, and 18 *S. carpocapsae* nematodes from 3 different biological replicates, respectively; we also recorded 6, 5, and 10 nematodes that had no colonizing bacteria, and 7, 0, and 6 nematodes with PIV-colonizing bacteria, respectively. We assessed AIC-localization at 23/29, 7/12, and 18/28 and PIV-localization at 7/13, 0/5, and 6/16. This approach underestimates the frequency of nematode colonization, but was necessary because we were unable to distinguish uncolonized

“AIC”-nematodes from uncolonized “PIV”-nematodes. Importantly, despite the underestimation of colonization, we still observed sufficient nematode colonization in each of our tests to identify a significant colonization defect of bacteria that did not carry the SR1 genes (either mutant *X. nematophila* or wild type *X. szentirmai*).

REFERENCES

1. **Pace NR.** 1997. A molecular view of microbial diversity and the biosphere. *Science* **276**:734-740.
2. **Bright M, Bulgheresi S.** 2010. A complex journey: transmission of microbial symbionts. *Nature Reviews Microbiology* **8**:218-230.
3. **Parniske M.** 2008. Arbuscular mycorrhiza: the mother of plant root endosymbioses. *Nature Reviews Microbiology* **6**:763-775.
4. **Popp C, Ott T.** 2011. Regulation of signal transduction and bacterial infection during root nodule symbiosis. *Current Opinion in Plant Biology* **14**:458-467.
5. **Ruby EG.** 2008. Symbiotic conversations are revealed under genetic interrogation. *Nature Reviews Microbiology* **6**:752-762.
6. **Bird AF, Akhurst RJ.** 1983. The nature of the intestinal vesicle in nematodes of the family Steinernematidae. *International Journal for Parasitology* **13**:599-606.
7. **Poinar GO.** 1966. The presence of *Achromobacter nematophilus* in the infective stage of a *Neoaplectana* sp. (Steinernematidae: Nematoda). *Nematologica* **12**:105-108.
8. **Snyder H, Stock SP, Kim SK, Flores-Lara Y, Forst S.** 2007. New insights into the colonization and release processes of *Xenorhabdus nematophila* and the morphology and ultrastructure of the bacterial receptacle of its nematode host, *Steinernema carpocapsae*. *Applied and Environmental Microbiology* **73**:5338-5346.
9. **Wouts WM.** 1980. Biology, life cycle, and redescription of *Neoaplectana bibionis* Bovien, 1937 Nematoda: Steinernematidae. *Journal of Nematology* **12**:62-72.
10. **Richards GR, Goodrich-Blair H.** 2009. Masters of conquest and pillage: *Xenorhabdus nematophila* global regulators control transitions from virulence to nutrient acquisition. *Cellular Microbiology* **11**:1025-1033.
11. **Wang JX, Bedding RA.** 1996. Population development of *Heterorhabditis bacteriophora* and *Steinernema carpocapsae* in the larvae of *Galleria mellonella*. *Fundamental and Applied Nematology* **19**:363-367.
12. **Popiel I, Grove DL, Friedman MJ.** 1989. Infective juvenile formation in the insect parasite *Steinernema feltiae*. *Parasitology* **99**:77-81.
13. **Martens EC, Goodrich-Blair H.** 2005. The *Steinernema carpocapsae* intestinal vesicle contains a subcellular structure with which *Xenorhabdus nematophila* associates during colonization initiation. *Cellular Microbiology* **7**:1723-1735.
14. **Hirao A, Ehlers R-U, Strauch O.** 2010. Life cycle and population development of the entomopathogenic nematodes *Steinernema carpocapsae* and *S. feltiae* (Nematoda, Rhabditida) in monoxenic liquid culture. *Nematology* **12**:201-210.
15. **Hirao A, Ehlers RU.** 2010. Influence of inoculum density on population dynamics and dauer juvenile yields in liquid culture of biocontrol nematodes *Steinernema carpocapsae*

- and *S. feltiae* (Nematoda: Rhabditida). Applied Microbiology and Biotechnology **85**:507-515.
16. **Vivas EI, Goodrich-Blair H.** 2001. *Xenorhabdus nematophilus* as a model for host-bacterium interactions: *rpoS* is necessary for mutualism with nematodes. Journal of Bacteriology **183**:4687-4693.
 17. **Wang J, Bedding RA.** 1998. Population dynamics of *Heterorhabditis bacteriophora* and *Steinernema carpocapsae* in *in vitro* monoxenic solid culture. Fundamental and Applied Nematology **21**:165-171.
 18. **Martens EC, Heungens K, Goodrich-Blair H.** 2003. Early colonization events in the mutualistic association between *Steinernema carpocapsae* nematodes and *Xenorhabdus nematophila* bacteria. Journal of Bacteriology **185**:3147-3154.
 19. **Kim SK, Flores-Lara Y, Patricia Stock S.** 2012. Morphology and ultrastructure of the bacterial receptacle in *Steinernema nematodes* (Nematoda: Steinernematidae). Journal of Invertebrate Pathology **110**:366-374.
 20. **Akhurst RJ.** 1983. *Neoaplectana*-species - specificity of association with bacteria of the genus *Xenorhabdus*. Experimental Parasitology **55**:258-263.
 21. **Chapuis E, Emelianoff V, Paulmier V, Le Brun N, Pages S, Sicard M, Ferdy JB.** 2009. Manifold aspects of specificity in a nematode-bacterium mutualism. Journal of Evolutionary Biology **22**:2104-2117.
 22. **Cowles CE, Goodrich-Blair H.** 2008. The *Xenorhabdus nematophila* *nilABC* genes confer the ability of *Xenorhabdus* spp. to colonize *Steinernema carpocapsae* nematodes. Journal of Bacteriology **190**:4121-4128.
 23. **Sicard M, Ferdy JB, Pages S, Le Brun N, Godelle B, Boemare N, Moulia C.** 2004. When mutualists are pathogens: an experimental study of the symbioses between *Steinernema* (entomopathogenic nematodes) and *Xenorhabdus* (bacteria). Journal of Evolutionary Biology **17**:985-993.
 24. **Heungens K, Cowles CE, Goodrich-Blair H.** 2002. Identification of *Xenorhabdus nematophila* genes required for mutualistic colonization of *Steinernema carpocapsae* nematodes. Molecular Microbiology **45**:1337-1353.
 25. **Bhasin A, Chaston JM, Goodrich-Blair H.** 2012. Mutational analyses reveal overall topology and functional regions of NilB, a bacterial outer membrane protein required for host association in a model of animal-microbe mutualism. Journal of Bacteriology **194**:1763-1776.
 26. **Cowles CE, Goodrich-Blair H.** 2004. Characterization of a lipoprotein, NilC, required by *Xenorhabdus nematophila* for mutualism with its nematode host. Molecular Microbiology **54**:464-477.
 27. **Altun ZF, Hall DH.** 2009. Alimentary system, pharynx. doi:10.3908/wormatlas.1.3. Accessed 5 September.

28. **Baldwin JG, Perry RN.** 2004. Nematode morphology, sensory structure and function, p 175-257. *In* Chen ZX, Chen SY, Dickson DW (ed), *Nematol Adv Persp*, vol 1. CABI, Cambridge, MA.
29. **Altun ZF, Hall DH.** 2005. Handbook of *C. elegans* anatomy. <http://www.wormatlas.org/ver1/handbook/alimentary/alimentary1.htm>. Accessed
30. **Kaya HK, Gaugler R.** 1993. Entomopathogenic nematodes. *Annual Review of Entomology* **38**:181-206.
31. **Martens EC, Russell FM, Goodrich-Blair H.** 2005. Analysis of *Xenorhabdus nematophila* metabolic mutants yields insight into stages of *Steinernema carpocapsae* nematode intestinal colonization. *Molecular Microbiology* **51**:28-45.
32. **Lee MM, Stock SP.** 2010. A multilocus approach to assessing co-evolutionary relationships between *Steinernema* spp. (Nematoda: Steinernematidae) and their bacterial symbionts *Xenorhabdus* spp. (gamma-Proteobacteria: Enterobacteriaceae). *Systematic Parasitology* **77**:1-12.
33. **Sugar DR, Murfin KE, Chaston JM, Andersen AW, Richards GR, deLeon L, Baum JA, Clinton WP, Forst S, Goldman BS, Krasomil-Osterfeld KC, Slater S, Stock SP, Goodrich-Blair H.** 2012. Phenotypic variation and host interactions of *Xenorhabdus bovienii* SS-2004, the entomopathogenic symbiont of *Steinernema jollieti* nematodes. *Environmental Microbiology* **14**:924-939.
34. **Endo BY, Nickle WR.** 1995. Ultrastructure of anterior and mid-regions of infective juveniles of *Steinernema feltiae*. *Fundamental and Applied Nematology* **18**:271-294.
35. **Murfin KE, Chaston JM, Goodrich-Blair H.** 2012. Visualizing bacteria in nematodes using fluorescent microscopy. *Journal of Visualized Experiments* **e4298**:10.3791/4298.
36. **Ciche TA, Kim KS, Kaufmann-Daszczuk B, Nguyen KC, Hall DH.** 2008. Cell invasion and matricide during *Photorhabdus luminescens* transmission by *Heterorhabditis bacteriophora* nematodes. *Applied and Environmental Microbiology* **74**:2275-2287.
37. **Blaxter ML, De Ley P, Garey JR, Liu LX, Scheldeman P, Vierstraete A, Vanfleteren JR, Mackey LY, Dorris M, Frisse LM, Vida JT, Thomas WK.** 1998. A molecular evolutionary framework for the phylum Nematoda. *Nature* **392**:71-75.
38. **Goodrich-Blair H, Clarke DJ.** 2007. Mutualism and pathogenesis in *Xenorhabdus* and *Photorhabdus*: two roads to the same destination. *Molecular Microbiology* **64**:260-268.
39. **Gage DJ.** 2002. Analysis of infection thread development using Gfp- and DsRed-expressing *Sinorhizobium meliloti*. *Journal of Bacteriology* **184**:7042-7046.
40. **Wollenberg MS, Ruby EG.** 2009. Population structure of *Vibrio fischeri* within the light organs of *Euprymna scolopes* squid from two Oahu (Hawaii) populations. *Applied and Environmental Microbiology* **75**:193-202.

41. **Kubota N, Kanemori M, Sasayama Y, Aida M, Fukumori Y.** 2007. Identification of endosymbionts in *Oligobranchia mashikoi* (Siboglinidae, Annelida). *Microbes and Environments* **22**:136-144.
42. **Nussbaumer AD, Fisher CR, Bright M.** 2006. Horizontal endosymbiont transmission in hydrothermal vent tubeworms. *Nature* **441**:345-348.
43. **Frank SA.** 1996. Host-symbiont conflict over the mixing of symbiotic lineages. *Proceedings of the Royal Society of London Series B-Biological Sciences* **263**:339-344.
44. **Xu J, Hurlbert RE.** 1990. Toxicity of irradiated media for *Xenorhabdus* spp. *Applied and Environmental Microbiology* **56**:815-818.
45. **Teal TK, Lies DP, Wold BJ, Newman DK.** 2006. Spatiometabolic stratification of *Shewanella oneidensis* biofilms. *Applied and Environmental Microbiology* **72**:7324-7330.
46. **Sicard M, Le Brun N, Pages S, Godelle B, Boemare N, Moulia C.** 2003. Effect of native *Xenorhabdus* on the fitness of their *Steinernema* hosts: contrasting types of interaction. *Parasitology Research* **91**:520-524.
47. **Bao Y, Lies DP, Fu H, Roberts GP.** 1991. An improved Tn7-based system for the single-copy insertion of cloned genes into chromosomes of Gram-negative bacteria. *Gene* **109**:167-168.
48. **Stabb EV, Ruby EG.** 2002. RP4-based plasmids for conjugation between *Escherichia coli* and members of the Vibrionaceae. *Methods in Enzymology* **358**:413-426.
49. **Flores-Lara Y, Renneckar D, Forst S, Goodrich-Blair H, Stock P.** 2007. Influence of nematode age and culture conditions on morphological and physiological parameters in the bacterial vesicle of *Steinernema carpocapsae* (Nematoda: Steinernematidae). *Journal of Invertebrate Pathology* **95**:110-118.

APPENDIX 4

NiID CRISPR RNA contributes to *Xenorhabdus nematophila* colonization of symbiotic host nematodes

This appendix has been published as:

Veesenmeyer JL, Andersen AW, Lu X, Hussa EA, **Murfin KE**, Chaston JM, Dillman AR, Wassarman KM, Sternberg PW, and Goodrich-Blair H. "The CRISPR/cas system of *Xenorhabdus nematophila* contributes to colonization of symbiotic host nematodes." *Mol Microbiol.* 2014 Sep;93(5):1026-42. doi: 10.1111/mmi.

ABSTRACT

The bacterium *Xenorhabdus nematophila* is a mutualist of entomopathogenic *Steinernema carpocapsae* nematodes and facilitates infection of insect hosts. *X. nematophila* colonizes the intestine of *S. carpocapsae* which carries it between insects. In the *X. nematophila* colonization-defective mutant *niID6::Tn5*, the transposon is inserted in a region lacking obvious coding potential. We demonstrate that the transposon disrupts expression of a single CRISPR RNA, NiID RNA. A variant NiID RNA also is expressed by *X. nematophila* strains from *S. anatoliense* and *S. websteri* nematodes. Only *niID* from the *S. carpocapsae* strain of *X. nematophila* rescued the colonization defect of the *niID6::Tn5* mutant, and this mutant was defective in colonizing all three nematode host species. NiID expression depends on the presence of the associated Cas6e but not Cas3, components of the Type I-E CRISPR-associated machinery. While *cas6e* deletion in the complemented strain abolished nematode colonization, its disruption in the wild-type parent did not. Likewise, *niID* deletion in the parental strain did not impact colonization of the nematode, revealing that the requirement for NiID is evident only in certain genetic backgrounds. Our data demonstrate that NiID RNA is conditionally necessary for mutualistic host colonization and suggest that it functions to regulate endogenous gene expression.

INTRODUCTION

Entomopathogenic *Steinernema spp.* nematodes are mutualistically associated with bacteria of the genus *Xenorhabdus* (1). Together, these symbiont pairs infect, kill, and reproduce within insect hosts. A specialized infective juvenile (IJ) stage of the *Steinernema* nematode transmits bacterial symbionts between insects, ensuring maintenance of the symbiosis through generations. The association between *S. carpocapsae* and its symbiont *X. nematophila* has been well studied with regard to cellular and molecular aspects of symbiosis, particularly with respect to the mechanisms by which the IJ is colonized (2-4). The bacteria occupy a region known as the receptacle in the anterior portion of the IJ intestine (5-10). Although the processes by which *X. nematophila* bacteria are selected and gain entry to the receptacle remain obscure, only one or two individual clones are founders for the final population (~30-200 CFU/IJ) that ultimately fills the space (4, 8).

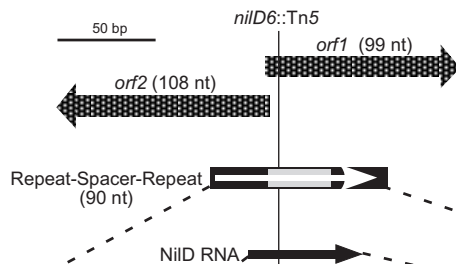
To better understand the bacterial molecular factors necessary during colonization of the IJ nematode, a signature tagged mutagenesis screen to identify *X. nematophila* mutants defective in this process was conducted in the *S. carpocapsae* nematode-associated strain *X. nematophila* HGB081 AN6/1 (hereafter referred to as XnSc 081) (11). In one of the mutants identified in this screen, *nilD6::Tn5*, the transposon had inserted into a region of the genome lacking obvious coding potential. Complementation studies then confirmed the *nilD* region was necessary for nematode colonization but was dispensable for virulence in an insect model of infection (11). Bioinformatic analyses have since indicated that the *nilD* locus encodes a single, free-standing CRISPR (clustered regularly interspaced short palindromic repeats) element comprising one spacer and two repeats, which was disrupted by the transposon insertion (Figure A4.1).

CRISPRs are genetic elements broadly distributed among bacteria and archaea and can provide resistance to foreign nucleotide sequences (12). CRISPRs comprise a series of short

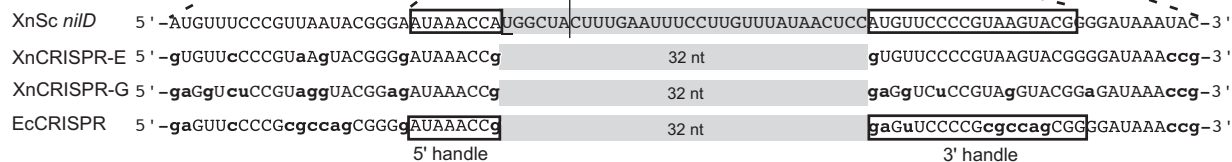
A.



B.



C.



D.

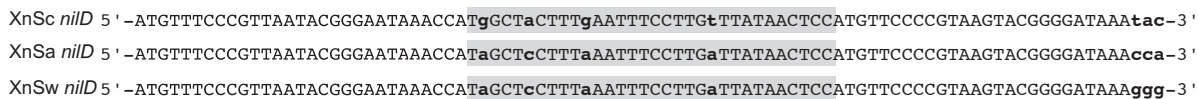


Figure A4.1 Schematic representation of the *niID* CRISPR locus. **A.** Schematic diagram of the *X. nematophila* genomic regions containing CRISPR loci, *cas/cse* genes, and *niID*. The bracket indicates the 3240-bp region previously sequenced in the HGB081 (XnSc 081) strain background (AY077466) (11), which is identical in the sequenced ATCC 19061 (HGB800/XnSc 800) genome (NC_014228.1). Line arrows represent open reading frames, with gene names indicated above each. CRISPR loci are represented by hatched rectangles and are named CRISPR-E and CRISPR-G according to their position on the *X. nematophila* genome, with *niID*, shown as a black rectangle, considered CRISPR-F. The location of the *niID6::Tn5* transposon insertion within *niID* is indicated. The gray shaded box represents the 135-bp leader sequence of CRISPR-E. White arrowheads indicate the predicted orientations of CRISPR-E and -G transcription, based on comparison to *E. coli* CRISPR transcription. **B.** Detail of the *niID* locus, showing the two small overlapping open reading frames (*orf1* and *orf2*) represented by checkered block arrows. The positions of *niID* locus repeats and spacer are indicated by black and gray rectangles, respectively. The white arrow indicates the predicted orientation of transcription based on comparison to *E. coli* CRISPR transcription. The black arrow represents the position of the small RNA transcript encoded by the *niID* locus. The position of the *niID6::Tn5* insertion site is indicated by a line. **C.** Sequence of NiID RNA aligned with CRISPR small RNAs predicted to be encoded by *X. nematophila* (XnCRISPR-E and -G) and CRISPR RNAs expressed in *E. coli* (EcCRISPR). Spacer regions are shaded in gray. Lower case, bold nucleotides indicate those that differ from NiID RNA. The 5' and 3' handles as described by Brouns *et al.* (2009), and experimentally determined for NiID RNA are boxed. The underlined "U" in the *niID* spacer sequence is necessary for colonization (11). **D.** Alignment of *niID* locus repeat-spacer-repeat sequences of *X. nematophila* (*carpocapsae*) (XnSc *niID*), *X. nematophila* (*anatoliense*) (XnSa *niID*), and *X. nematophila* (*websteri*) (XnSw *niID*). Lower case bold letters indicate nucleotides that differ among the three sequences.

repeat sequences that are separated by variable regions, called spacers. Many CRISPR spacers exhibit identity to sequences, termed proto-spacers, within bacteriophage genomes or other mobile DNA elements (13-16). This observation led to the discovery that CRISPR elements encode a rapidly evolving acquired immune defense system against incoming phages and plasmids (reviewed in (12, 17)). CRISPR arrays are transcribed as single RNA molecules that are then processed by components of the Cas (CRISPR associated sequences) machinery into individual CRISPR RNA (crRNA) molecules (18-20). There are three major classes of CRISPR systems (Types I-III). These three types are further subdivided into several subtypes, differentiated by criteria including the phylogeny of the *cas* genes and the sequence of the CRISPR repeats (21, 22). In *E. coli*, a type I-E system, five proteins, Cse1 (Cas subtype E. coli), Cse2, Cas7, Cas5, and Cas6e (previously named CasA, B, C, D, and E, respectively) are associated in a complex termed "Cascade" and Cas6e, a putative RNA binding protein, is the subunit responsible for RNA processing (19, 20, 23). Processed crRNAs target and interact with proto-spacer encoding DNA or RNA molecules, resulting in gene silencing and/or degradation (24). A 6-8 nt seed sequence within the crRNA exhibits 100% identity to the target and is predicted to guide the interaction between the crRNA and the proto-spacer (25, 26). CRISPR targeting and silencing also require the presence of a short, proto-spacer adjacent motif (PAM) within the exogenous target sequence, located directly upstream of the seed sequence. The PAM provides a mechanism by which the system differentiates between target and non-target (e.g. endogenous) sequences, thereby preventing potentially lethal auto-immunity due to targeting of chromosomal "self" sequences (27, 28). The hybridization of the crRNA molecule to the PAM-encoding DNA sequence results in the formation of an R-Loop within the crRNA that acts as a binding site for another member of the Cas protein family, Cas3. Cas3 contains helicase and nuclease activities that are responsible for degradation of the target molecule (29-31). Evolution of resistance to new challenges occurs by the addition of spacers to

the promoter-proximal end of the CRISPR repeat array, in a Cas1 and Cas2-dependent process (12).

In addition to providing resistance to exogenous sequences, *E. coli* CRISPRs have activity against lysogeny and induction of temperate bacteriophages (32). Induction of the CRISPR-Cas system results in *E. coli* cell death if crRNA targets are present on the chromosome, but the system also selects for bacterial populations that have lost prophages. Other functions attributed to CRISPR-Cas systems include modulation of bacterial community behaviors, gene expression, and DNA repair (33-37). Lastly, recent studies have implicated or established a role for CRISPR-Cas systems in promoting virulence of several pathogens including *Legionella pneumophila*, *Campylobacter jejuni*, and *Francisella novicida* (38-41). Thus, the repertoire of cellular activities impacted by CRISPR-Cas appears to be diverse and much remains to be learned about these versatile elements particularly with regard to their influence on host interactions.

The work presented here was undertaken to determine the relationship of *niID* to the CRISPR-Cas system and its function in mutualistic colonization of host nematodes. We demonstrate that the *niID* locus expresses a CRISPR RNA molecule that contributes, in a Cas6e-dependent manner, to colonization of three distinct nematode species. Our data are consistent with a model that NiID functions to regulate endogenous bacterial sequences in a way that requires neither Cas3 nor perfect sequence identity to the target.

RESULTS

The niID locus is encoded within a CRISPR-Cas region. Heungens *et al.* (2002) previously reported a 3185-bp sequence (AY077466) of XnSc 081 containing the *niID* locus required for association with *S. carpocapsae* nematodes. Further sequence analysis revealed this locus encodes a CRISPR repeat element, comprising one spacer and two repeats, which is disrupted

by the transposon insertion in the colonization deficient strain *nilD6::Tn5* (Figure A4.1) (11).

Additional CRISPR repeat sequences were noted upstream of *nilD* (bracketed region in Figure A4.1 A). These data indicate that *X. nematophila* encodes multiple CRISPR loci and that disruption of one of these, *nilD*, can inhibit nematode colonization.

To gain further information on the chromosomal context of *nilD* and to identify other CRISPR loci, the genome of XnSc 081 was sequenced and compared to that of the published sequence of *X. nematophila* strain HGB800 (NC_014228; ATCC 19061, hereafter referred to as XnSc 800) (Table A4.S1). In both genomes there are six CRISPR elements (Table A4.S2), labeled alphabetically in order of their occurrence in the chromosome (A-E and G) in addition to *nilD* (CRISPR-F). In both genomes, the *nilD* locus is located approximately 250-nt downstream of CRISPR-E. The *nilD* CRISPR is most similar to loci C and E: Each of these three loci (*nilD*, CRISPR-C, and CRISPR-E) encodes 32-nt spacer sequences and 29-nt repeats that are similar in sequence to those of *E. coli* K12 (11) (Figure A4.1 C). In turn, the *nilD* repeat sequences are similar, but not identical, to those of the loci C and E. In the 29 nt comprising each repeat, 6 and 4 differences occurred in the left and right repeats of *nilD* respectively, relative to the CRISPR-E repeats (Figure A4.1 C), indicating the *nilD* locus has diverged from the other CRISPR loci in the genome.

Encoded downstream of *nilD* is the previously sequenced *gloA* gene, as well as *cas* genes and CRISPR locus G (Figure A4.1 A). The sequences of each of these regions are identical between XnSc 081 and XnSc 800. CRISPR loci are preceded by A/T rich leader sequences containing promoters driving CRISPR transcription (42). These leaders can be necessary for CRISPR function (43, 44) and their sequence tends to be conserved within, but not across, species (45, 46). In both XnSc 800 and XnSc 081, a 99-nt sequence adjacent to CRISPR-E (Figure A4.1 A) is 93% identical to that found upstream of CRISPR-C, and is likely the leader sequence. This sequence is not found adjacent to any other CRISPR locus (A, B, D,

or G), nor is it found adjacent to *niID*, suggesting that these loci may be regulated in a manner distinct from CRISPR-C and -E.

The *X. nematophila* *cas* genes are of the Type I-E subset and include the broadly conserved *cas1*, *cas2*, and *cas3* genes, as well as *cse1* (*casA*), *cse2* (*casB*), *cas7* (*casC*), *cas5* (*casD*), and *cas6e* (*casE*) (Figure A4.1 A) (22, 47-49). Based on comparisons to *E. coli* and other systems (19, 29-31), we predict *cas3* encodes a protein with nuclease and helicase activity necessary for mediating degradation of crRNA-DNA hybrids, while the other five genes encode components of the ribonucleoprotein Cascade complex necessary for CRISPR RNA processing and target DNA degradation. In other systems *cas1* and *cas2* genes are not necessary for CRISPR RNA processing or activity, but rather encode nucleases that form a complex necessary for acquisition of new spacers (50, 51). In addition, *cas1* is involved in DNA repair and chromosome segregation (37), while *cas3* promotes plasmid replication in *E. coli* (52).

Genomic analyses indicate that the spacer composition of the *E. coli* Type I-E system diversifies more slowly than would be expected if the CRISPRs were primarily involved in immunity (53). To address if *X. nematophila* spacer content diversifies during association with nematode and insect hosts we isolated DNA from 10 individual colonies of *X. nematophila* from our laboratory stock population of *S. carpocapsae* IJ nematodes that had been maintained for ~15 years by repeated (~monthly) passage through *Galleria mellonella* insect larvae. These "evolved" *X. nematophila* are the result of >1500 rounds of the natural life cycle, comprising persistence in non-feeding IJ nematodes during storage in water, infection and growth within insect larvae (including exposure to insect-associated microbiota), and colonization of nematode IJs (54). In contrast, XnSc 800 and XnSc 081 stocks have been stored for a similar period frozen in glycerol without propagation. There were no spacer sequence differences in CRISPR loci C, E or *niID* in the 10 isolated colonies relative to each other or to the frozen stock strains

(data not shown), indicating that these loci are not evolving during laboratory passage through nematodes and insects. While we did not examine spacer content of the other 4 CRISPR loci in the evolved strain, the absence of spacer content changes in CRISPR loci C and E after more than 1500 passages through insects supports the idea that the CRISPR-Cas machinery in *X. nematophila* may function in a role outside of the canonical immunity against exogenous nucleic acids (55). Overall, the genomic analyses described above indicate that the *niID* locus, which is necessary for *X. nematophila* to colonize *S. carpocapsae* nematodes, encodes a non-canonical CRISPR element.

The niID CRISPR sequence is sufficient to promote nematode colonization. We previously reported that the colonization defect of the *niID6::Tn5* mutation was partially rescued by introduction of a plasmid (pSR2-312, Table A4.1) carrying a 312-bp fragment of wild type *niID*-containing DNA, confirming this region is necessary for colonization (11). Likewise, insertion of a 387-bp fragment encoding the *niID* locus (pEVS107-*niID*, Table A4.1) in single copy at the *attTn7* insertion site of the XnSc 081 *niID6::Tn5* genome (referred to hereafter as *niID6::Tn5 + niID*) was sufficient to restore nematode colonization, in this case to wild type levels (Figure A4.2 B). The DNA surrounding the transposon insertion encodes two putative divergent and overlapping small open reading frames, *orf1* and *orf2* that encompass the CRISPR element (11) (Figure A4.1 B) and may encode small peptides that could be involved in colonization. A plasmid carrying the *niID* sequence with a mutation at the common "T" of the start codons of these two ORFs did not rescue the colonization defect of the *niID6::Tn5* mutant (11). However, since this nucleotide is also the first within the 32-nt spacer (see underlined nucleotide in Figure A4.1 C), these previously reported data did not clarify if *orf1*, *orf2*, or the CRISPR-like element is involved in colonization. To help address this question, we transformed the *niID6::Tn5* mutant with derivatives of plasmid pSR2-312 (11), containing the 312-bp fragment sufficient to rescue

Table A4.1 Strains and plasmids used in this study

Strain or plasmid	Relevant Characteristics	Source or Reference
<i>E. coli</i>		
DH5a	General cloning host	(69)
DH5a (<i>lpir</i>)	General cloning strain for maintenance of <i>oriR6K</i> plasmids	
S17-1 (<i>lpir</i>)	<i>E. coli</i> donor strain for conjugations	
<i>X. nematophila</i>		
HGB081 (XnSc 081)	Rifampicin resistant derivative of wild-type <i>X. nematophila</i> AN6/1 (carpocapsae)	S. Forst
HGB151	<i>X. nematophila</i> ATCC 19061 <i>rpoS1::kan</i>	(65)
HGB315	HGB081 <i>nilD6::Tn5</i>	(11)
HGB829	HGB315 <i>nilD6::Tn5</i> pECM20- <i>gfp</i>	(8)
HGB1186	HGB315 <i>nilD6::Tn5</i> pECM20- <i>gfp sup-1</i>	This study
HGB1578	HGB081 <i>Dcas3-3::kan</i>	This study
HGB1695	HGB081 <i>DcasE4::kan</i> (<i>cas6e</i> mutant)	This study
HGB1418 (XnSa 1418)	<i>X. nematophila</i> (<i>anatoliense</i>) isolated from <i>S. anatoliense</i> nematodes	This study
HGB1419 (XnSw 1419)	<i>X. nematophila</i> (<i>websteri</i>) isolated from <i>S. websteri</i> nematodes	This study
HGB1421	<i>X. nematophila</i> strain of unknown origin	S. P. Stock
HGB007 (XnSc 007)	Wild-type <i>X. nematophila</i> (<i>carpocapsae</i>) ATCC 19061, acquired in 1995	ATCC
HGB800 (XnSc 800)	Wild-type <i>X. nematophila</i> (<i>carpocapsae</i>) ATCC 19061, acquired in 2003	ATCC
HGB1764	XnSc 081 <i>nilD56::kan</i>	This study
HGB1756	XnSc 800 <i>nilD56::kan</i>	This study
HGB1940	HGB315 <i>nilD6::Tn5 attTn7::Tn7/nilD</i>	This study
HGB1986	HGB315 <i>nilD6::Tn5 attTn7::Tn7/nilD-SDM</i>	This study
HGB1901	XnSc 081 <i>Dcas3-5::strep</i>	This study
HGB1909	XnSc 081 <i>DcasE6::strep</i> (<i>cas6e</i> mutant)	This study
HGB1907	HGB1940 <i>Dcas3-5::strep</i>	This study
HGB1915	HGB1940 <i>DcasE6::strep</i> (<i>cas6e</i> mutant)	This study
<i>X. bovienii</i>		
HGB1166	ATCC 35271 <i>X. bovienii attTn7::miniTn7</i>	
HGB1167	ATCC 35271 <i>X. bovienii attTn7::miniTn7/SR1</i> (containing <i>nilA</i> , <i>nilB</i> , and <i>nilC</i>)	(67)
HGB1649	HGB1166 pECMXb-Empty	This study
HGB1651	HGB1166 pECMXb-SR2; <i>nilD+</i>	This study
HGB1653	HGB1167 pECMXb-Empty; <i>nilABC+</i>	This study
HGB1655	HGB1167 pECMXb-SR2; <i>nilD+ nilABC+</i>	This study
Plasmids		
pBCSK+	General cloning vector, Cm ^R ,	Stratagene
pCR2.1 [®] -TOPO	General cloning vector, Amp ^R , Kan ^R	Invitrogen, Carlsbad, CA
pCR2.1-TOPOmini	General cloning vector, Amp ^R	This study
pTopoSR2-2	312-bp XnSc 007 <i>nilD</i> region amplified with KPH62 and KPH63 primers and cloned into pCR2.1 [®] -TOPO	(11)
pSR2-312	Apal-Sacl fragment from pTopoSR2-2 subcloned into	(11)

	pBCSK+, formerly named pBCSR2-2	
pAWA1	137-bp XnSc 007 <i>niID</i> region PCR amplified from HGB007 chromosomal DNA with primers KPH57 and KPH58 and cloned into pCR®II-TOPO	This study
pCR2.1-TOPO- <i>niID</i> - <i>XnSa</i>	pCR2.1-TOPO- <i>niID</i> modified by site directed mutagenesis to match the <i>niID</i> spacer sequence of XnSa and XnSw. Use for RPA analysis.	This study
pEVS107	Source of Kan ^r cassette for <i>cas3</i> and <i>cas6e</i> mutations	(76)
pEVS107- <i>niID</i>	Kan ^R ; vector for insertion of 387-bp <i>niID</i> fragment at <i>attTn7</i> site of XnSc 081	This study
pEVS107- <i>niID</i> -SDM	Kan ^R ; pEVS107- <i>niID</i> altered by site directed mutagenesis to change NiID RNA spacer sequence	This study
pKNG101	Sm ^R ; <i>oriR6K</i> suicide vector	(77)
pECM20	pECM2 containing a 614-bp chromosomal insert from XnSc 007	(8)
pECMXb-Empty	pECM20 with <i>X. bovienii</i> sequence replacing the <i>X. nematophila</i> insertion sequence	This study
pECMXb-SR2	pECMXb-Empty with 312bp <i>niID</i> region from pTopoSR2-2 in the XbaI site	This study
pKNG <i>cas3-5::strep</i>	Sm ^R ; pKNG101 with <i>Dcas3::strep</i> for replacing <i>cas3</i> gene with Sm ^R cassette	This study
pKNG <i>casE6::strep</i>	Sm ^R ; pKNG101 with <i>DcasE::strep</i> for replacing <i>cas6e</i> gene with Sm ^R cassette	This study
pKR100	Cm ^R ; <i>oriR6K</i> suicide vector	
pKR100 <i>niID56::kan</i>	Kan ^R , Cm ^R ; pKNG101 with <i>Dcas-3::kan</i> for replacing <i>niID</i> encoding region with Kan ^R cassette.	This study
pBS-5S	AmpR	(78)

A.

nilD-XnSc CCA-TGGCtACTTTgAAtTTcCTtGTtTAtAAcTCc-ATG
nilD-SDM CCA-TGGCaACaTTaAAaTTaCTaGTaTAaAAaTCa-ATG

B.

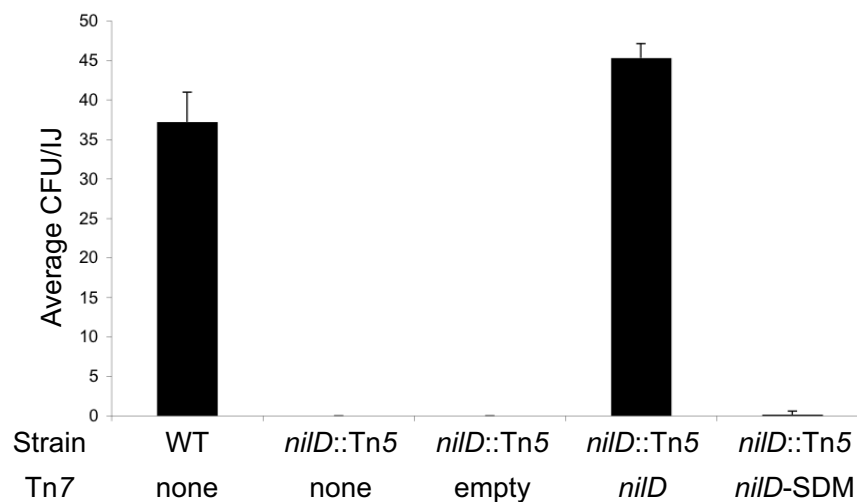


Figure A4.2 Wild type, but not mutant *nilD* provided in trans complements the colonization defect of the *nilD6*::Tn5 mutant. A. Alignment of the spacer sequences of *X. nematophila* (from *S. carpocapsae*) wild type *nilD* (*nilD*-XnSc) and the mutated allele (*nilD*-SDM). B. XnSc 081, XnSc 081 *nilD*::Tn5, and complemented strains were co-cultivated with axenic *S. carpocapsae* nematodes. The average colony forming units (CFU) colonizing the resulting progeny infective juveniles was measured by sonication and dilution plating.

colonization. Deletions were made in the pSR2-312 backbone such that the 5' (DL) and/or the 3' (DR) ends of the 312-bp *niID* region were truncated (Table A4.1, Figure A4.S1). These constructs were transformed into either the *niID6::Tn5* mutant or its wild-type parent XnSc 081 and transformants were tested for the ability to colonize IJ nematodes (Table A4.S3). Constructs lacking substantial regions of *orf1* or *orf2* were able to rescue the colonization defect of the *niID6::Tn5* mutant, indicating that neither ORF is required in its entirety to encode the colonization determinant. In contrast, the deletion constructs in which portions of the CRISPR repeat-spacer sequence are truncated were unable to rescue the colonization defect of the *niID6::Tn5* mutant. Furthermore, a plasmid (pSR2-DR90/DL84, Table A4.1) carrying a 137-bp central fragment containing the 90-nt *niID* CRISPR-like region did rescue the colonization defect of the *niID6::Tn5* mutant. These data support the hypothesis that within the *niID* locus, the CRISPR-like sequences, not the short coding regions are necessary for colonization.

The role of the predicted NiID RNA in colonization was investigated further by introducing base substitutions that would alter the putative NiID RNA sequence but not the Orf1 or Orf2 peptide coding sequences (Figure A4.2 A). This construct (pEVS107-*niID*-SDM, Table A4.1) was introduced in single copy in the *attTn7* site on the XnSc 081 *niID6::Tn5* genome and the colonization phenotypes of the resulting strains were examined. Complementation with this construct failed to restore nematode colonization, indicating that NiID RNA rather than either Orf peptide is essential for nematode colonization and further supporting the predicted function of NiID as a crRNA (Figure A4.2 B). Consistent with this conclusion, attempts to detect expression of the Orf1 and Orf2 peptides by immunoblot and assaying *lacZ* translational fusions were unsuccessful (data not shown), indicating that these factors may not be stably expressed.

***niID* encodes a small RNA transcript expressed during growth in lab culture and colonization of nematodes.** *E. coli* CRISPR repeats are transcribed and processed into small

RNAs of ~57 nt (19). We sought to determine if the *niID* locus similarly expresses a small RNA. Northern blots were insufficiently sensitive to detect an RNA transcript from the *niID* region (data not shown). We therefore performed an RNase protection assay (RPA) using probes containing *niID* sequence specific for either sense or anti-sense RNAs (relative to the transcript orientation of the CRISPR-like element predicted by comparison to *E. coli* (19)). No protected signal was observed in any reactions specific for anti-sense RNA (data not shown). In contrast, RNA harvested from wild type cultures, but not from the *niID6::Tn5* mutant, protected a fragment of approximately 58-nt when probes specific for the sense strand were used (Figure A4.3 A), indicating the *niID* region encodes a 58-nt RNA that is expressed under *in vitro* growth conditions. Similar results were observed when RNA was extracted from wild type bacteria harvested from IJ stage *S. carpocapsae* nematodes (Figure A4.3 B), demonstrating that the NiID RNA is also expressed during mutualistic interactions with its nematode host. Additionally, RPA analysis of RNA isolated from *X. nematophila* wild type cells grown under various *in vitro* conditions indicate that NiID RNA levels are elevated in nutrient-limited or aged cells (Figure A4.S2 A). Higher NiID RNA levels were detected after growth in LB supplemented with 2, 2'-dipyridil (an Fe(II) chelator) relative to LB alone or with additional supplementation with exogenous Fe₂SO₃, indicating NiID RNA levels may increase after iron limitation (Figure A4.S2 B).

Primer extension was used to determine the 5' end of the ~58-nt NiID RNA (Figure A4.3 C). The run-off fragment indicates that the 5' end of NiID RNA is an adenine (designated +1 and indicated by an asterisk in Figure A4.3 C) seven nucleotides upstream of the spacer region. In addition to this 5' end, we occasionally observed run off fragments consistent with the +2U as the 5' end (data not shown), which may indicate flexibility in processing or transcription initiation. The mapped 5' end of NiID RNA and the predicted 5' end match the 5' and 3' handles identified for *E. coli* crRNAs (19) (Figure A4.1 C). These results confirm that the *niID* locus encodes a

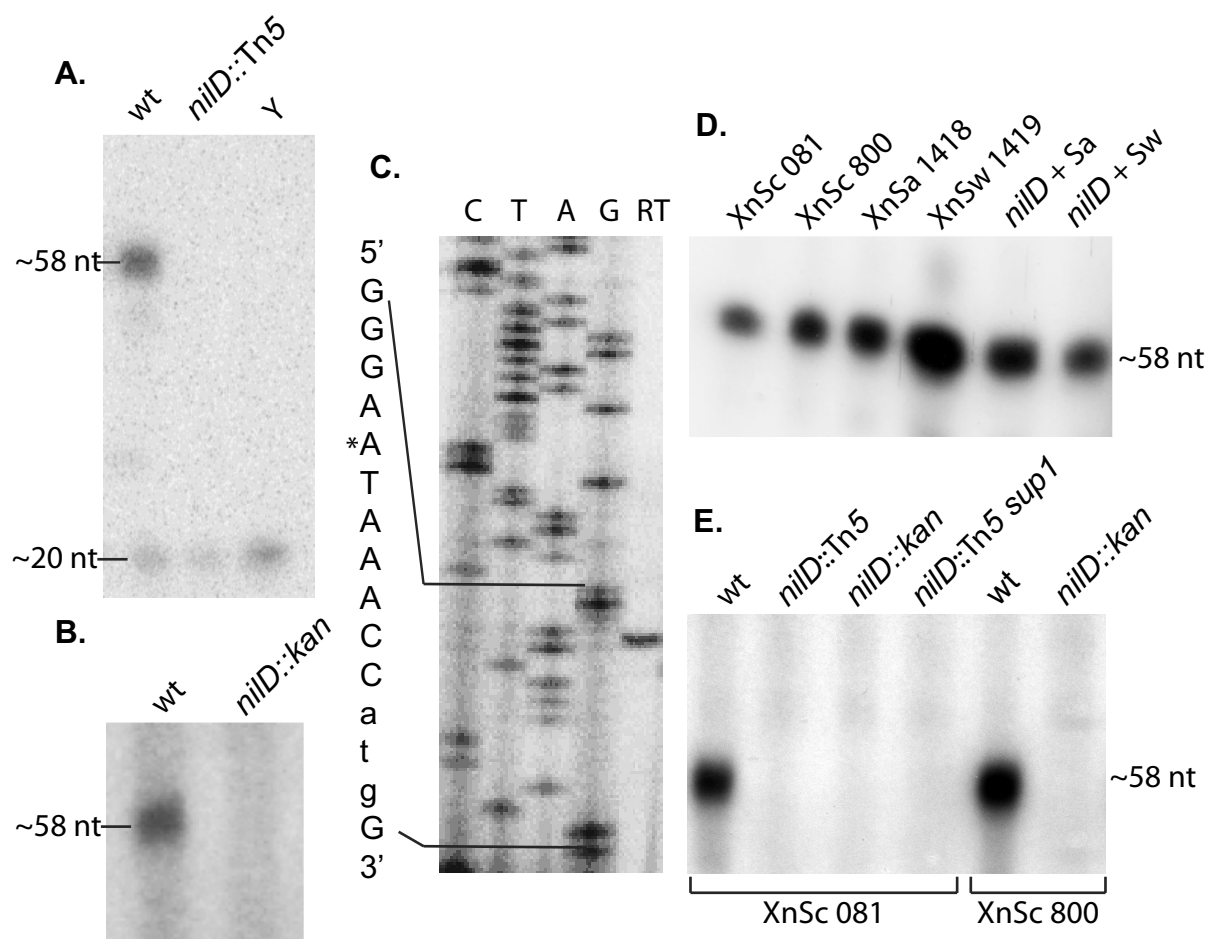


Figure A4.3 The *nilD* locus of *X. nematophila* encodes a small RNA. RNase protection analysis, using a radiolabeled NiID RNA-specific probe, was used to detect expression of the NiID RNA in RNA harvested from *X. nematophila* strains during both *in vitro* growth (panels **A**, **C**, **E**) and mutualistic interactions with the nematode host (panel **B**). Primer extension analysis was performed on RNA isolated from laboratory grown *X. nematophila* cultures to map the 5' end of NiID RNA (panel **C**). **A** RNA was harvested from stationary phase cultures of *X. nematophila* Sc 081, and *X. nematophila* Sc 081 *nilD6::Tn5*. The probe was also incubated with yeast RNA (Y) as a negative control. Radioactive markers (not shown) were used to estimate the sizes of the labeled fragments as indicated on the left. The 20-nt band represents the smallest nuclease-resistant single stranded RNA product of RNase cleavage. **B** To assay for *in vivo* expression of NiID, RNA was extracted from Sc 081 and Sc 081 *nilD56::kan* harvested from

infective-juvenile stage *S. carpocapsae* nematodes after co-cultivation. **C** RNA isolated from wild type *X. nematophila* HGB800 (ATCC19061) after overnight growth in LB was used as a template for reverse transcriptase extension (RT) from the radioactively labeled primer AAP2. The resulting products were loaded on each gel adjacent to a sequencing ladder (C, T, A, and G lanes) derived from the same primer on pAWA1 template DNA. The relevant sequence is indicated to the left of the panel. The asterisk represents the starting nucleotide of the observed product. The lower case atg in the sequence to the left of the panel indicates the predicted start codon of *orf1*. **D**. To determine if the *NilD* RNA is expressed in distinct *X. nematophila* strains, RNA was harvested from the indicated strains: XnSc 081, XnSc 800 and strains harvested from *S. anatoliense* and *S. websteri* nematodes (XnSa 1418 and XnSw 1419, respectively). Likewise, RNA was harvested from *nilD6::Tn5* strains complemented with the *nilD* locus derived from XnSa 1418 and XnSw 1419 (*nilD* + Sa and *nilD* + Sw, respectively). **E**. RNA was isolated from wild type *X. nematophila* strains (XnSc 081 and XnSc 800), *nilD* mutant strains (*nilD::Tn5* or *nilD::kan*), and the *nilD6::Tn5* suppressor strain (XnSc 081 *nilD::Tn5 sup1*). For each panel, each image was processed in its entirety with Adobe Photoshop CS3 to optimize visibility of bands by adjusting brightness and contrast.

small CRISPR RNA (genome coordinates: 3579434...3579491), hereafter referred to as NiID RNA (Figure A4.1 C).

NiID RNA expression requires Cas6e. To investigate the role of the Cas machinery in NiID RNA processing and nematode colonization, we used allelic exchange to generate mutations in *cas6e*, a gene predicted to encode an endoribonuclease responsible for processing of CRISPR transcripts into small RNAs, and in *cas3*, which is predicted to encode a helicase/nuclease required for CRISPR-mediated resistance to infection (19, 29). RPA was used to detect *X. nematophila* NiID RNA and northern hybridization, using a general crRNA probe, was used to detect total CRISPR RNA in wild type and *cas* mutants (Figure A4.4). In the XnSc 081 background, CRISPR small RNAs were absent in the *cas6e* mutant, but were present in the *cas6e* mutant complemented with the *cas6e* gene on a plasmid (compare Figure A4.4 B lanes 4 and 5 with lane 6). CRISPR RNAs were also apparent in the *cas3* mutant (Figure A4.4 B, lane 3). These data indicate that, as in *E. coli*, *cas6e* but not *cas3* is necessary for normal processing of crRNAs (19). Furthermore, crRNAs were expressed in the *niID6::Tn5* mutant (Figure A4.4 B, lane 2), suggesting that the nematode colonization defect of this mutant is not due to general disruption of crRNA expression. RPA analysis revealed NiID RNA, like other crRNAs, is apparent in the *cas3*-deficient (Figure A4.4 A, lanes 3 and 8) but not the *cas6e*-deficient strains (Figure A4.4 A, lanes 4, 5, 9, and 10), when expressed from its native locus (in the HGB081 background) or from the *attTn7* locus (in the *niID6::Tn5 + niID* background). Furthermore, providing a wild-type copy of the *cas6e* gene on a plasmid restored NiID processing (Figure A4.4 A, lanes 6 and 11). These results establish that the expression of the 58-nt NiID RNA depends on a component of the Cas machinery, further supporting its identity as a CRISPR RNA.

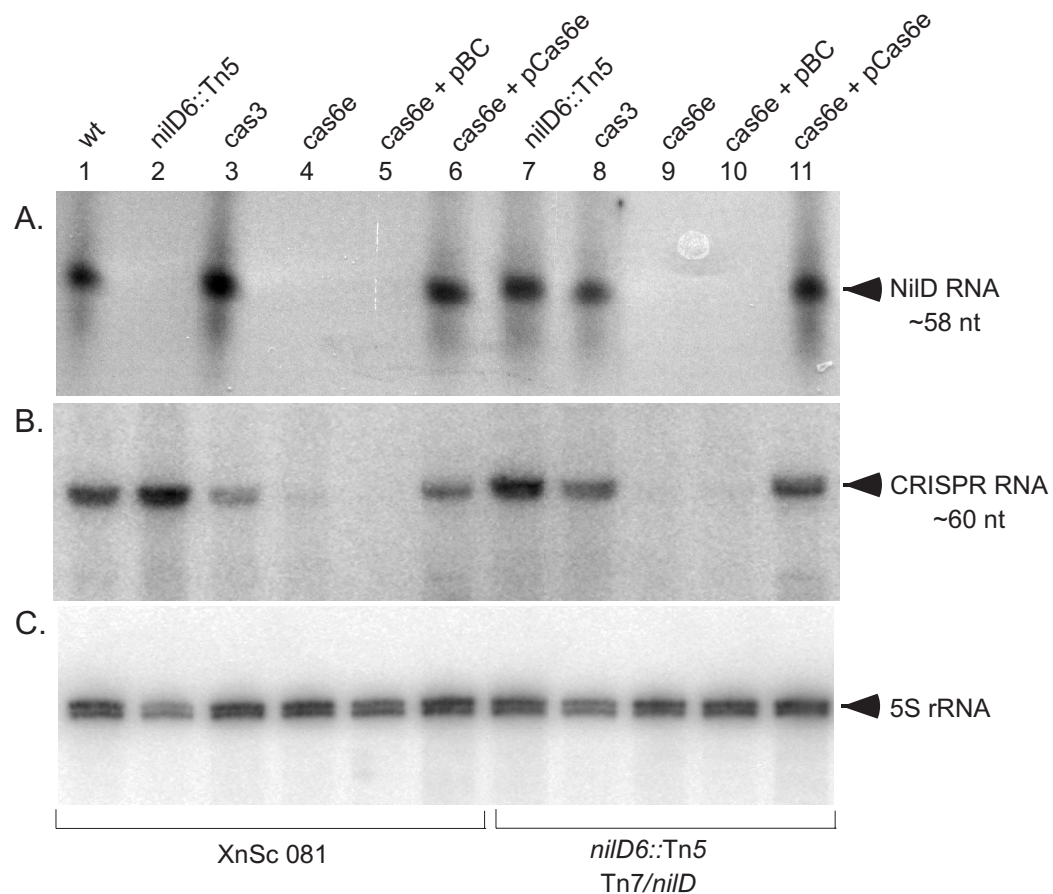


Figure A4.4 *cas6e* is necessary for presence of CRISPR RNA, but not for NiID RNA or colonization of *S. carpocapsae* nematodes. RNA was isolated from XnSc 081 wild type (wt), *nilD6::Tn5*, *Dcas-3::strep* (*cas3*), and *DcasE::strep* (*cas6e*) with or without the empty vector control (pBC) or the *cas6e* complement plasmid (pCas6e). All cells were grown to stationary phase in LB at 30°C. RNase protection assays using radiolabeled AAP2 primer (A) were used to detect NiID RNA while radiolabeled primers AAP1 (B) or Xn 5S RNA (C) were used in northern blots to detect CRISPR RNA and 5S RNA respectively. CRISPR RNA is detected as a band of ~60 nt. 5S RNA was detected as a band of ~113 nt.

***niID* and *casE* are only necessary for colonization in a specific genetic background.** Our data indicate that NiID RNA is not processed in the absence of *cas6e*. Furthermore, in *E. coli*, Cas3 is predicted to be required for processed crRNA function. We therefore predicted that in *X. nematophila* *cas6e* and *cas3*, like *niID*, would be required for nematode colonization. We first tested this by replacing the *cas6e* and *cas3* genes with a streptomycin resistance cassette in XnSc 081 and the *niID6::Tn5* mutant with (Tn7-*niID*) or without (eTn7) *niID*, generating a panel of *cas6e::strep* and *cas3::strep* strains. As predicted, disruption of *cas6e* in the *niID6::Tn5* + *niID* strain resulted in a significant colonization defect, which was rescued by providing a wild type copy of *cas6e* on a plasmid (Figure A4.5 B). These data are consistent with the model that the function of Cas6e in colonization is to process NiID RNA into a crRNA, although we have not ruled out the possibility that it has a NiID-independent function in colonization. Contrary to our prediction, deletion of *cas3* resulted in no significant effects on nematode colonization. Therefore, in contrast to crRNAs in other systems, NiID activity is independent of Cas3.

Surprisingly, neither the *cas6e::strep* nor the *cas3::strep* mutations caused a colonization defect in the XnSc 081 strain background (the parent of the *niID6::Tn5* mutant) (Figure A4.5 A), raising the possibility that the requirement for NiID RNA is specific to the *niID6::Tn5* background. To further explore this hypothesis, *niID* was replaced by allelic exchange with a kanamycin resistance cassette in the XnSc 081 and XnSc 800 wild type backgrounds. Like XnSc 081 *cas6E::strep*, the resulting strains, XnSc 081 *niID56::kan* and XnSc 800 *niID56::kan* mutants colonized *S. carpocapsae* to wild type levels (Table A4.2), despite a lack of NiID RNA detected by RPA (Figure A4.3 E and Figure A4.4 A).

These data verify that NiID and Cas6e are required for mutualism, but only within a specific genetic background of *X. nematophila*, suggesting a synthetic allele arose during the transposon mutagenesis process that gave rise to *niID6::Tn5*. To examine possible synthetic mutations present in this background, we sequenced and compared the *niID6::Tn5* draft

Table A4.2 A *nilD::kan* mutation does not confer a colonization defect in the HGB081 and HGB800 backgrounds.

<u>Relevant Alleles</u>	Average CFU of strain/IJ \pm standard error (n \geq 3) ^a	
	XnSc 081	HGB800
none	66.36 \pm 2.57	50.03 \pm 4.02
<i>nilD::kan</i>	60.03 \pm 3.86	61.73 \pm 0.96
<i>nilD::kan cas3::str</i>	60.52 \pm 5.97	60.05 \pm 3.17
<i>nilD::kan cas6e::str</i>	58.83 \pm 2.76	58.72 \pm 2.80

^aIn this experiment the *nilD6::Tn5* strain colonized at 0.10 ± 0.01 CFU/IJ. None of the values shown in the table were significantly different from each other, but all were significantly different from the *nilD6::Tn5* strain ($p < 0.001$ using one-way ANOVA with Tukey's post-test).

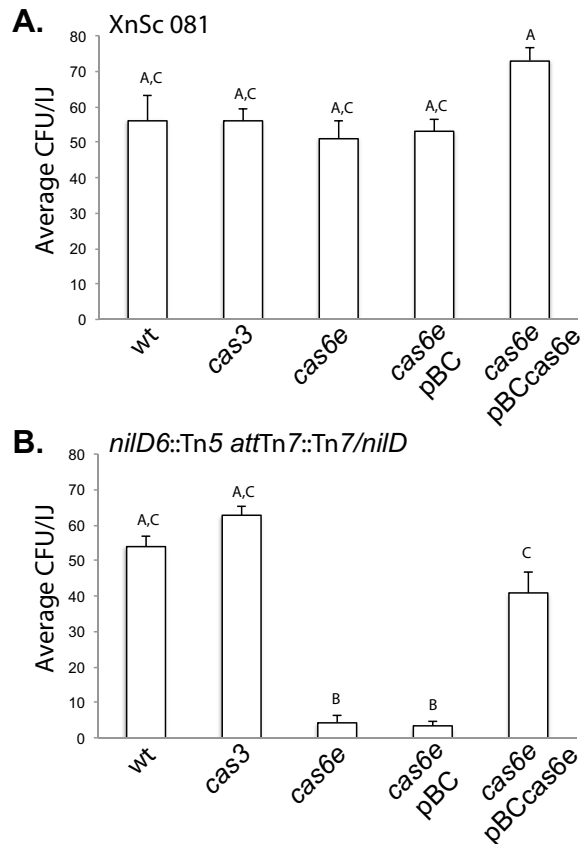


Figure A4.5 *cas6e* is necessary for colonization in the *nilD6::Tn5 attTn7::Tn7/nilD* background. Colonization ability was measured for **(A)** XnSc 081 and **(B)** *nilD6::Tn5 attTn7::Tn7/nilD* (the *nilD* mutant with wild type *nilD* expressed in trans at the *attTn7* site). Each strain carried wild type *cas* genes (wt) or *cas3* and *cas6e* mutations. In each background, the colonization phenotypes of the *cas6e* mutant carrying the control vector pBC or wild type *cas6e* (pBC*cas6e*) was also assessed. Each strain was co-cultivated with axenic *S. carpocapsae* nematodes and colony forming units (CFU) within the resulting progeny infective juveniles (IJ) was measured by sonication and dilution plating. The average CFU of strain/IJ \pm standard error ($n \geq 5$) is shown. In this experiment the uncomplemented *nilD6::Tn5* strain colonized at 0.22 ± 0.11 CFU/IJ. Different letters indicate significant differences in colonization levels between bacterial strains: $p < 0.0001$ One-way ANOVA with Tukey's post-test.

genome to that of its parent XnSc 081 and found only one difference, a single nucleotide variation (SNV) located within the intergenic region of genes XNC1_3346 and XNC1_3347 (T-3271541-C). Gene XNC1_3346 is predicted to encode a P4-like DNA primase while XNC1_3347 is a small hypothetical gene in the DUF1795 superfamily that is followed immediately by XNC1_3348, predicted to encode an Rhs-like, YD-repeat-containing protein of unknown function (Figure A4.S3). Overlapping XNC1_3346 is an 1147-bp repeat sequence that occurs with 80-87% identity in two other locations of the genome (one full length copy and one truncated copy), also overlapping with genes with homology to those encoding P4-like DNA primases (Figure A4.S3). The SNV occurs within this repetitive region and an alignment of the three repeat regions shows variability in the nucleotides around the SNV (Figure A4.S3 D). That the SNV associated with the *niID6::Tn5* strain background is located within a phage-encoding region is consistent with it being involved in the activity of the CRISPR-Cas system, potentially as a target for NiID RNA. However, no obvious regions of sequence identity or complementarity were observed between NiID RNA (repeats or spacer) and the region surrounding the SNV.

A suppressor of the niID6::Tn5 colonization phenotype. The low level of colonization observed for the *niID6::Tn5* mutant (~0.1 CFU/IJ; see for example Table A4.3) could reflect a majority of nematodes colonized by few bacterial cells, or full colonization (~50 bacteria) in one of many nematodes. The former phenotype might indicate the *niID6::Tn5* mutant has a defect in outgrowth (8), whereas the latter phenotype might indicate the *niID6::Tn5* mutant has a defect in initiation of colonization which can be occasionally suppressed. To distinguish between these possibilities we examined by epifluorescence microscopy the frequency of colonized nematodes after cultivation on a GFP-expressing *niID6::Tn5* strain (XnSc 829; Table A4.1). This analysis showed that the majority of individual nematodes were uncolonized and that approximately 1 in

600 nematodes were fully colonized (data not shown). To determine if rare colonization events were due to genetic or epi-genetic suppression of the *niID6::Tn5* mutation we examined the colonization phenotype of a colony isolate derived from *niID6::Tn5*-colonized nematodes. Upon re-cultivation with nematodes, this colony isolate, XnSc 1186 (*sup-1*) exhibited significantly higher levels of colonization than its *niID6::Tn5* parent (5.48 ± 0.57 vs. 0.15 ± 0.47 Avg. CFU/IJ respectively, $n \geq 6$, $p < 0.001$ by unpaired Student's t-test), despite the absence of detectable NiID RNA by RPA (Figure A4.3 E). These data indicate that the phenotype caused by the *niID6::Tn5* mutation can be suppressed, presumably by nucleotide or epigenetic changes elsewhere on the chromosome. The latter seems most likely, as sequencing of the XnSc 1186 *sup-1* genome did not reveal mutations that could explain the suppression phenotype (data not shown).

The niID locus contributes to XnSc 081 association with different nematode species. In addition to *S. carpocapsae*, *X. nematophila* associates with two other nematode species, *S. websteri* and *S. anatoliense* (56). To examine if NiID RNA is required for colonization of these other nematode hosts, the colonization phenotypes of the *niID6::Tn5* mutant and XnSc 081 in *S. anatoliense* and *S. websteri* were assessed. Similar to the phenotypes observed in *S. carpocapsae* colonization assays, XnSc 081 colonized *S. anatoliense* and *S. websteri* while the *niID6::Tn5* mutant displayed a marked defect in its ability to associate with these host nematode species (Table A4.3). In all three nematode hosts the colonization defect of the *niID6::Tn5* mutant was rescued by insertion of the XnSc 081 *niID* sequence at the *attTn7* insertion site (Table A4.3).

Strain specific NiID RNA variants are expressed in the S. anatoliense and S. websteri symbionts but do not rescue the niID6::Tn5 colonization defect. To determine if the *niID*

Table A4.3 *nilD* is required for *X. nematophila* colonization of *S. anatoliense* and *S. websteri* nematodes.

Bacterial Strain	<i>attTn7</i> locus insertion ^a	Average CFU/IJ ± standard deviation (n=3)		
		<i>S. carpocapsae</i>	<i>S. anatoliense</i>	<i>S. websteri</i>
XnSc 081	none	42.07 ± 11.01 ^A	34.40 ± 4.12 ^A	26.31 ± 6.20 ^A
XnSc 081 <i>nilD6::Tn5</i>	none	0.10 ± 0.04 ^B	0.36 ± 0.06 ^B	0.12 ± 0.15 ^B
XnSc 081 <i>nilD6::Tn5</i>	<i>nilD</i> -Sc	54.40 ± 7.95 ^A	38.60 ± 4.77 ^{A,C}	44.10 ± 7.03 ^{A,C}
XnSc 081 <i>nilD6::Tn5</i>	<i>nilD</i> -Sa	1.09 ± 0.24 ^B	1.08 ± 0.40 ^B	0.45 ± 0.23 ^B
XnSc 081 <i>nilD6::Tn5</i>	<i>nilD</i> -Sw	0.03 ± 0.02 ^B	0.25 ± 0.17 ^B	0.02 ± 0.14 ^B
XnSa	none	77.90 ± 16.58 ^{A,C}	59.40 ± 4.13 ^C	55.50 ± 16.61 ^{C,D}
XnSw	none	63.55 ± 12.97 ^{A,C}	28.45 ± 6.66 ^A	74.57 ± 4.74 ^D

^aA Tn7 transposon carrying *nilD* loci from XnSc (*nilD*-Sc), XnSa (*nilD*-Sa), or XnSw (*nilD*-Sw) was integrated at the *attTn7* locus. Different letters indicate significant differences between bacterial strains for colonization within each nematode species: p<0.05 using one-way repeated measures ANOVA (Prism v2.0, GraphPad, La Jolla, CA) with Tukey's post-test. Colonization levels achieved by each bacterial strain in the three nematode species were not significantly different except XnSw for which colonization of *S. anatoliense* nematodes was significantly lower than those of the other two nematode species (not shown).

locus is present in all *X. nematophila* strains regardless of the identity of their natural nematode host, we searched for it in *X. nematophila* strains from *S. anatoliense* and *X. websteri* (XnSa 1418 and XnSw 1419 respectively). Oligonucleotides (NiID 5' Apal and NiID 3' KpnI, Table A4.S4) complementary to flanking regions around the *niID* region of XnSc 081 successfully amplified products from XnSa 1418 and XnSw 1419 genomic DNA. In each case a product was obtained of similar size to that amplified from XnSc 081 and XnSc 800 (data not shown). The products amplified from XnSa 1418 and XnSw 1419 genomic DNA were cloned and sequenced. Relative to the *S. carpocapsae*-derived *X. nematophila* strains, the XnSa 1418 and XnSw 1419 *niID* regions encode an identical left repeat, 4-nt differences within the 32-nt spacer, and an identical right repeat except for the last 3 nt (Figure A4.1 D). Also, unlike the XnSc 081 *niID* sequence, the *niID* regions of XnSa 1418 and XnSw 1419 are not predicted to encode small overlapping open reading frames (data not shown).

To assess if the *niID* loci of XnSa 1418 and XnSw 1419 encode a NiID RNA molecule, we conducted RNase protection assays (RPA) using probes that match the XnSa 1418 *niID* sequence. RPA using this probe detected protected fragments in both the XnSa 1418 and XnSw 1419 samples that were similar in size to those that were detected (using XnSc specific probe) in the XnSc 081 and XnSc 800 samples (Figure A4.3 D). These data indicate that NiID RNA is expressed and processed similarly in all four Xn strains.

Given the divergence of the XnSa 1418 and XnSw 1419 *niID* spacers from those of Sc *X. nematophila* strains, we examined if the former could rescue the colonization defect of the *niID6::Tn5* mutant. The XnSa 1418 and XnSw 1419 *niID* sequences were cloned and inserted at the *attTn7* site of the XnSc 081 *niID6::Tn5* mutant, generating strains *niID6::Tn5 + niID-XnSa* (*niID + Sa*) and *niID6::Tn5 + niID-XnSw* (*niID + Sw*). RPA analysis was used to verify expression of the NiID RNA (Figure A4.3 D) while the colonization proficiency of the complemented strains was assessed using Sc nematodes (Table A4.3). As expected, insertion

of the XnSc *niID* sequence (strain *niID6::Tn5* + *niID*) was sufficient to restore wild type levels of colonization. In contrast, providing the XnSa 1418 and XnSw 1419 sequences failed to restore levels of colonization above the level of the *niID6::Tn5* mutant strain (Table A4.3). These results are consistent with our findings described above that alteration of the NiID RNA sequence was sufficient to disrupt the activity of this molecule. *niID6::Tn5* + *niID*-XnSa and *niID6::Tn5* + *niID*-XnSw were also deficient for colonization of *S. anatoliense* and *S. websteri* nematodes (Table A4.3), indicating that distinct *niID* sequences do not confer specificity for these nematode species.

To further explore the possible role of *niID* in host range specificity, we introduced it into *X. bovienii* (the symbiont of the nematode *S. jollieti*) that naturally lacks *niID* (57, 58). *X. bovienii* is unable to colonize *S. carpocapsae* unless it expresses the host-range specificity determinants *niIA*, *B*, and *C* (4, 59). We therefore expressed *niID* in *X. bovienii* with and without the *niIA*, *B*, and *C* genes. The presence of *niID* did not impact the colonization levels of *X. bovienii*: colonization of *S. carpocapsae* nematodes was below the level of detection (0.005 CFU/IJ) when *niID* was present without *niIA*, *B*, and *C*, and colonization levels of *X. bovienii* carrying *niIA*, *B*, and *C* were not increased by the presence of *niID* (data not shown).

CONCLUSIONS

The goal of this study was to elucidate the mechanistic role of the *X. nematophila niID* locus during colonization of *S. carpocapsae* host nematodes. Our work demonstrates that *niID* encodes a small RNA and that expression of this molecule is sufficient to rescue the colonization defect of the *niID6::Tn5* strain. Bioinformatic predictions indicated that NiID RNA is a member of the CRISPR RNA family. Consistent with this, we present experimental evidence that NiID RNA processing and colonization function requires *cas6e*, encoding a homolog of the *E. coli* CRISPR RNA processing Cascade complex endonuclease (Cas6e) (30). However,

unlike the CRISPR-Cas systems of other bacteria, NiID RNA function does not appear to require the helicase-nuclease Cas3 (29), since a *cas3* mutant does not display a colonization defect (Figure A4.5). This may indicate that the function of NiID RNA diverges from that of other crRNAs, and that its requirement in colonization does not include Cas3-mediated target degradation.

Several lines of evidence argue against the idea that the colonization function of NiID RNA is to restrict entry of exogenous DNA (plasmids and lytic bacteriophages), the initial primary function ascribed to crRNAs (19, 43). Instead, our data support the model that NiID RNA regulates endogenous sequences, as has been observed or suggested in other CRISPR-Cas systems (35, 36, 40, 60). First, the *niID6::Tn5* colonization defect is apparent in a closed system consisting only of a bacterial clonal population and the nematode host. Therefore, the only source of potentially toxic foreign DNA is the nematode. However, nematode lysates do not inhibit growth of *Xenorhabdus* strains in liquid culture and do not form plaques on bacterial lawns (data not shown). Further, BLASTn analyses (61) against the NCBI GenBank sequence database and to 13 other *Xenorhabdus* bacterial genomes (H. Goodrich-Blair, unpublished) failed to identify putative proto-spacers with identity to NiID (data not shown). While not conclusive, this fact is contrary to the idea that the NiID RNA targets a mobile genetic element present in other *Xenorhabdus* spp. Second, differences in the endogenous chromosome can bypass or cause the need for NiID RNA. The *niID6::Tn5* colonization defect is only apparent in a specific genomic background (Figure A4.5) in which suppressor alleles (e.g. *sup-1*) can arise that are able to colonize despite the absence of *niID* expression (Figure A4.3). Our genomic analysis indicates the strain background associated with the requirement for *niID* in colonization has a single distinguishing SNV, a T to C change at nt 3271541 in the intergenic region between a phage P4 primase and a region predicted to encode Rhs-like and associated elements (Figure A4.S3), while sequencing of the *sup-1* strain failed to identify any genetic alterations that could

account for the suppression phenotype (data not shown). These findings suggest that a single nucleotide change in the bacterial genome may confer dependence upon *niID* for colonization, whereas suppression may result from epigenetic or phase variability.

An alternative explanation for the role of NiID RNA in colonization is that it is required to control expression of an endogenous genetic element that is detrimental for host interactions, with the NiID RNA 32-nt spacer region conferring specificity for this element. Similar to the *E. coli* CRISPR system, NiID may control expression of its targets (32). Two models of CRISPR-Cas-mediated gene regulation are that the Cascade complex, including the crRNA binds to target mRNA to block translation or to promote Cas-3-mediated cleavage, or the Cascade complex binds to the DNA target and prevents transcription. Since a *cas-3* mutant does not display the same colonization defects as the *niID6::Tn5* mutant (Figure A4.5), our data are most consistent with the idea that the NiID RNA-Cascade complex blocks either transcription or translation, rather than triggering target degradation. Further insights into the mechanism of NiID RNA function await identification of its target(s). No proto-spacer with 100% identity is apparent in the genomes of XnSc 800 or XnSc 081, suggesting that low levels of similarity may be sufficient for NiID targeting. Conversely, complementation experiments using mutagenized XnSc 081 *niID* and the divergent *niID* loci of XnSa 1418 and XnSw 1419 failed to restore the colonization defect of *niID6::Tn5* (Table A4.3), revealing that some sequence integrity is essential. Furthermore, these data may indicate that the NiID RNA targets in strains XnSa 1418 and XnSw 1419 have diverged in sequence, and that the *niID* loci in those strains have co-evolved to maintain sequence identity. If true, further comparative sequence analysis of these strains could yield putative targets.

This report extends the limited number of studies demonstrating an impact of CRISPR-Cas systems on host-microbe interactions. The *cas2* gene of *Legionella pneumophila* is required for intracellular growth within host amoebae (38). Similar to our work, these

experiments were conducted in the absence of exogenous DNA or phage, suggesting that the requirement for *cas2* in *L. pneumophila* was independent of any interference-related functions. Likewise, a *cas2* mutant was not more sensitive upon exposure to UV light or to treatment with mitomycin C or nalidixic acid, indicating that the virulence defect was not due to the a potential role for Cas2 in DNA repair (data not shown). A recent study demonstrated *F. novicida* Cas9-mediated negative regulation of an endogenous gene encoding a lipoprotein. In the absence of *cas9*, aberrant expression of the lipoprotein triggered host immunity and reduced virulence of the pathogen (40). Together these and other studies have established a role for CRISPR-Cas machinery in facilitating pathogen virulence (41). The work presented here demonstrates these systems can also function in mutualistic associations. Though still enigmatic, the role of *NilD* RNA and its synthetic allele in nematode colonization should be clarified by identifying its molecular target, and in turn the function of this target in either promoting or inhibiting the colonization process.

ACKNOWLEDGEMENTS

We wish to thank Amy Cavanagh (UW-Madison) for technical support on northern blots and RPAs, and Jonathan Klassen (UConn-Storrs) and the Magnifying Genome team for their assistance in genome analysis and annotation. We gratefully acknowledge former and current members of the Goodrich-Blair lab: Dr. Kurt Heungens for preliminary data on the *nilD* locus, James Weger and Nick Feirer for contributions to *cas* mutant phenotypic analyses, and Ángel Casanova-Torres for quantitative reverse transcriptase PCR analysis of putative target genes. We thank Dr. Brian Tjaden (Wellesley College) for providing the Target RNA program for *X. nematophila*, S. Patricia Stock and S. Forst for collaborative work on *S. anatoliense* and *S. websteri*, and Caitilyn Allen and Katrina Forest (UW-Madison) for helpful discussions. Work in the Goodrich-Blair lab was funded by a grant from the National Science Foundation IOS-0950873. XL was

supported by the UW-Madison Graduate School research funds. JMC and KEM were supported by a National Institutes of Health (NIH) National Research Service Award T32 (AI55397) 'Microbes in Health and Disease'. J.M.C. was also supported by a National Science Foundation (NSF) Graduate Research Fellowship. EAH was supported by the National Institutes of Health grant 1F32AI084441. ARD was supported by a United States Public Health Service Training Grant (T32GM07616), and the Howard Hughes Medical Institute, with which PWS is an investigator. The authors have no conflict of interest to declare.

MATERIALS AND METHODS

Organisms and growth conditions. Strains used in this study are listed in Table A4.1. Unless otherwise noted, cultures were grown at 30°C in LB broth (62). *X. nematophila* growth media were stored in the dark or supplemented with 0.1% pyruvate (63). Media were supplemented with kanamycin (Km, 50 µg/ml), rifampicin (Rif, 100 µg/ml), ampicillin (Amp, 150 µg/ml), streptomycin (Sm, 25 µg/ml), or chloramphenicol (Cm, 30 µg/ml) where appropriate. For indicated RNA isolations, cultures were supplemented with 500 µM Fe₂SO₃, 100 µM 2,2-dipyridyl or 1 µM deferoxamine (Sigma-Aldrich, St. Louis, MO). The nematodes *Steinernema carpocapsae* (Weiser) All, obtained from Harry Kaya, and *S. anatoliense* (Al-Jubiha Jordan) and *S. websteri* (Peru), obtained from S. Patricia Stock, were reared in *Galleria mellonella* wax moth larvae (64). For *in vitro* co-cultures nematodes were grown at room temperature (20-26°C) on lipid agar (LA) plates with lawns of test *X. nematophila* strains as previously described (65). Defined medium was as previously described (66) except that glutamate was added at 100 mg l⁻¹ and Bacto agar (Sigma-Aldrich, St. Louis, MO) was used instead of noble agar. *X. nematophila* strains from *S. anatoliense* and *S. websteri* were isolated by surface sterilization of 1000-10000 IJ nematodes for 3 min in 0.5% NaOCl as described previously (11). Surface-sterilized nematode were sonicated for 1 min (67) and dilution plated onto LB + 0.1% pyruvate agar. Individual colonies were streaked for isolation, cultured overnight at 30°C, and frozen in glycerol stocks. Bacterial identity was verified by Sanger sequencing of the 16S gene using primers 27F and 1492R (Table A4.S4) (68).

DNA manipulations and biochemical assays. Plasmids used in this study are listed in Table A4.1. To create pCR2.1-TOPOmini, which lacks the Kan^R cassette, primers TOPO2.1mini_Fwd_NcoI and TOPO2.1mini_Rev_NcoI (Table A4.S4) were used to amplify the backbone of the plasmid pCR2.1-TOPO. The amplified product was cut with NcoI and self-

ligated. Standard protocols were used for the isolation of chromosomal DNA, DNA digestion, electrophoresis, and electroporation (69). Enzymes for DNA manipulations were obtained from Promega (Fitchburg, WI), New England Biosciences (Ipswich, MA) or Fermentas (Pittsburg, PA). Plasmid isolations and gel purifications were performed using appropriate kits (Qiagen, Germantown, MD). PCR amplification was performed using ExTaq polymerase, PrimeStar polymerase (Takara Shuzo, Kyoto, Japan) or PFU Ultra (Agilent Technologies, Madison, WI) and appropriate buffers on 100 ng *Xenorhabdus* chromosomal template-DNA, 0.2 μ M each primer, 0.4 mM dNTPs, and 2.5 U of polymerase. After 2 min incubation at 95°C, 30 cycles of 20 s at 95°C, 30 s at an annealing temperature appropriate for each primer pair, and 60-s kb⁻¹ at 72°C, were conducted, followed by 7 min incubation at 72°C.

pECMXb-Empty and pECMXb-SR2 construction, conjugation into *X. bovienii*. The pECMXb-Empty vector was constructed from pECM20 (8) by replacing the *X. nematophila* insertion sequence with a 588-bp fragment of *X. bovienii* intergenic genomic DNA (coordinates 390649-391236 of *X. bovienii* SS-2004; NC_013892.1) to facilitate homologous recombination of the plasmid into the *X. bovienii* genome. The pECM20 plasmid was divergently amplified on either side of the *X. nematophila* insert site to replace the insertion with the restriction sites for Apal and KpnI. Primers used were pECM20_Xb_F and pECM20_Xb_R (Table A4.S4). A predicted intergenic region of *X. bovienii* was amplified using primers pECMXb_insert_F and pECMXb_insert_R, and the sequence was inserted into pECMXb using Apal and KpnI. The insert was confirmed by sequencing using primers pECMXb_seq_F and pECMXb_seq_R (Table A4.S4). For construction of pECMXb-SR2, the SR2 region was sub-cloned from pTopoSR2-2 into the pECMXb XbaI site using XbaI and SpeI.

The pECMXb-Empty and pECMXb-SR2 plasmids were conjugated in *X. bovienii* 1166 and 1167 using previously described methods (70). Ex-conjugants were grown on LB media

supplemented with 15 µg/ml of chloramphenicol to select for insertion of the plasmid. Integration of pECMXb-Empty and pECMXb-SR2 into the genome was confirmed by positive PCR results using primers pECMXb_integratation_F and pECMXb_integration_R (Table A4.S4).

Isolation of *X. nematophila cas* and *niID* mutants. The 4,857 bp DNA fragment containing 2,751 bp *cas3* gene and its up-stream (1,213 bp) and down-stream (893 bp) sequences were amplified from HGB800 chromosomal DNA using Pfu DNA polymerase (Stratagene, Santa Clara, CA) and primers *cas3UpFwd_SpeI* and *cas3DownRev_XbaI*. Likewise, the 2,553 bp DNA fragment containing 678-bp *cas6e* (termed *casE* in strain designations) and its up-stream (1,233 bp) and down-stream (642 bp) sequences were amplified using primers *casEUpF_SpeI* and *casEDownR_XbaI*, respectively (Table A4.S4). The resulting fragments were digested with *XbaI* and *SpeI* and cloned into plasmid pCR2.1-TOPOmini between *XbaI* and *SpeI* sites. The *ahp* kanamycin resistance cassette and its promoter region were amplified from plasmid pEVS107 using primers *Kan-CleanRev_EcoRV_NEW* and *Kan-FullFwd_NheI_NEW* (Table A4.S4) digested with *NheI* and *EcoRV*, and used to replace the 2,362 bp *NheI-EcoRV* region (89-2451 bp) within the *cas3* gene and the 26-321 bp region of the *cas6e* gene, generating pCR2.1 mini $\Delta cas3::kan$ and pCR2.1 mini $\Delta casE4::kan$.

To create $\Delta cas6e::strep$ and *cas3::strep* insertion constructs used in this study, the Kan^R cassettes in pCR2.1 mini $\Delta casE4::kan$ (HGB1692) and pCR2.1 mini $\Delta cas3-3::kan$ were removed by cutting with *EcoRV* and *NheI*. The remaining backbone of the plasmid was ligated to *EcoRV/SpeI* fragment, containing the Sm^R cassette from pKNG101, to form pCR2.1 mini $\Delta casE6::strep$ and pCR2.1 mini $\Delta cas3-5::strep$. The $\Delta casE6::strep$ and $\Delta cas3-5::strep$ fragments were cut from the pCR2.1 mini backbone using *SpeI* and *XbaI* and cloned into the *SpeI* site of the mobilizable suicide plasmid pKNG101, generating pKNGD*casE6::strep* and pKNGD*cas3-5::strep*. The resulting constructs were maintained by electroporating into *E. coli*

SM10 (λ pir) cells and then introduced into HGB081, HGB800 and HGB1940 (Table A4.1) by conjugation, as described previously (71). Ex-conjugants were grown on LB agar containing 25 μ g/ml streptomycin overnight and subsequently grown on LB agar plus 5% sucrose to select for sucrose-resistant ex-conjugants that had excised the vector. The Sm^R phenotype was verified, and deletion of the *cas6e* or *cas3* gene fragments was confirmed by PCR amplification.

For deletion of the *niID* region, a 1,542 bp fragment upstream of *niID* was amplified from the XnSc 081 chromosome using PFU Ultra polymerase and the dNiID Up 5' Sall and dNiID Up 3' Apal primers. Likewise, a 1,082 bp fragment downstream of *niID* was amplified using the dNiID Dwn 5' Apal and dNiID 3' SacI primers while the Kan^R cassette was amplified from plasmid pEVS107 using primers Kan 5' Apal and Kan 3' Apal (Table A4.S4). PCR fragments were digested using appropriate restriction enzymes and then ligated into pKR100 plasmid, linearized with Sall and SacI enzymes, generating pKR100-*niID56::kan*. The resulting construct was maintained by electroporation of *E. coli* S17.1 (λ pir) and introduced into HGB081 and HGB800 by conjugation. Ex-conjugants were grown on LB agar containing 50 μ g/ml kanamycin overnight and then screened for loss of resistance to chloramphenicol. The deletion of the *niID* locus was confirmed by PCR and RPA was utilized to confirm NiID RNA was not being produced.

Complementation studies. To generate *niID* truncation constructs, portions of the *niID* locus were amplified (using primers indicated in parentheses) and cloned into pCR2.1[®]-TOPO to create pTopoSR2-DR90 (KHP62 and KHP58), -DR126 (KHP62 and KHP64), -DL84 (KHP57 and KHP63), -DL132 (KHP55 and KHP63), -DL161 (KHP36N and KHP63), and -DR90/DL84 (KHP57 and KHP58) (Table A4.S4). Once constructed, all fragments were subcloned from pCR2.1[®]-TOPO into pBCSK+ using Apal and SacI to create pSR2-DR90, pSR2-DR126, etc. To generate a stable *niID* complemented strain, a 387-nt fragment encoding the *niID* crRNA region

and approximately 175-nt upstream, was amplified using PrimeStar polymerase (Takara Shuzo, Kyoto, Japan) and primers *niID* 5' *Apal* and *niID* 3' *KpnI* (Table A4.S4). The *niID* PCR fragment and the Tn7-insertion vector, pEVS107 (Table A4.1), were digested with *Apal* and *KpnI* restriction enzymes and ligated using T4 DNA ligase (New England Biosciences). The resulting vector, pEVS107-*niID*, was maintained by electroporating into competent S17.1 λ *pir* *E. coli* cells followed by selection on LB plates supplemented with kanamycin.

To complement the *niID*-deficient strain (*niID6::Tn5*) with a *niID* region encoding synonymous base mutations within the spacer sequence, pEVS107-*niID* was subjected to a series of site directed mutagenesis reactions. The pEVS107-*niID* vector was first amplified using the *NiID* SDM set 1F and 1R primers (Table A4.S4) to generate base substitutions within codons 2 and 3 in the *niID* spacer region. The resulting construct was then further mutated using *NiID* SDM sets 2 through 5 (Table A4.S4) to generate synonymous base substitutions within codons 4-11, forming pEVS107-*niID*-SDM (Table A4.1). For site directed mutagenesis reactions, approximately 3 μ g of pEVS107-*niID* DNA were mixed with 15 pmol of each primer, 4 μ l of DMSO, 50 μ mol dNTP mix, 5 μ l PFU Ultra buffer and 1 μ l PFU ultra polymerase (2.5 units/ μ l) (Agilent Technologies) in 50 μ l of total volume. After 1 minute at 95°C, the resulting mixtures were incubated at 95°C for 1 min, 56°C for 50 s, and 72°C for 10 min for 25 cycles, followed by 10 additional min at 72°C. Following amplification, template DNA was digested by incubation with 10 units of *Apal* restriction enzyme at 37°C for 1 hr and the resulting PCR product was maintained by electroporation into S17.1 λ *pir* *E. coli* cells and selection on LB supplemented with kan. All plasmids were sequenced to ensure that the appropriate mutations were present and that no additional mutations had occurred within the *niID* region.

To generate the *casE* complementation construct, the *cas6e* gene was amplified using the *CasE* 5' *XbaI* and *CasE* 3' *EcoRV* primers (Table A4.S4) and PrimeStar polymerase (Takara Shuzo, Kyoto, Japan). The PCR product and pBluescript (pBCSK+) vector (Stratagene, La

Jolla, CA) were subjected to restriction digestion with XbaI and EcoRV enzymes and ligated using T4 ligase. The resulting vector, pBC-*casE* (Table A4.1), was introduced into Top 10 *E. coli* cells (Invitrogen, Carlsbad, CA) and maintained by selection on LB plates supplemented with chloramphenicol.

Complementation of *Xenorhabdus* strains was performed as previously described (71, 72). Briefly, for complementation of the *niID* mutation, overnight cultures of *niID6::Tn5*, S17.1 + pEVS107-*Tn7/niID* and the transposition helper strain S17.1 + pUX-BF13 (72), were diluted 1:100 in LB and incubated for 3 h at 30°C. After incubation, 900 µl of *X. nematophila* culture was mixed with 600 µl of S17.1 + pEVS107-*Tn7/niID*, and 500 µl S17.1 + pUX-BF13. The mixture was then pelleted by centrifugation, resuspended in 30 µl of LB and spotted onto LB plates supplemented with 0.1% pyruvate. Approximately 18 h after plating, cells were scraped into 1 ml of LB and 50 µl were plated onto LB supplemented with 0.1% pyruvate, and containing ampicillin and erythromycin for selection. Resistant colonies were screened for proper insertion at the Tn7 site by PCR analysis. For complementation with *niID* truncation or *cas6e* constructs, chemically competent *X. nematophila* strains were generated as previously described (73) and transformed with 200 ng of individual vector constructs. Transformants were plated on LB supplemented with 0.1% pyruvate and chloramphenicol.

RNA isolations and analyses. For RNA isolation from cultured bacteria, *X. nematophila* strains were grown for 18 h in either liquid LB or LB containing 100 µM dipyriddyI (to promote optimal NiID expression) and 0.1% pyruvate. Cultures were then diluted and cells were harvested during stationary phase or during late log phase (OD₆₀₀ of 1.0). Alternatively, for analysis of gene expression on solid media, cells were harvested from LA agar plates after 1 or 8 d of incubation, or from defined medium plates after 1 d. All strains were grown at either 20° or 30°C. RNA for RPA was isolated from individual strains using Trizol Reagent (Life

Technologies, Madison, WI), as previously described (74). The presence of approximately equal amounts of RNA between treatments was confirmed by agarose gel-electrophoresis (data not shown). Small RNA for northern analysis of CRISPR RNAs was isolated using mirVana kits (Applied Biosystems, Life Technologies, Madison, WI) according to manufacturer methods except for modifications to facilitate cell lysis as previously described (75).

For isolation of RNA from symbiotic bacteria, approximately 100,000 nematodes were harvested from lipid agar plates, suspended in LB, and lysed by sonication for 1 minute in a water bath sonicator. *Xenorhabdus* bacteria were harvested by centrifugation and RNA was isolated using Trizol Reagent (Life Technologies, Madison, WI), as described above.

Primer extension experiments. For primer extension, PAGE purified primers AAP1 and AAP2 (Table A4.S4) were radioactively labeled using T4 Polynucleotide Kinase and $\gamma^{32}\text{P}$ -ATP (Perkin Elmer, Waltham, MA) for 30 min at 37°C. Excess nucleotides were removed using a QIAquick® (Nucleotide Removal kit, Qiagen, Valencia, CA). Labeled primer was hybridized to 5 µg of total cell RNA in Avian Myeloblastosis Virus Reverse Transcriptase (AMV-RT) buffer (Promega, Madison, WI) by heating to 80°C for 10 min and slow cooling to 37°C. The primer was extended by AMV-RT enzyme at 37°C, precipitated, and resuspended in gel loading buffer (Promega, Madison, WI). A plasmid-based copy of *X. nematophila* SR2-2 region was cycle sequenced using *fmoI*® DNA Cycle Sequencing System kit (Promega, Madison, WI) and the labeled primer. The sequencing reaction was stopped using *fmoI*® sequencing stop solution (Promega, Madison, WI). Samples were electrophoresed on a 12% polyacrylamide gel (National Diagnostics, Charlotte, NC) that was then dried and imaged on a Storm860 phosphorimager (Molecular Dynamics, Sunnyvale, CA).

RNase protection assays. RPA analyses were performed using the Ambion RPA III kit™

method (Ambion Inc., Austin, TX), following manufacturer recommendations. Probes for XnSc *nilD* were generated by transcription from pAWA1 (Table A4.1) template containing a 137 bp fragment containing the *nilD* locus of XnSc. For generation of a probe complementary to the *nilD* region of XnSa and XnSw, site directed mutagenesis was utilized to alter the spacer region of *nilD* within TOPOSR2-2. SDM was performed as described above using PFU Ultra polymerase and primers RPA SDM 5' and 3' (Table A4.S4) to generate pTOPO-*nilD*-Sa (Table A4.1). Complementary transcripts were amplified and radioactively labeled with $\alpha^{32}\text{P}$ -UTP (PerkinElmer, Waltham, MA) using the MAXIscript®-T7 reaction (Ambion, Austin, TX). Labeled transcripts were separated on a 10% polyacrylamide gel (National Diagnostics Inc, Charlotte, NC) and probes were gel purified. 10 μg of sample RNA was then hybridized to $1\text{-}2 \times 10^5$ cpm of purified probe and RNase treated using a 1:100 dilution of RNase A/T1 enzyme (Ambion, Austin, TX). The RNase treated samples were electrophoresed on 10% polyacrylamide gels and visualized using XAR ECL- film (Kodak, Rochester, NY). A no-RNase control was also run to confirm probe integrity.

Northern. Total small RNA was separated on 12% denaturing polyacrylamide MOPS gels, transferred to uncharged nylon membrane, and probed first for crRNAs with pAAP1 oligonucleotide (which anneals to the conserved 3' repeat of all crRNAs; Table A4.S4) using methods previously described for LNA probes except that 2.5 μg small RNA was loaded per lane and hybridization was done at 50°C (75). Membranes were then reprobed with a full length RNA probe to *E. coli* 5S RNA (generated from pBS-5S) as previously described (74).

Nematode colonization assays. For colonization assays, lawns of individual bacterial strains were grown on lipid agar for 48 hours. Aposymbiotic infective juvenile-stage nematodes were generated by cultivation on a non-colonizing *rpoS* mutant, then surface sterilized, using a diluted

bleach solution, and applied to the bacterial lawns (65). In each experiment, two independent cultures of each strain were used as replicates, and 3 plates per replicate were seeded. Approximately one week post-inoculation, plates were water trapped for harvesting of IJs. Roughly 10^4 progeny IJs were then harvested from each plate (65), surface sterilized and disrupted by sonication. The macerates were dilution plated on selective media to quantify CFU/IJ as previously described (11). For *niID* deletion analyses, XnSc 081 and *niID6::Tn5* were transformed (73) with the plasmids indicated for each experiment and transformants were co-cultivated with nematodes on LA plates containing rifampicin and chloramphenicol. For *casE* complementation analyses, strains containing pBC-*casE* were grown on lipid agar plates supplemented with 10 $\mu\text{g/ml}$ Cm and 1 mM IPTG.

Sequencing of *X. nematophila* strains. The genomes of *X. nematophila* strains XnSc 081, *niID6::Tn5*, and *niID6::Tn5 sup-1* were sequenced using Illumina paired-end libraries (mean insert length = 300bp) yielding approximately 20-30 million 75 base-pair, paired-end reads for each strain. The resulting reads were trimmed for quality and then used in a reference alignment with respect to XnSc 800 using CLC Genomics Workbench 5.1 (CLC Bio). Assembled genomes were then analyzed for deletions, insertions and single nucleotide variations using CLC Genomics Workbench 5.1. SNVs were manually inspected for verification. Regions where low sequence coverage was obtained (fewer than 8 reads of coverage) were amplified and cloned from individual genomes and then sequenced. Because of significant genomic differences between XnSc 800, XnSa 1418 and XnSw 1419, performing reference alignments was not feasible. As a result, CLC Genomics Workbench 5.1 software was utilized to generate *de novo* genome assemblies using the reads from XnSa 1418 and XnSw 1419.

Accession numbers: Genomes have been submitted and accession numbers are pending. The

project accession number for HGB081 *X. nematophila* AN6/1 genome (XNC2) is PRJEB5061

while the project accession numbers for *X. nematophila* anatoliense (XNA1) and *X. nematophila* websteri (XNW1) are ERS451357 and ERS451358, respectively.

REFERENCES

1. **Stock SP, Goodrich-Blair H.** 2008. Entomopathogenic nematodes and their bacterial symbionts: The inside out of a mutualistic association. *Symbiosis* **46**:65-76.
2. **Goodrich-Blair H.** 2007. They've got a ticket to ride: *Xenorhabdus nematophila*-*Steinernema carpocapsae* symbiosis. *Curr Op Microbiol* **10**:225-230.
3. **Herbert EE, Goodrich-Blair H.** 2007. Friend and foe: the two faces of *Xenorhabdus nematophila*. *Nat Rev Microbiol* **5**:634-646.
4. **Chaston JM, Murfin KE, Heath-Heckman EA, Goodrich-Blair H.** 2013. Previously unrecognized stages of species-specific colonization in the mutualism between *Xenorhabdus* bacteria and *Steinernema* nematodes. *Cell Microbiol* **15**:1545-1559.
5. **Poinar GO.** 1966. The presence of *Achromobacter nematophilus* in the infective stage of a *Neoaplectana* sp. (Steinernematidae: Nematoda). *Nematologica* **12**:105-108.
6. **Wouts WM.** 1980. Biology, life cycle, and redescription of *Neoaplectana bibionis* Bovien, 1937 Nematoda: Steinernematidae. *J Nematol* **12**:62-72.
7. **Bird AF, Akhurst RJ.** 1983. The nature of the intestinal vesicle in nematodes of the family Steinernematidae. *Int J Parasitol* **13**:599-606.
8. **Martens EC, Heungens K, Goodrich-Blair H.** 2003. Early colonization events in the mutualistic association between *Steinernema carpocapsae* nematodes and *Xenorhabdus nematophila* bacteria. *J Bacteriol* **185**:3147-3154.
9. **Flores-Lara Y, Renneckar D, Forst S, Goodrich-Blair H, Stock P.** 2007. Influence of nematode age and culture conditions on morphological and physiological parameters in the bacterial vesicle of *Steinernema carpocapsae* (Nematoda: Steinernematidae). *J Invertebr Pathol* **95**:110-118.
10. **Snyder HA, Stock SP, Kim SK, Flores-Lara Y, Forst S.** 2007. New insights into the colonization and release process of *Xenorhabdus nematophila* and the morphology and ultrastructure of the bacterial receptacle of its nematode host, *Steinernema carpocapsae*. *Appl Environ Microbiol* **73**:5338-5346.
11. **Heungens K, Cowles CE, Goodrich-Blair H.** 2002. Identification of *Xenorhabdus nematophila* genes required for mutualistic colonization of *Steinernema carpocapsae* nematodes. *Mol Microbiol* **45**:1337-1353.
12. **Barrangou R, Marraffini LA.** 2014. CRISPR-Cas systems: Prokaryotes upgrade to adaptive immunity. *Mol Cell* **54**:234-244.
13. **Bolotin A, Quinquis B, Sorokin A, Ehrlich SD.** 2005. Clustered regularly interspaced short palindrome repeats (CRISPRs) have spacers of extrachromosomal origin. *Microbiol* **151**:2551-2561.
14. **Mojica FJ, Diez-Villasenor C, Garcia-Martinez J, Soria E.** 2005. Intervening sequences of regularly spaced prokaryotic repeats derive from foreign genetic elements. *J Mol Evol* **60**:174-182.

15. **Pourcel C, Salvignol G, Vergnaud G.** 2005. CRISPR elements in *Yersinia pestis* acquire new repeats by preferential uptake of bacteriophage DNA, and provide additional tools for evolutionary studies. *Microbiol* **151**:653-663.
16. **Deveau H, Barrangou R, Garneau JE, Labonte J, Fremaux C, Boyaval P, Romero DA, Horvath P, Moineau S.** 2008. Phage response to CRISPR-encoded resistance in *Streptococcus thermophilus*. *J Bacteriol* **190**:1390-1400.
17. **Sorek R, Lawrence CM, Wiedenheft B.** 2013. CRISPR-mediated adaptive immune systems in bacteria and archaea. *Annu Rev Biochem* **82**:237-266.
18. **Barrangou R, Fremaux C, Deveau H, Richards M, Boyaval P, Moineau S, Romero DA, Horvath P.** 2007. CRISPR provides acquired resistance against viruses in prokaryotes. *Science* **315**:1709-1712.
19. **Brouns SJ, Jore MM, Lundgren M, Westra ER, Slijkhuis RJ, Snijders AP, Dickman MJ, Makarova KS, Koonin EV, van der Oost J.** 2008. Small CRISPR RNAs guide antiviral defense in prokaryotes. *Science* **321**:960-964.
20. **Carte J, Wang R, Li H, Terns RM, Terns MP.** 2008. Cas6 is an endoribonuclease that generates guide RNAs for invader defense in prokaryotes. *Genes Dev* **22**:3489-3496.
21. **Makarova KS, Aravind L, Wolf YI, Koonin EV.** 2011. Unification of Cas protein families and a simple scenario for the origin and evolution of CRISPR-Cas systems. *Biol Direct* **6**:38.
22. **Makarova KS, Haft DH, Barrangou R, Brouns SJ, Charpentier E, Horvath P, Moineau S, Mojica FJ, Wolf YI, Yakunin AF, van der Oost J, Koonin EV.** 2011. Evolution and classification of the CRISPR-Cas systems. *Nat Rev Microbiol* **9**:467-477.
23. **Jore MM, Lundgren M, van Duijn E, Bultema JB, Westra ER, Waghmare SP, Wiedenheft B, Pul U, Wurm R, Wagner R, Beijer MR, Barendregt A, Zhou K, Snijders AP, Dickman MJ, Doudna JA, Boekema EJ, Heck AJ, van der Oost J, Brouns SJ.** 2011. Structural basis for CRISPR RNA-guided DNA recognition by Cascade. *Nat Struct Mol Biol* **18**:529-536.
24. **Gasiunas G, Sinkunas T, Siksnyus V.** 2014. Molecular mechanisms of CRISPR-mediated microbial immunity. *Cell Mol Life Sci* **71**:449-465.
25. **Semenova E, Jore MM, Datsenko KA, Semenova A, Westra ER, Wanner B, van der Oost J, Brouns SJ, Severinov K.** 2011. Interference by clustered regularly interspaced short palindromic repeat (CRISPR) RNA is governed by a seed sequence. *Proc Natl Acad Sci USA* **108**:10098-10103.
26. **Wiedenheft B, van Duijn E, Bultema JB, Waghmare SP, Zhou K, Barendregt A, Westphal W, Heck AJ, Boekema EJ, Dickman MJ, Doudna JA.** 2011. RNA-guided complex from a bacterial immune system enhances target recognition through seed sequence interactions. *Proc Natl Acad Sci USA* **108**:10092-10097.

27. **Mojica FJ, Diez-Villasenor C, Garcia-Martinez J, Almendros C.** 2009. Short motif sequences determine the targets of the prokaryotic CRISPR defence system. *Microbiol* **155**:733-740.
28. **Westra ER, Semenova E, Datsenko KA, Jackson RN, Wiedenheft B, Severinov K, Brouns SJ.** 2013. Type I-E CRISPR-Cas systems discriminate target from non-target DNA through base pairing-independent PAM recognition. *PLoS Genet* **9**:e1003742.
29. **Sinkunas T, Gasiunas G, Fremaux C, Barrangou R, Horvath P, Siksnys V.** 2011. Cas3 is a single-stranded DNA nuclease and ATP-dependent helicase in the CRISPR/Cas immune system. *EMBO J* **30**:1335-1342.
30. **Westra ER, van Erp PB, Kunne T, Wong SP, Staals RH, Seegers CL, Bollen S, Jore MM, Semenova E, Severinov K, de Vos WM, Dame RT, de Vries R, Brouns SJ, van der Oost J.** 2012. CRISPR immunity relies on the consecutive binding and degradation of negatively supercoiled invader DNA by Cascade and Cas3. *Mol Cell* **46**:595-605.
31. **Sinkunas T, Gasiunas G, Waghmare SP, Dickman MJ, Barrangou R, Horvath P, Siksnys V.** 2013. *In vitro* reconstitution of Cascade-mediated CRISPR immunity in *Streptococcus thermophilus*. *EMBO J* **32**:385-394.
32. **Edgar R, Qimron U.** 2010. The *Escherichia coli* CRISPR system protects from lambda lysogenization, lysogens, and prophage induction. *J Bacteriol* **192**:6291-6294.
33. **Methe BA, Webster J, Nevin K, Butler J, Lovley DR.** 2005. DNA microarray analysis of nitrogen fixation and Fe(III) reduction in *Geobacter sulfurreducens*. *Appl Environ Microbiol* **71**:2530-2538.
34. **Viswanathan P, Murphy K, Julien B, Garza AG, Kroos L.** 2007. Regulation of *dev*, an operon that includes genes essential for *Myxococcus xanthus* development and CRISPR-associated genes and repeats. *J Bacteriol* **189**:3738-3750.
35. **Zegans ME, Wagner JC, Cady KC, Murphy DM, Hammond JH, O'Toole GA.** 2009. Interaction between bacteriophage DMS3 and host CRISPR region inhibits group behaviors of *Pseudomonas aeruginosa*. *J Bacteriol* **191**:210-219.
36. **Aklujkar M, Lovley DR.** 2010. Interference with histidyl-tRNA synthetase by a CRISPR spacer sequence as a factor in the evolution of *Pelobacter carbinolicus*. *BMC Evol Biol* **10**:230.
37. **Babu M, Beloglazova N, Flick R, Graham C, Skarina T, Nocek B, Gagarinova A, Pogoutse O, Brown G, Binkowski A, Phanse S, Joachimiak A, Koonin EV, Savchenko A, Emili A, Greenblatt J, Edwards AM, Yakunin AF.** 2010. A dual function of the CRISPR-Cas system in bacterial antiviral immunity and DNA repair. *Mol Microbiol* **79**:484-502.
38. **Gunderson FF, Cianciotto NP.** 2013. The CRISPR-associated gene *cas2* of *Legionella pneumophila* is required for intracellular infection of amoebae. *mBio* **4**.
39. **Louwen R, Horst-Kreft D, de Boer A, van der Graaf L, de Knecht G, Hamersma M, Heikema A, Timms A, Jacobs B, Wagenaar J, Endtz H, van der Oost J, Wells J,**

- Nieuwenhuis E, van Vliet A, Willemsen P, van Baarlen P, van Belkum A.** 2013. A novel link between *Campylobacter jejuni* bacteriophage defence, virulence and Guillain-Barré syndrome. *Eur J Clin Microbiol Infect Dis* **32**:207-226.
40. **Sampson TR, Saroj SD, Llewellyn AC, Tzeng YL, Weiss DS.** 2013. A CRISPR/Cas system mediates bacterial innate immune evasion and virulence. *Nature* **497**:254-257.
41. **Louwen R, Staals R, Endtz H, van Baarlen P, van der Oost J.** 2014. The role of CRISPR-Cas systems in virulence of pathogenic bacteria. *Microbiol Molec Biol Rev* **78**:74-88.
42. **Pul U, Wurm R, Arslan Z, Geissen R, Hofmann N, Wagner R.** 2010. Identification and characterization of *E. coli* CRISPR-cas promoters and their silencing by H-NS. *Mol Microbiol* **75**:1495-1512.
43. **Marraffini LA, Sontheimer EJ.** 2008. CRISPR interference limits horizontal gene transfer in staphylococci by targeting DNA. *Science* **322**:1843-1845.
44. **Sorek R, Kunin V, Hugenholtz P.** 2008. CRISPR--a widespread system that provides acquired resistance against phages in bacteria and archaea. *Nat Rev Microbiol* **6**:181-186.
45. **Jansen G, Thijssen KL, Werner P, van der Horst M, Hazendonk E, Plasterk RHA.** 1999. The complete family of genes encoding G proteins of *Caenorhabditis elegans*. *Nat Genet* **21**:414-419.
46. **Lillestol RK, Redder P, Garrett RA, Brugger K.** 2006. A putative viral defence mechanism in archaeal cells. *Archaea* **2**:59-72.
47. **Haft DH, Selengut J, Mongodin EF, Nelson KE.** 2005. A guild of 45 CRISPR-associated (Cas) protein families and multiple CRISPR/Cas subtypes exist in prokaryotic genomes. *PLoS Comput Biol* **1**:e60.
48. **Makarova KS, Grishin NV, Shabalina SA, Wolf YI, Koonin EV.** 2006. A putative RNA-interference-based immune system in prokaryotes: computational analysis of the predicted enzymatic machinery, functional analogies with eukaryotic RNAi, and hypothetical mechanisms of action. *Biol Direct* **1**:7.
49. **Chakraborty S, Snijders AP, Chakravorty R, Ahmed M, Tarek AM, Hossain MA.** 2010. Comparative network clustering of direct repeats (DRs) and *cas* genes confirms the possibility of the horizontal transfer of CRISPR locus among bacteria. *Mol Phylogenet Evol* **56**:878-887.
50. **Fineran PC, Charpentier E.** 2012. Memory of viral infections by CRISPR-Cas adaptive immune systems: acquisition of new information. *Virology* **434**:202-209.
51. **Nuñez JK, Kranzusch PJ, Noeske J, Wright AV, Davies CW, Doudna JA.** 2014. Cas1-Cas2 complex formation mediates spacer acquisition during CRISPR-Cas adaptive immunity. *Nat Struct Mol Biol* doi:10.1038/nsmb.2820.

52. **Ivancic-Bace I, Radovcic M, Bockor L, Howard JL, Bolt EL.** 2013. Cas3 stimulates runaway replication of a ColE1 plasmid in *Escherichia coli* and antagonises RNaseHI. *RNA Biol* **10**.
53. **Touchon M, Charpentier S, Clermont O, Rocha EP, Denamur E, Branger C.** 2011. CRISPR distribution within the *Escherichia coli* species is not suggestive of immunity-associated diversifying selection. *J Bacteriol* **193**:2460-2467.
54. **Richards GR, Goodrich-Blair H.** 2009. Masters of conquest and pillage: *Xenorhabdus nematophila* global regulators control transitions from virulence to nutrient acquisition. *Cell Microbiol* **11**:1025-1033.
55. **Takeuchi N, Wolf YI, Makarova KS, Koonin EV.** 2012. Nature and intensity of selection pressure on CRISPR-associated genes. *J Bacteriol* **194**:1216-1225.
56. **Lee MM, Stock SP.** 2010. A multilocus approach to assessing co-evolutionary relationships between *Steinernema* spp. (Nematoda: Steinernematidae) and their bacterial symbionts *Xenorhabdus* spp. (gamma-Proteobacteria: Enterobacteriaceae). *Syst Parasitol* **77**:1-12.
57. **Chaston JM, Suen G, Tucker SL, Andersen AW, Bhasin A, Bode E, Bode HB, Brachmann AO, Cowles CE, Cowles KN, Darby C, de Leon L, Drace K, Du Z, Givaudan A, Herbert Tran EE, Jewell KA, Knack JJ, Krasomil-Osterfeld KC, Kukor R, Lanois A, Latreille P, Leimgruber NK, Lipke CM, Liu R, Lu X, Martens EC, Marri PR, Medigue C, Menard ML, Miller NM, Morales-Soto N, Norton S, Ogier JC, Orchard SS, Park D, Park Y, Qurollo BA, Sugar DR, Richards GR, Rouy Z, Slominski B, Slominski K, Snyder H, Tjaden BC, van der Hoeven R, Welch RD, Wheeler C, Xiang B, Barbazuk B, et al.** 2011. The entomopathogenic bacterial endosymbionts *Xenorhabdus* and *Photorhabdus*: convergent lifestyles from divergent genomes. *PLoS ONE* **6**:e27909.
58. **Sugar DR, Murfin KE, Chaston JM, Andersen AW, Richards GR, Deleon L, Baum JA, Clinton WP, Forst S, Goldman BS, Krasomil-Osterfeld KC, Slater S, Stock SP, Goodrich-Blair H.** 2012. Phenotypic variation and host interactions of *Xenorhabdus bovienii* SS-2004, the entomopathogenic symbiont of *Steinernema jolietii* nematodes. *Env Microbiol* **14**:924-939.
59. **Cowles CE, Goodrich-Blair H.** 2008. The *Xenorhabdus nematophila* *nilABC* genes confer the ability of *Xenorhabdus* spp. to colonize *Steinernema carpocapsae* nematodes. *J Bacteriol* **190**:4121-4128.
60. **Cady KC, O'Toole GA.** 2011. Non-identity-mediated CRISPR-bacteriophage interaction mediated via the Csy and Cas3 proteins. *J Bacteriol* **193**:3433-3445.
61. **Altschul SF, Madden TL, Schaffer AA, Zhang J, Zhang Z, Miller W, Lipman DJ.** 1997. Gapped BLAST and PSI-BLAST: a new generation of protein database search programs. *Nucleic Acids Res* **25**:3389-3402.
62. **Miller JH.** 1972. *Experiments in Molecular Genetics*. Cold Spring Harbor Laboratory Press, Cold Spring Harbor, N. Y.

63. **Xu J, Hurlbert RE.** 1990. Toxicity of irradiated media for *Xenorhabdus* spp. Appl Environ Microbiol **56**:815-818.
64. **Kaya HK, Stock SP.** 1997. Techniques in insect nematology, p 281-324. In Lacey LA (ed), Manual of Techniques in Insect Pathology. Academic Press, London.
65. **Vivas EI, Goodrich-Blair H.** 2001. *Xenorhabdus nematophilus* as a model for host-bacterium interactions: *rpoS* is necessary for mutualism with nematodes. J Bacteriol **183**:4687-4693.
66. **Orchard SS, Goodrich-Blair H.** 2004. Identification and functional characterization of a *Xenorhabdus nematophila* oligopeptide permease. Appl Environ Microbiol **70**:5621-5627.
67. **Cowles CE, Goodrich-Blair H.** 2004. Characterization of a lipoprotein, NilC, required by *Xenorhabdus nematophila* for mutualism with its nematode host. Mol Microbiol **54**:464-477.
68. **Lane DJ.** 1991. 16S/23S rRNA sequencing, p 115-175. In Stackebrandt E, Goodfellow M (ed), Nucleic acid techniques in bacterial systematics. Blackwell, Oxford.
69. **Sambrook J, Fritsch EF, Maniatis T.** 1989. Molecular Cloning: a Laboratory Manual, second ed. Cold Spring Harbor Laboratory Press, Cold Spring Harbor, NY.
70. **Murfin KE, Chaston J, Goodrich-Blair H.** 2012. Visualizing bacteria in nematodes using fluorescence microscopy. J Vis Exp **68**:e4298.
71. **Forst SA, Tabatabai N.** 1997. Role of the histidine kinase, EnvZ, in the production of outer membrane proteins in the symbiotic-pathogenic bacterium *Xenorhabdus nematophilus*. Appl Environ Microbiol **63**:962-968.
72. **Bao Y, Lies DP, Fu H, Roberts GP.** 1991. An improved Tn7-based system for the single-copy insertion of cloned genes into chromosomes of Gram-negative bacteria. Gene **109**:167-168.
73. **Xu J, Lohrke S, Hurlbert IM, Hurlbert RE.** 1989. Transformation of *Xenorhabdus nematophilus*. Appl Environ Microbiol **55**:806-812.
74. **Wassarman KM, Storz G.** 2000. 6S RNA regulates *E. coli* RNA polymerase activity. Cell **101**:613-623.
75. **Cavanagh AT, Sperger JM, Wassarman KM.** 2012. Regulation of 6S RNA by pRNA synthesis is required for efficient recovery from stationary phase in *E. coli* and *B. subtilis*. Nucleic Acids Res **40**:2234-2246.
76. **McCann J, Stabb EV, Millikan DS, Ruby EG.** 2003. Population dynamics of *Vibrio fischeri* during infection of *Euprymna scolopes*. Appl Environ Microbiol **69**:5928-5934.
77. **Kaniga K, Delor I, Cornelis GR.** 1991. A wide-host-range suicide vector for improving reverse genetics in Gram-negative bacteria: inactivation of the *blaA* gene of *Yersinia enterocolitica*. Gene **109**:137-141.

78. **Trotochaud AE, Wassarman KM.** 2005. A highly conserved 6S RNA structure is required for regulation of transcription. *Nat Struct Mol Biol* **12**:313-319.

SUPPLEMENTAL MATERIALS

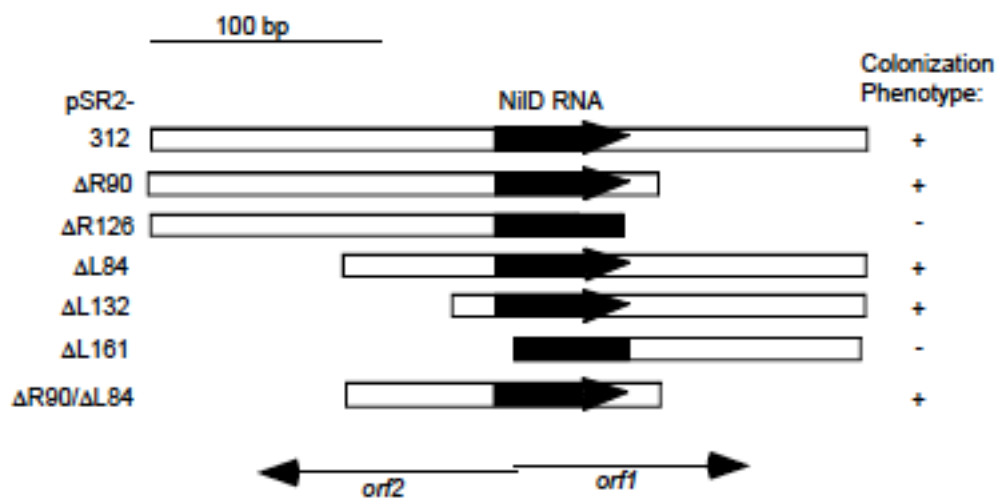


Figure A4.S1 Deletion analysis of the *niID* region indicates neither *orf1* nor *orf2* is required in its entirety to rescue the colonization defect of the *niID6::Tn5* mutant in plasmid complementation assays. Schematic representations of the deletion constructs tested for their ability to complement the colonization defect of the XnSc HGB081 *niID6::Tn5* mutant. The name of the plasmid carrying each fragment is shown on the left and is named according to whether the deletion truncates the 5' (ΔL) and/or 3' (ΔR) ends, and the size of the deleted region. *orf1* and *orf2* positions are indicated by arrows at the bottom of the figure, and the region encoding the 58-nt NiID RNA (see main text and Figure A4.1) is shaded in black, with an arrow representing the full NiID RNA sequence and a rectangle indicating a truncation of the NiID RNA coding sequence. The colonization phenotype of XnSc HGB081 *niID6::Tn5* carrying each plasmid construct is indicated to the right (see Table A4.S3 for data).

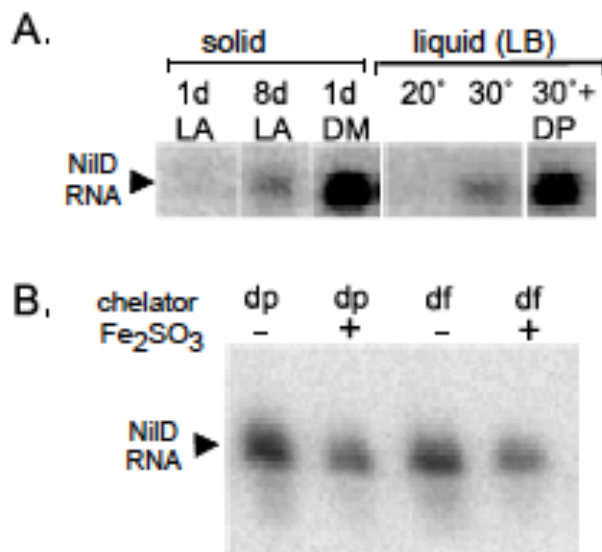


Figure A4.S2

A) NiID RNA expression under various conditions. Protection assays were performed with RNA isolated from wild-type HGB081 cells cultured on solid (lanes 1-3) or liquid (lanes 4-6) medium. RNA was isolated from cells growing on LA for 1 (lane 1) or 8 (lane 2) days or on solid defined medium (DM) for 1 day (lane 3). Cells were grown in liquid LB at 20°C (lane 4) or 30°C (lane 5) or in LB supplemented with 2,2-dipyridyl (DP) at 30°C (lane 6). A representative experiment is shown; similar results were obtained in 2 independent experiments. Little NiID RNA-protected fragment was observed on LA plates after 1 d of incubation, with substantially more at 8 d, suggesting NiID RNA is elevated in nutrient-limited or aged cells. Indeed, NiID RNA was more abundant in *X. nematophila* incubated 1 d on a solid defined medium (see experimental procedures) than in 1 d LA plates (compare lanes 1 and 3), further suggesting that NiID RNA abundance is affected by nutrient availability. The elevated levels of NiID RNA do not appear to be the result of slow growth, since higher levels were not observed in cells grown at 20°C relative to cells grown at the optimal *X. nematophila* growth temperature (30°C). Instead, increased NiID RNA levels may be triggered by iron limitation since higher levels were detected after growth in LB supplemented with 2, 2-dipyridil (an Fe(II) chelator) than in LB alone

(compare lanes 5 and 6).

B) NilD RNA expression during growth with iron chelators. Protection assays were performed with RNA isolated from wild-type HGB081 cells cultured in LB + 2,2-dipyridyl (lane 1, dp, -), LB + 2,2-dipyridyl + Fe₂SO₃ (lane 2, dp, +), LB + deferoxamine (Lane 3, df, -), or LB + deferoxamine + Fe₂SO₃ (lane 4, df, +). A representative experiment is shown; similar results were obtained in 2 independent experiments. RNA (i.e. protected fragment) levels similar to that found in LB grown cultures (data not shown) were observed in *X. nematophila* cells grown in the presence of iron chelators specific for Fe(II) or Fe(III) without exogenously added iron (Average \pm SD, n=2, radioactivity relative to growth in LB: Deferoxamine, 1.19 ± 0.14 ; 2,2- dipyridyl, 0.94 ± 2.0). This result is in contrast to those obtained and shown in Figure A4.S2 A, in which RNA levels were higher in the presence of chelator than in its absence. However, levels of iron in LB media preparations were not controlled, and it is likely that the LB-grown cells shown in Fig. S2B had already begun to experience iron limitation when they were harvested. Indeed, when Fe₂SO₃ was included in addition to the iron chelators the level of protected fragment was lower than that during growth in LB alone (Average \pm SD, n=2, radioactivity relative to growth in LB: Deferoxamine + Fe₂SO₃, 0.54 ± 0.06 ; 2,2-dipyridyl + Fe₂SO₃, 0.59 ± 0.03). No protected fragments were detected in samples of RNA isolated from HGB315 nilD6::Tn5 cells grown under each of these conditions (data not shown).

Within each panel, all samples were run on a single gel, but for A, irrelevant lanes were removed by manipulation in Adobe Photoshop after visualization was enhanced through contrast.

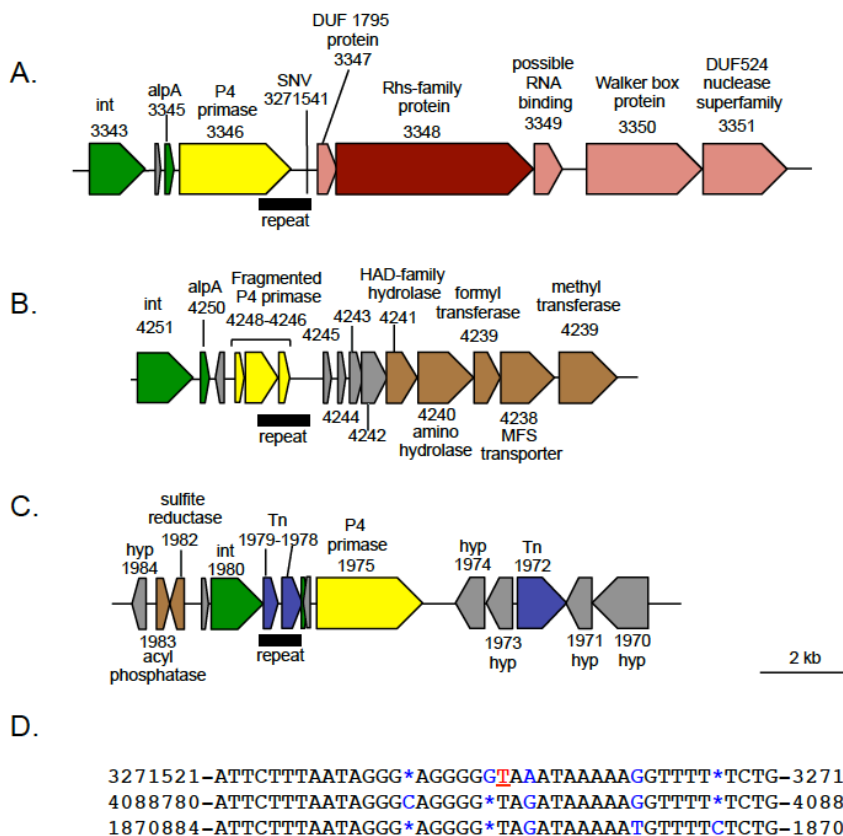


Figure A4.S3 (A) Genomic context of the single nucleotide variant (SNV), C-3271541-T, that distinguishes the nilD6::Tn5 strain background from the XnSc 081 parent background. The SNV occurs within a 1147-bp sequence (black rectangle) that is repeated in two other regions of the genome, one at full length (B) and the other truncated by 208-nt (C). Predicted open reading frames (box arrows) are labeled with their XNC1_ORF designation and predicted putative function. The boxes representing predicted P4 primases encoded at each locus are yellow whereas additional predicted functional categories are indicated by the following color scheme: Maroon (Rhs-family protein); Light red (potential Rhs-related proteins); Green (phage-related); Brown (metabolic); Blue (transposon and IS elements); Gray (hypothetical ORFs). A 2-kb scale bar for A-C is shown on the lower right. (D) Alignment of 40-nt of the repeat region surrounding the SNV (red underlined nucleotide). Within the 40-nt, sequence differences among the three repeats are highlighted as blue text and asterisks mark indels.

Table A4.S1 Regions of genome differences between XnSc 081 and XnSc 800

Mutation	Gene ID	Gene name/Function	Effect on Coding Sequence
SNVS			
T241,233C	XNC1_0274	<i>fabR</i> , transcriptional repressor fragment	Synonymous
G241,237C	XNC1_0274		Synonymous
T270,582G	XNC1_0323	<i>rpsC</i> , 30S ribosomal subunit protein S3	H139Q
A270,617T	XNC1_0323		E151V
C270,642T	XNC1_0323		Synonymous
C270,880G	XNC1_0324	Hypothetical	Synonymous
C270,896A	XNC1_0324		Q40K
T270,940G	XNC1_0325	<i>rlpP</i> , 50S ribosomal subunit protein L16	V8G
T636,807G	XNC1_0743	<i>oppA3</i> , ABC Transporter family	D2E
A653,167T	Upstream of XNC1_0754	<i>ahpC</i> , alkyl hydroperoxide reductase	NA ¹
T804,168G	XNC1_0935	Hypothetical	M15L
C941,069A	XNC1_1064	<i>lpxC</i> , NAG deacetylase	NA
T941,071A	XNC1_1064		
T941,131G	XNC1_1064		V15G
T976,807A	XNC1_1092	Hypothetical	Y40*
C1,065,676A	Upstream XNC1_1197	e14 prophage tail fiber protein	NA
G1,081,851C	Downstream XNC1_1212	Phage modular protein D	NA
G1,081,856C	Downstream XNC1_1212		NA
T1,081,865C	Downstream XNC1_1212		NA
G1,081,878C	Downstream XNC1_1212		NA
T1,081,884,G	Downstream XNC1_1212		NA
T1,081,890G	Downstream XNC1_1212		NA
T1,195,432C	XNC1_1332	<i>mrd</i> , peptidoglycan synthetase	K195E
A1,422,830T	XNC1_1543	<i>infA</i> , Protein chain initiation factor	L8*
C1,422,833T	XNC1_1543		G7D
C1,712,985T	XNC1_1774	Hypothetical	With Below Q44S
A1,712,986C	XNC1_1774		Q44S
A2,598,811T	Downstream XNC1_2635	NA	NA
G2,898,177A	XNC1_2903	DnaG primase like seq	Synonymous
G2,982,740A	Upstream of XNC1_2997	Chiting binding protein	NA
T3,490,398G	XNC1_3605 Operon	GroEL chaperone operon	NA
C3,490,857G	XNC1_3606 Operon	GroEL chaperone operon	NA
T3,495,578A	Downstream XNC1_3616	BamHI control element	NA
G3,704,993A	XNC1_3848	<i>pcm</i>	Q156*
G3,839,515A	Upstream XNC1_3977	Hypothetical	NA
T3,839,518A	Upstream XNC1_3977		NA
T3,839,519A	Upstream XNC1_3977		NA
A3,839,525C	Upstream XNC1_3977		NA
A3,839,526G	Upstream XNC1_3977		NA
A3,839,634G	XNC1_3978	<i>gmhB</i>	C156R
A3,839,640G	XNC1_3978		F154L
C3,839,695T	XNC1_3978		Synonymous
G3,839,718T	XNC1_3978		L128M
T3,839,751A	XNC1_3978		M117L
C3,933,193G	XNC1_4062	<i>imp</i> , organic solvent tolerance protein	Synonymous
G3,933,205T	XNC1_4062		K246N
A3,933,207T	XNC1_4062		N247I
G3,933,223T	XNC1_4062		E252D
C3,933,272A	XNC1_4062		H269N
A4,204,557T	XNC1_4379	<i>rpoB</i> , RNA polymeras subunit	D516V
Frameshift Mutations			
-36,438A	XNC1_0034	<i>gidA</i> , glucose-inhibited division protein	G19fs
-241,252A	XNC1_0274	<i>fabR</i> , transcriptional repressor	NA

Table A4.S2 CRISPR loci of *X. nematophila* (HGB800) designated alphabetically according to their chromosomal position.

CRISPR Region	Coordinates (HGB800 genome)	Repeat #	Notable features
A	881776-882019	2	Spacer identical to that of CRISPR-B
B	1814239-1814329	2	Spacer identical to that of CRISPR-A. Encoded near 3' end of repeat region C.
C	1814463-1815955	25	Spacer 22 is 100% identical to XNC1_3681, a XnSc chromosomal gene of unknown function
D	3320125-3320276	3	Highly divergent repeat sequence
E	3577918-3579107	20	CAS-proximal (upstream); Spacer 4 is 100% identical to XNC1_2560 (<i>xptE1</i>), a XnSc chromosomal gene predicted to encode an A subunit of Tc toxin
<i>nilD</i>	3579434..3579491	2	Necessary for nematode colonization
G	3589391_3590272	16	CAS-proximal (downstream)

Table A4.S3 Colonization analysis of HGB315 (*nilD6::Tn5*) carrying SR2 deletion constructs^a

Plasmid	<i>orf1</i>	<i>orf2</i>	RNA	XnSc 081	XnSc 081
				wild-type	<i>nilD6::Tn5</i>
pBCSK+	n.a.	n.a.	n.a.	37.3 ± 12.3	0.8 ± 0.1
pSR2-312	+	+	+	38.3 ± 13.3	43.6 ± 16.5
pSR2-ΔR90	-	+	+	31.9 ± 2.2	49.1 ± 23.9
pSR2-ΔR126	-	+	-	53.8 ± 23.7	0.1 ± 0.0
pSR2-ΔL84	+	-	+	18.7 ± 5.4	90.3 ± 43.8
pSR2-ΔL132	+	-	+	15.6 ± 4.5	40.9 ± 23.5
pSR2-ΔL161	+	-	-	40.3 ± 20.6	0.1 ± 0.0
pSR2-ΔR90/ΔL84	-	-	+	32.1 ± 11.4	53.4 ± 4.0

a. Each construct was tested 3 independent times and colonization data represent average cfu/IJ ± standard error.

Table A4.S4 Oligonucleotides used in this study

Name	Sequence (5'-3')
PCR Amplification and Sequencing	
KHP36N	CATGGCTACTTTGAATTTCC
KHP55	ATGTTTCCCGTTAATACGG
KHP57	GAAGAAAGATAAAGAATTGG
KHP58	TATTTATCCCGTACTTACG
KHP62	TATACCTACAGTGCTTTACC
KHP63	TCAACGAAAAACAAGAAGC
KHP64	ACAAGGAAATTCAAAGTAGCC
KHP65	CTACCATTTTTTCAGCCAAT
NiID 5' Apal	AAAGGGCCCTCTACCATTTTTTCAGC
NiID 3' KpnI	AAAGGTACCCTAGATATGCAAATTC
SR-2 Websteri 5'	ATTTCCCGCCGGATTAATATGCCAAAACCT
SR-2 Websteri 3'	CGTACTTACGGGAACACATCATTGCCTGAACA
RPA Probe SDM 5'	CCATAGCTCCTTTAAATTTCTTGATTATAACTCCATGTTCCCGG
RPA Probe SDM 3'	CGGGGAACATGGAGTTATAATCAAGGAAATTTAAAGGAGCTATGG
27F	AGAGTTTGATCATGGCTCAG
1492R	TACGGTTACCTTGTACGACTT
Primer Extension and Northern	
AAP1	CCGTACTTACGGGGAACATGG
AAP2	GGAGTTATAAACAAGGAAATTC
Mutant Construction	
dNiID Up 5' Sall	AAAGTCGACTGTGCCCCAATGCG
dNiID Up 3' Apal	AAAGGGCCCTACTATTTCGT
dNiID Dwn 5' Apal	AAAGGGCCCGAATCCGTTCTATTC
dNiID Dwn 3' SacI	AAAGAGCTCAATTCCAACCTGACTCCG
Kan 5' Apal	AAAGGGCCCCCACGTTGTGTCTCAAAATCT CTG
Kan 3' Apal	AAAGGGCCCTTAGAAAAACTCATGGAGCATCAAATG
Cas3UpFwd_Spel	ATATATACTAGTCCATGGCTACTTTGAATTTCTTG
Cas3DownRev_XbaI	ATATATTCTAGACGGATTCCACCGATAGGGTG
Kan-Clean Rev_EcoRV_NEW	ATATATGATATCTTAGAAAAACTCATCGAGCATC AAATG
Kan-FullFwd NheI_NEW	ATATATGCTAGCCACGTTGTGTCTCAAAATCTCTG
casEUupF_Spel	ATATATACTAGTCTTTACCGCCGTGGACGAT
casEDownR_XbaI	ATATATTCTAGAATAAAGGTTTACCCGTGTGCAGA
casEDownF_EcoRV	ATATATGATATCGATTCCAGGCAACAGCGGC
casEUupR2_NheI	ATATATGCTAGCGCAAGGTGACTTTAGACAG ATACA
NiID SDM set 1F (bases 2-3)	CGGGAATAAACCATGGCCACCTTGAATTTCTTGTT
NiID SDM set 1R (bases 2-3)	AACAAGGAAATTCAGGTGGCCATGGTTTAT TCCCG
NiID SDM set 2F (bases 4-5)	GAATAAACCATGGCCACCTTAAACTTCTTG TTTATAAC
NiID SDM set 2R (bases 4-5)	GTTATAAACAAGGAAGTTAAGGTGGCCAT GGTTTATTC
NiID SDM set 3F (bases 6-7)	CCATGGCCACCTTAAACTTTCTCGTTTATA ACTCCATG
NiID SDM set 3R (bases 6-7)	CATGGAGTTATAAACGAGAAAGTTAAGGT GGCCATGG
NiID SDM set 4F (bases 8-9)	GCCACCTTAAACTTTCTCGTGTACAACCTCC ATGTTCCCG
NiID SDM set 4R (bases 8-9)	GGGGAACATGGAGTTGTACACGAGAAAGTT TAAGGTGGC
NiID SDM set 5F (bases 10-11)	CTTAAACTTTCTCGTGTACAATTCTATGTTCCC CGTAAGTAC
NiID SDM set 5R (bases 10-11)	GTACTTACGGGGAACATAGAATTGTACACGAGA AAGTTTAAG
CasE 5' XbaI	AAATCTAGACCGATGTATCTGTCTAAAGTCACC
CasE 3' EcoRV	AAAGATATCCCATTACAGCGCCCTTATCAG
Vector Construction	
TOPO2.1mini_Fwd_NcoI	ATATATCCATGGCGATGCCTGC
TOPO2.1mini_Rev_NcoI	ATATATCCATGGTCCATTCGCCATTCAGGC
pECM20_Xb_F	GGGCCCCGGATCAGATCTCGTTGTGTCTCA
pECM20_Xb_R	GGGCCCCNNNGGTACCGTGTGACCTGCAGATGGAGA
pECMXb_insert_F	GGGCCCCAGACGACATTGGCTGACTTGA
pECMXb_insert_R	GGTACCAAACCTAAATCACAAAAAGCACA
pECMXb_seq_F	AGGCCGGATAAAACTTGTGC
pECMXb_seq_R	TGGGACAACCTCCAGTGAAGAG
pECMXb_integration_F	ATTGTTGATCGTGAGAAGTCCG
pECMXb_integration_R	CTCCAATAAAGCGAATCCAG